A UNIFIED ANALYSIS OF STIFFENER REINFORCED COMPOSITE BEAMS WITH ARBITRARY CROSS-SECTION

by

GIANFRANCO RIOS

Presented to the Faculty of the Graduate School of

The University of Texas at Arlington in Partial Fulfillment

of the Requirements

for the Degree of

DOCTOR OF PHILOSOPHY

THE UNIVERSITY OF TEXAS AT ARLINGTON

December 2009

ACKNOWLEDGEMENTS

I would like to thank my beloved parents, Luis Enrique Rios and Marghe Lombardi de Rios, for their support and guidance; and my brother Giancarlo Rios. Also, my girlfriend Nhat Linh Do for all her love, support, and never ending encouragement. And my special dog Chewy for his companionship and unconditional love.

I would like to express my sincere appreciation and gratitude to my supervising professor, Dr. Wen S. Chan for his guidance, patience, support, and encouragement. I would also like to thank the committee members: Dr. Lawrence, Dr. Nomura, Dr. Wang, and Dr. Huang for their valuable advice and assistant.

November 19, 2009

ABSTRACT

A UNIFIED ANALYSIS OF STIFFENER REINFORCED
COMPOSITE BEAMS WITH ARBITRARY
CROSS-SECTION

Gianfranco Rios, PhD

The University of Texas at Arlington, 2009

Supervising Professor: Wen S. Chan

A number of methods are available to analyze the laminated composite beams using smear property of laminate stiffness ignoring unsymmetrical behavior of laminates. Some include their effect of laminate but did not include the unsymmetrical effect of the cross-section of the beam. On the other hand, using finite element method to analyze the beam is dependent on the structural configurations including the laminate lay-up sequence.

An analytical method was developed from lamination theory in order to study the structural response of composite laminated beams. The present method is capable of predicting the axial and bending stiffnesses, the centroid location, and the stresses in each ply of the whole structure. The results were compared with finite element methods.

Laminated beams studied in this research include the beams with a rectangular cross-section bonded with a stiffener. The stiffener placed in both aligned and non-aligned position with respect to the centerline of the beam is considered.

Thin-walled beams with circular and airfoil sections are also studied. A parametrization method to define the median of the cross-section is developed. Then the stress analysis is conducted.

For two laminates aligned bonded together top and bottom, the present method results agree very well with the finite element results for all the cases less the unsymmetrical case. For the non-aligned case, all the results agree. On the other hand, the results also are close to each other for the laminates bonded side by side less the un-balanced case. Finally, for the circular and airfoil cross-sections the results agree with the finite element results.

TABLE OF CONTENTS

LIST OF ILLUSTRATIONS

Figure Page

LIST OF TABLES

Table Page

LIST OF SYMBOLS

$[a]$: Extensional compliance matrix of laminate.

a^*: Extensional compliance reduced to 1 dimension.

a_{11}^c: a_{11} referred to the centroid of the cross-section.

$[A]$: Extensional stiffness matrix of laminate.

A^*: Extensional stiffness reduced to 1 dimension.

A_1^*: Extensional stiffness of the beam reduced to 1 dimension.

A_2^*: Extensional stiffness of the stiffener reduced to 1 dimension.

$\overline{A}_x$: Axial stiffness.

$\overline{A}_x^{Narrow}$: Axial stiffness of a narrow beam.

$\overline{A}_x^{Narrow,\ Sym}$: Axial stiffness of a symmetric narrow beam.

$\overline{A}_x^{Wide}$: Axial stiffness of a wide beam.

$\overline{A}_x^{Wide,\ Sym}$: Axial stiffness of a symmetric wide beam.

$[b]$: Extensional-flexibility coupling matrix of laminate.

b^*: Extensional-flexibility coupling reduced to 1 dimension.

b_{11}^c: b_{11} referred to the centroid of the cross-section.

$[B]$: Extensional-bending coupling stiffness matrix of laminate.

B^*: Extensional-bending coupling reduced to 1 dimension.

B_1^*: Extensional-bending coupling of the beam reduced to 1 dimension.

B_2^*: Extensional-bending coupling of the stiffener reduced to 1 dimension.

$[d]$: Bending flexibility matrix of laminate.

d^*: Bending flexibility reduced to 1 dimension.

$[D]$: Bending stiffnesses matrix of laminate.

D^*: Bending stiffnesses reduced to 1 dimension.

D_1^*: Bending stiffnesses of the beam reduced to 1 dimension.

D_2^*: Bending stiffnesses of the stiffener reduced to 1 dimension.

$\overline{D}_x$: Bending stiffness in the yy-direction.

$\overline{D}_x^{Narrow}$: Bending stiffness of a narrow beam.

$\overline{D}_x^{Narrow,\ Sym}$: Bending stiffness of a symmetric narrow beam.

$\overline{D}_x^{Wide}$: Bending stiffness of a wide beam.

$\overline{D}_x^{Wide,\ Sym}$: Bending stiffness of a symmetric wide beam.

$\overline{D}_x^{Smeared}$: Bending stiffness according to smeared properties approach.

$\overline{D}_y$: Bending stiffness in the zz-direction.

$\overline{D}'_{xy}$: Bending stiffness in the yz-direction.

$\widetilde{E}_x$: Equivalent Young's Modulus of laminate.

h: Thickness of laminate.

L: Length of the beam.

L_o: Width of the airfoil.

m: Cosine of the angle $(m = \cos\theta)$.

$[M]$: Moment matrix per unit width of laminate.

M_x: Moment per unit width of laminate due to loading along the x-direction.

$\overline{M}_x^c$:Total moment of laminate applied in the centroid of the cross-section.

M_x^c: Moment per unit width of laminate applied in the centroid of the cross-section.

M_{x1}: Moment per unit width in the beam.

M_{x2} : Moment per unit width in the stiffener.

$\overline{M}_x$: Total moment of laminate due to loading along the x-direction.

M_{xy} : Torsion per unit width applied to laminate.

M_y : Moment per unit width applied to laminate.

M_z : Moment per unit width applied to laminate around z.

n: Sine of the angle $(m = \sin\theta)$.

$[N]$: In-plane force matrix per unit width acting on laminate.

N_x : Normal force per unit width in the x-direction applied to laminate.

$\overline{N}_x^c$: Total normal force applied in the centroid of the cross-section.

N_x^c : Normal force per unit width applied in the centroid of the cross-section.

N_{x1} : Normal force per unit width in the x-direction applied to the beam.

N_{x2} : Normal force per unit width in the x-direction applied to the stiffener.

$\overline{N}_x$: Total normal force in the x-direction applied to laminate.

N_{xy} : Shear in-plane force per unit width applied to laminate.

N_y : Normal force per unit width in the y-direction applied to laminate.

$[Q]$: Reduced stiffness matrix of the composite (in a general form).

$[Q]_{1-2}$: Reduced stiffness matrix of lamina.

$[\overline{Q}]_k$: Reduced stiffness matrix of k^{th} lamina.

$[\overline{Q}]_{x-y}$: Reduced stiffness matrix of laminate.

R_m : Mean radius.

$[S]$: Reduced compliance matrix of the composite (in a general form).

$[S]_{1-2}$: Reduced compliance matrix of lamina.

$[\bar{S}]_{x-y}$: Reduced compliance matrix of laminate.

$[T_{\sigma}(\theta)]$: Stress transformation matrix.

$[T_{\varepsilon}(\theta)]$: Strain transformation matrix.

y_1 : is the distance from the centroid of the whole cross-section to the centroid of the beam.

y_2 : is the distance from the centroid of the whole cross-section to the centroid of the stiffener.

$\bar{y}_c$: is the distance from the right of the cross-section to the centroid of the beam and stiffener bonded together.

$\bar{y}_{c1}$: is the distance from the right of the cross-section to the centroid of the beam.

$\bar{y}_{c2}$: is the distance from the right of the cross-section to the centroid of the stiffener.

w : Width of the composite laminate.

w_1 : Width of the composite beam or laminate 1.

w_2 : Width of the composite stiffener or laminate 2.

z: Distance from the mid-plane to certain lamina or centroid.

z_1 : is the distance from the centroid of the whole cross-section to the midplane of the beam.

$\bar{z}_1$: is the distance from the bottom of the cross-section to the midplane of the beam.

z_2 : is the distance from the centroid of the whole cross-section to the midplane of the stiffener.

$\bar{z}_2$: is the distance from the bottom of the cross-section to the midplane of the stiffener.

$\bar{z}_c$: is the distance from the bottom of the cross-section to the centroid of the beam and the stiffener bonded together.

$\bar{z}_{c1}$: is the distance from the bottom of the cross-section to the centroid of the beam.

$\bar{z}_{c1}$: is the distance from the bottom of the cross-section to the centroid of the stiffener.

γ_{xy}^{0} : Mid-plane in-plane shear strain of laminate.

$\gamma_{xy,k}$: In-plane shear strain of k[th] lamina.

ε_{x}^{0} : Mid-plane strain in the x-direction of laminate.

ε_{x1}^{0} : Mid-plane strain in the x-direction of the beam.

ε_{x2}^{0} : Mid-plane strain in the x-direction of the stiffener.

ε_{x}^{c} : Axial strain of the centroid of the structure cross-section.

ε_{y}^{0} : Mid-plane strain in the y-direction of laminate.

$[\varepsilon]_{1-2}$: Strain matrix in 1-2 coordinates.

$[\varepsilon]_{x-y}$: Strain matrix in x-y coordinates.

$\varepsilon_{x,k}$: Normal strain in the x-direction of k[th] lamina.

$\varepsilon_{y,k}$: Normal strain in the y-direction of k[th] lamina.

θ: Angle ply of a lamina about z-coordinate.

κ : Curvature matrix of laminate.

$\kappa_{x}, \kappa_{y}, \kappa_{xy}$: Curvatures of the laminate mid-plane.

κ_{x1} : Curvature of the beam mid-plane.

κ_{x2} : Curvature of the stiffener mid-plane.

κ_{x}^{c} : Curvature of the centroid of the structure cross-section.

ρ : Distance from the midplane to the centroid of the cross-section.

σ_1: Normal stress along the fibers of the composite ply.

σ_2: Normal stress transversal to the direction of the fibers.

σ_3: Normal stress perpendicular to the ply plane.

$[\sigma]_{1-2}$: Stress matrix of laminate in 1-2 coordinates.

$[\sigma]_{x-y}$: Stress matrix of laminate in x-y coordinates.

$\sigma_{x,k}$: Normal stress in the x-direction of k^{th} lamina.

$\sigma_{y,k}$: Normal stress in the y-direction of k^{th} lamina.

$\tilde{\sigma}_x$: Average stress in the x-direction acting on laminate.

τ_{23} or τ_4, τ_{13} or τ_5, τ_{12} or τ_6: Shear stresses of the composite.

$\tau_{xy,k}$: In-plane shear stress of k^{th} lamina.

CHAPTER 1

INTRODUCTION

1.1 Composite Materials Overview

1.1.1 Definition

A structural composite is a material system consisting of two or more phases on a macroscopic scale, whose mechanical performance and properties are designed to be superior to those of the constituent materials acting independently. One of the phases is usually stiffer and stronger used as the reinforcement, whereas the less stiff and weaker phase is used as the matrix.

Some of the properties that can be improved by forming a composite material are: strength, stiffness, corrosion resistance, wear resistance, attractiveness, weight, fatigue life, temperature-dependent behavior, thermal insulation, thermal conductivity, and acoustical insulation.

1.1.2 Ancient History

Composite materials have been around humans since they first grabbed a stick of wood or a bone. Wood consists of strong and flexible cellulose fibers surrounded and held together by a stiffer material called lignin [1]. Also, bone is a composite of the strong yet soft protein collagen and the hard, brittle mineral apatite [1]. However, these are natural materials. The first time recorded in history when mankind started building composite materials was in the form of reinforced bricks made out of straw and mud in the ancient Egypt.

In the nineteenth century, iron rods were used to reinforce masonry, leading to the development of steel-reinforced concrete. Phenolic resin reinforced with asbestos fibers was introduced in the beginning of the last century.

But it was not until 1937 that the history of modern composites began when salesmen from the Owens Corning Fiberglass Company began to sell fiberglass around the United States [2]. In 1930, fiberglass was born when an engineer became intrigued by a fiber that was formed during the process of applying lettering to a glass milk bottle [2].

The first fiberglass boat was made in 1942, accompanied by the use of reinforced plastics in aircraft and electrical components. By 1947, a fully composite body automobile had been made and tested. This car was reasonably successful and led to the development of the Corvette in 1953 which was made using fiberglass performs [2].

In the submarine industry, as early as the 1960s, cylindrical models were being built and tested in an effort to build a pressure hull (that are subjected to massive compressive loads at extreme depths) with a strength-to-weight ratio superior to high-strength steel [3]. In 1954, the U.S. Navy developed a fiberglass replacement for the aluminum fairwaters (a hydrodynamic cowling that surrounds the submarine's sail) that were fitted on submarines [3].

In 1962, the high-strength carbon fibers production began and laminated composites were introduced.

In the aircraft industry, the transition from wood to aluminum began in the 1930s and was spurred to completion by World War II. Carbon and glass composites were gradually introduced in the 1970s and 1980s and continues even today [4]. Starting in the late 1970s, applications of composites expanded widely to the aircraft, marine, automotive, sporting goods, and biomedical industries. The 1980s marked a significant increase in high-modulus fiber utilization. The 1990s marked the further expansion to infrastructure. Recently, Glare, a specific type of fiber-metal laminate (FML) made from aluminum and fiberglass composite, is now poised to be only the third new material to be used in aircraft primary structures [5].

Since late 1990s, composite materials has widely been used in new aircraft structures including Bell Helicopter V22, Lockheed F22 and F35, Airbus A380, and Boeing 777 and 787 models.

1.1.3 Classification

Based on types of fiber reinforcements, composite material is classified as,

i) Continuously fiber-reinforced composites

a) Unidirectional fiber-reinforced composites
b) Fabric composites

ii) Discontinuously fiber-reinforced composites

a) Short fiber-reinforced composites (chopped fiber-reinforced composites)
   - Aligned short fiber-reinforced composites
   - Randomly short fiber-reinforced composites
b) Particulate fibrous reinforced composites

iii) Hybrid composites (multiple types of fibers)

In this dissertation, all the investigation will be done with unidirectional fiber-reinforced composites. This type of composite has the highest efficiency and potential for different structural components. They are called high-performance structural composites, where the normally continuous fiber reinforcement is the backbone of the material, which determines its stiffness and strength in the fiber direction and the matrix provides protection for the sensitive fibers, bonding, support, and local stress transfer from one fiber to another.

1.1.4 Advantages and Disadvantages

The main advantages of composite materials are: low density, high specific stiffness (modulus to density ratio), and high specific strength (strength to density ratio). The higher specific stiffness and strength are the main reason of selecting composites for aircraft structures. However, there are many other advantages that should be taken into consideration: corrosion resistance, long fatigue life, wear resistance, favorable life cycle cost, low thermal expansion, thermal insulation and conductivity, acoustic insulation, and design flexibility.

Some disadvantages of laminated composites are: relative low toughness, low impact resistance, intolerant to out-of-the-plane loads, sensitive to temperature and moisture conditions, requirement of sophisticated nondestructive techniques for detection and monitoring of damage growth, multiple failure modes, and more complex analysis to study them.

1.2 Literature Review on Composite Beams

Numerous researches have been done and books published in the area of composite beams. In review of composite beam study, discussions are divided into three areas: analytical studies, experiment studies, and finite element analyses.

1.2.1 Analytical Studies

In composite materials structures, the designer has the capability to achieve new types of elastic coupling because of their directionality property. These coupling can be generated through the proper selection of the lamination configuration (i.e. ply orientation and stacking sequence) [6-8]. In this sense, for thin-walled beams there are two basic lamination scheme configurations: one of them, referred to as the circumferentially uniform stiffness (CUS) configuration that results in bending-twist and extension-shear elastic couplings, and the other one, referred to as circumferentially asymmetric stiffness (CAS) configuration that features the extension-twist and bending-shear elastic coupling. Song et al. [9] presented analytical solutions of the static response of composite I-beams loaded at their free-end cross-section, and analyzed within the CUS and CAS ply-angle configurations. The analysis highlighted the influence of a number of non-classical effects such as transverse shear, warping inhibition and, directionality property of constituent material systems. They separated their experiment results for CAS and CUS beam configurations. For CAS beam configuration, the transverse shear effect is more prominent in flapping than in lagging degree of freedom. In addition, compared to the case of the free warping, the warping inhibition diminishes the twist angle. For CUS beam configuration, the lagging displacement increases with the increase of the ply-angle, or in another words, with the increase of the lagging-transverse shear stiffness coupling. In addition, the flapping deflection decreases with the increase of the ply-angle, i.e., with the increase of the flapping stiffness. Finally, in the

CAS case, the warping restraint plays a much stronger effect than in the CUS case. In addition, in the CUS case, for the warping restraint twist model the ply-angles have a more distinct effect on twist distribution as compared to the CAS case. As we can see, this analysis provides for the first time a wide presentation, highlighting the importance of a number of essential non-classical effects in composite I-beams.

Razaqpur [10] highlighted the major differences between the methods of analysis for isotropic and anisotropic laminate structures. He identified the various coupling effects. In addition, he suggested in how frame analysis and finite element programs for structures composed of isotropic materials can be modified to make them suitable for the analysis of anisotropic advanced composite structures.

Parnas and Katirci [11] focused their studies in composite pressure vessels. They developed an analytical procedure to design and predict the behavior of fiber reinforced composite pressure vessels. The classical lamination theory and generalized plane strain model are used in the formulation of the elastic problem. The effective elastic properties were formulated neglecting the effect of curvature.

In thin-walled composite beams, Kollar and Springer [12] studied deeply open and closed-sections subjected to axial load and bending. They found closed-form solutions for axial, bending, and torsional stiffnesses as well as the centroids locations for different cross-sections. In addition, they studied transversely loaded thin-walled beams and shear stiffness and compliances of thin-walled open and closed-sections beams. Vasiliev [13] studied open and closed-sections under bending and torsion. In addition, he included the calculation of the cross-section shear center. Hodges [14] worked with open and closed-sections of anisotropic thin-walled beams. Barbero [15] developed a method to study thin-walled beams and to calculate axial, bending, and torsional stiffnesses. In addition, he also included the transverse shear stress in his theory. Altenbach et al. [16] modeled and analyzed thin-walled folded composite structures. Turtle [17] developed a method to calculate the effective axial and bending rigidities of composite beams with solid and thin-walled sections.

Barbero [18] performed stress analysis on pultruded composite I-beams and several failure criteria are used to predict first-ply failure of the member and the failure mode. In addition, Barbero et al. [19] investigated the bending behavior of glass fiber reinforced composite beams. They showed that the bending stiffness is low compared to that of steel sections of the same shape. They concluded that shear deformation effects are important for composite beams. This is due to relatively low elastic modulus of glass fibers when compared to steel and the low shear modulus of matrix resin. The mindlin plate theory takes into account the effect of transverse shear deformation which makes it valid for thick plate situation. Performance of this mindlin theory for thick and moderately thin plates is good, but it faces some deficiencies when applied to thin plates. This is due to numerical over stiffness effect or locking caused by shear terms as the thickness of the plate is reduced. Therefore, Suresh and Malhotra [20] presented a finite element method for the determination of transverse displacement and layer-wise stress distribution of thin-walled plate structures assembled from flat plates. The finite element formulation is based on mindlin plate theory which takes shear deformation of the beam into consideration. Finally, effect of material and lay-up sequence on the structural behavior of rectangular cross-section thin-walled composite box beam under uniformly distributed load on the top face with end supports was studied. Some parameters were defined as the shear correction factors, introduced to account for the fact that through the thickness, shear strain distribution is not uniform [21]. The finite element formulation is used to study the effect of fiber orientation and boundary condition on the deflection and layer wise stresses of the box beam made of glass-epoxy, Kevlar-epoxy, boron-epoxy and graphite-epoxy composites. The FEM aspect ratios of the element in the mesh were also defined. Finally, basically they made four main experiments. They simulated a square isotropic plate, a square laminated composited plate, an isotropic box beam, and a laminated composite box beam. All of them were compared with data available and the results agreed.

Mamalis et al. [22] focus their work on theoretical analysis of the failure mechanism of the stable mode of collapse of thin-walled fiberglass composite tubes under static axial compression.

A simple analytical beam theory can still be quite beneficial for several reasons. First, having more variables in the analysis than necessary can obscure a clear understanding of phenomena being studied. In addition, there have been lot researches in the area of composite thin-walled beam theory. However, shell bending strain measures were neglected in all those papers. For all those two reasons, Volovoi and Hodges [23] built a simple composite beam theory that contains only the four classical beam variables (extensional, torsional, and two bending variables corresponding to transverse deflections in two orthogonal directions) from a general variational-asymptotic framework that takes the shell bending strain measures effect into account. In addition, they developed closed form expressions for the stiffness matrices of single- and double-celled composite thin-walled beams. For most layups, all of the previous theories render practically identical results, which might explain why the deficiency of those theories was not realized earlier. However, for certain material properties the deviation of all those results from the asymptotically correct results might be significant. The results correlation with a finite element based solution is excellent, which show that local shell bending strain measures can be important for such beams.

Wu et al. [24] presented a new method for analyzing the shear lag and shear deformation effects on symmetrically laminated thin-walled composite box beams under bending load. The method is based on the theory of composite laminated plates and is deduced by means of the principle of minimum potential energy.

Dechao et al. [25] developed a series of hierarchical warping functions to analyze the static and dynamic problems of thin walled composite laminated helicopter rotors composed of several layers with single closed cell. In addition, since the composite laminate is usually composed of many layers of different layout orientation, the warping distribution along the thickness is not uniform. Hence, an improved technology based upon the successive corrective warping functions and varying warping distribution along the thickness is developed. He concluded that, the thinner the skin, the larger the ratio of width to height of the beam, and the higher the ratio of Young's modulus to shear modulus, the higher the effects of warping will be.

Mitra et al. [26] developed a new composite thin wall beam element of arbitrary cross-section with open or closed contour. The formulation incorporated the effect of elastic coupling, restrained warping, transverse shear deformation associated with thin walled composite structures. In thin walled composite beam, the end restrains causes non uniform out-of-plane torsional warping as opposed to Saint Venant's assumptions. This effect is predominant in open section beam and in such cases Vlasov theory is normally adopted to incorporate restrained warping effect, which causes considerable change in the effective torsional stiffness.

1.2.2 Experiment Studies

Armanios et al. [27] presented analytical and experimental studies on laminated composite strips exhibiting extension-twist coupling. They obtained the closed-form expressions relating applied extension to twisting rotation; and the contribution of axial force to the twisting moment were isolated. The results were compare with finite element and experimental results. A set of pretwisted laminated composite strips made of a graphite/cyanate material system was used for the testing. An especially design equipment was designed to allow the laminate to twist freely under axial loading and measure the twist angle associated with applied axial force. Test results agreed with the analytical model.

Bank and Mosallam [28] described a pilot experimental study of concrete slabs constructed of normal weight portland cement concrete and reinforced with fiber-reinforced-plastic grating. They compared the flexural stiffness to each other and to theoretical predictions.

Drummond and Chan [29] analytically and experimentally studied the bending stiffness of composites I-beam. Different configurations were tested for pre-buckled stiffness, buckling moment, and ultimate moment. The results were compared with FEM model and test specimens; where all the results agree very well.

Previous investigations showed that it is important to include the non-classical effect, such a section warping and transverse shear effects, in the modeling of thin-walled composite beams. In addition, in those previous works, it is assumed that the tangential stress is negligible

when compared to the axial stress. However, it has been shown that this assumption results in overestimated stiffnesses [30-34]. In Salim and Davalos [35] work, the tangential stresses are not assumed to be zero. The classical Vlasov theory of isotropic thin-walled sections [36] is extended to sections made of composite laminates. The shear deformation of the cross section is accounted for in the formulation of the theory by including the shear properties of the walls in the warping function. All possible elastic couplings such as extension-torsion, bending-extension, and bending-torsion are included in the present model. The torsional response of open and single- and multicell closed sections is considered in this paper. The analytical modeling for a general open-closed composite cross section is presented first, followed by application to wide-flange and box beams. To validate the presented model, single- and double-cell FRP-pultruded composite box beam were tested under tip torsional loads, and their structural response in terms of angle of twist were recorded. Two different laminated box sections were tested, and the analytical model agreed well with the experimental results.

1.2.3 Finite Element Analyses

Thin-walled composite structures are present in many applications, especially in the aircraft and civil industries. The thin-walled beams of open cross-sections are used extensively in space systems as space erectable booms installed on spacecraft; in aeronautical industry both as direct load-carrying members and as stiffener members. In addition, they are used as well in marine and civil engineering, whereas the I-beams, in the fabrication of flexbeams of bearingless helicopter rotor [37].

Thin- walled structures are integral part of an aircraft [26]. That is the reason why many researchers consider it in their studies and published it in scholarly articles.

Chan and his students focused on thin-walled beams with different cross-sections. Among their studies, Chan and Dermirhan [38] considered first a circular cross section thin-walled composite beam. They developed a new and simple closed-form method to calculate its bending stiffness. Then, Lin and Chan [39] continued the work with an elliptical cross section thin-walled composite beam. Later, Syed and Chan [40] included hat-sectioned composite beams. And most

recently, Rao and Chan [41] expanded the work to consider laminated tapered tubes. They developed a closed-form analytical model to study for axial deformation and angle twist of thin-walled composite tubes with a tapered cross section subjected to axial and torsion loading.

Several non-classical behaviors are exhibited by thin-walled composite structures which includes the effect of elastic coupling, transverse shear deformation and restrained torsional warping [26].

Ascione et al. [42] presented a method that formulates a one-dimensional kinematical model that is able to study the static behavior of fiber-reinforced polymer thin-walled beams. It's well known that the statics of composite beam is strongly influenced by shear deformability because of the low values of the elastic shear moduli. Such a feature cannot be analyzed by Vlasov's theory, which assumes that the shear strains are negligible along the middle line of the cross-section. Many authors [43-47] had tried to modify Vlasov's theory and other theories in order to take into account this effect. However, they assumed non-zero mid-plane shear strain. In their work, they took into account the effects of shear deformability within the context of a simplified one-dimensional model, only depending on the coordinate along the beam axis. In addition, a one-dimensional FE approach is also proposed in order to overcome the difficulties related to a 3D analysis of these deformations. As expected, the presence of shear deformation results in higher deflection than predicted by Vlasov's theory.

Ferrero et al. [48] proposed that the stress field in thin-walled composite beams due to a twisting moment is not correctly modeled by classical analytical theories, so numerical modeling is essential. Therefore, they developed a method with a simple way of determining stress and stiffness in this type of structures where the constrained warping effect can be taken into account. They worked with both open and closed cross sections. Also, to check the validity of the method for structures made of composite materials, a beam with thin, composite walls were studied. This beam was free to warp. The results were validated by 4 different methods: this method presented, classical method on uniform twisting in which is assumed to be constant in the wall thickness, NASTRAN FEA, and CPAO which is a software they developed as well.

Wu et al. [49] presented a procedure for analyzing the mechanical behavior of laminated thin-walled composite box beam under torsional load without external restraint. Some analyses have been formulated to analyzed composite box beam with varying levels of assumptions [50-53]. However, none of them dealt with the ply stress of composite box beams, or the free torsional characteristics of composites box beam with consideration of shear-extension coupling effects. In fact, because a composite box beam consist of four composite panels and ply stresses along the thickness of each panel distribute unequally and vary with the ply angle, the analysis of ply stress is of particular importance for the strength design of composite box beams; on the other hand, for composite box beams the mechanical characteristics of free torsion (without external restraint) are distinctly different from those of restraint torsion and should be given enough attention. Therefore, their present research investigates those matters. Numerical results correlate very well with the results of model tests and FEA. However, the analysis results indicate that during the process of torsion, although without external restraint, the internal restraint between plies caused by the coupling effect may induce the longitudinal displacement of fibers, which means for composite box beams, in general, the free torsion may not exist definitely, and may be replaced by a concept of torsion without external restraint.

Lee and Lee [37] developed a general analytical model applicable to the flexural, torsional, and flexural-torsional behavior of an I-section composite beam subjected to vertical and torsional load. This model is based on the classical lamination theory, and accounts for the coupling of flexural and torsional responses for arbitrary laminate stacking sequence configuration. Governing equations are derived from the principle of the stationary value of total potential energy. Numerical results are obtained for thin-walled composites under vertical and torsional loading, addressing the effects of fiber angle, and laminate stacking sequence. It was found that the beam with fiber angle change in the flanges is more sensitive to angle of twist than that of fiber angle change in the web. For both cases, the minimum angle of twist occurs near 45°, that is, because the torsional rigidity becomes maximum value at that value. The last experiment presented was a cantilever beam under point load. This case is that both flanges are anti-symmetric angle-ply stacking sequence and the web is assumed to be unidirectional. The

results showed that it exhibits flexural-torsional coupling. In addition, they showed that the load eccentricity does not affect the vertical displacements.

Chattopadhyay et al. [54] presented a new theory based on a refined higher order displacement field of a plate with eccentricity, that is a three-dimensional model which approximates the elasticity solution so that the box beam cross-sectional properties are not reduced to one-dimensional beam parameters. Both in-plane and out-of-plane warping were included automatically in the formulation. The results showed that piezoelectric actuation significantly reduces the deflection along the box beam span and therefore can be used to control the magnitude of rotor blade vibrations.

1.3 Objective of this Research

In practical engineering analysis, structural members are often idealized as a beam. As it is well known, these beams are one-dimensional structures; however, two-dimensional properties are inherent in composite materials. Furthermore, analyses of beams are often done using smeared property in computing their sectional properties. In doing so, the effect of un-symmetry of the structure is not included.

In analyzing composite structures, one often divides the structure into several laminates. Then, lamination theory is used to perform the laminate analysis. On the other hand, finite element method is used to conduct the structural analysis. Analysis by FEM is still for some cases time consuming, expensive, complex, structural dependent, and probably not the most favorable method for optimal design. Therefore, there is the need to develop a simple method that can accurately analyze axial and bending stiffnesses of these composite beams.

For a thin-walled beam with arbitrary tubular cross-section, a parametric method is used to determine the contour of the cross-section. The stiffness model developed by Chan and his students was modified to determine the axial and bending stiffnesses of the tubular structure with airfoil cross-section.

A new analytical method was developed based on lamination theory in order to study the behavior of these bonded composite laminates. This method is capable of predicting the axial and bending stiffnesses, the centroid location, and the stresses in each ply of the whole structure. The results were compared with finite element method.

1.4 Outline of the Dissertation

Chapter 2 presents a brief review of lamination theory, axial and bending stiffnesses of laminated beam with narrow and wide cross-sections.

Chapter 3 presents a new analytical method to calculate the centroid, axial and bending stiffnesses, as well as ply stresses of a beam with and without a stiffener bonded together. A stiffener bonded on the top of the parent laminate is analyzed. Both stiffener aligned and unaligned with the centerline of laminate width is considered. In addition the axial and bending stiffnesses of a z-stiffener were included.

A new method to calculate the axial and bending stiffnesses as well as the ply stresses of two laminates bonded side by side is included in Chapter 4.

Chapter 5 presents a method to calculate the axial and bending stiffnesses and the ply stresses of a composite beam with arbitrary cross-section. The circular cross-section beam and an airfoil composite beam cases were studied.

Concluding remarks and future work are included in Chapter 6.

CHAPTER 2

BASIC PROPERTIES OF COMPOSITE LAMINATED BEAMS

In most structural applications, composite materials are used in the form of thin laminates which are constructed by stacking multiple laminas together. Instead of analyzing layer by layer, the mid-plane of the laminate is selected as a reference plane. Then, the in-plane structural properties of each ply are translated into this plane. This analysis method is termed as "Lamination Theory". Since composite layer is very thin in thickness comparing to its in-plane dimensions, a plane stress condition ($\sigma_3=\tau_{13}=\tau_{23}=0$) is enforced. With this assumption, the properties of the composite laminate reduces from 3-D to 2-D. On the other hand, fiber composites are often used in the form of beam structures, because beams are common in applications [55]. A beam is one dimensional structure. Hence, the two-dimensional properties of laminate can not be directly applied to a one-dimensional beam. This chapter will cover the development of constitutive equation for a laminated beam.

In structural beam analysis, equivalent axial and bending stiffnesses as well as centroid of the beam cross-section is often used. Expressions of these properties in terms of composite properties will be also included in this chapter.

2.1 Brief Review of Lamination Theory

In this section, a brief description of lamina and laminate constitutive relationships are described. Two coordinate systems, 1-2-3 coordinates and x-y-z coordinates are often used to designate the lamina and the laminate levels, respectively. The 1-coordinate is the direction along the fibers of the composite ply; the 2-coordinate is the transversal direction to the fibers but in the plane of the ply; and the 3-coordinate is perpendicular to the ply plane. The x-y-z coordinates is often selected at the mid-plane of the laminates.

Laminates are usually very thin structures; thus, the main assumption of lamination theory is that composite laminates can be considered to be under plane stress, with all of the out-of-the-plane stress components being equal to zero. That is,

$$\sigma_3 = 0 \ , \ \tau_{23} = \tau_4 = 0 \text{ , and } \tau_{13} = \tau_5 = 0 \tag{2.1}$$

As a result, the orthotropic stress-strain relation reduced to a 3 by 3 matrix in a composite lamina. The reduced compliance matrix $[S]_{1\text{-}2}$ can be written as,

$$[\varepsilon]_{1-2} = [S]_{1-2}[\sigma]_{1-2} \tag{2.2}$$

The inverse of the reduced compliance matrix $[S_{1\text{-}2}]$ is the reduced stiffness matrix $[Q_{1\text{-}2}]$,

$$[Q]_{1-2} = [S]_{1-2}^{-1} \tag{2.3}$$

These reduced compliance [S] and stiffness matrices [Q] are in the general form; that is, it does not matter in which coordinate system they are, they could be in the 1-2 or x-y coordinate systems. However, when there is an angle ply (this angle will be denoted by the Greek letter θ) different than 0°, the reduced compliance $[S]_{1-2}$ and stiffness $[Q]_{1-2}$ will be changed by the transformation matrices to the x-y coordinate system $[\overline{S}]_{x-y}$ and $[\overline{Q}]_{x-y}$, respectively (Eqs. 2.4 and 2.5).

$$[\overline{Q}]_{x-y} = [T_\sigma(-\theta)] \cdot [Q]_{1-2} \cdot [T_\varepsilon(\theta)] \tag{2.4}$$

$$[\overline{S}]_{x-y} = [T_\varepsilon(-\theta)] \cdot [S]_{1-2} \cdot [T_\sigma(\theta)] \tag{2.5}$$

where the transformation matrices are defined as,

$$[T_\sigma(\theta)] = \begin{bmatrix} m^2 & n^2 & 2mn \\ n^2 & m^2 & -2mn \\ -mn & mn & m^2 - n^2 \end{bmatrix} \text{ and } [T_\varepsilon(\theta)] = \begin{bmatrix} m^2 & n^2 & mn \\ n^2 & m^2 & -mn \\ -2mn & 2mn & m^2 - n^2 \end{bmatrix} \tag{2.6}$$

$$m = \cos\theta$$
$$n = \sin\theta$$

$[T_\sigma(\theta)]$ and $[T_\varepsilon(\theta)]$ are referred as the stress and strain transformation matrices, respectively.

The results presented were valid for a single lamina. However, when all the plies or laminas are combined together, they are called laminate.

In general for any k[th] layer, the strain can be in terms of the strain in the mid-plane laminate $(\varepsilon_x^0, \varepsilon_y^0, \gamma_{xy}^0)$, and the curvature of that mid-plane $(\kappa_x, \kappa_y, \kappa_{xy})$, as shown,

$$\begin{bmatrix} \varepsilon_x \\ \varepsilon_y \\ \gamma_{xy} \end{bmatrix}_k = \begin{bmatrix} \varepsilon_x^0 \\ \varepsilon_y^0 \\ \gamma_{xy}^0 \end{bmatrix} + z \begin{bmatrix} \kappa_x \\ \kappa_y \\ \kappa_{xy} \end{bmatrix} \tag{2.7}$$

The stresses in any k[th] layer can be found multiplying the mechanical strain by its stiffness.

$$\begin{bmatrix} \sigma_x \\ \sigma_y \\ \tau_{xy} \end{bmatrix}_k = [\overline{Q}]_k \begin{bmatrix} \varepsilon_x \\ \varepsilon_y \\ \gamma_{xy} \end{bmatrix}_k \tag{2.8}$$

The resultant forces and moments per unit width of the laminate can be obtained by integrating the stresses of each ply through the thickness as shown.

$$\begin{bmatrix} N_x \\ N_y \\ N_{xy} \end{bmatrix} = \sum_{k=1}^{n} \int_{h_{k-1}}^{h_k} \begin{bmatrix} \sigma_x \\ \sigma_y \\ \tau_{xy} \end{bmatrix}_k dz \tag{2.9}$$

$$\begin{bmatrix} M_x \\ M_y \\ M_{xy} \end{bmatrix} = \sum_{k=1}^{n} \int_{h_{k-1}}^{h_k} \begin{bmatrix} \sigma_x \\ \sigma_y \\ \tau_{xy} \end{bmatrix}_k z dz \tag{2.10}$$

The loads and moments directions are defined in Figure 2.1.

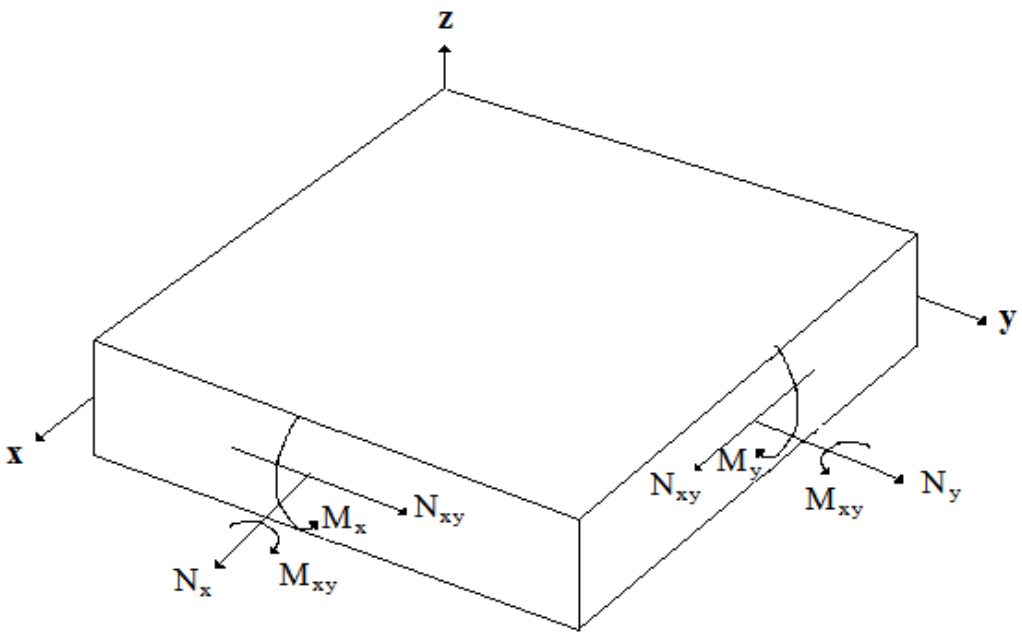

Figure 2.1 Definition of moments and loads in lamination theory

Substituting the expression of stress and strain of each ply, the constitutive equation of the laminate can be expressed as:

$$\begin{bmatrix} N \\ M \end{bmatrix} = \begin{bmatrix} A & B \\ B & D \end{bmatrix} \cdot \begin{bmatrix} \varepsilon^0 \\ \kappa \end{bmatrix} \tag{2.11}$$

or

$$\begin{bmatrix} \varepsilon^0 \\ \kappa \end{bmatrix} = \begin{bmatrix} a & b \\ b^T & d \end{bmatrix} \cdot \begin{bmatrix} N \\ M \end{bmatrix} \tag{2.12}$$

where $\begin{bmatrix} a & b \\ b^T & d \end{bmatrix} = \begin{bmatrix} A & B \\ B & D \end{bmatrix}^{-1}$. (2.13)

The stiffness matrices [A], [B], and [D] are defined as,

$$[A] = \sum_{k=1}^{n} [\overline{Q}_{x-y}]_k (h_k - h_{k-1}) \tag{2.14}$$

$$[B] = \frac{1}{2} \sum_{k=1}^{n} [\overline{Q}_{x-y}]_k (h_k^2 - h_{k-1}^2) \tag{2.15}$$

$$[D] = \frac{1}{3} \sum_{k=1}^{n} [\overline{Q}_{x-y}]_k (h_k^3 - h_{k-1}^3) \tag{2.16}$$

h_k and h_{k-1} are the coordinates of the upper and lower surface of the k[th] layer, respectively. It should be noted that [A], [B], and [D] matrices are symmetrical since $[\overline{Q}_{x-y}]_k$ matrix is symmetrical.

To better understand each term of the [ABD] matrix (Eq. 2.11), it is expanded below,

$$\begin{bmatrix} N_x \\ N_y \\ N_{xy} \\ M_x \\ M_y \\ M_{xy} \end{bmatrix} = \begin{bmatrix} A_{11} & A_{12} & A_{16} & B_{11} & B_{12} & B_{16} \\ A_{12} & A_{22} & A_{26} & B_{12} & B_{22} & B_{26} \\ A_{16} & A_{26} & A_{66} & B_{16} & B_{26} & B_{66} \\ B_{11} & B_{12} & B_{16} & D_{11} & D_{12} & D_{16} \\ B_{12} & B_{22} & B_{26} & D_{12} & D_{22} & D_{26} \\ B_{16} & B_{26} & B_{66} & D_{16} & D_{26} & D_{66} \end{bmatrix} \cdot \begin{bmatrix} \varepsilon_x^o \\ \varepsilon_y^o \\ \gamma_{xy}^o \\ \kappa_x \\ \kappa_y \\ \kappa_{xy} \end{bmatrix} \tag{2.17}$$

[A] matrix is called in-plane extensional stiffness matrix because it directly relates in-plane strains $(\varepsilon_x^0, \varepsilon_y^0, \gamma_{xy}^0)$ to in-plane forces per unit width (N_x, N_y, N_{xy}). A_{11} and A_{22} are called the axial extension stiffness, A_{12} is the stiffness due to Poisson's ratio effect, A_{16} and A_{26} are the stiffness due to shear coupling, and A_{66} is the shear stiffness.

On the other hand, [B] is called extensional-bending coupling stiffness matrix. This matrix relates in-plane strains to bending moments and curvatures to in-plane forces. This coupling effect does not exist for isotropic materials. Thus, if $B_{ij}\neq 0$, in-plane forces produce flexural and twisting deformation in addition to in-plane deformation; moments as well produce extensional and shear deformation of the middle surface in addition to flexural and twisting deformation. B_{11} and B_{22} are the coupling stiffness due to direct curvature, B_{12} is the coupling stiffness due to Poisson's ratio effect, B_{16} and B_{26} are the extension-twisting coupling stiffness or shear-bending coupling stiffness, and B_{66} is the shear-twisting coupling stiffness.

[D] matrix is the bending stiffness matrix because it relates curvatures $(\kappa_x, \kappa_y, \kappa_{xy})$ to bending moments per unit width (M_x, M_y, M_{xy}). D_{11} and D_{22} are the bending stiffness, D_{12} is the bending stiffness due to Poisson's ratio effect, D_{16} and D_{26} are the bending-twisting coupling, and D_{66} is the twisting stiffness [15].

Inverting the stiffness matrix [ABD], the compliance matrix is obtained,

$$\begin{bmatrix} \varepsilon_x^o \\ \varepsilon_y^o \\ \gamma_{xy}^o \\ \kappa_x \\ \kappa_y \\ \kappa_{xy} \end{bmatrix} = \begin{bmatrix} a_{11} & a_{12} & a_{16} & b_{11} & b_{12} & b_{16} \\ a_{21} & a_{22} & a_{26} & b_{21} & b_{22} & b_{26} \\ a_{16} & a_{26} & a_{66} & b_{61} & b_{62} & b_{66} \\ b_{11} & b_{21} & b_{61} & d_{11} & d_{12} & d_{16} \\ b_{12} & b_{22} & b_{62} & d_{12} & d_{22} & d_{26} \\ b_{16} & b_{26} & b_{66} & d_{16} & d_{26} & d_{66} \end{bmatrix} \cdot \begin{bmatrix} N_x \\ N_y \\ N_{xy} \\ M_x \\ M_y \\ M_{xy} \end{bmatrix} \tag{2.18}$$

Equation 2.18 has been written in several composite books with the assumption that [b] is symmetric; however, this is incorrect, in general. Equations 2.12 and 2.18 emphasize this issue, showing that [b] and $[b^T]$ must be used simultaneous in order to build the compliance matrix which needs to be symmetric.

2.2 Special Cases of Laminates

There are special cases of laminates in which some terms in the stiffness matrix (Eq. 2.17) and the compliance matrix (Eq. 2.18) vanish. This makes them to have specific structural response only archived in certain laminate configurations.

2.2.1 Balanced vs. Un-balanced Laminate

A laminate is balanced if plies with identical material properties and thickness have equal number of +θ and -θ as angle ply in the laminate lay-up. In addition, 0° and 90° angle ply are self-balanced. A balanced laminate could be symmetric or un-symmetric.

The advantage of a balanced laminated is that there is no extension-shear coupling because A_{16} and A_{26} vanish (Eq. 2.19).

$$A_{16} = A_{26} = 0 \tag{2.19}$$

On the other hand, an un-balanced laminate exhibits an extension-shear coupling effect.

2.2.2 Symmetric, Un-symmetric, and Anti-symmetric Laminate

A laminate is symmetric if plies with identical material properties, thickness, and orientation are symmetrically located with respect to the reference plane of the laminate. For these laminates, it can be proved that [B] matrix, the coupling stiffness is zero. This implies there is no extension-bending coupling effect when the laminate is loaded. In other words, the in-plane load induces in-plane deformation and the bending load causes the curvature of the laminate. Furthermore, the symmetric laminates exhibit no distortion or warpage in hygrothermal environment or after fabrication. Hence, a symmetric laminate is the most desirable laminate configuration in design practice.

On the other hand, an un-symmetric laminate is any other laminate that is not symmetric. For these laminates, [B] matrix does not vanish and as a result the laminate will experience extension-bending coupling as well as distortion and warpage in hygrothermal environment or after fabrication.

A symmetric laminate can eliminate the bending effect when it is loaded in tension. However, both symmetric and un-symmetric laminates will exhibit bending-twisting coupling under bending.

An anti-symmetric laminate is a balanced laminate but its +θ and -θ layers are in an anti-symmetric position with respect to its mid-plane. For this laminates, it is balanced but un-symmetric. This laminates gives a non-zero [B] matrix but a zero value of the D_{16} and D_{26} terms. This implies that the laminate exhibits extension-bending coupling but no bending-twisting coupling effect.

2.3 Evaluation of Stiffness of Composite Beams

Evaluation of the axial, bending, and torsion stiffnesses is for predicting structural response of structural members under load. In aircraft industry, wing and fuselage structures consist of a collection of basic structural elements. Each component, as a whole, acts like a beam and a torsion member. As an example, the box beam consists of stringers (axial members) that are located at the maximum allowable distance from the neutral axis to achieve the most bending capability, and the thin skin (shear panel), which encloses a large area to provide a large torque capability. This dissertation focuses only in the axial and bending stiffnesses.

2.3.1 Axial Stiffness

The axial stiffness of the material can be seen as a resistance of the structure to deform along the loading direction. It is a proportional constant that relates the applied force and its strain response. In design practice, the axial stiffness of a structure is evaluated at a load that does not exceed the proportional limit of the material.

2.3.1.1 Isotropic Material

For a structure made of isotropic material, the force and strain relationship can be easily written as

$$\overline{N}_x = (EA)\varepsilon_x \tag{2.20}$$

where $\overline{N}_x$ is the total applied force to the structure, and the term EA is known as the axial stiffness and it is simply the modulus of the material times the structural cross-section (Eq. 2.21).

$$\boxed{Axial\_stiffness = \overline{A}_x = EA} \tag{2.21}$$

It is obvious that the axial stiffness of axial members cannot be increased or decreased by simply changing the shape of the cross section.

2.3.1.2 Composite Laminate

From the compliance matrix (Eq. 2.18), assuming all the loads are zero (N_y=N_{xy}=M_x=M_y=M_{xy}=0) and applying only N_x, the first equation of the system becomes,

$$\varepsilon_x^o = \mathrm{a}_{11} \cdot N_x \tag{2.22}$$

$$\overline{N}_x = \left(\frac{w}{a_{11}} \right) \varepsilon_x^o$$

$$\boxed{\overline{A}_x = \frac{w}{a_{11}}} \tag{2.23}$$

The width of the composite laminate is represented by the letter w. Units of the width are inches and a_{11} is “in/lb”. As a result, the units of the total axial stiffness are “lb”, just the same as for isotropic material (Eq. 2.21).

In composites, an equivalent Young’s Modulus is equal to the inverse of a_{11} multiplied by the total height of the laminate. From Equation 2.22,

$$\varepsilon_x^o = \mathrm{a}_{11} \cdot N_x \quad \rightarrow \quad \frac{\tilde{\sigma}_x}{\varepsilon_x^o} = \frac{1}{\mathrm{a}_{11} h} \quad \rightarrow \quad \tilde{E}_x = \frac{1}{a_{11} h} \tag{2.24}$$

where h is the total thickness of the laminate and "$\tilde{\sigma}_x$" is the averaged stress acting on it.

Therefore, the axial stiffness can be seen as this equivalent Young's Modulus multiplied by the area of the cross-section of the beam. This gives exactly the same result as Equation 2.23.

$$\boxed{\overline{A}_x = \tilde{E}_x A = \frac{w}{a_{11}}} \tag{2.25}$$

Equations 2.23 and 2.25 reduce to Equation 2.21 when using isotropic material properties. Substituting Equation 2.24 "$a_{11} = \frac{1}{\tilde{E}_x h}$" into 2.23, $\overline{A}_x = \tilde{E}_x hw = EA$ which is the same axial stiffness found for isotropic materials.

2.3.2 Bending Stiffness

The bending stiffness is defined as the resistance of the structure from bending. In other words, the bending stiffness is the proportional constant that relates the bending moment and its induced curvature. Mathematically, it can be written as

$$\overline{M}_x = \overline{D}_x \cdot \kappa_x$$

2.3.2.1 Isotropic Material

For isotropic materials, the bending stiffness "$\overline{D}_x$" can be expresses as

$$\boxed{Bending\_stiffness = \overline{D}_x = EI} \tag{2.26}$$

where I is the moment of inertia of the cross-section.

Except for pure moment loading, a beam is designed to carry both bending moments and transverse shear forces as the latter usually produce the former. For a beam of a large span/depth ratio, the bending stress is usually more critical than the transverse shear stress. From the ratio $\frac{\sigma_{MAX}}{\tau_{MAX}} = \frac{4L}{h}$ it is evident that bending stress plays a more dominant role than transverse shear stress if the span-to-depth ratio is large (as in wing structures) [56].

2.3.2.2 Composite Materials (Smeared Property Approach)

Equation 2.25 shows that, in order to calculate the axial stiffness, it is possible to calculate an equivalent Young's Modulus for the composite and multiplied it by the area of the cross-section. Therefore, using an analogous approach, the equivalent Young's Modulus (Eq. 2.24) of the composite multiplied by the inertia of the cross-section gives the bending stiffness.

$$\boxed{\overline{D}_x^{Smeared} = \tilde{E}_x I = \frac{1}{h a_{11}} I} \tag{2.27}$$

Once again, when using isotropic material properties in Equation 2.27, it reduces to Equation 2.26, because $\tilde{E}_x$ reduces to E.

2.4 Parallel Axis Theorem

The laminate properties such as the stiffness matrices [A], [B], and [D] are derived at a reference axis of the laminate. In lamination theory, the reference axis is chosen in the mid-plane of the laminate. In practice, the reference axis may be selected at another place like the centroid for example. In those cases, those stiffness matrices [A], [B], and [D] must be translated to the other reference axis by the Parallel Axis Theorem. The primed and unprimed notations refer to the new and original coordinate systems (Fig. 2.2), respectively. ρ is the distance measuring from the original coordinate system to the new coordinate system.

$$\begin{aligned} [A'] &= [A] \\ [B'] &= [B] - \rho[A] \\ [D'] &= [D] - 2\rho B] + \rho^2[A] \end{aligned} \tag{2.28}$$

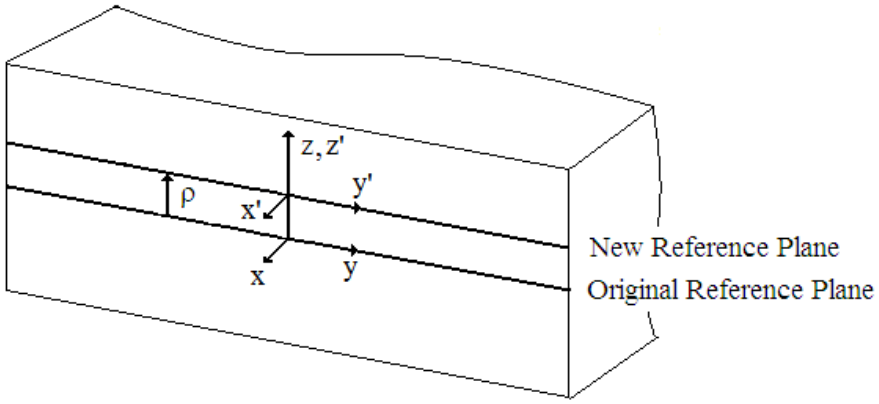

Figure 2.2 Reference planes

The shift of the stiffness matrices has been derived and given in many textbooks [12]. In some cases, it is desired to shift the compliance matrices instead of the stiffness matrices. The expressions of the compliance matrices are obtained as

$$\begin{aligned} [a'] &= [a] + \rho([b] + [b^T]) + \rho^2[d] \\ [b'] &= [b] + \rho[d] \\ [d'] &= [d] \end{aligned} \tag{2.29}$$

The detail derivation of the compliance matrices shift Equations (Eq. 2.29) can be found in Appendix A. It is noted that the extensional stiffness [A'] and the flexibility matrices [d'] remain unchanged when the axis is shifted.

2.5 Axial and Bending Stiffness in Laminated Rectangular cross-section Beams

The axial and bending stiffnesses of composite beam depend on the deformation of the configuration of the cross-section. The configuration deformation is affected by the width of the beam. Hence, in order to perform the analysis, narrow and wide beams need to be considered separately. Wide and narrow refer to the aspect ratio of the cross-section, that is, the ratio of the cross-section width to height. The difference between these two cases lies in the anticlastic effect, which refers to the transverse distortion of the beam [55].

2.5.1 Narrow Beams

For a narrow beam the axial strain distributions give rise to a deformation of the cross-section in the transverse direction because the Poisson effect [55] (Fig. 2.3). A narrow beam is a beam in which its width-height ratio is small. Therefore, the load N_x and moment M_x acting on the axial direction are only considered; the loads and moments in the other directions are neglected.

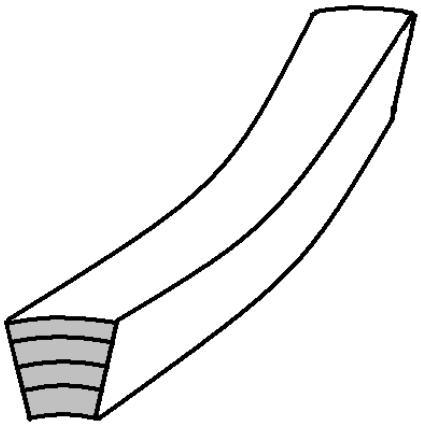

Figure 2.3 Narrow beam deformed cross-section

Substituting $N_y = N_{xy} = M_y = M_{xy} = 0$ in Equation 2.18 give the following equations [57],

$$\varepsilon_x^0 = \mathrm{a}_{11} \cdot N_x + \mathrm{b}_{11} \cdot M_x$$

$$\kappa_x = \mathrm{b}_{11} \cdot N_x + \mathrm{d}_{11} \cdot M_x$$

Writing them in the matrix from and inverting it,

$$\begin{bmatrix} \varepsilon_x^0 \\ \kappa_x \end{bmatrix} = \begin{bmatrix} a_{11} & b_{11} \\ b_{11} & d_{11} \end{bmatrix} \cdot \begin{bmatrix} N_x \\ M_x \end{bmatrix} \quad \text{and} \quad \begin{bmatrix} N_x \\ M_x \end{bmatrix} = \begin{bmatrix} a_{11} & b_{11} \\ b_{11} & d_{11} \end{bmatrix}^{-1} \cdot \begin{bmatrix} \varepsilon_x^0 \\ \kappa_x \end{bmatrix}$$

$$N_x = \frac{d_{11}}{a_{11}d_{11} - b_{11}^2} \cdot \varepsilon_x^0 \tag{2.30}$$

$$M_x = \frac{a_{11}}{a_{11}d_{11} - b_{11}^2} \cdot \kappa_x \tag{2.31}$$

From Equation 2.30, the axial stiffness can be extracted since N_x is the axial force per unit width acting on the composite. Therefore, substituting $N_x = \frac{\overline{N}_x}{w}$ in Equation 2.30, the axial stiffness becomes,

$$\boxed{\overline{A}_x^{Narrow} = \frac{wd_{11}}{a_{11}d_{11} - b_{11}^2}} \tag{2.32}$$

It is important to highlight that Equation 2.32 reduces to Equations 2.23 and 2.25 when the lay-up is symmetric; in this case, b_{11} becomes zero (Eq. 2.33). Therefore, when the lay-up is symmetric, the smeared property gives the same answer as the narrow beam does. However, when the lay-up is un-symmetric, the answers are different. For a symmetric cross-section, Equation 2.32 reduces to 2.33.

$$\boxed{\overline{A}_x^{Narrow,\ Sym} = \frac{w}{a_{11}}} \tag{2.33}$$

Similarly, from Equation 2.31 can be extracted the bending stiffness of a narrow beam. Substituting $M_x = \frac{\overline{M}}{w}$ in Equation 2.31, it is possible to conclude that,

$$\boxed{\overline{D}_x^{Narrow} = \frac{wa_{11}}{a_{11}d_{11} - b_{11}^2}} \tag{2.34}$$

Once again, when the lay-up is symmetric, b_{11} vanishes, and Equation 2.34 reduces to,

$$\boxed{\overline{D}_x^{Narrow,\ Sym} = \frac{w}{d_{11}}} \tag{2.35}$$

This result is very important since there is a significant difference between the smeared property bending stiffness (Eq. 2.27) and the narrow beam bending stiffness (Eq. 2.34). The smeared property approach bending stiffness does not take the order of the stacking sequence into consideration. As emphasized earlier, the smeared property approach considers only an equivalent Young's Modulus and multiplied it by the inertia of the cross-section; therefore, the effect of the stacking sequence on the bending stiffness is not taken into account. This ignorance is acceptable if the laminate is very thin and the distance from the bending axis is relative large (e.g. like I-section). However, if the laminate is thick and the distance from the bending axis is very small, the stacking sequence will have a significant effect on the bending stiffness. This effect is only included in narrow beam approach (Eq. 2.34) since d_{11} contains that information.

2.5.2 Wide Beams

Opposite to a narrow beam, a wide beam, acting essentially as a plate, does not show distortion of the cross-section except at the outer edges [55] (Fig. 2.4). A wide beam is a beam in which its width-height ratio is large. As a result of this, its curvatures κ_y and κ_{xy} are restrained.

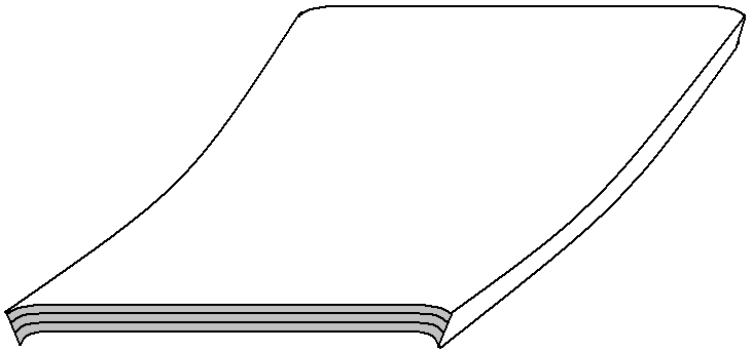

Figure 2.4 Wide beam deformed cross-section

Substituting $\varepsilon_y^o = \gamma_{xy}^o = \kappa_y = \kappa_{xy} = 0$ in Equation in 2.17 gives the following equations,

$$N_x = A_{11}\varepsilon_x^0 + B_{11}\kappa_x$$

$$M_x = B_{11}\varepsilon_x^0 + D_{11}\kappa_x$$

Just as before, writing them in the matrix from and inverting it,

$$\begin{bmatrix} N_x \\ M_x \end{bmatrix} = \begin{bmatrix} A_{11} & B_{11} \\ B_{11} & D_{11} \end{bmatrix} \cdot \begin{bmatrix} \varepsilon_x^0 \\ \kappa_x \end{bmatrix} \quad \text{and} \quad \begin{bmatrix} \varepsilon_x^0 \\ \kappa_x \end{bmatrix} = \begin{bmatrix} A_{11} & B_{11} \\ B_{11} & D_{11} \end{bmatrix}^{-1} \cdot \begin{bmatrix} N_x \\ M_x \end{bmatrix}$$

$$\varepsilon_x^0 = \frac{D_{11}}{A_{11}D_{11} - B_{11}^2} \cdot N_x \tag{2.36}$$

$$\kappa_x = \frac{A_{11}}{A_{11}D_{11} - B_{11}^2} \cdot M_x \tag{2.37}$$

Rearranging Equation 2.36, it is possible to relate the axial force per unit width and the axial strain.

$$N_x = \left(A_{11} - \frac{B_{11}^2}{D_{11}} \right) \cdot \varepsilon_x^0 \tag{2.38}$$

As usually, substituting $N_x = \frac{\overline{N}_x}{w}$ in Equation 2.38, and the axial stiffness can be extracted.

$$\boxed{\overline{A}_x^{Wide} = w\left(A_{11} - \frac{B_{11}^2}{D_{11}} \right)} \tag{2.39}$$

When the lay-up is symmetric, B_{11} vanishes and Equation 2.39 reduces to,

$$\boxed{\overline{A}_x^{Wide,\ Sym} = wA_{11}} \tag{2.40}$$

Similarly, rearranging Equation 2.37, and substituting $M_x = \frac{\overline{M}}{w}$, the bending stiffness of a wide beam can be found.

$$\boxed{\overline{D}_x^{Wide} = w\left(D_{11} - \frac{B_{11}^2}{A_{11}} \right)} \tag{2.41}$$

Once again, when the lay-up is symmetric, B_{11} vanishes and Equation 2.41 reduces to,

$$\boxed{\overline{D}_x^{Wide,\ Sym} = wD_{11}} \tag{2.42}$$

2.5.3 General Beam

There is no clear distinction between the wide and narrow beams. For a general laminated beam, the structural response exhibits in-between the two above mentioned cases.

2.6 Centroid

The centroid is a significant sectional property of the structure's cross-section that is used to determine the response.

2.6.1 Isotropic Material

For isotropic materials, the centroid depends only of geometric parameters (Eq. 2.43).

$$y_c = \frac{\sum y_i A_i}{\sum A_i} \quad \text{and} \quad z_c = \frac{\sum z_i A_i}{\sum A_i} \tag{2.43}$$

where y_c and z_c are the centroid locations of each element i, and A_i is the cross-section area of element i.

2.6.2 Composite Laminate

In composites, the centroid is defined as the location where an axial load N_x^c does not cause a change in curvature κ_x^c and a bending moment M_x^c does not produce axial strain ε_x^c. In other words, the load acting at the centroid decouples the structural response between axial extension and bending. Hence, the centroid of the laminate cross-section can be obtained from the following procedure. From Equation 2.18, it is possible to obtain the axial strain and curvature referred to the centroid instead of the mid-plane.

$$\varepsilon_x^c = a_{11}^c N_x^c + b_{11}^c M_x^c \tag{2.44}$$

From the centroid definition the application of bending moment does not contribute to the axial strain of the beam. Hence, $b_{11}{}^{c}$ must be equal to zero ($b_{11}^{c} = 0$). With aid of Equation 2.29, we have,

$$b_{11}^{c} = b_{11} + \rho d_{11} = 0$$

$$\rho = -\frac{b_{11}}{d_{11}} \tag{2.45}$$

where ρ is the distance from the mid-plane axis to the centroid of the laminate.

It should be noted that for a symmetric laminate $\rho = 0$. This implies that the centroid coincides with the mid-plane axis of the laminate.

2.6.3 Smeared Property Approach

As explained earlier, the smeared property approach uses an equivalent Young's Modulus to calculate the axial and bending stiffnesses (Eq. 2.24). This equivalent Young's Modulus is base on the assumption that it is constant through all the laminate. Therefore, for smeared property approach, the centroid is always going to be at the mid-plane of each laminate; however, if working with two laminates bonded together, the equivalent Young's Modulus will be different for each laminate. With the help of Equation 2.46 is possible to calculate the centroid through the smeared property approach.

$$z_{c}^{Smeared} = \frac{(E_1 A_1)\bar{z}_1 + (E_2 A_2)\bar{z}_2}{(E_1 A_1) + (E_2 A_2)} \tag{2.46}$$

where $\bar{z}_1$ is the distance from the bottom of the cross-section to the mid-plane of laminate 1; and $\bar{z}_2$ is the distance from the same bottom of the cross-section to the mid-plane of laminate 2.

CHAPTER 3

STIFFENER REINFORCED LAMINATED BEAMS

Bonding composite laminates together is a common practice in today industry. This could be done for reparation of a damage composite structure, for reinforcement, or to created new compound structures. A theory was developed from lamination theory in order to study the behavior of these bonded composite laminates. This theory is capable of predicting the axial and bending stiffnesses, the centroid location, and the stresses generated in each ply of the whole structure due to axial and bending loads.

This chapter considers two different laminates bonded together one on the top of the other one. First, we consider the two laminates are aligned together, and then, we consider the case when they are not aligned. The results were compared with lamination theory and finite element method.

Typical MATLAB program used in the calculations are included in Appendix C.

3.1 Constitutive Equations of Composite Beam

Since the beam is narrow and long, moment M_y and twisting curvature k_{xy} in the y-plane can be ignored. For a laminated beam under an axial load, a bending moment M_x, an M_{xy} may be induced. Conversely, a bending moment in a laminated beam may induce the in-plane deformation. In this case, the following assumptions will be assumed in this study $N_y = N_{xy} = M_y = 0$ and $\kappa_{xy} = 0$. Substituting these assumptions in Equation 2.18, Equation 3.1 is obtained

$$\begin{bmatrix} \varepsilon_x^o \\ \kappa_x \\ \kappa_{xy} \end{bmatrix} = \begin{bmatrix} a_{11} & b_{11} & b_{16} \\ b_{11} & d_{11} & d_{16} \\ b_{16} & d_{16} & d_{66} \end{bmatrix} \cdot \begin{bmatrix} N_x \\ M_x \\ M_{xy} \end{bmatrix} \tag{3.1}$$

Since $\kappa_{xy} = 0$, Equation 3.1 can be rewritten as,

$$\begin{bmatrix} \varepsilon_x^o \\ \kappa_x \end{bmatrix} = \begin{bmatrix} a^* & b^* \\ b^* & d^* \end{bmatrix} \cdot \begin{bmatrix} N_x \\ M_x \end{bmatrix} \tag{3.2}$$

Where,

$$a^* = \left(a_{11} - \frac{b_{16}^2}{d_{66}} \right) \qquad b^* = \left(b_{11} - \frac{b_{16} d_{16}}{d_{66}} \right) \qquad d^* = \left(d_{11} - \frac{d_{16}^2}{d_{66}} \right) \tag{3.3}$$

Equation 3.2 is the constitutive equation of laminated beam. It should be noted that if the laminate is symmetric, $b^* = 0$. Inverting Equation 3.2,

$$\begin{bmatrix} N_x \\ M_x \end{bmatrix} = \begin{bmatrix} A^* & B^* \\ B^* & D^* \end{bmatrix} \begin{bmatrix} \varepsilon_x^o \\ \kappa_x \end{bmatrix} \tag{3.4}$$

Where,

$$A^* = \left(\frac{d^*}{a^* d^* - b^{*2}} \right) \qquad B^* = \left(\frac{-b^*}{a^* d^* - b^{*2}} \right) \qquad D^* = \left(\frac{a^*}{a^* d^* - b^{*2}} \right) \tag{3.5}$$

The centroid of composite beam can be calculate similar to the way it is calculated in lamination theory; however, instead of using Equation 2.45, the reduced properties to one dimension must be used, that is,

$$\rho = -\frac{b^*}{d^*} \tag{3.6}$$

3.2 Aligned Rectangular Strip Stiffener Reinforcement

An aligned stiffener bonded or co-cured in a laminated beam as shown in Figure 3.1 is considered in this section. The bondline thickness is ignored in this study.

3.2.1 Description of the Geometry

The laminated beam is assumed to be thin in thickness and narrow in its width compared to its length. Figure 3.2 shows a cross-section of a laminated beam with a stiffener reinforcement at the top of the beam.

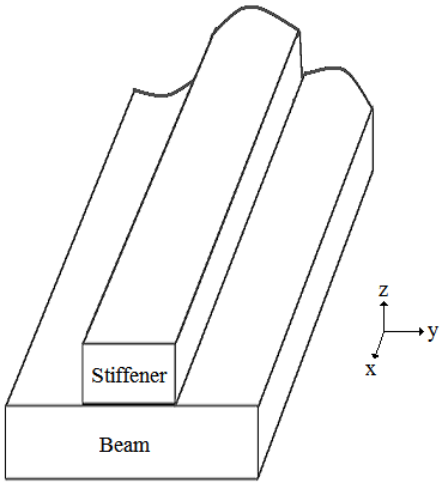

Figure 3.1 Laminated beam with a stiffener reinforcement on the top

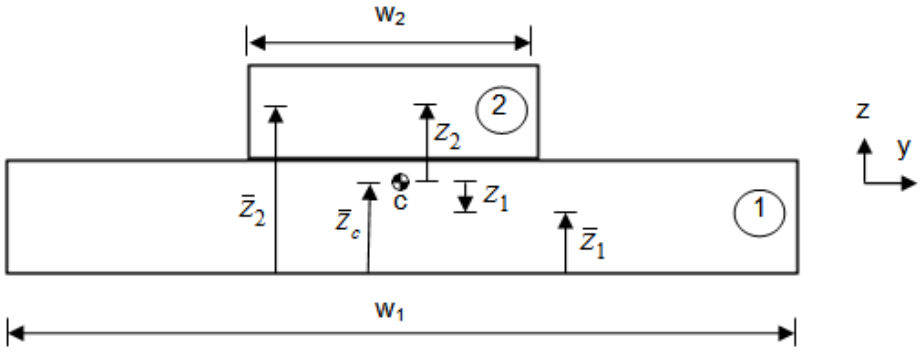

Figure 3.2 Stiffener at the center of laminate beam

$\bar{z}_1$ is the distance from the bottom of the cross-section to the mid-plane of the beam. $\bar{z}_c$ is the distance from the bottom to the centroid of the whole structure. On the other hand, z_1

is the distance from this centroid to the mid-plane of the beam. Similar notation is used for stiffener. In addition, w_1 is the width of the beam and w_2 is the width of the stiffener (Fig. 3.2).

3.2.2 Equivalent Axial Stiffness

Let assume a total load $\overline{N}_x^c$ be applied at the centroid of the beam cross-section. An axial load and a bending moment for each laminate are induced as shown in Figure 3.3. Let N_{x1}, N_{x2}, M_{x1}, and M_{x2} be the axial load and moment per unit width of laminate 1 (beam) and 2 (stiffener), respectively.

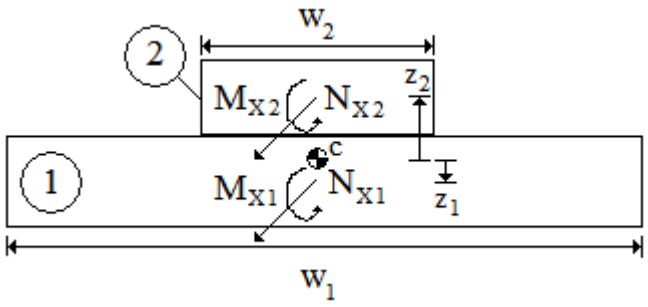

Figure 3.3 Axial forces and moments acting on centroids of the beam and stiffener

Considering the force balanced,

$$\overline{N}_x^c = w_1 N_{x1} + w_2 N_{x2} \tag{3.7}$$

Substituting Equation 3.4 into 3.7 for each laminate, it is obtained,

$$\overline{N}_x^c = w_1(A_1^* \varepsilon_{x1}^o + B_1^* \kappa_{x1}) + w_2(A_2^* \varepsilon_{x2}^o + B_2^* \kappa_{x2}) \tag{3.8}$$

ε_{x1}^o and ε_{x2}^o are the mid-plane strain of laminate 1 and 2 in x-direction and κ_{x1} and κ_{x2} are the curvature of each laminate. Because of the two laminates perfectly bonded, the curvature of each laminate should be equal to the one of the entire bonded laminate. The mid-plane strain of each laminate can be in terms of the mid-plane strain and the curvature of the entire bonded laminate as

$$\varepsilon_x = \varepsilon_x^c + z\kappa_x^c \tag{3.9}$$

Since the load is applied to the centroid of a composite beam, there is no curvature induced to the entire cross-section of the laminate. Therefore, $\kappa_{x1} = \kappa_{x2} = \kappa_x^c = 0$ and $\varepsilon_{x1}^o = \varepsilon_{x2}^o = \varepsilon_x^c$. Consequently, Equation 3.8 becomes,

$$\overline{N}_x^c = (w_1 A_1^* + w_2 A_2^*)\varepsilon_x^c \tag{3.10}$$

Comparing Equation 3.10 with Equation 2.20 the equivalent axial stiffness of the whole structure $\overline{A}_x$ can be expressed as

$$\boxed{\overline{A}_x = w_1 A_1^* + w_2 A_2^*} \tag{3.11}$$

3.2.3 Equivalent Bending Stiffness

In a similar way, the equivalent bending stiffness can be determined. Let a bending moment $\overline{M}_x^c$ be applied at the centroid of the beam. The equilibrium equations of moments (Fig. 3.3) give,

$$\overline{M}_x^c = w_1 N_{x1} z_1 + w_1 M_{x1} + w_2 N_{x2} z_2 + w_2 M_{x2} \tag{3.12}$$

Substituting back Equations 3.4 into 3.12,

$$\begin{aligned}\overline{M}_x^c &= w_1(A_1^* \varepsilon_{x1}^o + B_1^* \kappa_{x1}) z_1 + w_1(B_1^* \varepsilon_{x1}^o + D_1^* \kappa_{x1}) + \\ &+ w_2(A_2^* \varepsilon_{x2}^o + B_2^* \kappa_{x2}) z_2 + w_2(B_2^* \varepsilon_{x2}^o + D_2^* \kappa_{x2})\end{aligned} \tag{3.13}$$

With aid of Equation 3.9, we have

$$\varepsilon_{x1}^o = z_1 \kappa_x^c \quad \textit{and} \quad \varepsilon_{x2}^o = z_2 \kappa_x^c \tag{3.14}$$

In addition, $\kappa_{x1} = \kappa_{x2} = \kappa_x^c$. Therefore,

$$\overline{M}_x^c = [w_1 A_1^* z_1^2 + w_1 B_1^* z_1 + w_1 B_1^* z_1 + w_1 D_1^* + w_2 A_2^* z_2^2 + w_2 B_2^* z_2 + w_2 B_2^* z_2 + w_2 D_2^*]\kappa_x^c \tag{3.15}$$

By definition, we have the equivalent bending stiffness of the whole structure expressed as shown below.

$$\boxed{\overline{D}_x = w_1 A_1^* z_1^2 + 2 w_1 B_1^* z_1 + w_1 D_1^* + w_2 A_2^* z_2^2 + 2 w_2 B_2^* z_2 + w_2 D_2^*} \tag{3.16}$$

3.2.4 Centroid

The centroid is the location where the summation of the moments of the cross-sectional area equal zero. The centroid can be calculated taking summation of moments of the axial loads acting on the centroids of each laminate and equating them to the total axial force acting on the centroid of the whole structure. Referring Figure 3.4, we obtain

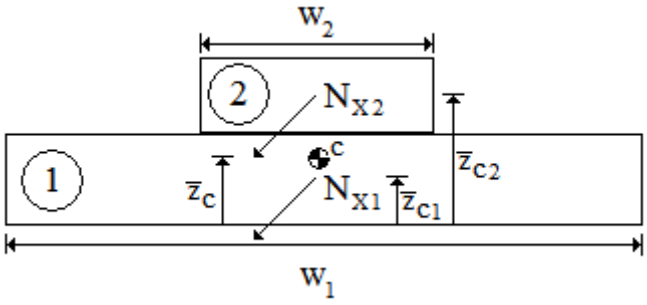

Figure 3.4 Axial force acting the centroids of each laminate

$$\bar{z}_{c1} N_{x1} w_1 + \bar{z}_{c2} N_{x2} w_2 = \bar{z}_c \overline{N}_x^c \tag{3.17}$$

Substituting Equation 3.4 and 3.7 into 3.17,

$$\bar{z}_c = \frac{\bar{z}_{c1}(A_1^* \varepsilon_{x1}^o + B_1^* \kappa_{x1}) w_1 + \bar{z}_{c2}(A_2^* \varepsilon_{x2}^o + B_2^* \kappa_{x2}) w_2}{w_1(A_1^* \varepsilon_{x1}^c + B_1^* \kappa_{x1}^c) + w_2(A_2^* \varepsilon_{x2}^c + B_2^* \kappa_{x2}^c)} \tag{3.18}$$

No curvatures of each laminate as well as the whole structure are induced because of all the forces are assumed to be acting on their centroid. Hence, we have $\kappa_{x1} = \kappa_{x2} = \kappa_x^c = 0$ resulting in $\varepsilon_{x1}^o = \varepsilon_{x2}^o = \varepsilon_x^c$. Consequently, Equation 3.18 becomes,

$$\boxed{\bar{z}_c = \frac{\bar{z}_{c1} w_1 A_1^* + \bar{z}_{c2} w_2 A_2^*}{w_1 A_1^* + w_2 A_2^*}} \tag{3.19}$$

This last equation gives the centroid position of the whole section as a function of the properties of the laminated beam and the laminated stiffener.

Another approach to calculate the centroid is based upon the axial forces acting on the mid-plane of each laminate plus the moment generate due to the translation of this force from the centroid to the mid-plane of the beam and stiffener (Fig. 3.5) As a result, the summation of moments becomes (Eq. 3.20),

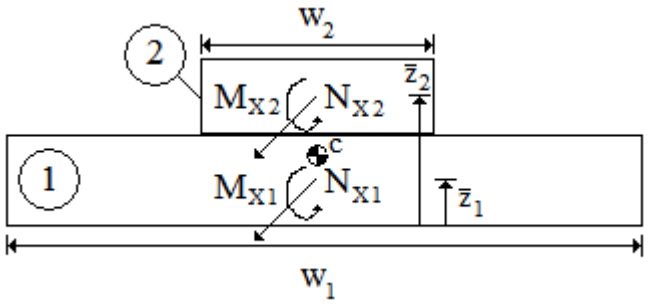

Figure 3.5 Axial forces and moments acting on the mid-plane of each laminate

$$\bar{z}_c \overline{N}_x^c = \bar{z}_1 N_{x1} w_1 + w_1 M_{x1} + \bar{z}_2 N_{x2} w_2 + w_2 M_{x2} \tag{3.20}$$

Substituting Equation 3.4 and 3.7 into 3.20,

$$\bar{z}_c = \frac{\bar{z}_1 (A_1^* \varepsilon_{x1}^o + B_1^* \kappa_{x1}) w_1 + w_1 (B_1^* \varepsilon_{x1}^o + D_1^* \kappa_{x1}) + \bar{z}_2 (A_2^* \varepsilon_{x2}^o + B_2^* \kappa_{x2}) w_2 + w_2 (B_2^* \varepsilon_{x2}^o + D_2^* \kappa_{x2})}{w_1 (A_1^* \varepsilon_{x1}^c + B_1^* \kappa_{x1}^c) + w_2 (A_2^* \varepsilon_{x2}^c + B_2^* \kappa_{x2}^c)} \tag{3.21}$$

As explained before, we have $\kappa_{x1} = \kappa_{x2} = \kappa_x^c = 0$, and $\varepsilon_{x1}^o = \varepsilon_{x2}^o = \varepsilon_x^c$. Consequently, Equation 3.21 becomes,

$$\boxed{\bar{z}_c = \frac{\bar{z}_1 A_1^* w_1 + w_1 B_1^* + \bar{z}_2 A_2^* w_2 + w_2 B_2^*}{w_1 A_1^* + w_2 A_2^*}} \tag{3.22}$$

Appendix B proof that Equation 3.22 reduces to Equation 3.19. Therefore, both are equivalent.

3.3 Results Comparison of Centroid Calculations

In this study, first was considered an isotropic material, aluminum was chosen with a Young Modulus of 10.498e6 psi and a Poisson's ratio of 0.33. After that, a composite material was used. The composite's properties were the following E_1=18.2e6 psi, E_2=E_3=1.41e6, v_{12}= v_{23}= v_{13}=0.27, and G_{12}=G_{23}=G_{13}=0.92e6 psi. The laminate consisted of 12 plies of 0.005 inches each one.

3.3.1 Isotropic Material

In order to validate the present method is necessary to evaluate an isotropic material because the answer can be calculated easily. An isotropic material rectangular cross-section is broken in two pieces as shown in Figure 3.6; therefore, it is possible to treat each piece like an independent laminate.

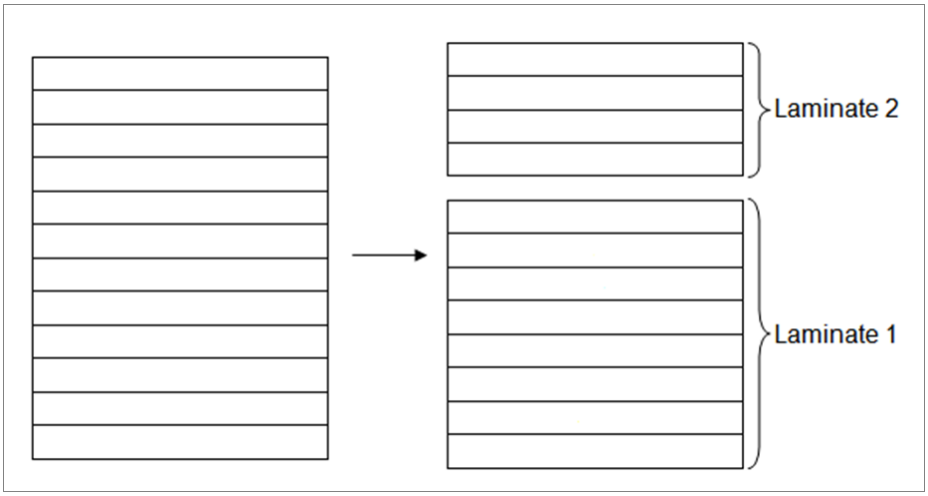

Figure 3.6 Isotropic Laminates

Table 3.1 lists the results of the centroid z_c calculated by three different methods. The results show excellent agreement each other. Equation 2.45 is the centroid calculated from lamination theory. On the other hand, Equation 3.6 is the centroid calculated through a modified lamination theory for composite beams.

Table 3.1 Results for isotropic material

	Present Method	Eq. 2-45	Diff %	Eq. 3-6	Diff %	Smeared Prop. Approach	Diff %
		$-b_{11}/d_{11}$		-b*/d*			
z_c [tply]	6.0000	6.0000	0.0	6.0000	0.0	6.0000	0.0

3.3.2 Symmetric Laminate

A symmetric laminate $[\pm 45_2/0_2]_S$ of graphite/epoxy is split into two pieces in three different cases as shown in Figure 3.7.

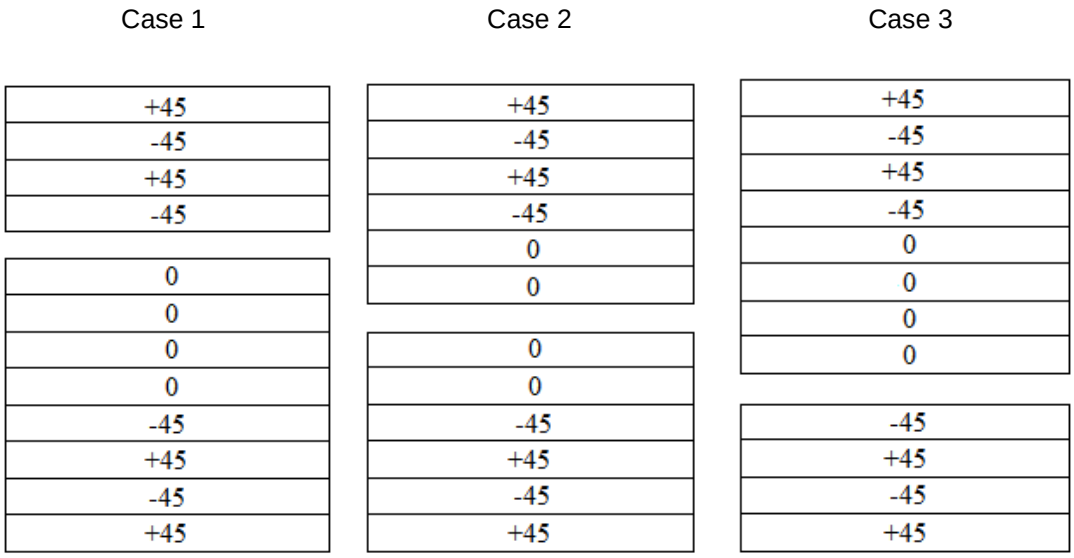

Figure 3.7 Composite Laminate $[\pm 45_2/0_2]_S$

The centroid calculations in terms of ply thickness are presented in the Table 3.2. The present method gives excellent results for symmetric and balanced laminate. On the other hand, the smeared property approach results are far.

Table 3.2 Results for Composite $[\pm 45_2/0_2]_s$

		Present Method	Eq. 2-45	Diff %	Eq. 3-6	Diff %	Smeared Prop. Approach	Diff %
			$-b_{11}/d_{11}$		-b*/d*			
Case 1	z_c [tply]	5.9970	6.0000	0.1	6.0000	0.1	5.1176	-14.7
Case 2	z_c [tply]	6.0000	6.0000	0.0	6.0000	0.0	6.0000	0.0
Case 3	z_c [tply]	6.0030	6.0000	-0.1	6.0000	-0.1	6.8824	14.6

3.3.3 Un-symmetric and Balanced Laminate

A layup $[\pm 45/0/90]_{3T}$ of un-symmetric laminate is going divided into two pieces, layer by layer as shown in Figure 3.8.

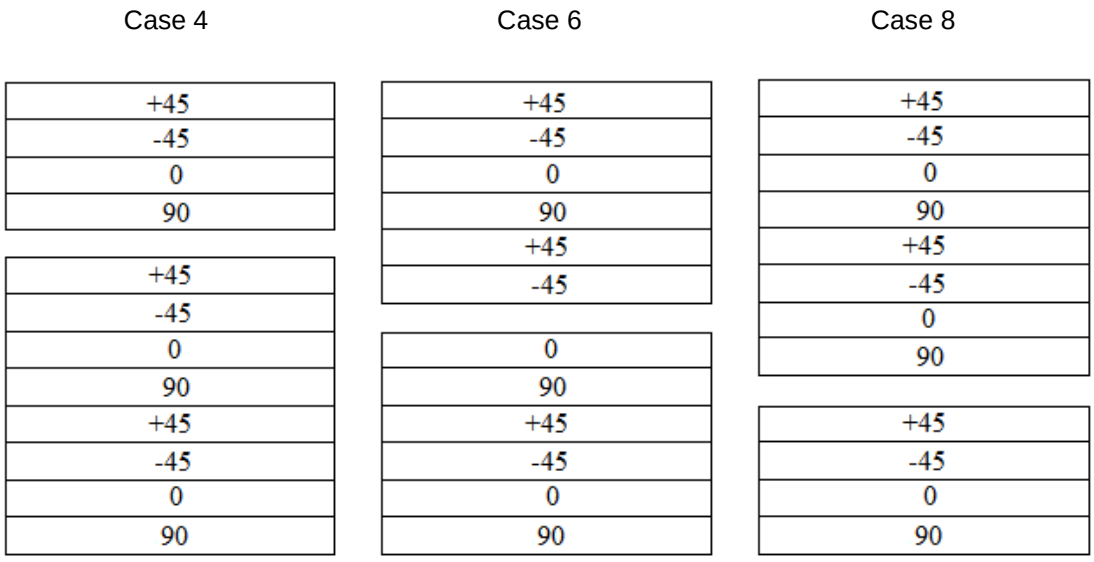

Figure 3.8 Three different case where the un-symmetric laminate

The first case (Table 3.3) was the top laminate containing just 1 ply and the bottom laminate containing 11 plies. The results listed in Table 3.3 indicate that a less than 2% difference of the calculated centroid is observed among the present, laminate and laminated beam methods. However, a smeared property method gives a slightly higher difference. It should be noted that the laminate is an un-symmetric but quasi-isotropic laminate. When the laminate is loaded, the curvature is induced. Using the smear property of laminate, the induced curvature is ignored. The results are also plotted in Figure 3.9.

Even though the beam of case 4 is identical to the stiffener in case 8 (and the beam in case 8 is identical as well as the stiffener in case 4), case 4 and 8 produce different results because the height of those beam and stiffener are different in each case.

Table 3.3 Results for un-symmetric laminate $[\pm 45/0/90]_{3T}$ ply by ply

Case #	Stiffener	Beam		Present Method	Eq. 2-45	Diff %	Eq. 3-6	Diff %	Smeared Prop. Approach	Diff %
	# plies	# plies			$-b_{11}/d_{11}$		$-b^*_{11}/d^*_{11}$			
1	1	11	z_c [tply]	5.7174	5.8261	1.9	5.8282	1.9	5.6558	-1.1
2	2	10	z_c [tply]	5.7284	5.8261	1.7	5.8282	1.7	5.3799	-6.1
3	3	9	z_c [tply]	5.7341	5.8261	1.6	5.8282	1.6	5.6399	-1.6
4	4	8	z_c [tply]	5.7144	5.8261	2.0	5.8282	2.0	5.8178	1.8
5	5	7	z_c [tply]	5.7761	5.8261	0.9	5.8282	0.9	5.6630	-2.0
6	6	6	z_c [tply]	5.8209	5.8261	0.1	5.8282	0.1	5.5842	-4.1
7	7	5	z_c [tply]	5.8204	5.8261	0.1	5.8282	0.1	6.5176	12.0
8	8	4	z_c [tply]	5.9257	5.8261	-1.7	5.8282	-1.6	6.1822	4.3
9	9	3	z_c [tply]	5.9249	5.8261	-1.7	5.8282	-1.6	5.9121	-0.2
10	10	2	z_c [tply]	5.8863	5.8261	-1.0	5.8282	-1.0	6.2861	6.8
11	11	1	z_c [tply]	5.8882	5.8261	-1.1	5.8282	-1.0	6.3987	8.7

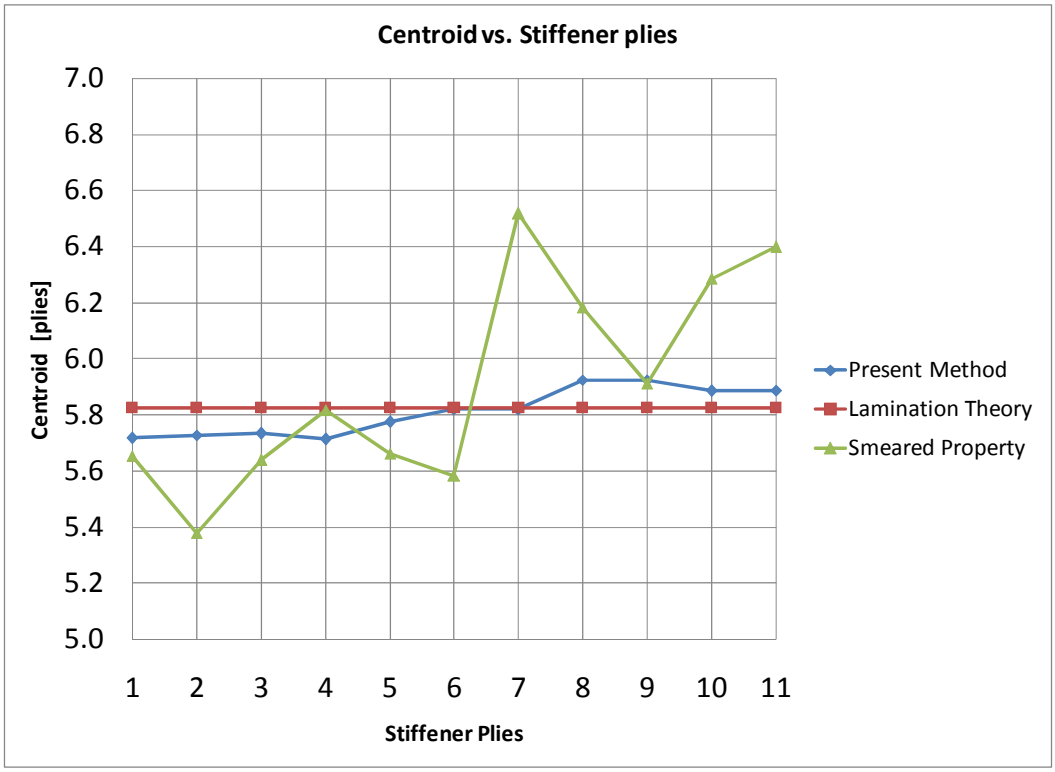

Figure 3.9 Plot of un-symmetric laminate $[\pm 45/0/90]_{3T}$ ply by ply results

3.3.4 Un-symmetric and Un-balanced Laminate

An un-balanced and un-symmetric $[15_2/30_2/45_2/60_2/75_2/90_2]_T$ laminate was considered. Three different cases are considered as shown in Figure 3.10.

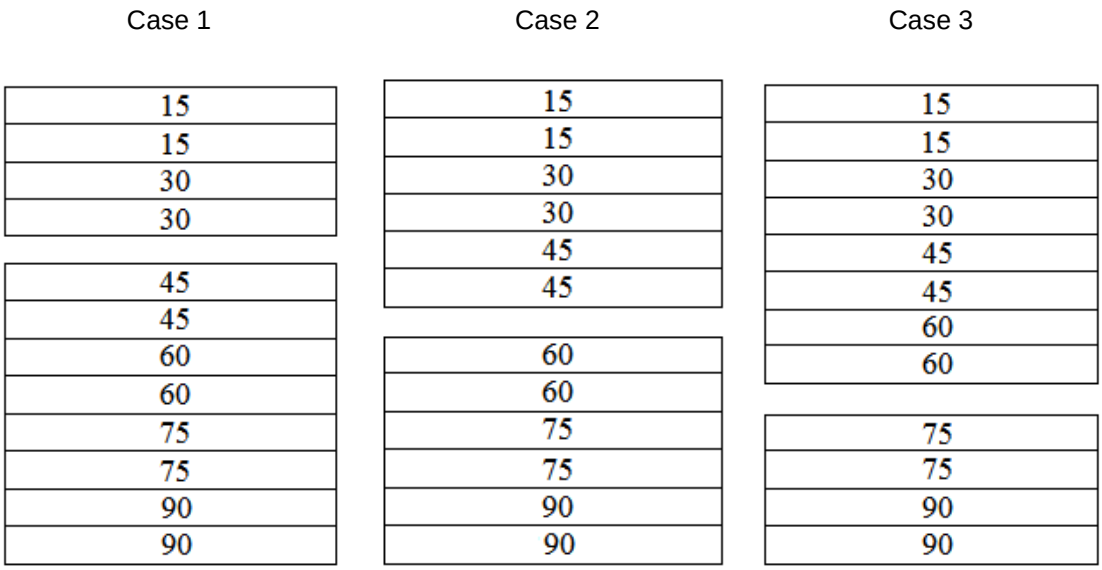

Figure 3.10 Three different case for un-balanced laminate

Once again, the present method gives results close to the laminate and laminated beam methods compared with the smear method (Table 3.4). It should be noted that the smeared property approach neglects the shear deformation and curvature of the laminates; as results, the high percentage difference from the other two methods.

Table 3.4 Results for un-balanced $[15_2/30_2/45_2/60_2/75_2/90_2]_T$ laminate

		Present Method	**Eq. 2-45**	**Diff %**	**Eq. 3-6**	**Diff %**	**Smeared Prop. Approach**	**Diff %**
			$-b_{11}/d_{11}$		**-b*/d***			
Case 1	z_c [tply]	8.3940	8.4131	0.2	8.9460	6.6	7.7195	-8.0
Case 2	z_c [tply]	8.5700	8.4131	-1.8	8.9460	4.4	7.2944	-14.9
Case 3	z_c [tply]	8.7234	8.4131	-3.6	8.9460	2.6	6.8356	-21.6

3.4 Ply Stress Calculations

The stresses in each laminate can be calculated through the following procedure.

$$\begin{aligned} N_{x1} &= A_1^*(\varepsilon_x^c + z_1\kappa_x^c) + B_1^*\kappa_{x1} \\ M_{x1} &= B_1^*(\varepsilon_x^c + z_1\kappa_x^c) + D_1^*\kappa_{x1} \end{aligned} \quad \textit{or} \quad \begin{pmatrix} N_{x1} \\ M_{x1} \end{pmatrix} = \begin{bmatrix} A_1^* & B_1^* + z_1A_1^* \\ B_1^* & D_1^* + z_1B_1^* \end{bmatrix} \begin{pmatrix} \varepsilon_x^c \\ \kappa_x^c \end{pmatrix} \tag{3.23}$$

where ε_x^c *and* κ_x^c *can be obtained from the stiffnesses,*

$$\varepsilon_x^c = \frac{\overline{N}_x^c}{\overline{A}_x} \qquad \text{and} \qquad \kappa_x^c = \frac{\overline{M}_x^c}{\overline{D}_x} \tag{3.24}$$

To calculate the strains in the mid-plane of laminate 1,

$$\begin{pmatrix} \varepsilon_x^o \\ \varepsilon_y^o \\ \gamma_{xy}^o \\ \kappa_x \\ \kappa_y \\ \kappa_{xy} \end{pmatrix}_1 = \begin{bmatrix} a_{11} & b_{11} & b_{16} \\ a_{21} & b_{21} & b_{26} \\ a_{61} & b_{61} & b_{66} \\ b_{11} & d_{11} & d_{16} \\ b_{12} & d_{21} & d_{26} \\ b_{16} & d_{61} & d_{66} \end{bmatrix}_1 \begin{pmatrix} N_{x1} \\ M_{x1} \\ M_{xy1} \end{pmatrix}$$

where $M_{xy1} = -\frac{1}{(d_{66})_1}[(b_{16})_1 N_{x1} + (d_{61})_1 M_{x1}]$, *since* $\kappa_{xy1} = 0$.

And to calculate the strain in each ply of laminate 1,

$$\begin{pmatrix} \varepsilon_x \\ \varepsilon_y \\ \gamma_{xy} \end{pmatrix}_{k1} = \begin{pmatrix} \varepsilon_x^o \\ \varepsilon_y^o \\ \gamma_{xy}^o \end{pmatrix}_1 + z_{k1} \begin{pmatrix} \kappa_x \\ \kappa_y \\ \kappa_{xy} \end{pmatrix}_1$$

Finally, to calculate the stresses in each ply of laminate 1,

$$\begin{pmatrix} \sigma_x \\ \sigma_y \\ \tau_{xy} \end{pmatrix}_{k1} = \begin{bmatrix} & \overline{Q}_{k1} & \\ & & \end{bmatrix} \begin{pmatrix} \varepsilon_x \\ \varepsilon_y \\ \gamma_{xy} \end{pmatrix}_{k1}$$

Similarly, the equation for laminate 2 can be determined.

3.5 Finite Element Model

A model was built in ANSYS to simulate the composite laminates. Two laminates of 10 inches long and 0.5 inches wide were bonded together. The bottom one constituted by 8 plies and the top one of 4 plies. So this was equivalent of a total of 12 plies laminate (since both widths were the same). Each ply with a thickness of 0.005 inches.

The element used was solid46, a 3D block element with 8 nodes and 3 degrees of freedom per node. The mesh generated was 320 elements through the length, 16 through the width, and 2 per ply. This gives a total of 136,425 nodes.

Two cases were considered an axial load and a moment were applied. An axial load of 1 lb was applied at the centroid of the cross-section (Figure 3.11).

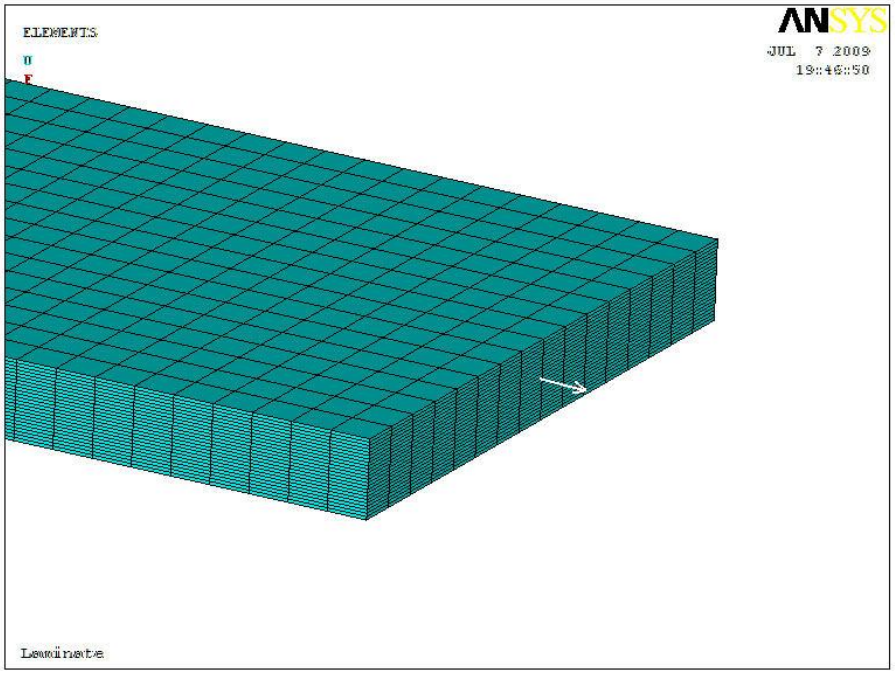

Figure 3.11 $\overline{N}_x^c$ applied to the centroid of the cross-section

The other case was the moment applied. A pair of forces were assigned to generate the moment; each force being a 1 lb and acting one ply away from the centroid of the cross-section

(that is 0.005 inches). This generates a total moment of 0.01 lb-in. A typical mesh for this case is shown in Figure 3.12.

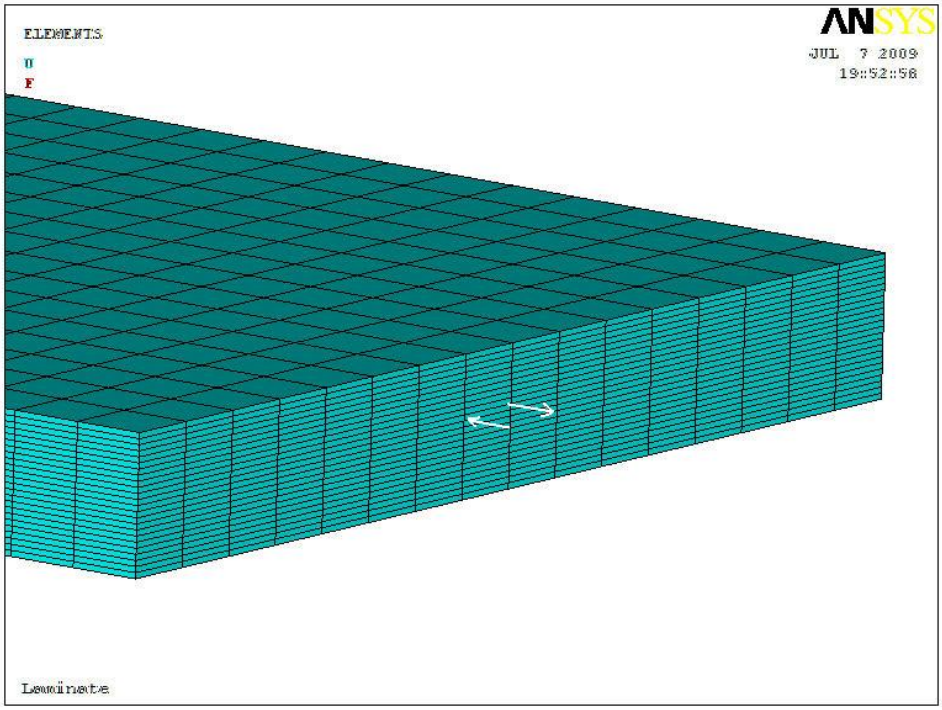

Figure 3.12 Two forces generating $\overline{M}_x^c$

The boundary conditions were applied as follows (Fig. 3.13): the whole plane on the other side of the laminate were constricted in the x-direction (axial direction). The middle of the laminate in the y-direction was constrained in that direction (U_y=0). And the location of the centroid in the z-direction was constrained in that direction (U_z=0) as well.

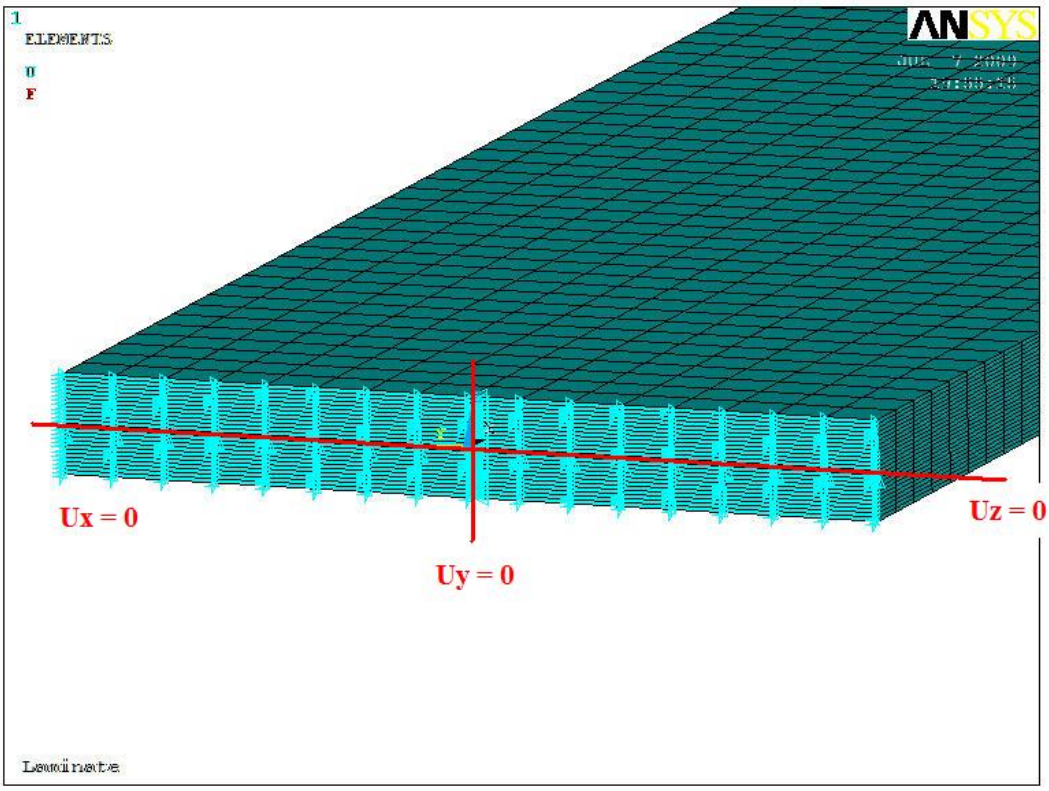

Figure 3.13 Applied Boundary Conditions

Aluminum was chosen with a Young Modulus of 10.498 Msi and a Poisson ratio of 0.33. After that, a composite material was used. The composite's properties were the following E_1=18.2e6 psi, E_2=E_3=1.41e6, v_{12}= v_{23}= v_{13}=0.27, G_{12}=G_{23}=G_{13}=0.92e6 psi, and t_{ply}=0.005 in.

Three cases of composite material models were simulated. The laminates $[0_6]_S$, $[\pm 45_2/0_2]_s$ and $[\pm 45/0/90]_{3T}$ were studied.

3.6 Finite Element Results

3.6.1 Axial and Bending Stiffnesses obtained from FEM

The axial stiffnesses were calculated from the FEM model by the following equation.

$$\overline{A}_x = \frac{FL}{2(U_{x|at\ x=L/2})}$$

To avoid distortions of the results by the boundary conditions or the applied load, the results were read half way through the length of the beam; that is at L/2. And F is the applied load.

The bending stiffnesses were calculated from the FEM model by first determining the curvature of the beam, κ_x^c, and then dividing the applied moment by it.

$$\overline{M}_x^c = \overline{D}_x \kappa_x^c \quad \rightarrow \quad \overline{D}_x = \frac{\overline{M}_x^c}{\kappa_x^c}$$

3.6.2 Centroid Locations

The centroids z_c were calculated using Equation 3.22. The axial stiffnesses were calculated through Equation 3.11. Finally, the bending stiffnesses were calculated using Equation 3.16. The units of the centroid z_c are in numbers of ply thicknesses since its value was divided by that thickness.

As it was explained before, the centroid is defined as the location where an axial load does not cause a change in curvature and a bending moment does not produce axial strain. In other words, the load acting at the centroid decouples the structural response between axial extension and bending. Therefore, it was checked that for an applied axial load at the centroid there were no bending (curvature) and for an applied moment at the centroid of the cross-section, there were no axial displacement.

Finally, all the axial displacements (for the axial stiffness and centroid) and z-vertical displacements (for the bending stiffness and centroid) were read at the centroid of the cross-section. The mesh was done extremely careful so there was nodes presents in the centroids of each case. For the first three cases there was not major problem since the centroid of the whole cross-section corresponds with a line between plies since all these three cases the whole cross-section have symmetric layups. However, for the last case, the whole cross-section layup were un-symmetric, so special care was needed in order to ensure the mesh have node in the centroid of the cross-section.

3.6.3 Comparison of Laminate Stiffnesses

Four cases were considered in this study. They are isotropic material, all 0° ply laminate, symmetric and balanced laminate, and un-symmetric laminate in the overlapped region. All of the results are listed in Table 3.5.

Table 3.5 Comparison of the axial and bending stiffnesses for different cases

		units	Present Method	FEM	Diff%	Smeared Prop. Approach	Diff%	Theoretical Solution	Diff%
ISO	$\overline{A}_x$	[lb]	314,940	314,941	0.0	314,940	0.0	314,940	0.0
	$\overline{D}_x$	[lb-in²]	94.48	94.51	0.0	94.48	0.0	94.48	0.0
$[0_8]_s$	$\overline{A}_x$	[lb]	546,000	546,001	0.0	546,000	0.0	546,000	0.0
	$\overline{D}_x$	[lb-in²]	163.80	163.85	0.0	163.80	0.0	163.80	0.0
$[\pm 45_2/0_2]_s$	$\overline{A}_x$	[lb]	245,084	246,475	0.6	246,690	0.7	N/A	
	$\overline{D}_x$	[lb-in²]	33.14	33.08	-0.2	74.01	123.3		
$[\pm 45/0/90]_{3T}$	$\overline{A}_x$	[lb]	206,856	214,335	3.5	214,797	3.8	N/A	
	$\overline{D}_x$	[lb-in²]	57.77	60.90	5.1	64.44	11.5		

First, to confirm the procedure and equations was correct, an isotropic material was used to be able to calculate the centroid and axial and bending stiffnesses by close-from theoretical solution. Those results were also compared to the FEM model to validate the model as well. The results matched perfectly giving confidence that the FEM model and equations were right.

The next step was to compare those equations with the composite FEM model since, unfortunately, there is not close-form theoretical solution. The first case was all the plies with an angle ply of 0°. The bottom laminate consists of 8 plies and the top laminate consists of 4 plies. The results are extremely good.

The next step was to consider a symmetric total laminate. Strictly speaking, because two laminate are being bonded together, neither of those laminates were symmetric; however, when bonded together the layup of the total cross-section is symmetric. Once again the bottom laminate had 8 plies and the top laminate had 4 plies. In this case, the bottom laminate layup was

$[0_4/\text{-}45/45/\text{-}45/+45]_T$ and the top laminate layup was $[\pm 45_2]_T$. The results are in excellent agreement.

Finally, in order to try to cover all the possible cases, the last selection was to consider an un-symmetric laminate (once again when bonded together both laminates). That is the bottom laminate with a layup of $[\pm 45/0/90]_{2T}$ and the top laminate with a layup of and $[\pm 45/0/90]_T$. For this case the results were 5% difference between the present and finite element method.

3.6.4 Ply Stresses of Isotropic Material

3.6.4.1 Beam Laminate under Axial Load, $\overline{N}_x^c$

Figure 3.14 through 3.16 show the stresses through the cross-section of two isotropic laminates bonded together subjected to an axial load. The horizontal axis represents each ply of the whole cross-section. The first 8 plies are the bottom laminate and the last 4 plies are the laminate at the top, for a total of 12 plies. The applied axial load was 1 lb; however, in composite notation, this load must be divided by the width of the laminate which is 0.5 inches. Therefore, applied load in composite notation is $N_x^c = 2\,lb/in$.

For theoretical solution it is known that $\sigma_x=F_x/A$. The total height cross-section is 8 plies multiplied by 0.005 inches which is the thickness of each ply plus 4 plies multiplied by 0.005 inches; that is 12x0.005=0.06 inches. Therefore, the area of the total cross-section is 0.03 in^2 and the axial stress is 33.33 psi which confirms the results from the FEM model (Figure 3.14). The transversal and shear stresses are decoupled from axial extension for isotropic materials; therefore, as expected $\sigma_y=0$ and $\tau_{xy}=0$ (Figures 3.15 and 3.16).

All of the ply stresses calculated by three different methods are listed in Table 3.6.

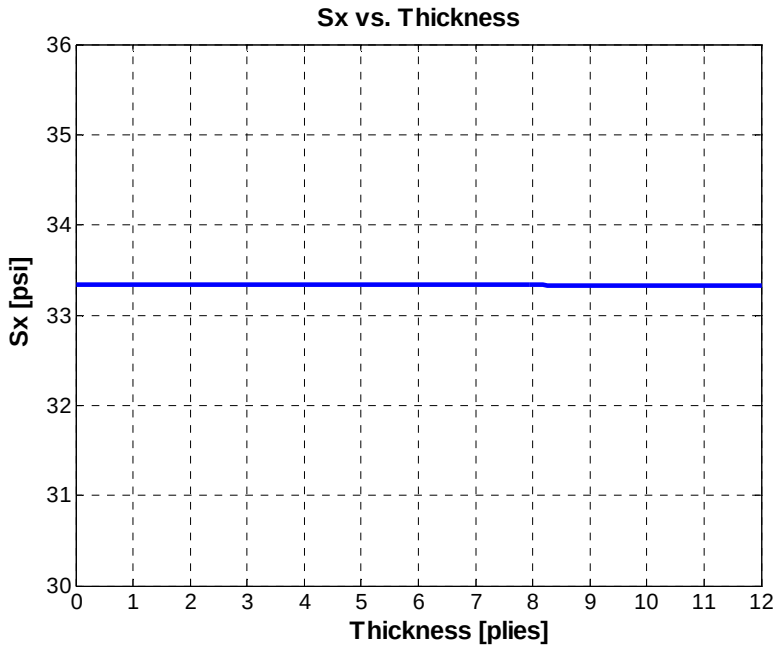

Figure 3.14 FEM axial stress due to $\overline{N}_x^c$ in isotropic material

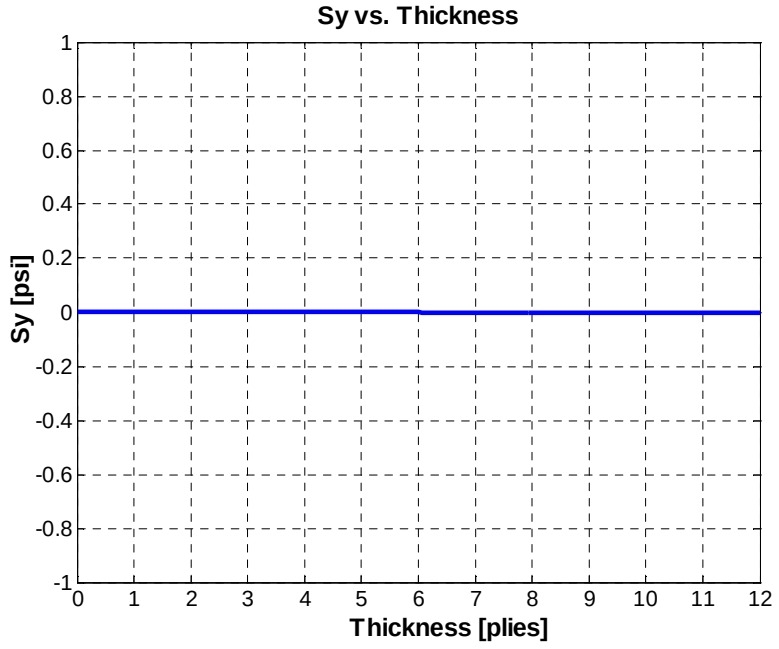

Figure 3.15 FEM transversal stress due to $\overline{N}_x^c$ in isotropic material

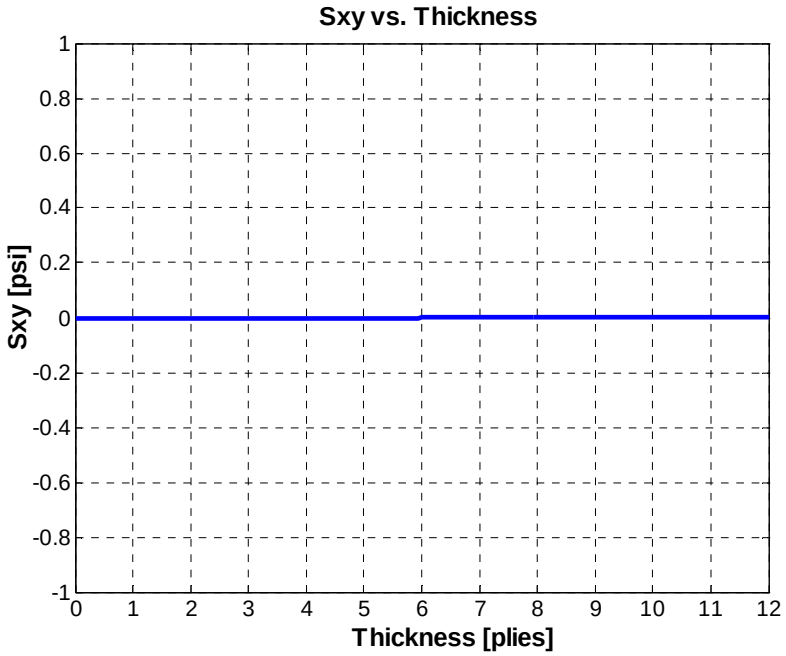

Figure 3.16 FEM shear stress due to $\overline{N}_x^c$ in isotropic material

Table 3.6 Stresses due to $\overline{N}_x^c$ applied to isotropic material

			σ_x		σ_y		τ_{xy}	
			[psi]	%Diff	[psi]	%Diff	[psi]	%Diff
ply #12	ISO	Lamination Theory	33.33		0.00		0.00	
		FEM	33.33	0.0	0.00	0.0	0.00	0.0
		Prensent Method	33.33	0.0	0.00	0.0	0.00	0.0
ply #11	ISO	Lamination Theory	33.33		0.00		0.00	
		FEM	33.33	0.0	0.00	0.0	0.00	0.0
		Prensent Method	33.33	0.0	0.00	0.0	0.00	0.0
ply #10	ISO	Lamination Theory	33.33		0.00		0.00	
		FEM	33.33	0.0	0.00	0.0	0.00	0.0
		Prensent Method	33.33	0.0	0.00	0.0	0.00	0.0
ply #9	ISO	Lamination Theory	33.33		0.00		0.00	
		FEM	33.33	0.0	0.00	0.0	0.00	0.0
		Prensent Method	33.33	0.0	0.00	0.0	0.00	0.0
ply #8	ISO	Lamination Theory	33.33		0.00		0.00	
		FEM	33.33	0.0	0.00	0.0	0.00	0.0
		Prensent Method	33.33	0.0	0.00	0.0	0.00	0.0
ply #7	ISO	Lamination Theory	33.33		0.00		0.00	
		FEM	33.33	0.0	0.00	0.0	0.00	0.0
		Prensent Method	33.33	0.0	0.00	0.0	0.00	0.0
ply #6	ISO	Lamination Theory	33.33		0.00		0.00	
		FEM	33.33	0.0	0.00	0.0	0.00	0.0
		Prensent Method	33.33	0.0	0.00	0.0	0.00	0.0
ply #5	ISO	Lamination Theory	33.33		0.00		0.00	
		FEM	33.33	0.0	0.00	0.0	0.00	0.0
		Prensent Method	33.33	0.0	0.00	0.0	0.00	0.0
ply #4	ISO	Lamination Theory	33.33		0.00		0.00	
		FEM	33.33	0.0	0.00	0.0	0.00	0.0
		Prensent Method	33.33	0.0	0.00	0.0	0.00	0.0
ply #3	ISO	Lamination Theory	33.33		0.00		0.00	
		FEM	33.33	0.0	0.00	0.0	0.00	0.0
		Prensent Method	33.33	0.0	0.00	0.0	0.00	0.0
ply #2	ISO	Lamination Theory	33.33		0.00		0.00	
		FEM	33.33	0.0	0.00	0.0	0.00	0.0
		Prensent Method	33.33	0.0	0.00	0.0	0.00	0.0
ply #1	ISO	Lamination Theory	33.33		0.00		0.00	
		FEM	33.33	0.0	0.00	0.0	0.00	0.0
		Prensent Method	33.33	0.0	0.00	0.0	0.00	0.0
	Force Balance	Lamination Theory	400.00	x0.0025=	1.0000			
		FEM	400.01	x0.0025=	1.0000			
		Present Method	400.00	x0.0025=	1.0000			

To check on the force balance, the summation of all the stresses was calculated and listed at the bottom of each table. Then they were multiplied by the area of each ply (0.0025 in^2) to obtain the total force (Table 3.6).

The present method results match perfectly with the FEM and the lamination theory results, which validates the new method and FEM model.

3.6.4.2 Beam Laminate under Bending Moment, $\overline{M}_x^c$

Now for the same isotropic bonded laminates, a moment is applied at the centroid of the whole cross-section. This moment is generated by a pair of axial forces acting on a distance of one ply of the centroid each one in different directions. The total moment applied is 2x(1lb)x(0.005in)=0.01lb-in. Just like before, the transversal and shear stresses are decoupled from bending for isotropic materials; therefore, as expected σ_y=0 and τ_{xy}=0 (Figures 3.18 and 3.19). On the other hand, the axial stress is a linear function from the bottom to the top of the cross-section (Figure 3.17). The maximum axial stress is $\sigma_{x,max}$=Mc/I; that is, $\sigma_{x,max}$= (0.01lb_in)(6x0.005in)/(1/12x0.5inx(12X0.005in)^3)= 33.33 psi, this is exactly the output of the FEM simulation (Figure 3.17). All of the stresses calculated by three different methods are tabulated in Table 3.7.

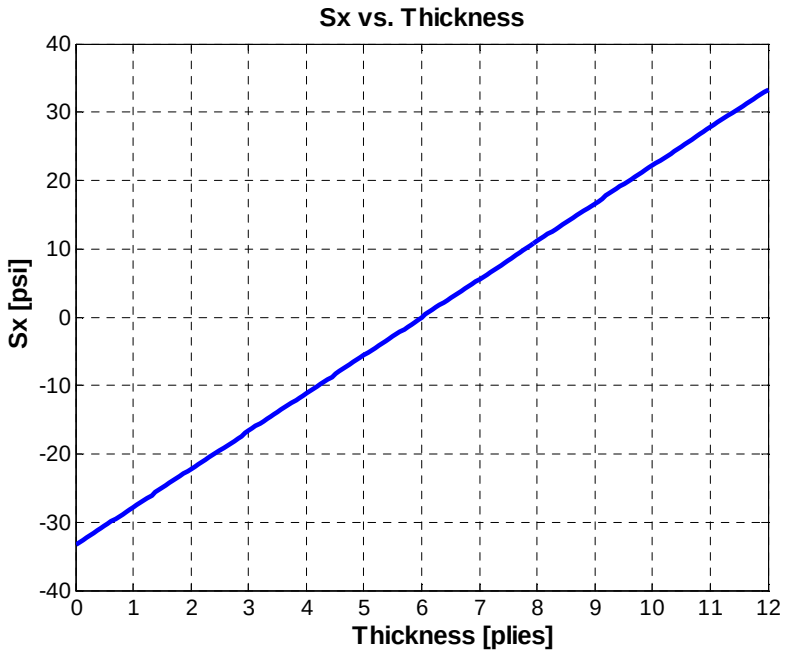

Figure 3.17 FEM axial stress due to $\overline{M}_x^c$ in isotropic material

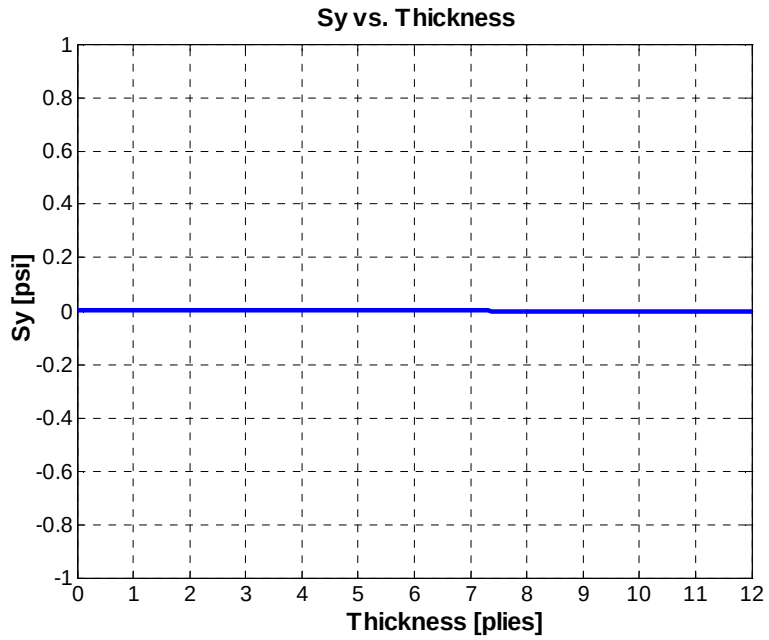

Figure 3.18 FEM transversal stress due to $\overline{M}_x^c$ in isotropic material

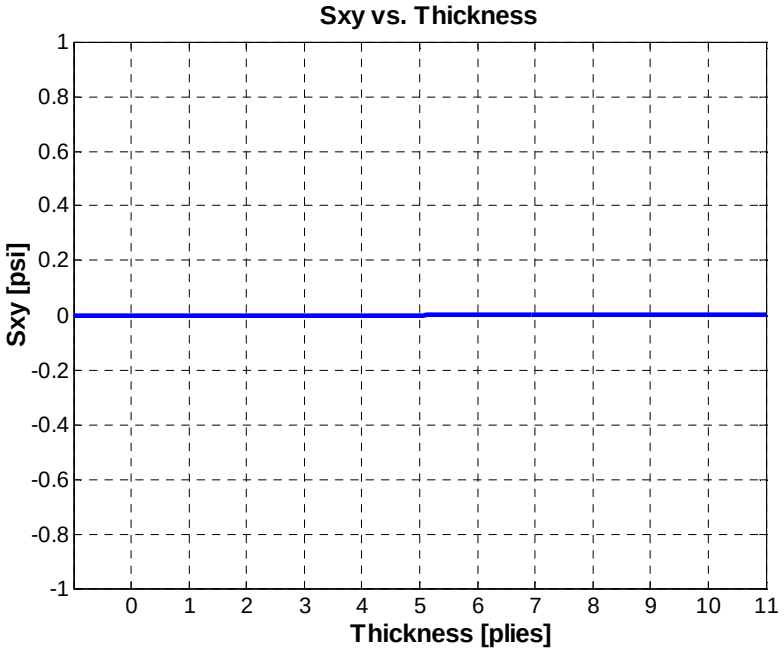

Figure 3.19 FEM shear stress due to $\overline{M}_x^c$ in isotropic material

The results are listed in Table 3.7.

Table 3.7 Stresses due to $\overline{M}_x^c$ applied to isotropic material

			σ_x		σ_y		τ_{xy}	
			[psi]	%Diff	[psi]	%Diff	[psi]	%Diff
ply #12	ISO	Lamination Theory	30.56		0.00		0.00	
		FEM	30.56	0.0	0.00	0.0	0.00	0.0
		Prensent Method	30.56	0.0	0.00	0.0	0.00	0.0
ply #11	ISO	Lamination Theory	25.00		0.00		0.00	
		FEM	25.00	0.0	0.00	0.0	0.00	0.0
		Prensent Method	25.00	0.0	0.00	0.0	0.00	0.0
ply #10	ISO	Lamination Theory	19.44		0.00		0.00	
		FEM	19.45	0.0	0.00	0.0	0.00	0.0
		Prensent Method	19.44	0.0	0.00	0.0	0.00	0.0
ply #9	ISO	Lamination Theory	13.89		0.00		0.00	
		FEM	13.89	0.0	0.00	0.0	0.00	0.0
		Prensent Method	13.89	0.0	0.00	0.0	0.00	0.0
ply #8	ISO	Lamination Theory	8.33		0.00		0.00	
		FEM	8.33	0.0	0.00	0.0	0.00	0.0
		Prensent Method	8.33	0.0	0.00	0.0	0.00	0.0
ply #7	ISO	Lamination Theory	2.78		0.00		0.00	
		FEM	2.78	0.0	0.00	0.0	0.00	0.0
		Prensent Method	2.78	0.0	0.00	0.0	0.00	0.0
ply #6	ISO	Lamination Theory	-2.78		0.00		0.00	
		FEM	-2.78	0.0	0.00	0.0	0.00	0.0
		Prensent Method	-2.78	0.0	0.00	0.0	0.00	0.0
ply #5	ISO	Lamination Theory	-8.33		0.00		0.00	
		FEM	-8.33	0.0	0.00	0.0	0.00	0.0
		Prensent Method	-8.33	0.0	0.00	0.0	0.00	0.0
ply #4	ISO	Lamination Theory	-13.89		0.00		0.00	
		FEM	-13.89	0.0	0.00	0.0	0.00	0.0
		Prensent Method	-13.89	0.0	0.00	0.0	0.00	0.0
ply #3	ISO	Lamination Theory	-19.44		0.00		0.00	
		FEM	-19.45	0.0	0.00	0.0	0.00	0.0
		Prensent Method	-19.44	0.0	0.00	0.0	0.00	0.0
ply #2	ISO	Lamination Theory	-25.00		0.00		0.00	
		FEM	-25.00	0.0	0.00	0.0	0.00	0.0
		Prensent Method	-25.00	0.0	0.00	0.0	0.00	0.0
ply #1	ISO	Lamination Theory	-30.56		0.00		0.00	
		FEM	-30.56	0.0	0.00	0.0	0.00	0.0
		Prensent Method	-30.56	0.0	0.00	0.0	0.00	0.0

All the axial, transversal, and shear stresses from lamination theory match perfectly with those from the FEM model and the present method.

3.6.5 Ply Stresses of 0° Laminate

3.6.5.1 $\overline{N}_x^c$ acting on the $[0_4]_S$ and $[0_2]_S$ of parent and stiffener

Repeating the same procedure but this time instead of using an isotropic material, a composite material was used. For this first try with composites, all the plies were chosen to be at an angle ply of 0° to avoid any shear deformation or other undesired effects. Therefore, the transversal and shear stresses are decoupled from axial extension; that is why $\sigma_y=0$ and $\tau_{xy}=0$ were expected (Fig. 3.21 and 3.22). Once again the axial stress (Fig. 3.20) can be calculated as before $\sigma_x=F_x/A=33.33$psi, just like the FEM model output.

The results listed in Table 3.8.

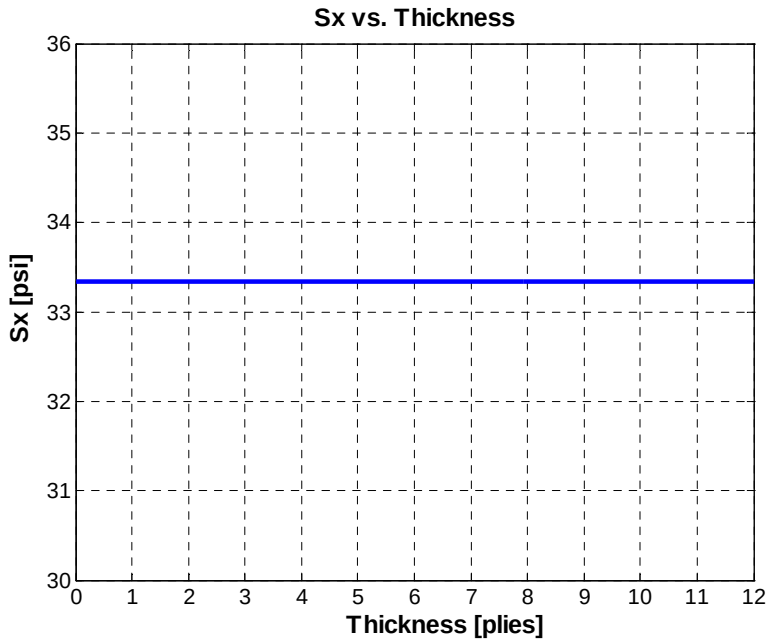

Figure 3.20 FEM axial stress due to $\overline{N}_x^c$ in $[0_4]_S$ and $[0_2]_S$ of parent and stiffener

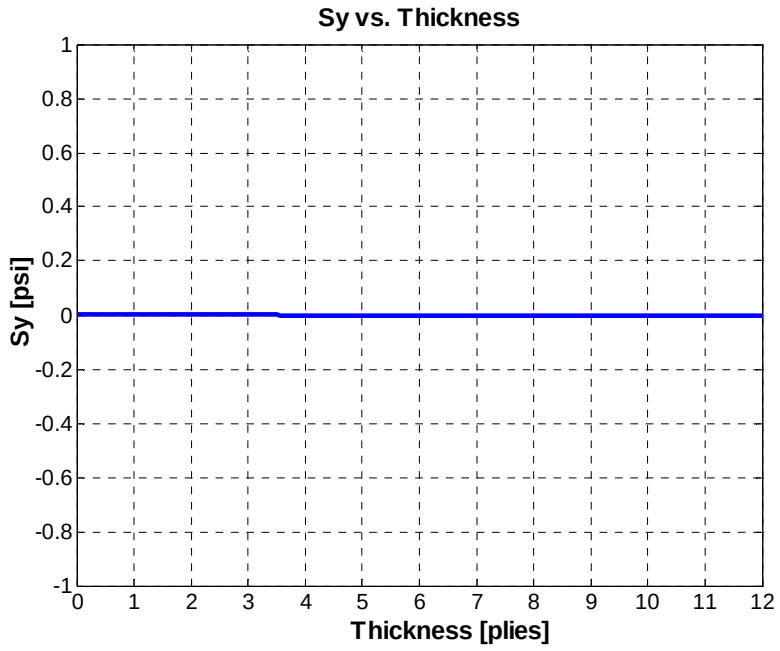

Figure 3.21 FEM transverse stress due to $\overline{N}_x^c$ in $[0_4]_S$ and $[0_2]_S$ of parent and stiffener

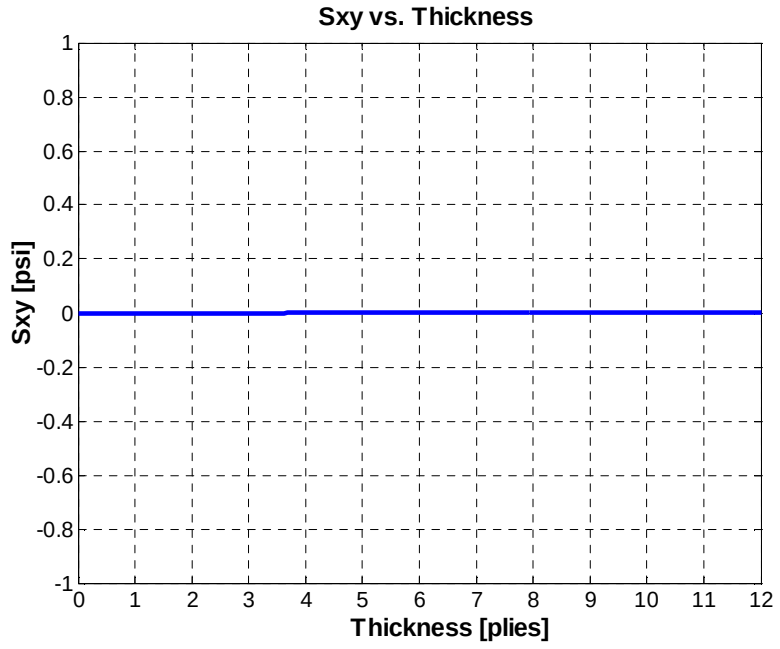

Figure 3.22 FEM shear stress due to $\overline{N}_x^c$ in $[0_4]_S$ and $[0_2]_S$ of parent and stiffener

Table 3.8 Stresses due to $\overline{N}_x^c$ applied to $[0_4]_S$ and $[0_2]_S$ of parent and stiffener

			σ_x		σ_y		τ_{xy}	
			[psi]	%Diff	[psi]	%Diff	[psi]	%Diff
ply #12	0	Lamination Theory	33.33		0.00		0.00	
		FEM	33.33	0.0	0.00	0.0	0.00	0.0
		Prensent Method	33.33	0.0	0.00	0.0	0.00	0.0
ply #11	0	Lamination Theory	33.33		0.00		0.00	
		FEM	33.33	0.0	0.00	0.0	0.00	0.0
		Prensent Method	33.33	0.0	0.00	0.0	0.00	0.0
ply #10	0	Lamination Theory	33.33		0.00		0.00	
		FEM	33.33	0.0	0.00	0.0	0.00	0.0
		Prensent Method	33.33	0.0	0.00	0.0	0.00	0.0
ply #9	0	Lamination Theory	33.33		0.00		0.00	
		FEM	33.33	0.0	0.00	0.0	0.00	0.0
		Prensent Method	33.33	0.0	0.00	0.0	0.00	0.0
ply #8	0	Lamination Theory	33.33		0.00		0.00	
		FEM	33.33	0.0	0.00	0.0	0.00	0.0
		Prensent Method	33.33	0.0	0.00	0.0	0.00	0.0
ply #7	0	Lamination Theory	33.33		0.00		0.00	
		FEM	33.33	0.0	0.00	0.0	0.00	0.0
		Prensent Method	33.33	0.0	0.00	0.0	0.00	0.0
ply #6	0	Lamination Theory	33.33		0.00		0.00	
		FEM	33.33	0.0	0.00	0.0	0.00	0.0
		Prensent Method	33.33	0.0	0.00	0.0	0.00	0.0
ply #5	0	Lamination Theory	33.33		0.00		0.00	
		FEM	33.33	0.0	0.00	0.0	0.00	0.0
		Prensent Method	33.33	0.0	0.00	0.0	0.00	0.0
ply #4	0	Lamination Theory	33.33		0.00		0.00	
		FEM	33.33	0.0	0.00	0.0	0.00	0.0
		Prensent Method	33.33	0.0	0.00	0.0	0.00	0.0
ply #3	0	Lamination Theory	33.33		0.00		0.00	
		FEM	33.33	0.0	0.00	0.0	0.00	0.0
		Prensent Method	33.33	0.0	0.00	0.0	0.00	0.0
ply #2	0	Lamination Theory	33.33		0.00		0.00	
		FEM	33.33	0.0	0.00	0.0	0.00	0.0
		Prensent Method	33.33	0.0	0.00	0.0	0.00	0.0
ply #1	0	Lamination Theory	33.33		0.00		0.00	
		FEM	33.33	0.0	0.00	0.0	0.00	0.0
		Prensent Method	33.33	0.0	0.00	0.0	0.00	0.0
	Force Balance	Lamination Theory	400.00	x0.0025=	1.0000			
		FEM	400.01	x0.0025=	1.0000			
		Present Method	400.00	x0.0025=	1.0000			

The results agree perfectly. In addition, a force balanced check was done to make sure all the summation of stresses in the cross-section equate the applied force so there is equilibrium. It is shown that the force balanced for the three methods ($\overline{N}_x^c = 1\,lb$).

3.6.5.2 $\overline{M}_x^c$ acting on the $[0_4]_S$ and $[0_2]_S$ of parent and stiffener

For the bending case the results are what was expected; $\sigma_y=0$ and $\tau_{xy}=0$ (Figure 3.24 and 3.25). And for the axial stress $\sigma_{x,max}=Mc/I=33.33$ psi (Figure 3.23).

All the stresses are listed in Table 3.9.

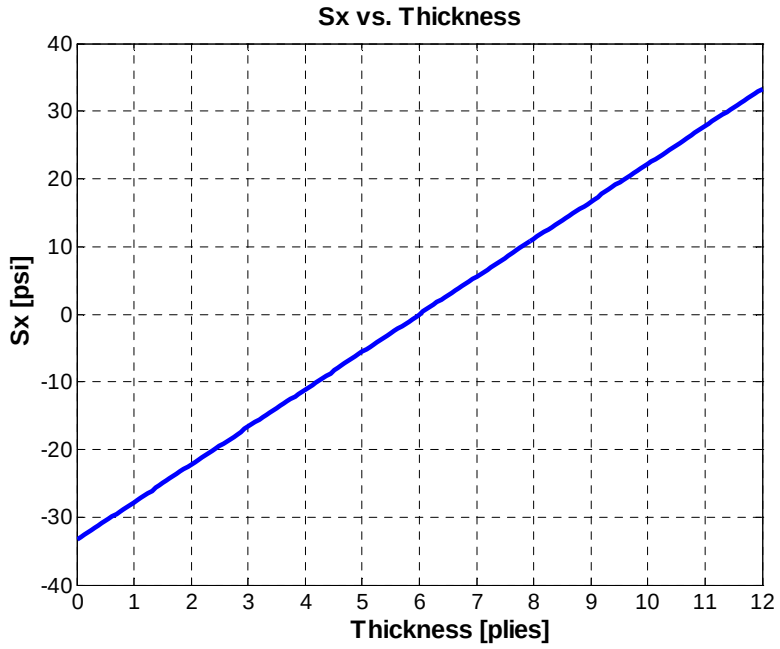

Figure 3.23 FEM axial stress due to $\overline{M}_x^c$ in $[0_4]_S$ and $[0_2]_S$ of parent and stiffener

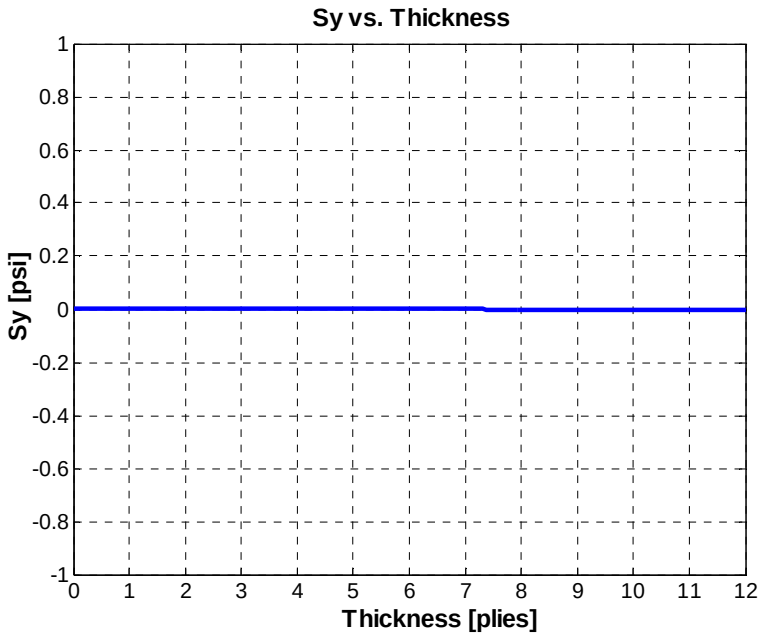

Figure 3.24 FEM transverse stress due to $\overline{M}_x^c$ in $[0_4]_S$ and $[0_2]_S$ of parent and stiffener

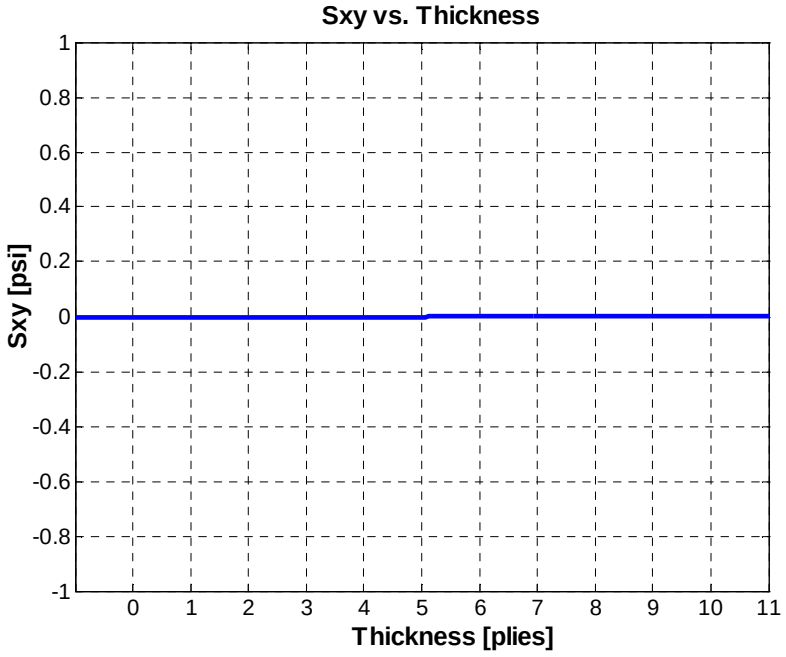

Figure 3.25 FEM shear stress due to $\overline{M}_x^c$ in $[0_4]_S$ and $[0_2]_S$ of parent and stiffener

Table 3.9 Stresses due to $\overline{M}_x^c$ applied to $[0_4]_S$ and $[0_2]_S$ of parent and stiffener

			σ_x		σ_y		τ_{xy}	
			[psi]	%Diff	[psi]	%Diff	[psi]	%Diff
ply #12	0	Lamination Theory	30.56		0.00		0.00	
		FEM	30.56	0.0	0.00	0.0	0.00	0.0
		Prensent Method	30.56	0.0	0.00	0.0	0.00	0.0
ply #11	0	Lamination Theory	25.00		0.00		0.00	
		FEM	25.00	0.0	0.00	0.0	0.00	0.0
		Prensent Method	25.00	0.0	0.00	0.0	0.00	0.0
ply #10	0	Lamination Theory	19.44		0.00		0.00	
		FEM	19.45	0.0	0.00	0.0	0.00	0.0
		Prensent Method	19.44	0.0	0.00	0.0	0.00	0.0
ply #9	0	Lamination Theory	13.89		0.00		0.00	
		FEM	13.89	0.0	0.00	0.0	0.00	0.0
		Prensent Method	13.89	0.0	0.00	0.0	0.00	0.0
ply #8	0	Lamination Theory	8.33		0.00		0.00	
		FEM	8.33	0.0	0.00	0.0	0.00	0.0
		Prensent Method	8.33	0.0	0.00	0.0	0.00	0.0
ply #7	0	Lamination Theory	2.78		0.00		0.00	
		FEM	2.78	0.0	0.00	0.0	0.00	0.0
		Prensent Method	2.78	0.0	0.00	0.0	0.00	0.0
ply #6	0	Lamination Theory	-2.78		0.00		0.00	
		FEM	-2.78	0.0	0.00	0.0	0.00	0.0
		Prensent Method	-2.78	0.0	0.00	0.0	0.00	0.0
ply #5	0	Lamination Theory	-8.33		0.00		0.00	
		FEM	-8.33	0.0	0.00	0.0	0.00	0.0
		Prensent Method	-8.33	0.0	0.00	0.0	0.00	0.0
ply #4	0	Lamination Theory	-13.89		0.00		0.00	
		FEM	-13.89	0.0	0.00	0.0	0.00	0.0
		Prensent Method	-13.89	0.0	0.00	0.0	0.00	0.0
ply #3	0	Lamination Theory	-19.44		0.00		0.00	
		FEM	-19.45	0.0	0.00	0.0	0.00	0.0
		Prensent Method	-19.44	0.0	0.00	0.0	0.00	0.0
ply #2	0	Lamination Theory	-25.00		0.00		0.00	
		FEM	-25.00	0.0	0.00	0.0	0.00	0.0
		Prensent Method	-25.00	0.0	0.00	0.0	0.00	0.0
ply #1	0	Lamination Theory	-30.56		0.00		0.00	
		FEM	-30.56	0.0	0.00	0.0	0.00	0.0
		Prensent Method	-30.56	0.0	0.00	0.0	0.00	0.0

All the stresses match perfectly among three different methods for the bending case of a composite beam.

3.6.6 Ply Stresses of [±45$_2$/0$_2$]$_s$ Symmetric Laminate

3.6.6.1 $\overline{N}_x^c$ acting on the parent laminate [0$_4$/-45/45/-45/+45]$_T$ and the stiffener [±45$_2$]$_T$

For this case, the beam contains a bottom laminate with [0$_4$/-45/45/-45/+45]$_T$ layup and a top laminate with [±45$_2$]$_T$ layup bonded together. Since the top and bottom laminate are not symmetrical, there is no decoupled between the transversal and shear stresses and the axial extension.

Since the axial load was applied to the centroid of the whole cross-section, there is not bending, all the axial stresses are constant within the same fiber orientation of the ply (see Fig. 3.26). In addition, the 0° plies have much more axial stress than the ±45° ones, which makes totally sense since the first ones are stiffer than the second ones.

Table 3.10 lists all the stress results.

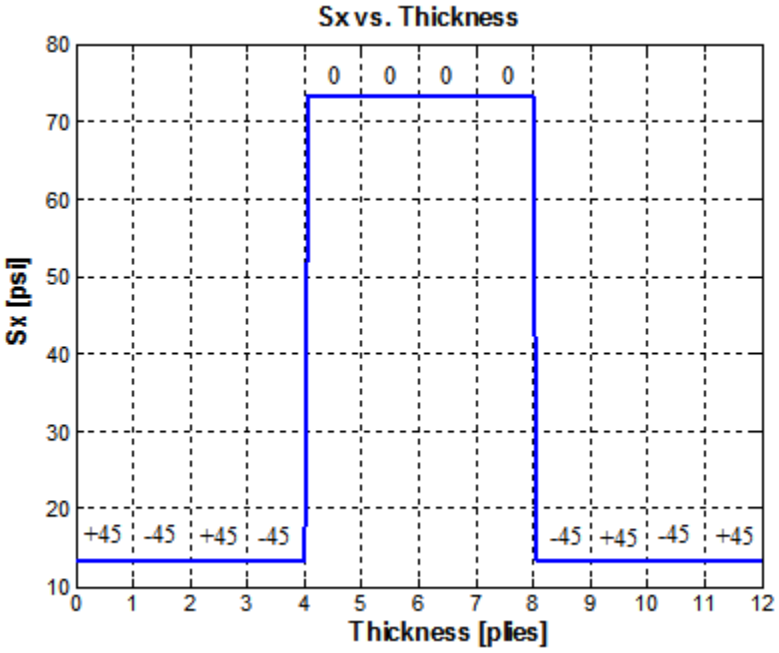

Figure 3.26 FEM axial stress due to $\overline{N}_x^c$ in [0$_4$/-45/45/-45/+45]$_T$ and [±45$_2$]$_T$ of parent and stiffener

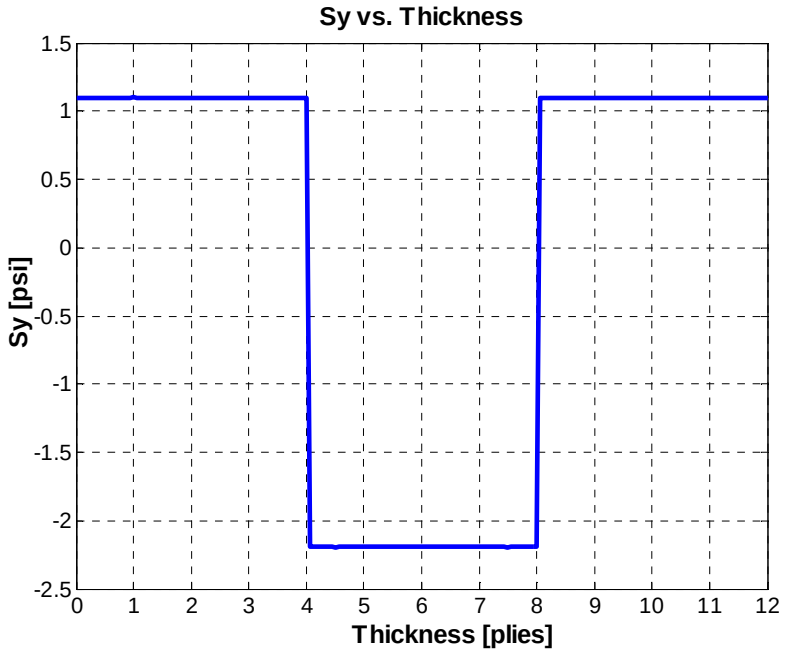

Figure 3.27 FEM transverse stress due to $\overline{N}_x^c$ in $[0_4/-45/45/-45/+45]_T$ and $[\pm 45_2]_T$ of parent and stiffener

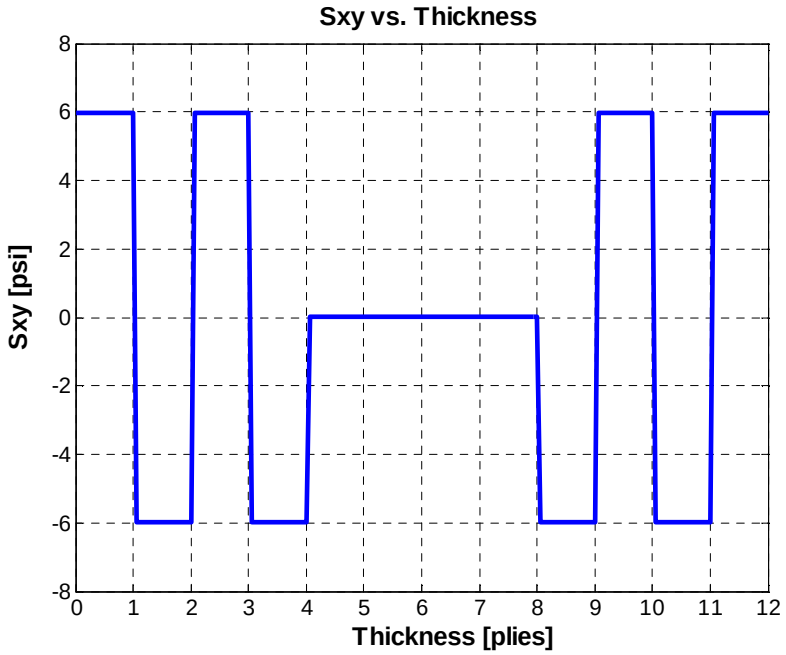

Figure 3.28 FEM shear stress due to $\overline{N}_x^c$ in $[0_4/-45/45/-45/+45]_T$ and $[\pm 45_2]_T$ of parent and stiffener

Table 3.10 Stresses due to $\overline{N}_x^c$ applied to $[0_4/-45/45/-45/45]_T$ and $[\pm 45_2]_T$ of parent and stiffener

			σ_x		σ_y		τ_{xy}	
			[psi]	%Diff	[psi]	%Diff	[psi]	%Diff
ply #12	45	Lamination Theory	13.41		1.09		5.98	
		FEM	13.42	0.1	1.09	-0.2	5.98	0.1
		Prensent Method	12.73	-5.1	0.00	-100.0	5.25	-12.2
ply #11	-45	Lamination Theory	13.41		1.09		-5.98	
		FEM	13.42	0.1	1.10	0.2	-5.98	0.1
		Prensent Method	12.73	-5.1	0.00	-100.0	-5.25	-12.2
ply #10	45	Lamination Theory	13.41		1.09		5.98	
		FEM	13.42	0.1	1.09	-0.1	5.98	0.1
		Prensent Method	12.73	-5.1	0.00	-100.0	5.25	-12.2
ply #9	-45	Lamination Theory	13.41		1.09		-5.98	
		FEM	13.42	0.1	1.09	0.0	-5.98	0.1
		Prensent Method	12.73	-5.1	0.00	-100.0	-5.25	-12.2
ply #8	0	Lamination Theory	73.19		-2.19		0.00	
		FEM	73.25	0.1	-2.19	0.2	0.00	0.0
		Prensent Method	74.25	1.5	-0.05	-97.8	0.10	0.0
ply #7	0	Lamination Theory	73.19		-2.19		0.00	
		FEM	73.25	0.1	-2.19	0.0	0.00	0.0
		Prensent Method	74.14	1.3	-0.46	-79.1	0.10	0.0
ply #6	0	Lamination Theory	73.19		-2.19		0.00	
		FEM	73.25	0.1	-2.19	0.0	0.00	0.0
		Prensent Method	74.03	1.1	-0.87	-60.3	0.10	0.0
ply #5	0	Lamination Theory	73.19		-2.19		0.00	
		FEM	73.25	0.1	-2.19	0.2	0.00	0.0
		Prensent Method	73.91	1.0	-1.28	-41.6	0.10	0.0
ply #4	-45	Lamination Theory	13.41		1.09		-5.98	
		FEM	13.42	0.1	1.09	0.0	-5.98	0.1
		Prensent Method	14.56	8.6	2.83	158.8	-7.03	17.7
ply #3	45	Lamination Theory	13.41		1.09		5.98	
		FEM	13.42	0.1	1.09	-0.1	5.98	0.1
		Prensent Method	14.25	6.3	1.99	82.2	6.83	14.3
ply #2	-45	Lamination Theory	13.41		1.09		-5.98	
		FEM	13.42	0.1	1.10	0.2	-5.98	0.1
		Prensent Method	12.13	-9.6	-0.67	-161.0	-4.59	-23.3
ply #1	45	Lamination Theory	13.41		1.09		5.98	
		FEM	13.42	0.1	1.09	-0.2	5.98	0.1
		Prensent Method	11.82	-11.8	-1.51	-237.6	4.39	-26.6
	Force Balance	Lamination Theory	400.00	x0.0025=	1.0000			
		FEM	400.33	x0.0025=	1.0008			
		Present Method	400.00	x0.0025=	1.0000			

The axial stresses from the present method are in agreement compared with lamination theory. In addition, for 0° plies the results agree better than for ±45° ones. For the transversal and shear stresses the results are very small, so the percentual difference is exaggerated; however, looking closely to the values, the difference is small.

3.6.6.2 $\overline{M}_x^c$ acting on $[0_4/-45/45/-45/+45]_T$ and $[\pm 45_2]_T$ of parent and stiffener

For the bending case, again the axial stress is way more significant than the transversal or shear stresses. In addition, the axial stress is a linear function with jumps between plies as expected (Fig. 3.29 through 3.31). Once again, the 0° plies have a greater axial stress than the ±45° as expected as well.

Table 3.11 lists all the ply stresses.

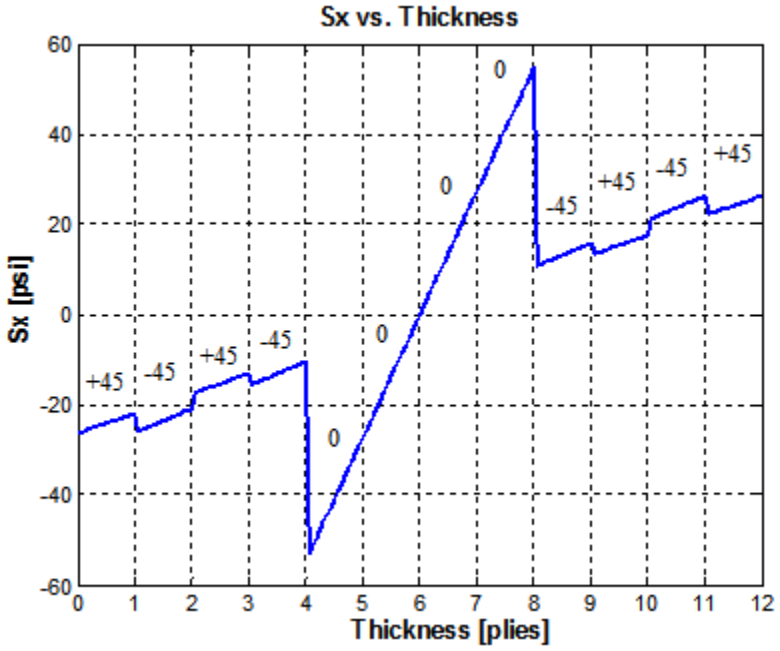

Figure 3.29 FEM axial stress due to $\overline{M}_x^c$ in $[0_4/-45/45/-45/+45]_T$ and $[\pm 45_2]_T$ of parent and stiffener

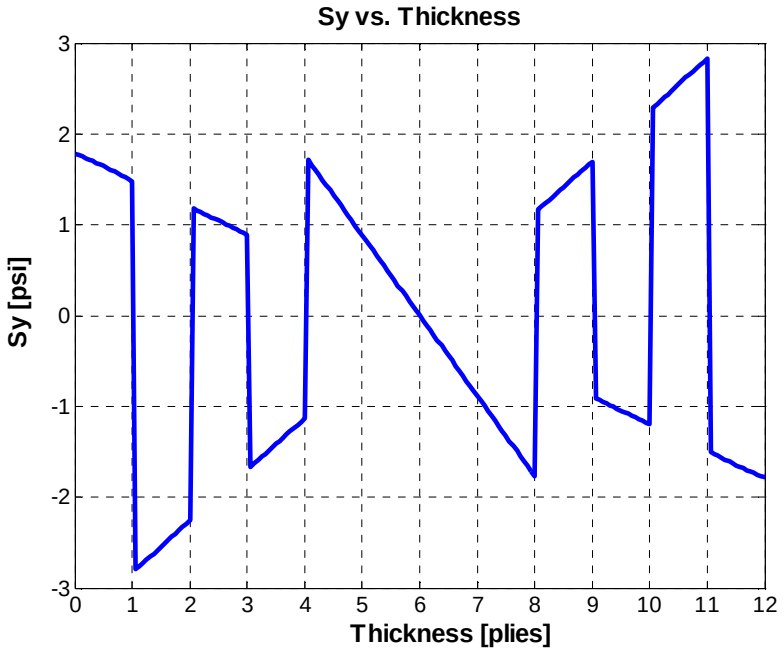

Figure 3.30 FEM transversal stress due to $\overline{M}_x^c$ in [0₄/-45/45/-45/+45]$_T$ and [±45₂]$_T$ of parent and stiffener

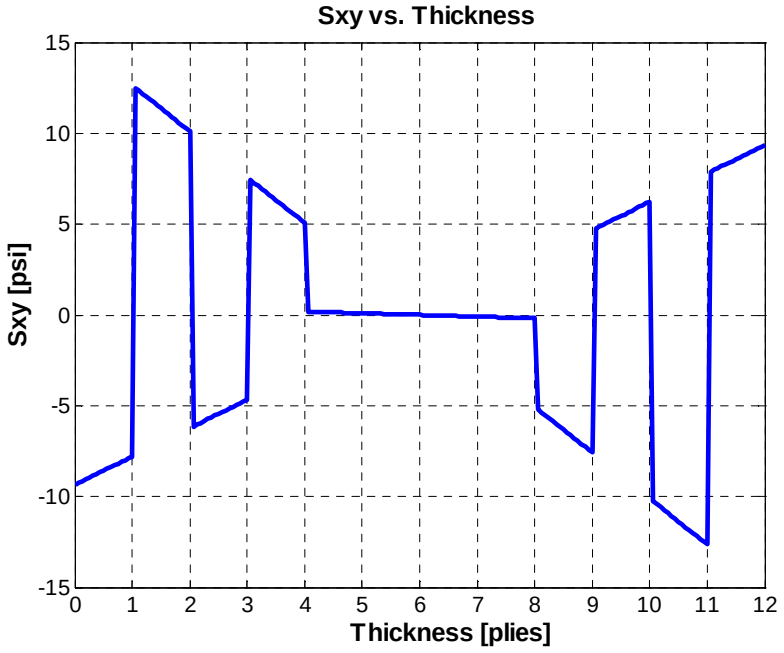

Figure 3.31 FEM shear stress due to $\overline{M}_x^c$ in [0₄/-45/45/-45/+45]$_T$ and [±45₂]$_T$ of parent and stiffener

Table 3.11 Stresses due to $\overline{M}_x^c$ applied to $[0_4/-45/45/-45/45]_T$ and $[\pm 45_2]_T$ of parent and stiffener

			σ_x		σ_y		τ_{xy}	
			[psi]	%Diff	[psi]	%Diff	[psi]	%Diff
ply #12	45	Lamination Theory	24.19		-1.57		8.64	
		FEM	24.15	-0.2	-1.65	4.8	8.56	-0.9
		Prensent Method	25.29	4.5	-0.43	-72.8	9.95	15.2
ply #11	-45	Lamination Theory	23.54		2.46		-11.27	
		FEM	23.65	0.5	2.55	3.7	-11.37	0.9
		Prensent Method	22.29	-5.3	1.16	-52.7	-9.95	-11.7
ply #10	45	Lamination Theory	15.40		-1.00		5.50	
		FEM	15.37	-0.2	-1.05	4.8	5.45	-0.9
		Prensent Method	15.37	-0.2	-1.16	16.1	5.56	1.2
ply #9	-45	Lamination Theory	13.08		1.36		-6.26	
		FEM	13.14	0.5	1.41	3.7	-6.32	0.9
		Prensent Method	12.36	-5.5	0.43	-68.6	-5.56	-11.2
ply #8	0	Lamination Theory	40.98		-1.32		-0.14	
		FEM	41.03	0.1	-1.33	0.2	-0.14	3.6
		Prensent Method	40.91	-0.2	-0.98	-25.9	0.18	-230.5
ply #7	0	Lamination Theory	13.66		-0.44		-0.05	
		FEM	13.68	0.1	-0.44	-0.1	-0.05	3.6
		Prensent Method	13.68	0.1	-0.15	-65.7	0.18	-491.4
ply #6	0	Lamination Theory	-13.66		0.44		0.05	
		FEM	-13.68	0.1	0.44	-0.1	0.05	3.7
		Prensent Method	-13.56	-0.7	0.68	53.5	0.18	291.4
ply #5	0	Lamination Theory	-40.98		1.32		0.14	
		FEM	-41.03	0.1	1.33	0.2	0.14	3.6
		Prensent Method	-40.80	-0.4	1.51	13.8	0.18	30.5
ply #4	-45	Lamination Theory	-13.08		-1.36		6.26	
		FEM	-13.14	0.5	-1.41	3.7	6.32	0.9
		Prensent Method	-12.41	-5.1	-0.56	-59.1	5.59	-10.8
ply #3	45	Lamination Theory	-15.40		1.00		-5.50	
		FEM	-15.37	-0.2	1.05	4.8	-5.45	-0.9
		Prensent Method	-15.73	2.2	0.72	-27.7	-5.94	8.1
ply #2	-45	Lamination Theory	-23.54		-2.46		11.27	
		FEM	-23.65	0.5	-2.55	3.7	11.37	0.9
		Prensent Method	-22.30	-5.2	-1.25	-49.1	9.95	-11.7
ply #1	45	Lamination Theory	-24.19		1.57		-8.64	
		FEM	-24.15	-0.2	1.65	4.9	-8.56	-0.9
		Prensent Method	-25.62	5.9	0.03	-97.9	-10.30	19.3

The results match very well with the lamination theory prediction. Once again, the 0° plies results agree better than for ±45° ones. And the percentual difference is once aga in magnified for the transversal and shear stresses.

3.6.7 Ply Stresses of [±45/0/90]$_{3T}$ Un-symmetric Laminate

3.6.7.1 $\overline{N}_x^c$ acting on [±45/0/90]$_{2T}$ and [±45/0/90]$_T$ of parent and stiffener

For the un-symmetric case, the beam contains a bottom laminate of [±45/0/90]$_{2T}$ and a top laminate of [±45/0/90]$_T$ bonded together. The results are present in Figures 3.32 through 3.34 and listed in Table 3.12.

For this case, the lamination theory was modified. The reference plane was not the mid-plane of the total laminate but the centroid of the total cross-section. This was done only in this case because this is the only case with the centroid at a different location than the mid-plane. The compliance matrices were shifted from the mid-plane to the centroid using Equation 2.29.

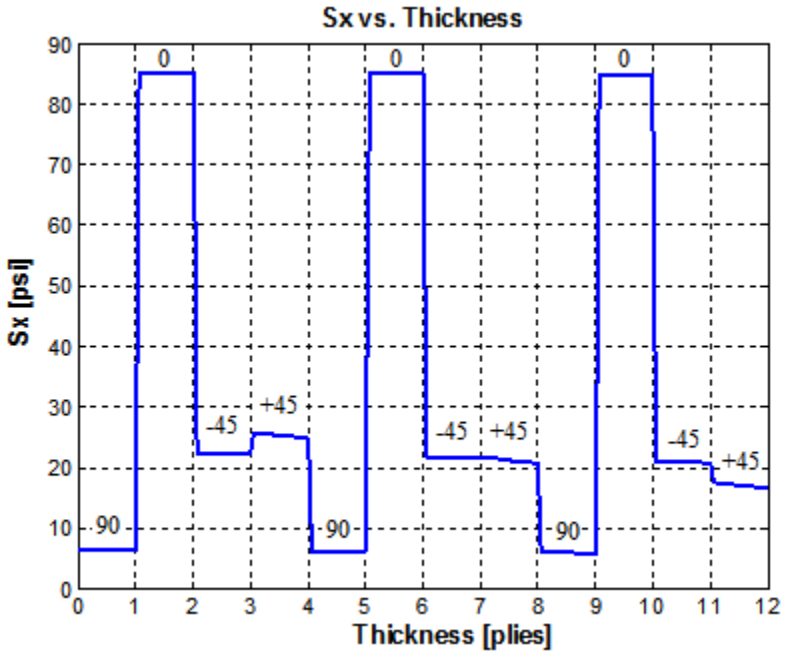

Figure 3.32 FEM axial stress due to $\overline{N}_x^c$ in [±45/0/90]$_{2T}$ and [±45/0/90]$_T$ of parent and stiffener

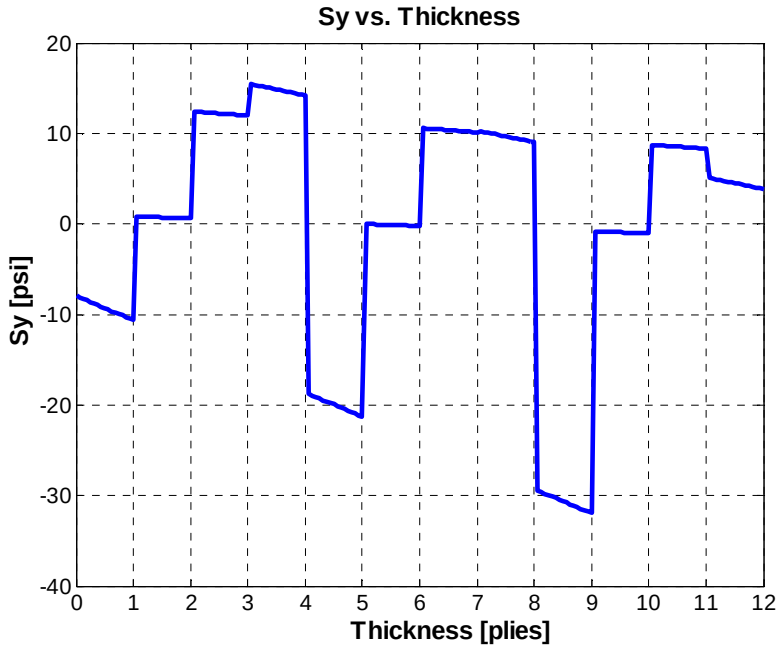

Figure 3.33 FEM transverse stress due to $\overline{N}_x^c$ in $[\pm 45/0/90]_{2T}$ and $[\pm 45/0/90]_T$ of parent and stiffener

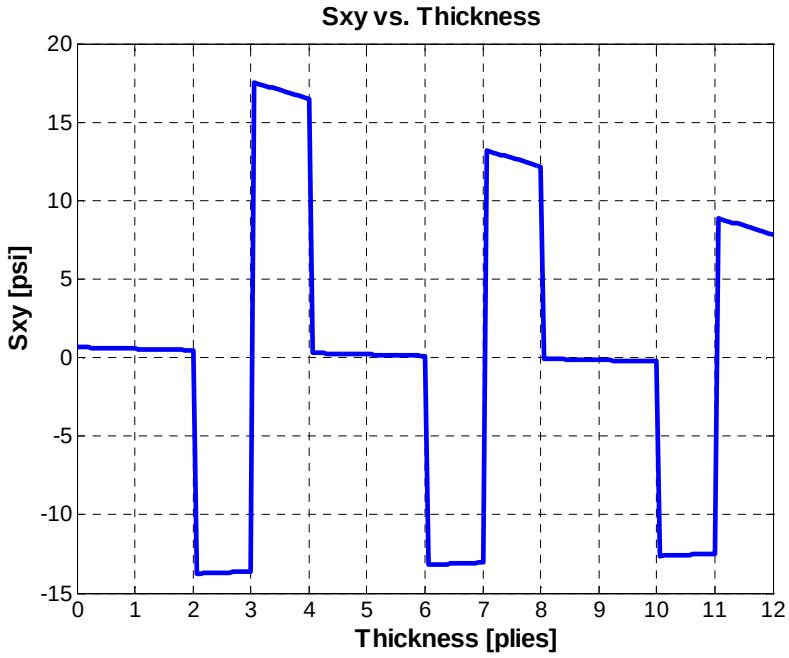

Figure 3.34 FEM shear stress due to $\overline{N}_x^c$ in $[\pm 45/0/90]_{2T}$ and $[\pm 45/0/90]_T$ of parent and stiffener

Table 3.3.12 Stresses due to $\overline{N}_x^c$ applied to $[\pm 45/0/90]_{2T}$ and $[\pm 45/0/90]_T$ of parent and stiffener

			σ_x [psi]	%Diff	σ_y [psi]	%Diff	τ_{xy} [psi]	%Diff
ply #12	45	Lamination Theory	17.05		4.47		8.34	
		FEM	17.17	0.7	4.51	0.8	8.40	0.7
		Prensent Method	15.15	-11.2	-0.72	-116.2	6.51	-22.0
ply #11	-45	Lamination Theory	20.81		8.49		-12.48	
		FEM	20.94	0.6	8.55	0.6	-12.56	0.6
		Prensent Method	16.41	-21.1	2.74	-67.8	-7.33	-41.3
ply #10	0	Lamination Theory	84.26		-0.92		-0.21	
		FEM	84.76	0.6	-0.93	0.6	-0.21	0.6
		Prensent Method	87.95	4.4	-0.13	-85.4	0.41	-298.6
ply #9	90	Lamination Theory	5.91		-30.44		-0.12	
		FEM	5.94	0.6	-30.62	0.6	-0.12	0.9
		Prensent Method	6.78	14.7	-1.88	-93.8	0.41	-454.0
ply #8	45	Lamination Theory	21.15		9.63		12.65	
		FEM	21.27	0.6	9.70	0.7	12.73	0.6
		Prensent Method	18.23	-13.8	4.30	-55.4	9.44	-25.4
ply #7	-45	Lamination Theory	21.57		10.32		-13.05	
		FEM	21.68	0.5	10.37	0.5	-13.12	0.5
		Prensent Method	18.59	-13.8	5.27	-48.9	-9.67	-25.9
ply #6	0	Lamination Theory	84.48		-0.10		0.16	
		FEM	84.90	0.5	-0.10	1.1	0.16	0.0
		Prensent Method	87.69	3.8	-1.08	947.8	0.12	-26.3
ply #5	90	Lamination Theory	6.13		-19.85		0.25	
		FEM	6.16	0.5	-19.95	0.5	0.25	0.1
		Prensent Method	6.19	1.0	-29.84	50.3	0.12	-53.4
ply #4	45	Lamination Theory	25.25		14.79		16.96	
		FEM	25.37	0.5	14.87	0.5	17.05	0.5
		Prensent Method	23.87	-5.4	12.41	-16.1	15.11	-10.9
ply #3	-45	Lamination Theory	22.34		12.15		-13.63	
		FEM	22.43	0.4	12.20	0.4	-13.69	0.4
		Prensent Method	24.23	8.5	13.38	10.1	-15.34	12.6
ply #2	0	Lamination Theory	84.70		0.72		0.52	
		FEM	85.04	0.4	0.72	0.3	0.52	0.3
		Prensent Method	88.21	4.1	0.82	14.9	0.12	-77.8
ply #1	90	Lamination Theory	6.35		-9.27		0.61	
		FEM	6.38	0.4	-9.29	0.2	0.61	0.3
		Prensent Method	6.71	5.6	-5.27	-43.2	0.12	-81.1
	Force Balance	Lamination Theory	400.00	x0.0025=	1.0000			
		FEM	402.05	x0.0025=	1.0051			
		Present Method	400.00	x0.0025=	1.0000			

The results are relative close to each other. The force balance indeed remains in equilibrium.

3.6.7.2 $\overline{M}_x^c$ acting on $[\pm 45/0/90]_{2T}$ and $[\pm 45/0/90]_{2T}$ *of parent and stiffener*

For the bending case, it was expected a linear relationship for the axial stress as explained many times before (Figures 3.35 through 3.37).

Table 3.13 lists all the results.

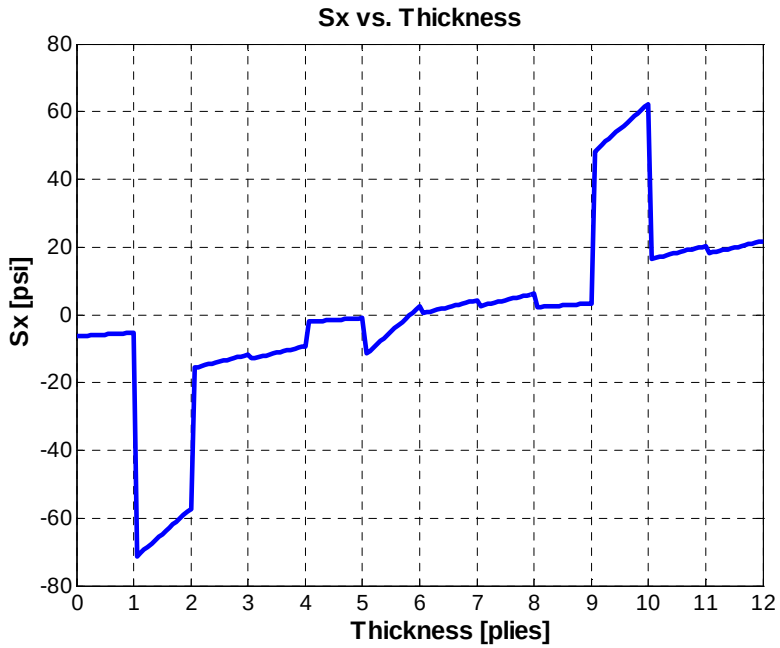

Figure 3.35 FEM axial stress due to $\overline{M}_x^c$ *in* $[\pm 45/0/90]_{2T}$ *and* $[\pm 45/0/90]_T$ *of parent and stiffener*

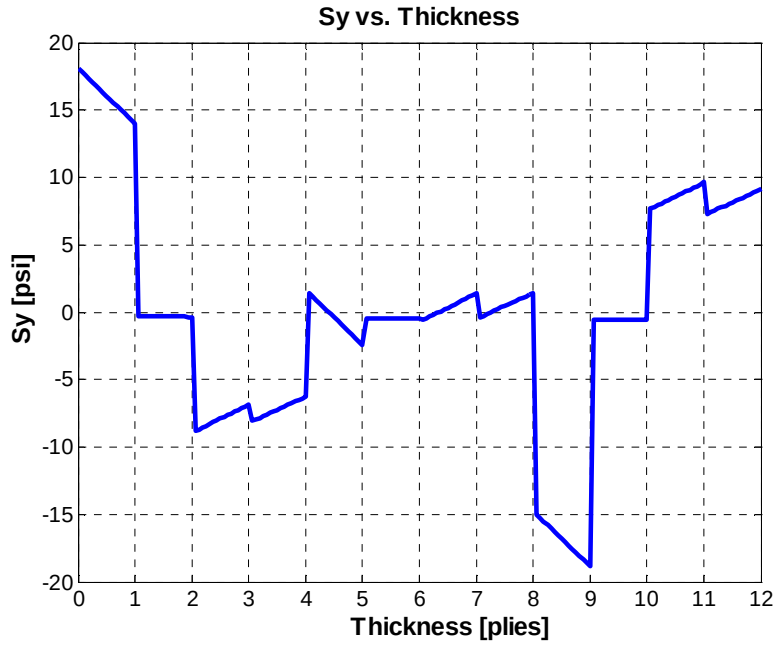

Figure 3.36 FEM transverse stress due to $\overline{M}_x^c$ in $[\pm 45/0/90]_{2T}$ and $[\pm 45/0/90]_T$ of parent and stiffener

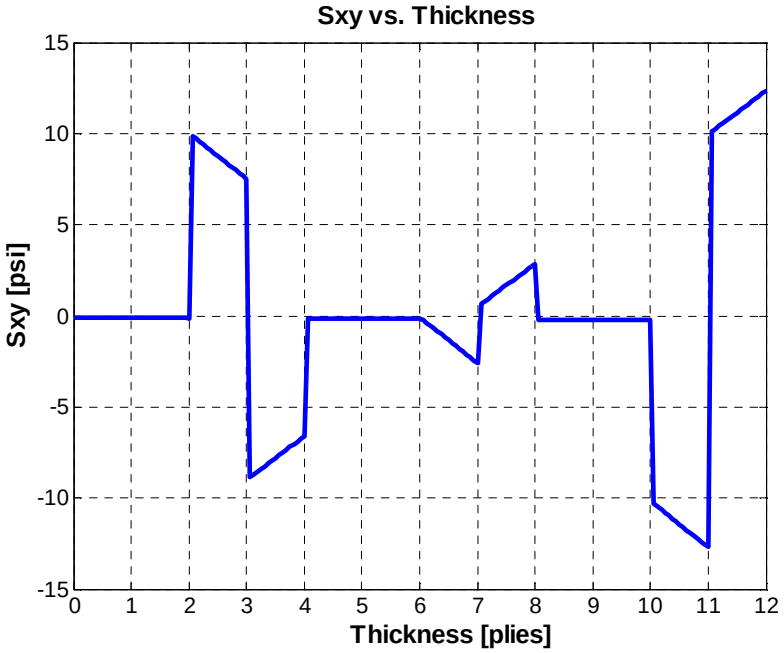

Figure 3.37 FEM shear stress due to $\overline{M}_x^c$ in $[\pm 45/0/90]_{2T}$ and $[\pm 45/0/90]_T$ of parent and stiffener

Table 3.13 Stresses due to $\overline{M}_x^c$ applied to the $[\pm 45/0/90]_{2T}$ and $[\pm 45/0/90]_T$ of parent and stiffener

			σ_x [psi]	%Diff	σ_y [psi]	%Diff	τ_{xy} [psi]	%Diff
ply #12	45	Lamination Theory	19.59		8.04		11.01	
		FEM	19.83	1.2	8.15	1.4	11.16	1.4
		Prensent Method	15.52	-20.8	-0.39	-104.9	6.38	-42.1
ply #11	-45	Lamination Theory	18.14		8.52		-11.34	
		FEM	18.31	1.0	8.59	0.8	-11.44	0.8
		Prensent Method	14.25	-21.4	2.09	-75.4	-6.59	-41.9
ply #10	0	Lamination Theory	54.21		-0.54		-0.24	
		FEM	54.82	1.1	-0.55	1.2	-0.24	-0.5
		Prensent Method	59.59	9.9	-0.57	3.9	0.11	-143.4
ply #9	90	Lamination Theory	2.72		-16.59		-0.23	
		FEM	2.75	1.1	-16.78	1.2	-0.23	0.0
		Prensent Method	3.38	24.5	-1.14	-93.2	0.11	-146.5
ply #8	45	Lamination Theory	4.26		0.45		1.65	
		FEM	4.32	1.5	0.47	4.5	1.68	2.0
		Prensent Method	6.67	56.6	3.13	601.8	3.70	124.1
ply #7	-45	Lamination Theory	2.21		0.33		-1.31	
		FEM	2.24	1.5	0.34	2.3	-1.33	1.5
		Prensent Method	4.32	95.7	2.64	702.6	-3.21	144.5
ply #6	0	Lamination Theory	-4.94		-0.43		-0.18	
		FEM	-4.95	0.2	-0.44	1.0	-0.18	2.0
		Prensent Method	-3.31	-33.0	-0.18	-58.5	-0.25	38.4
ply #5	90	Lamination Theory	-1.53		-0.34		-0.16	
		FEM	-1.54	0.8	-0.36	4.8	-0.17	2.8
		Prensent Method	-1.46	-4.7	0.87	-355.4	-0.25	52.4
ply #4	45	Lamination Theory	-11.07		-7.15		-7.71	
		FEM	-11.20	1.1	-7.24	1.3	-7.80	1.3
		Prensent Method	-11.76	6.2	-7.84	9.8	-8.42	9.2
ply #3	-45	Lamination Theory	-13.72		-7.86		8.72	
		FEM	-13.83	0.8	-7.91	0.6	8.77	0.6
		Prensent Method	-14.11	2.8	-8.33	6.0	8.91	2.2
ply #2	0	Lamination Theory	-64.10		-0.32		-0.11	
		FEM	-64.72	1.0	-0.33	0.8	-0.12	7.2
		Prensent Method	-66.45	3.7	-0.67	105.3	-0.25	118.4
ply #1	90	Lamination Theory	-5.77		15.91		-0.10	
		FEM	-5.83	1.0	16.07	1.0	-0.11	9.7
		Prensent Method	-6.14	6.3	10.38	-34.8	-0.25	155.2

3.7 Non-aligned Top-and-Bottom Laminates bonded together

This section includes the case when both laminates are not aligned with respect to y-coordinate as shown in Figure 3.38.

3.7.1 Description of the Geometry and Bi-axial Bending

All the distances in z-direction remains the same as in Figure 3.2; however, it is necessary to define some distance in the y-direction. $\bar{y}_{c1}$ is the distance from the most right of the cross-section to the centroid of the beam. Similarly, $\bar{y}_{c2}$ is the distance from the most right of the cross-section to the centroid of the stiffener. $\bar{y}_c$ is the distance from the most right of the cross-section to the centroid of the two laminate bonded together.

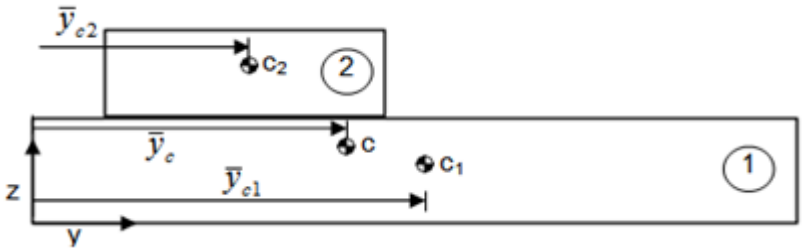

Figure 3.38 Non-aligned top and bottom laminates

If the beam is subjected to a bi-axial bending, as shown in Figure 3.39, the strain can be written as shown for isotropic materials [56] as

$$\varepsilon_x^o = \varepsilon_x^c + z\kappa_x^c + y\kappa_z^c$$

where κ_z is defined in the same manner as for κ_x shown below,

$$\kappa_z = -\frac{\partial^2 v}{\partial x^2} \qquad \text{and} \qquad \kappa_x = -\frac{\partial^2 w}{\partial x^2}$$

The bending moment about the x-axis and z-axis acting at the centroid can be defined as

$$\overline{M}_x^c = \overline{D}_x \kappa_x^c + \overline{D}_{xy}^{'} \kappa_z^c$$

$$\overline{M}_z^c = \overline{D}_{xy}^{'} \kappa_x^c + \overline{D}_y \kappa_z^c$$

where $\overline{M}_z^c = \int y \overline{\sigma}_x dA$.

It should be noted that the positive M_z points to –z-axis direction.

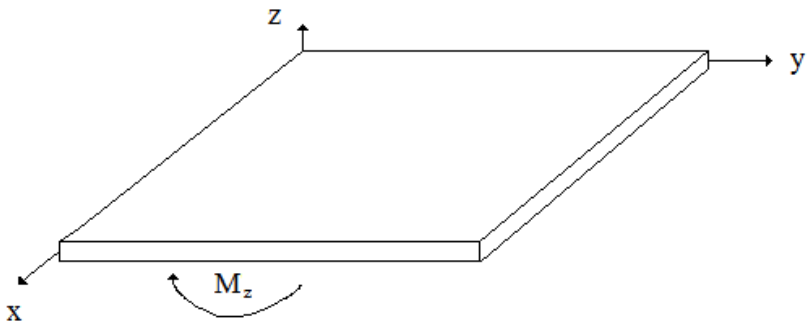

Figure 3.39 M_z applied to a laminate

3.7.2 Equivalent Axial Stiffness

The equivalent axial stiffness is the same as the case shown in section 3.2.2.

$$\overline{A}_x = w_1 A_1^* + w_2 A_2^*$$

3.7.3 Equivalent Bending Stiffnesses

Unlike aligned laminated beam, the equivalent bending stiffness $\overline{D}_x$, $\overline{D}_y$, and $\overline{D}_{xy}$ are required for performing stress analysis.

To obtain the bending stiffness $\overline{D}_x$, the results need to be read only at the curvature κ_x^c when applied $\overline{M}_x^c$, because, $\overline{M}_x^c = \overline{D}_x \kappa_x^c + \overline{D}_{xy}^{'} \kappa_z^c$. Therefore, the expression for, $\overline{D}_x$ is the same as the one obtained from the aligned laminated beam.

$$\overline{D}_x = w_1 A_1^* z_1^2 + 2 w_1 B_1^* z_1 + w_1 D_1^* + w_2 A_2^* z_2^2 + 2 w_2 B_2^* z_2 + w_2 D_2^*$$

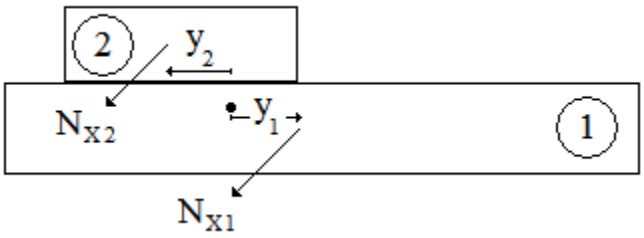

Figure 3.40 Axial load applied on the centroid of each laminate

Referring to Figure 3.40, we have

$$\overline{M}_z^c = \overline{N}_{x1} y_1 + \overline{N}_{x2} y_2$$

$$\overline{M}_z^c = w_1 N_{x1} y_1 + w_2 N_{x2} y_2$$

$$\overline{M}_z^c = w_1 (A_1^* \varepsilon_{x1}^o + B_1^* \kappa_{x1}) y_1 + w_2 (A_2^* \varepsilon_{x2}^o + B_2^* \kappa_{x2}) y_2$$

It is noted that y_1 and y_2 are often in opposite direction. On the other hand, the strains in the mid-planes of each laminate can be substituted by $\varepsilon_x^o = \varepsilon_x^c + z\kappa_x^c + y\kappa_z^c$, where $\varepsilon_x^c = 0$.

And realizing that all the curvature are the same $(\kappa_x = \kappa_x^c = \kappa_{x1} = \kappa_{x2})$. To obtain the bending stiffness $\overline{D}_{xy}^{'}$, the results need to be read only at the curvature κ_x^c when applied $\overline{M}_z^c$, because, $\overline{M}_z^c = \overline{D}_{xy}^{'} \kappa_x^c + \overline{D}_y \kappa_z^c$.

$$\overline{M}_z^c = [w_1 (A_1^* z_1 + B_1^*) y_1 + w_2 (A_2^* z_2 + B_2^*) y_2] \kappa_x^c$$

$$\boxed{\overline{D}_{xy}^{'} = w_1 (A_1^* z_1 + B_1^*) y_1 + w_2 (A_2^* z_2 + B_2^*) y_2} \qquad (3.25)$$

The last bending stiffness $\overline{D}_y$ can be calculated applying the same moment M_z but reading the curvature in z instead of x. The best way to treat this problem is using the help of stiffness for the web in the composite I-Beam theory.

$$\overline{M}_z^c = \left[A_1^* \left(\frac{w_1^3}{12} + y_1^2 w_1 \right) + A_2^* \left(\frac{w_2^3}{12} + y_2^2 w_2 \right) \right] \kappa_z^c$$

$$\boxed{\overline{D}_y = A_1^* \left(\frac{w_1^3}{12} + y_1^2 w_1 \right) + A_2^* \left(\frac{w_2^3}{12} + y_2^2 w_2 \right)} \quad (3.26)$$

3.7.4 Centroids

The vertical centroid z_c is calculated as shown in Equation 3.19.

$$\bar{z}_c = \frac{\bar{z}_{c1} w_1 A_1^* + \bar{z}_{c2} w_2 A_2^*}{w_1 A_1^* + w_2 A_2^*}$$

On the other hand, the horizontal centroid, y_c, can be obtained in an analogous way as z_c (Fig. 3.38).

$$\boxed{\bar{y}_c = \frac{\bar{y}_{c1} w_1 A_1^* + \bar{y}_{c2} w_2 A_2^*}{w_1 A_1^* + w_2 A_2^*}} \quad (3.27)$$

3.8 Finite Element Model

A model was built in ANSYS to simulate the composite laminates. Two laminates of 10 inches length; the bottom laminate of 8 plies was 0.5 inches wide while the top laminate of 4 plies was 0.25 inches wide. Both were bonded together.

The element used was solid46, a 3D block element with 8 nodes and 3 degrees of freedom per node. The mesh generated for the bottom laminate was 320 elements through the length, and 19 through the width. 2 elements per ply were used and special care was used in order to define nodes in the centroid of the whole cross-section which happens to be located in the bottom laminate. On the other hand, the top laminate mesh has 11 elements through the wide, and 2 elements per ply through the height. This gives a total of 160,821 nodes.

In order to evaluate the stiffnesses, three cases were considered an axial load $\overline{N}_x^c$ and two moments $\overline{M}_x^c$ and $\overline{M}_z^c$ were applied.

An axial load of 1 lb was applied at the centroid of the cross-section. The mesh was specially designed so when applying the other moments $\overline{M}_x^c$ and $\overline{M}_z^c$, there were nodes defined in the location where the pair of forces should act. That is why the mesh is not uniform around the centroid (Fig. 3.41).

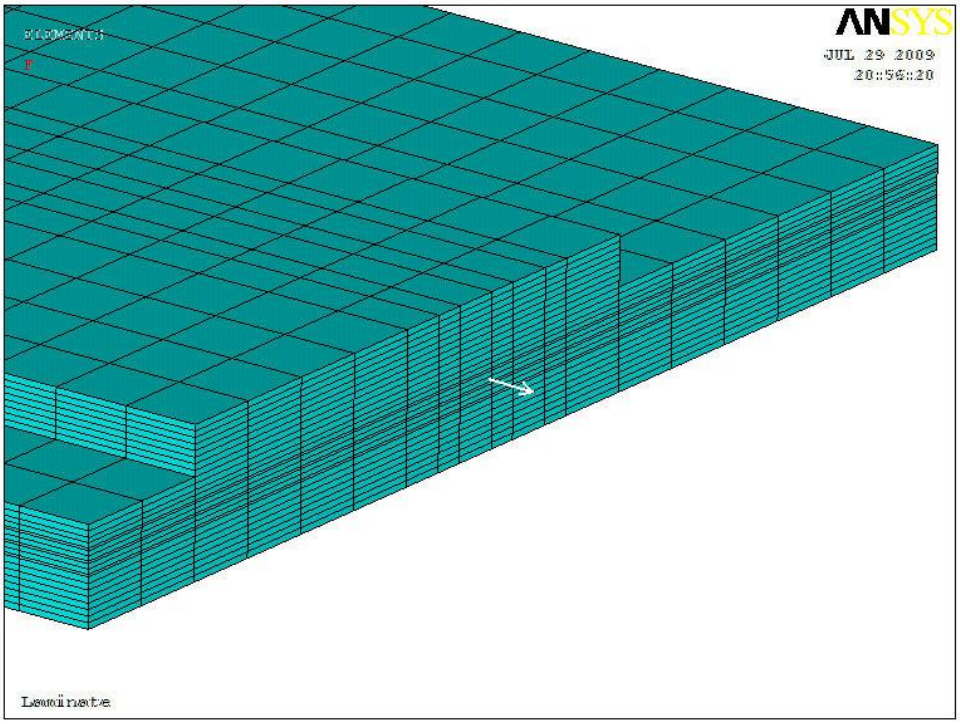

Figure 3.41 $\overline{N}_x^c$ applied to the centroid of the whole cross-section

The other case was the moment applied. A pair of forces were assigned to generate the moment; each force being a 1 lb and acting one ply away from the centroid of the cross-section (that is 0.005 inches). This generates a total moment of 0.01 lb-in. A typical mesh for this case is shown in Figure 3.42.

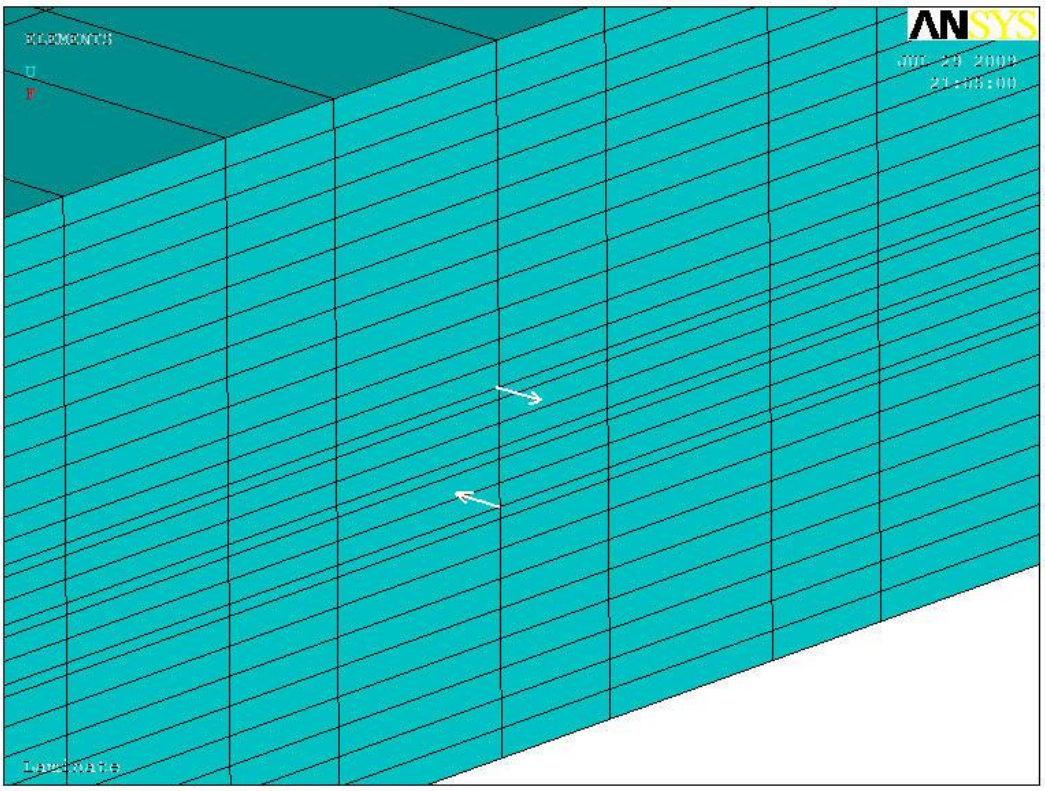

Figure 3.42 Two forces generating $\overline{M}_x^c$

The other moment $\overline{M}_z^c$ as defined in Figure 3.39 is generated by a pair of forces acting an equal distance from the centroid in opposite directions. Each force being a 1 lb and acting 0.03125 inches away from the centroid of the whole cross-section (Fig. 3.43). This generates a total moment of 0.0625 lb-in.

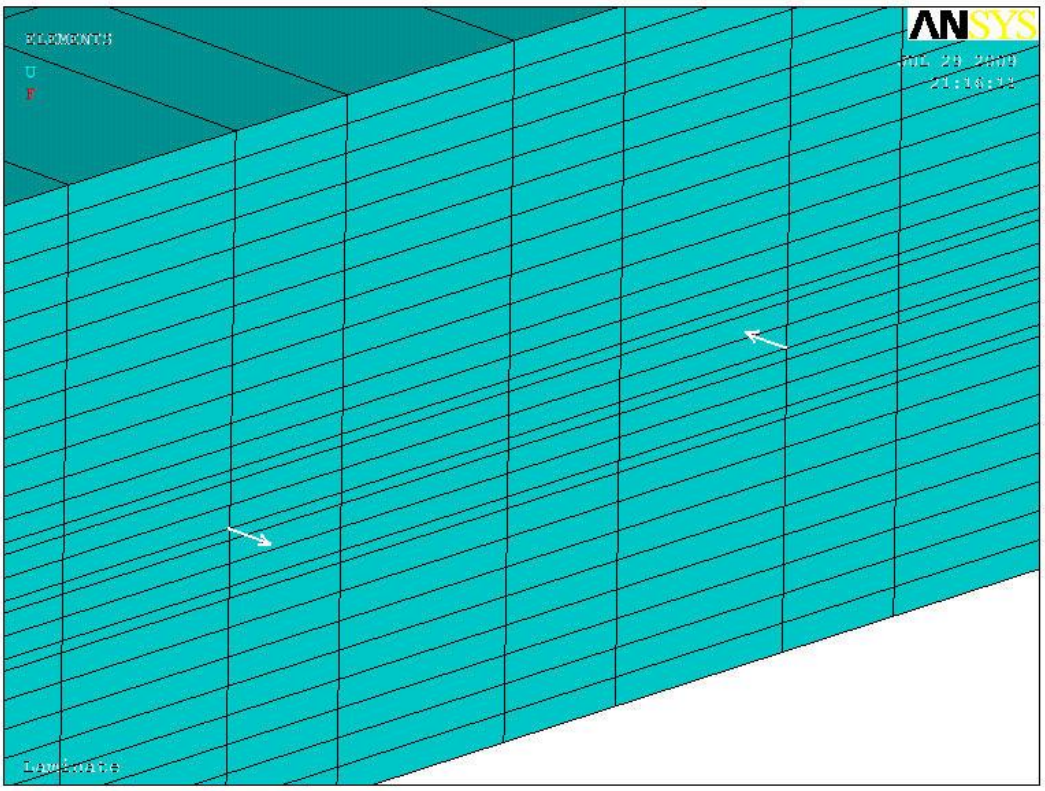

Figure 3.43 Two forces generating $\overline{M}_z^c$

The boundary conditions were applied has follows similar as before; however, the constrained planes were not the mid-planes but the centroid planes (Fig. 3.44). As before, the whole plane on the other side of the laminate was constrained in the x-direction (axial direction). The centroid plane y_c of the laminate in the y-direction was constrained in that direction (Uy=0). And the location of the centroid plane z_c in the z-direction was constrained in that direction (Uz=0) as well.

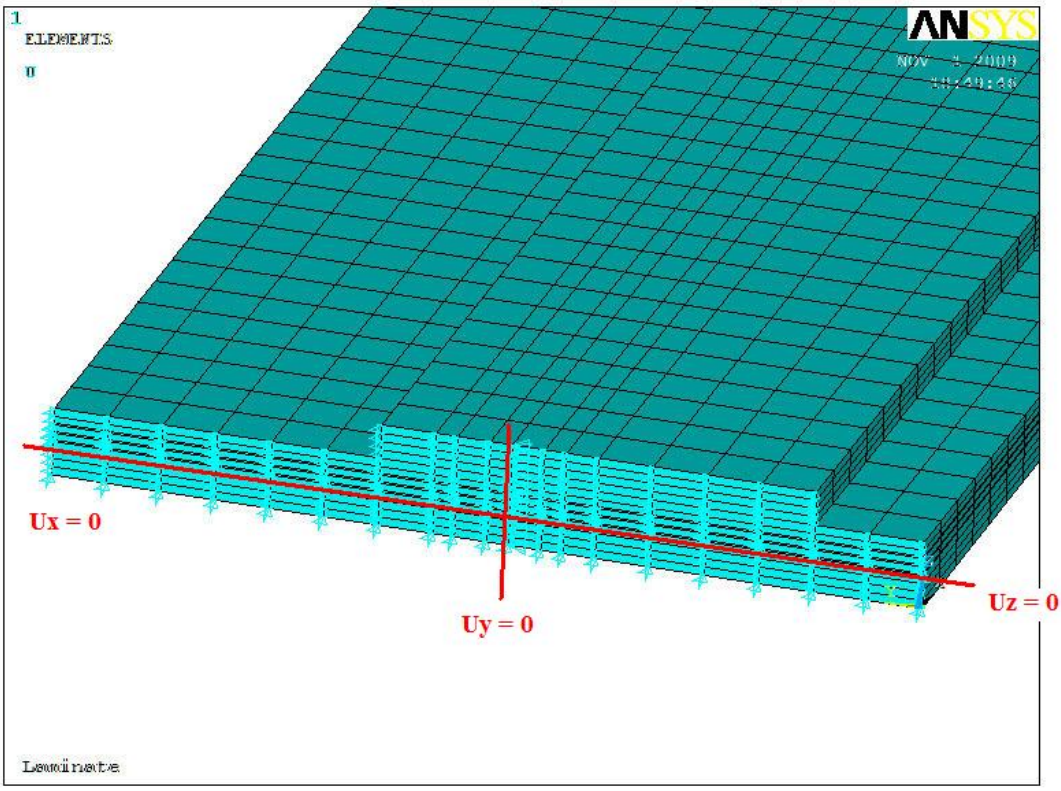

Figure 3.44 Applied boundary conditions

The same two materials were used for the simulations. First, the isotropic material was used to compare the results with closed form theoretical solutions.

For the composite material 3 cases were simulated. First all the plies to be 0°, that one ply of $[0_4]_S$ and the other of $[0_2]_S$. The second was the bottom laminate $[0_4/-45/45/-45/+45]_T$ and the top laminate $[\pm 45_2]_T$. And finally, the last case was the bottom laminate $[\pm 45/0/90]_{2T}$ and the top laminate $[\pm 45/0/90]_T$.

3.9 Comparison of the Axial and Bending Stiffnesses

3.9.1 Axial and Bending Stiffnesses obtained from FEM

The axial stiffnesses were calculated from the FEM model by the following equation.

$$\overline{A}_x = \frac{FL}{2(U_{x|at\ \mathrm{x=L/2}})}$$

To avoid distortions of the results by the boundary conditions or the applied load, the results were read half way through the length of the beam; that is at L/2. And F is the applied load.

For the bending stiffnesses some assumptions has to be made. It can be assumed that κ_z^c is very small compare to κ_x^c, ($\kappa_z^c << \kappa_x^c$), when $\overline{M}_x^c$ is applied. Therefore, $\overline{M}_x^c = \overline{D}_x \kappa_x^c + \overline{D}_{xy}^{'} \kappa_z^c$ reduces to simply $\overline{M}_x^c = \overline{D}_x \kappa_x^c$; and the bending stiffness $\overline{D}_x$ can be calculated from the FEM model by first determining the curvature of the beam, κ_x^c, and then dividing the applied moment by it.

$$\overline{M}_x^c = \overline{D}_x \kappa_x^c \quad \rightarrow \quad \overline{D}_x = \frac{\overline{M}_x^c}{\kappa_x^c}$$

In the same way, it can be assumed that κ_x^c is very small compare to κ_z^c, ($\kappa_x^c << \kappa_z^c$), when $\overline{M}_z^c$ is applied. In the same manner, $\overline{M}_z^c = \overline{D}_{xy}^{'} \kappa_x^c + \overline{D}_y \kappa_z^c$ reduces to $\overline{M}_z^c = \overline{D}_y \kappa_z^c$; therefore,

$$\overline{M}_z^c = \overline{D}_y \kappa_z^c \quad \rightarrow \quad \overline{D}_y = \frac{\overline{M}_z^c}{\kappa_z^c}$$

3.9.2 Centroid Locations

The centroid z_c and y_c were calculated using Equation 3.19 and 3.27, respectively. The axial stiffnesses were calculated through Equation 3.11 and the bending stiffnesses were calculated using Equations 3.16, 3.25, and 3.26.

The centroid rather than calculated from the FEM model was confirmed by it. As it was explained before, the centroid is defined as the location where an axial load does not cause a change in curvature and a bending moment does not produce axial strain. In other words, the load acting at the centroid decouples the structural response between axial extension and bending. Therefore, it was checked that for an applied axial load at the centroid there were not bending (curvature) and for an applied moment at the centroid of the cross-section, there were not axial displacement.

Finally, all the axial displacements (for the axial stiffness and centroid) and vertical and lateral displacements (for the bending stiffness) were read at the centroid of the cross-section. The mesh was done careful so there were nodes presents in the centroids of each case.

3.9.3 Method of obtaining $\overline{D}'_{xy}$

Let the moment being applied at the centroid of the laminate. Then we have

$$\overline{M}_x^c = \overline{D}_x \kappa_x^c + \overline{D}'_{xy} \kappa_z^c$$

$$\overline{M}_z^c = \overline{D}'_{xy} \kappa_x^c + \overline{D}_y \kappa_z^c$$

Solving the above equations, we have

$$\kappa_x^c = \frac{\overline{M}_x^c \overline{D}_y - \overline{M}_z^c \overline{D}'_{xy}}{\overline{D}_x \overline{D}_y - \overline{D}'^2_{xy}}$$

$$\kappa_z^c = \frac{-\overline{M}_x^c \overline{D}'_{xy} + \overline{M}_z^c \overline{D}_x}{\overline{D}_x \overline{D}_y - \overline{D}'^2_{xy}}$$

The strain at any given point can be written as

$$\varepsilon_x = \varepsilon_x^c + z\kappa_x^c + y\kappa_z^c$$

since $\varepsilon_x^c = 0$, we have

$$\varepsilon_x = \frac{\overline{D}_y \overline{M}_x^c - \overline{D}'_{xy} \overline{M}_z^c}{\overline{D}_x \overline{D}_y - \overline{D}'^2_{xy}} z + \frac{\overline{D}_x \overline{M}_z^c - \overline{D}'_{xy} \overline{M}_x^c}{\overline{D}_x \overline{D}_y - \overline{D}'^2_{xy}} y \tag{3.28}$$

Since the only moment applied was $\overline{M}_x^c$ ($\overline{M}_z^c = 0$), and the results were read at certain point where (y=0).

$$\overline{D}'_{xy} = \sqrt{\overline{D}_x \overline{D}_y - \frac{\overline{D}_y \overline{M}_x^c z}{\varepsilon_x}} \tag{3.29}$$

In this way the bending stiffness $\overline{D}'_{xy}$ was calculated from the FEM results.

3.9.4 Results Comparison

Four cases were considered in this study. They are isotropic material, all 0° ply laminate, symmetric and balanced laminate, and un-symmetric laminate in the overlapped region. All of the results are listed in Table 3.14.

The theoretical solution of $\overline{D}_x$, $\overline{D}_y$, and $\overline{D}'_{xy}$ for composite cases are not available. For isotropic material model, the composite laminated beam was input the isotropic material properties and the results matched perfectly with the closed-form solution. This gives confidence the developed equations are correct.

For all the cases the bottom laminate consists of 8 plies and the top laminate consists of 4 plies. The results match perfectly as before for the equations.

For the third case, the bottom laminate layup was $[0_4/\text{-}45/45/\text{-}45/+45]_T$ and the top laminate layup was $[\pm 45_2]_T$. The results are very excellent agreement.

Finally, the last cases contains the bottom laminate with a layup of $[\pm 45/0/90]_{2T}$ and a top laminate with a layup of $[\pm 45/0/90]_T$. For this case the results in excellent agreement as well except for $\overline{D}'_{xy}$.

Table 3.14 Comparison of the axial and bending stiffnesses for different cases

		units	Present Meth.	FEM	Diff%	Theoretical Sol.	Diff%
ISO	$\bar{z}_c$	[tply]	5.2	5.2		5.2	0.0
	$\bar{y}_c$	[in]	0.2375	0.2375		0.2375	0.0
	U_x	[in]		1.91E-05			
	$\bar{A}_x$	[lb]	262,450	262,453	0.0	262,450	0.0
	k_x	[1/in]		1.50E-04			
	$\bar{D}_x$	[lb-in²]	67.54	66.62	1.4	67.54	0.0
	k_z	[1/in]		1.32E-05			
	$\bar{D}_y$	[lb-in²]	4,812	4,720	1.9	4,812	0.0
	ε_x	[in/in]		5.13E-06			
	$\bar{D}'_{xy}$	[lb-in²]	-78.74	-78.71	0.0	-78.74	0.0
$[0_5]_s$	$\bar{z}_c$	[tply]	5.2	5.2		5.2	0.0
	$\bar{y}_c$	[in]	0.2375	0.2375		0.2375	0.0
	U_x	[in]		1.10E-05			
	$\bar{A}_x$	[lb]	455,000	455,000	0.0	455,000	0.0
	k_x	[1/in]		8.70E-05			
	$\bar{D}_x$	[lb-in²]	117.09	114.88	1.9	117.09	0.0
	k_z	[1/in]		7.64E-06			
	$\bar{D}_y$	[lb-in²]	8,342	8,183	1.9	8,342	0.0
	ε_x	[in/in]		2.96E-06			
	$\bar{D}'_{xy}$	[lb-in²]	-136.50	-136.49	0.0	-136.50	0.0
$[\pm 45_2/0_2]_s$	$\bar{z}_c$	[tply]	5.722	5.722			
	$\bar{y}_c$	[in]	0.2436	0.2436			
	U_x	[in]		2.17E-05			
	$\bar{A}_x$	[lb]	228,925	230,097	-0.5		
	k_x	[1/in]		3.81E-04			
	$\bar{D}_x$	[lb-in²]	25.67	26.28	-2.3	N/A	
	k_z	[1/in]		1.37E-05			
	$\bar{D}_y$	[lb-in²]	4,588	4,579	0.2		
	ε_x	[in/in]		1.22E-05			
	$\bar{D}'_{xy}$	[lb-in²]	-20.36	-20.18	0.9		
$[\pm 45/0/90]_{3T}$	$\bar{z}_c$	[tply]	4.939	4.939			
	$\bar{y}_c$	[in]	0.2387	0.2387			
	U_x	[in]		2.83E-05			
	$\bar{A}_x$	[lb]	173,458	176,991	-2.0		
	k_x	[1/in]		0.0002383			
	$\bar{D}_x$	[lb-in²]	40.75	41.96	-2.9	N/A	
	k_z	[1/in]		1.989E-05			
	$\bar{D}_y$	[lb-in²]	3,209	3,142	2.1		
	ε_x	[in/in]		8.35E-06			
	$\bar{D}'_{xy}$	[lb-in²]	-49.28	-70.23	-29.8		

3.10 Z-Stiffener

This section will utilize the equation developed in Section 3.7 in order to calculate the axial and bending stiffness of a stiffener with Z-shape.

From Equations 3.19 and 3.27 is possible to expand them to calculate the centroid of the Z stiffener case.

$$\bar{z}_c = \frac{\bar{z}_{c,f1} w_{f1} A^*_{f1} + \bar{z}_{c,f2} w_{f2} A^*_{f2} + \bar{z}_{c,w} w_w A^*_w}{w_{f1} A^*_{f1} + w_{f2} A^*_{f2} + w_w A^*_w} \tag{3.30}$$

$$\bar{y}_c = \frac{\bar{y}_{c,f1} w_{f1} A^*_{f1} + \bar{y}_{c,f2} w_{f2} A^*_{f2} + \bar{y}_{c,w} w_w A^*_w}{w_{f1} A^*_{f1} + w_{f2} A^*_{f2} + w_w A^*_w} \tag{3.31}$$

The subscripts f and w refer to the flage and the web laminates, respectively.

The axial stiffness can be calculated expanding Equation 3.11 for the Z stiffener case.

$$\overline{A}_x = w_{f1} A^*_{f1} + w_{f2} A^*_{f2} + w_w A^*_w \tag{3.32}$$

Finally, for the bending stiffnesses a combination of Equations 3.16, 3.25, and 3.26 must be taken into consideration.

$$\begin{aligned}\overline{D}_x &= w_{f1} A^*_{f1} z^2_{f1} + 2 w_{f1} B^*_{f1} z_{f1} + w_{f1} D^*_{f1} + w_{f2} A^*_{f2} z^2_{f2} + 2 w_{f2} B^*_{f2} z_{f2} \\ &+ w_{f2} D^*_{f2} + A^*_w \left(\frac{w^3_w}{12} + y^2_w w_w \right)\end{aligned} \tag{3.33}$$

$$\overline{D}_y = A^*_{f1} \left(\frac{w^3_{f1}}{12} + y^2_{f1} w_{f1} \right) + A^*_{f2} \left(\frac{w^3_{f2}}{12} + y^2_{f2} w_{f2} \right) + w_w A^*_w z^2_w + 2 w_w B^*_w z_w + w_w D^*_w \tag{3.34}$$

$$\overline{D}'_{xy} = w_{f1} (A^*_{f1} z_{f1} + B^*_{f1}) y_{f1} + w_{f2} (A^*_{f2} z_{f2} + B^*_{f2}) y_{f2} \tag{3.35}$$

As we can see in Figure 3.45 the top and bottom flanges have 0.25 inches in width and contain 12 plies of 0.005 inches each one. The web is 0.5 inches wide and contains only 4 plies

of the same thickness. The stiffener is 10 inches long. First an isotropic material is used, and then a composite material is used; just as before. The material properties are the same from the previous sections. The layup for the flanges is $[\pm 45/0_2/-45/45]_s$ and for the web is $[\pm 45]_s$.

The FEM model was built in ANSYS with 41,861 nodes constrained as a cantilever beam. For the axial force, 1 lb was used and the free side was constrained to have the same axial deformation (rigid region). On the other hand, for the bending case, a moment of 0.56 lb-in was used. The results are presented in the following table.

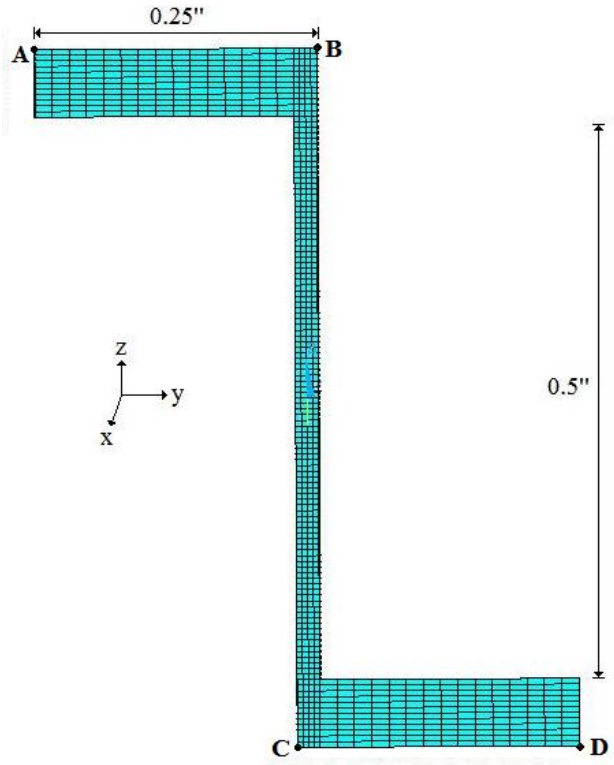

Figure 3.45 Z-stiffener dimensions

3.10.1 Stiffnesses Comparison

3.10.1.1 Isotropic Material

For isotropic material, Table 3.15 presents the results of the axial stiffness of the Z-stiffner. For the bending cases, Tables 3.16 and 3.17 lists the results for the bending stiffnesses and the curvatures.

Table 3.15 Axial stiffness of isotropic material Z-stiffener

FEM U_x [in]	FEM U_y [in]	FEM U_z [in]	FEM $\bar{A}_x$ [lb]	Theoretical $\bar{A}_x$ [lb]	Diff %	Eq. 3-11 $\bar{A}_x$ [lb]	Diff %
1.1845E-05	7.0018E-11	3.1290E-11	422,119	419,920	-0.52	419,920	-0.52

Table 3.16 Bending stiffness of isotropic material Z-stiffener

FEM U_x [in]	FEM U_y [in]	FEM U_z [in]	Th. $\bar{D}_x$ [lb-in²]	Eq. 3-16 $\bar{D}_x$ [lb-in²]	Diff %	Th. $\bar{D}_y$ [lb-in²]	Eq. 3-26 $\bar{D}_y$ [lb-in²]	Diff %	Th. $\bar{D}'_{xy}$ [lb-in²]	Eq. 2-25 $\bar{D}'_{xy}$ [lb-in²]	Diff %
-9.5400E-12	-1.3073E-03	-7.4756E-04	26,973	26,973	0.0	5,809	5,809	0.0	-10,141	-10,138	0.0

Table 3.17 Comparison of FEM and present method results of Z-stiffener

FEM Eq. 3-29 $\bar{D}'_{xy}$ [lb-in²]	Eq. 2-25 $\bar{D}'_{xy}$ [lb-in²]	Diff %	FEM k_x^c [1/in]	Eq. 3-36 k_x^c [1/in]	Diff %	FEM k_z^c [1/in]	Eq. 3-36 k_z^c [1/in]	Diff %
-10,239	-10,141	-1.0	5.980E-05	6.042E-05	1.0	1.046E-04	1.055E-04	0.8

The curvatures were compared as well through the following equations,

$$\kappa_x^c = \frac{\bar{M}_x^c \bar{D}_y}{\bar{D}_x \bar{D}_y - \bar{D}'^2_{xy}} \quad \text{and} \quad \kappa_z^c = \frac{-\bar{M}_x^c \bar{D}'_{xy}}{\bar{D}_x \bar{D}_y - \bar{D}'^2_{xy}} \tag{3.36}$$

3.10.1.2 Composite Material

For the composite cases, the layup is the following: for the flanges is $[\pm 45/0_2/\text{-}45/45]_s$ and for the web is $[\pm 45]_s$. The axial stiffness results are presented in Table 3.18. The bending stiffnesses are showed in Table 3.19 and the curvatures in Table 3.20. For the bending stiffnesses case, the results can not be read directly from the FEM model since there is coupling between them. Therefore, in order to compare them it was necessary to compare $\bar{D}'_{xy}$ which contains all of them (Eq. 3.29) and the curvatures (Eq. 3.36).

Table 3.18 Axial stiffness of composite material Z-stiffener

FEM U_x [in]	FEM U_y [in]	FEM U_z [in]	FEM $\overline{A}_x$ [lb]	Eq. 3-11 $\overline{A}_x$ [lb]	Diff %
1.7948E-05	-1.3583E-08	3.9978E-07	278,583	277,886	-0.25

Table 3.19 Bending stiffness of composite material Z-stiffener

FEM U_x [in]	FEM U_y [in]	FEM U_z [in]	Eq. 3-16 $\overline{D}_x$ [lb-in^2]	Eq. 3-26 $\overline{D}_y$ [lb-in^2]	Eq. 2-25 $\overline{D'}_{xy}$ [lb-in^2]	FEM Eq. 3-29 $\overline{D'}_{xy}$ [lb-in^2]	Diff %
-2.4375E-08	-1.9813E-03	-1.1297E-03	20,054	4,548	-7,943	-8,023	1.0

Table 3.20 Curvatures of composite material Z-stiffener

FEM k_x^0 [1/in]	Eq. 3-36 k_x^0 [1/in]	Diff %	FEM k_z^0 [1/in]	Eq. 3-36 k_z^0 [1/in]	Diff %
9.038E-05	9.064E-05	0.3	1.585E-04	1.583E-04	-0.1

3.10.2 Stress and Strain Comparison

3.10.2.1 Isotropic Material

For the isotropic case, the strains from Equation 3.28 were obtained and then multiplied by the Young's Modulus to calculate the stresses. These ones were compared with the FEM and theoretical results. This procedure was done for the point A, B, C, and D showed in Figure 3.45. All these results are listed in Table 3.20. All the results are very close to each other.

Table.3.20 Axial stresses of isotropic Z-stiffener

	y [in]	z [in]	Theoretical [psi]	Eq. 3-28 [psi]	Diff %	FEM [psi]	Diff %
A	-0.24	0.31	-69.13	-68.95	-0.3	-69.11	0.0
B	0.01	0.31	207.70	207.42	-0.1	207.91	0.1
C	-0.01	-0.31	-207.70	-207.42	-0.1	-207.91	0.1
D	0.24	-0.31	69.13	68.95	-0.3	69.11	0.0

3.10.2.2 Composite Material

For the composite case, the strains were obtained again from Equation 3.28. Since, it is not possible to calculate the stresses directly; the strains were used to perform the comparison. Table 3.21 contains the results. Once again, the results agree very well.

Table 3.21 Axial strains of composite Z-stiffener

	y	z	FEM	Eq. 3-28	Diff %
	[in]	[in]	[in/in]	[in/in]	
A	-0.24	0.31	-9.9654E-06	-9.8891E-06	-0.8
B	0.01	0.31	2.9800E-05	2.9667E-05	-0.4
C	-0.01	-0.31	-2.9792E-05	-2.9667E-05	-0.4
D	0.24	-0.31	9.9627E-06	9.8891E-06	-0.7

CHAPTER 4

LAMINATES BONDED SIDE BY SIDE

This chapter employs the concept used in Chapter 3; however, instead of bonding the laminates one on the top of the other, in this chapter, they are bonded side by side.

In this case the mid-planes of both laminates are at the same heights; therefore, instead of working with the centroids, the mid-planes will be used as a plane of reference.

The objective of this chapter is to calculate the equivalent axial and bending stiffnesses and the axial stress in each ply. Since the axial stress is the most significant stress present, it is the only stress consider.

All the beams on this chapter will be consider narrow beams.

4.1 Equivalent Axial Forces and Moments acting on each Laminate

To better understand the response of each laminate it is necessary to discompose the total applied load into two equivalent forces acting independently on each laminate as shown in Figure 4.1.

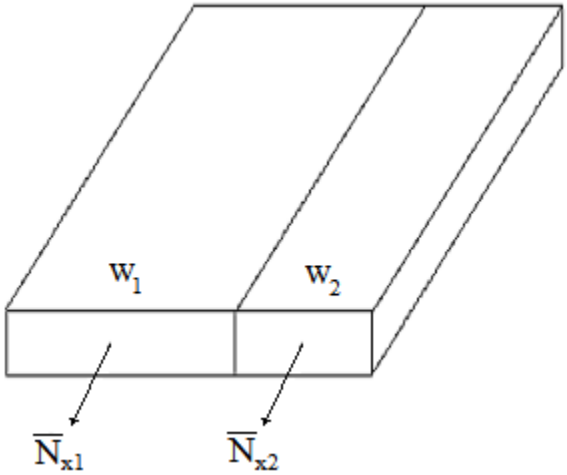

Figure 4.1 Total axial load discomposed into two loads acting on each laminate

Starting from the basis, the total axial load is the summation of the individual axial loads acting on each laminate.

$$\overline{N}_x = \overline{N}_{x1} + \overline{N}_{x2} \tag{4.1}$$

On the other hand, for narrow beams, these individual axial loads acting on each laminate can be related to the strain by Equation 2.30.

$$\overline{N}_x = w\left(\frac{d_{11}}{a_{11}d_{11} - b_{11}^2}\right)\varepsilon_x^0 \quad \rightarrow \quad \overline{N}_x = w\frac{1}{a^{**}}\varepsilon_x^0 \tag{4.2}$$

where, $a^{**} = \left(\frac{a_{11}d_{11} - b_{11}^2}{d_{11}}\right)$.

Substituting the last equation in Equation 4.1, and assuming that all the axial strains are equal; that is $\varepsilon_{x1}^o = \varepsilon_{x2}^o = \varepsilon_x^o$.

$$\overline{N}_x = \left(\frac{w_1}{a_1^{**}} + \frac{w_2}{a_2^{**}}\right)\varepsilon_x^o \qquad \rightarrow \qquad \overline{N}_x = \left(\frac{w_1 a_2^{**} + w_2 a_1^{**}}{a_1^{**} a_2^{**}}\right)\varepsilon_x^o \tag{4.3}$$

Now, substituting equation 4.2 for the second laminate, $\varepsilon_{x2}^0 = \frac{a_2^{**}\overline{N}_{x2}}{w_2}$, into 4.3,

$$\overline{N}_x = \left(\frac{w_1 a_2^{**} + w_2 a_1^{**}}{a_1^{**} w_2}\right)\overline{N}_{x2}$$

Rearranging for $\overline{N}_{x2}$,

$$\boxed{\overline{N}_{x2} = \overline{N}_x\left(\frac{a_1^{**} w_2}{w_1 a_2^{**} + w_2 a_1^{**}}\right)} \tag{4.4}$$

In an analogous manner, the axial force acting on the first laminate $\overline{N}_{x1}$ can be calculated as well.

$$\boxed{\overline{N}_{x1} = \overline{N}_x \left(\frac{a_2^{**} w_1}{w_1 a_2^{**} + w_2 a_1^{**}} \right)} \tag{4.5}$$

With $\overline{N}_{x1}$ and $\overline{N}_{x2}$ found, it is possible to treat each laminate individually with the equivalent axial load.

Similarly, for the bending case, the total applied moment can be decomposed into two equivalent moments acting on each laminate.

$$\overline{M}_x = \overline{M}_{x1} + \overline{M}_{x2} \tag{4.6}$$

On the other hand, for narrow beams, each of these individual moments acting on each laminate can be related to the curvature by Equation 2.31.

$$\overline{M}_x = w \left(\frac{a_{11}}{a_{11} d_{11} - b_{11}^2} \right) \kappa_x \quad \rightarrow \quad \overline{M}_x = w \frac{1}{d^{**}} \kappa_x \tag{4.7}$$

where, $d^{**} = \left(\frac{a_{11} d_{11} - b_{11}^2}{a_{11}} \right)$.

Substituting Equation 4.7 into 4.6, and assuming that all the curvatures are equal; that is $\kappa_{x1} = \kappa_{x2} = \kappa_x$.

$$\overline{M}_x = \left(\frac{w_1}{d_1^{**}} + \frac{w_2}{d_2^{**}} \right) \kappa_x \quad \rightarrow \quad \overline{M}_x = \left(\frac{w_1 d_2^{**} + w_2 d_1^{**}}{d_1^{**} d_2^{**}} \right) \kappa_x \tag{4.8}$$

Now, substituting Equation 4.7 for the second laminate, $\kappa_{x2} = \frac{d_2^{**} \overline{M}_{x2}}{w_2}$, into 4.8,

$$\overline{M}_x = \left(\frac{w_1 d_2^{**} + w_2 d_1^{**}}{d_1^{**} w_2} \right) \overline{M}_{x2} \tag{4.9}$$

Rearranging for $\overline{M}_{x2}$,

$$\boxed{\overline{M}_{x2} = \overline{M}_x \left(\frac{d_1^{**} w_2}{w_1 d_2^{**} + w_2 d_1^{**}} \right)} \tag{4.10}$$

In an analogous manner, the moment acting on the first laminate $\overline{M}_{x1}$ can be calculated as well.

$$\boxed{\overline{M}_{x1} = \overline{M}_x \left(\frac{d_2^{**} w_1}{w_1 d_2^{**} + w_2 d_1^{**}} \right)} \tag{4.11}$$

Once again, with $\overline{M}_{x1}$ and $\overline{M}_{x2}$ found, it is possible to treat each laminate individually with the equivalent applied moment.

4.2 Finite Element Model

A model was built in ANSYS to simulate the composite laminate. The model consists of 0.5 inches width laminate (left) bonded together side by side with a 0.25 inches width laminate (right). Both laminates have 12 plies of 0.005 inches thickness and were 10 inches long.

The element used was solid46, a 3D block element with 8 nodes and 3 degrees of freedom per node. The mesh generated for the model was 100 elements through the length, 24 elements through the width of the left laminate, 12 elements through the width of the right laminate, and 2 element per ply; therefore, a total of 93,425 nodes. The typical mesh is shown in Figure 4.2.

The axial load was applied as a pressure of 1 psi over all the surface of the free side. Because the cross-section area was 0.045 in^2, the total axial load was $\overline{N}_x = 0.045 \ lb$. The other side was constrained in all the directions as a cantilever beam.

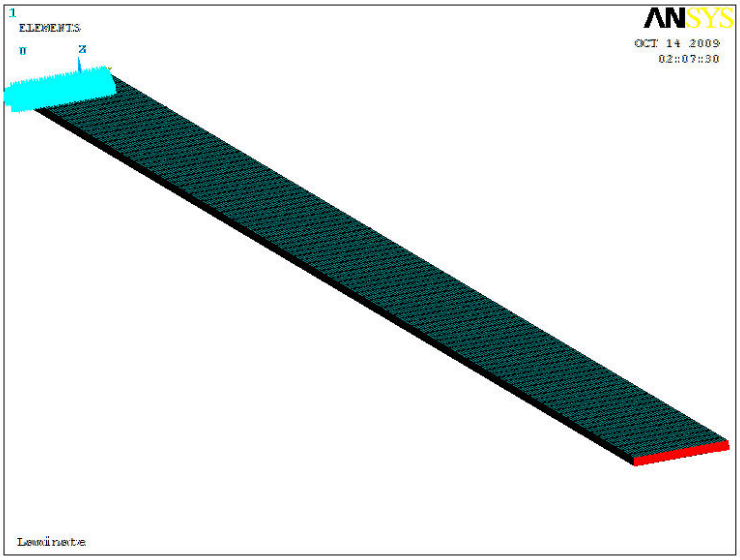

Figure 4.2 Mesh, loading, and boundary conditions of the model

For the bending case the loading was defined as follow. One side constrained in all the directions as a cantilever beam, just as before. The other side was loaded with a uniform outgoing force in the half top of the beam's cross-section. The half bottom was loaded with the same uniform force but inward (Fig. 4.3 and 4.4). The magnitude of the force was 0.1 lb per node and the total moment applied was calculated through the positions of all the nodes, $\overline{M}_x = 1.4330\ lb-in$.

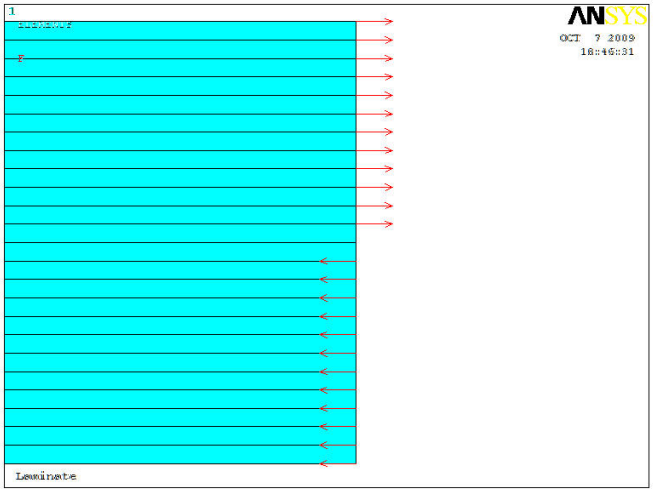

Figure 4.3 Lateral view of the loading for the bending case

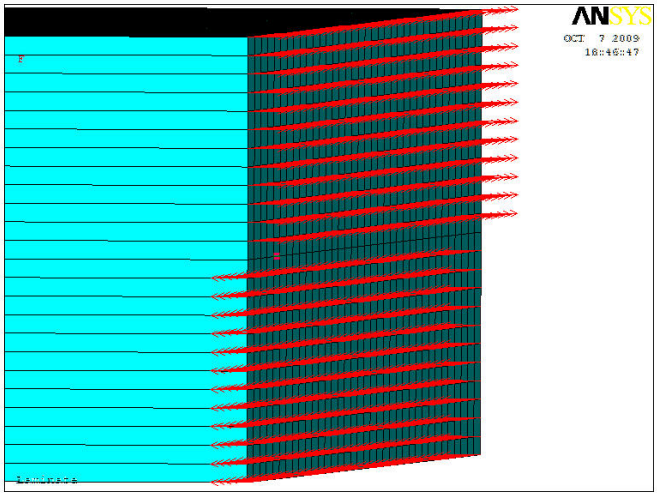

Figure 4.4 Perspective view of the loading for the bending case

4.3 Axial Stresses due to an Axial Loading and Bending

First an isotropic material was simulated in order to compare the results with the theoretical close-from solution. The isotropic material chosen was the same aluminum used in the previous chapter. As usually, the next step was to consider a composite material (it was used again the same composite material used in the previous chapter) with all the angle plies equal to 0° to avoid any shear deformation or undesired effe ct. Therefore, two laminates of $[0_6]_s$ were bonder together side by side. After that, two symmetric laminates were used $[\pm 45_2/0_2]_s$. Then, an anti-symmetric laminate $[\pm 45_2/0_4/\pm 45_2]_T$ were bonded with a symmetric laminate $[\pm 45_2/0_2]_s$. Finally, and un-balanced laminate $[45_4/0_2]_s$ and a symmetric laminate $[\pm 45_2/0_2]_s$ were bonded together. The results of these 5 cases are presented in the following section.

4.3.1 $\overline{N}_x$ acting on two Isotropic Laminates

The applied pressure to the cross-section was 1 psi. Therefore, the internal stress generated in each ply of each laminate is 1 psi as expected (Fig. 4.5). Both results were read half way through the length and width of each laminate. Table 4.1 lists the equivalent forces acting on each laminate and Table 4.2 shows the stresses acting on each ply of the laminates.

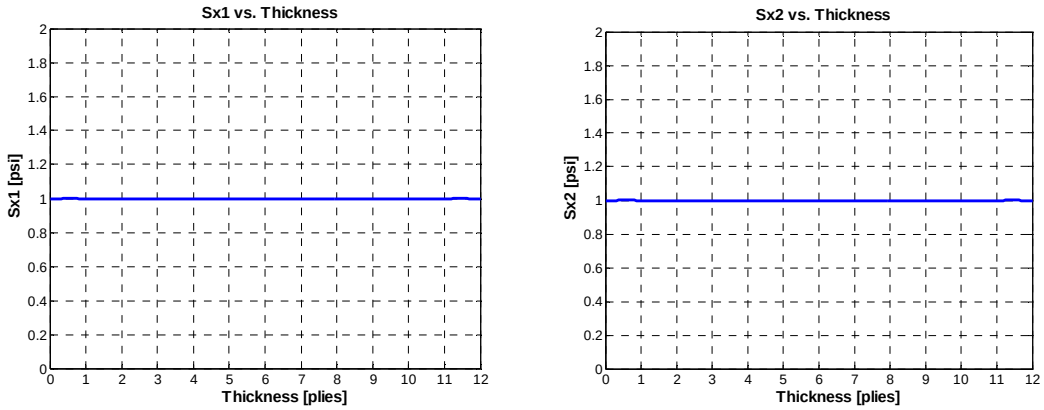

Figure 4.5 FEM axial stress through the thickness of each isotropic laminate

The total force applied to the model is 0.18 lb. a_1^{**} and a_2^{**} are calculated for each laminate using lamination theory. And $\overline{N}_{x1}$ and $\overline{N}_{x2}$ (Table 4.1) are calculating using Equations 4.4 and 4.5.

Table 4.1 Calculation of the equivalent axial load for each laminate

$\overline{N}_x$=	0.045	lb			
$(a_{11})_1$=	1.5876E-06	in/lb	$(a_{11})_2$=	1.5876E-06	in/lb
$(b_{11})_1$=	2.3327E-21	1/lb	$(b_{11})_2$=	2.3327E-21	1/lb
$(d_{11})_1$=	5.2920E-03	1/lb-in	$(d_{11})_2$=	5.2920E-03	1/lb-in
a^{**}_1=	1.5876E-06	in/lb	a^{**}_2=	1.5876E-06	in/lb
w_1=	0.5	in	w_2=	0.25	in
$\overline{N}_{x1}$=	0.030	lb	$\overline{N}_{x2}$=	0.015	lb

Table 4.2 Axial stresses in each isotropic-isotropic laminate

Laminate #1

			σ_x [psi]	%Diff
ply #12	ISO	FEM	1.00020	
		Present Method	1.00000	0.0
		Lamination Theory	1.00000	0.0
		Theoretical Sol.	1.00000	0.0
ply #11	ISO	FEM	1.00000	
		Present Method	1.00000	0.0
		Lamination Theory	1.00000	0.0
		Theoretical Sol.	1.00000	0.0
ply #10	ISO	FEM	0.99999	
		Present Method	1.00000	0.0
		Lamination Theory	1.00000	0.0
		Theoretical Sol.	1.00000	0.0
ply #9	ISO	FEM	0.99999	
		Present Method	1.00000	0.0
		Lamination Theory	1.00000	0.0
		Theoretical Sol.	1.00000	0.0
ply #8	ISO	FEM	1.00000	
		Present Method	1.00000	0.0
		Lamination Theory	1.00000	0.0
		Theoretical Sol.	1.00000	0.0
ply #7	ISO	FEM	1.00000	
		Present Method	1.00000	0.0
		Lamination Theory	1.00000	0.0
		Theoretical Sol.	1.00000	0.0
ply #6	ISO	FEM	1.00000	
		Present Method	1.00000	0.0
		Lamination Theory	1.00000	0.0
		Theoretical Sol.	1.00000	0.0
ply #5	ISO	FEM	1.00000	
		Present Method	1.00000	0.0
		Lamination Theory	1.00000	0.0
		Theoretical Sol.	1.00000	0.0
ply #4	ISO	FEM	1.00000	
		Present Method	1.00000	0.0
		Lamination Theory	1.00000	0.0
		Theoretical Sol.	1.00000	0.0
ply #3	ISO	FEM	1.00000	
		Present Method	1.00000	0.0
		Lamination Theory	1.00000	0.0
		Theoretical Sol.	1.00000	0.0
ply #2	ISO	FEM	1.00000	
		Present Method	1.00000	0.0
		Lamination Theory	1.00000	0.0
		Theoretical Sol.	1.00000	0.0
ply #1	ISO	FEM	1.00020	
		Present Method	1.00000	0.0
		Lamination Theory	1.00000	0.0
		Theoretical Sol.	1.00000	0.0

Laminate #2

			σ_x [psi]	%Diff
ply #12	ISO	FEM	1.00020	
		Present Method	1.00000	0.0
		Lamination Theory	1.00000	0.0
		Theoretical Sol.	1.00000	0.0
ply #11	ISO	FEM	1.00000	
		Present Method	1.00000	0.0
		Lamination Theory	1.00000	0.0
		Theoretical Sol.	1.00000	0.0
ply #10	ISO	FEM	0.99999	
		Present Method	1.00000	0.0
		Lamination Theory	1.00000	0.0
		Theoretical Sol.	1.00000	0.0
ply #9	ISO	FEM	0.99999	
		Present Method	1.00000	0.0
		Lamination Theory	1.00000	0.0
		Theoretical Sol.	1.00000	0.0
ply #8	ISO	FEM	1.00000	
		Present Method	1.00000	0.0
		Lamination Theory	1.00000	0.0
		Theoretical Sol.	1.00000	0.0
ply #7	ISO	FEM	1.00000	
		Present Method	1.00000	0.0
		Lamination Theory	1.00000	0.0
		Theoretical Sol.	1.00000	0.0
ply #6	ISO	FEM	1.00000	
		Present Method	1.00000	0.0
		Lamination Theory	1.00000	0.0
		Theoretical Sol.	1.00000	0.0
ply #5	ISO	FEM	1.00000	
		Present Method	1.00000	0.0
		Lamination Theory	1.00000	0.0
		Theoretical Sol.	1.00000	0.0
ply #4	ISO	FEM	1.00000	
		Present Method	1.00000	0.0
		Lamination Theory	1.00000	0.0
		Theoretical Sol.	1.00000	0.0
ply #3	ISO	FEM	1.00000	
		Present Method	1.00000	0.0
		Lamination Theory	1.00000	0.0
		Theoretical Sol.	1.00000	0.0
ply #2	ISO	FEM	1.00000	
		Present Method	1.00000	0.0
		Lamination Theory	1.00000	0.0
		Theoretical Sol.	1.00000	0.0
ply #1	ISO	FEM	1.00020	
		Present Method	1.00000	0.0
		Lamination Theory	1.00000	0.0
		Theoretical Sol.	1.00000	0.0

The finite element method axial stresses in each ply match perfectly with the present method results. At the same time, both the FEM model and the present method match with the theoretical solution and lamination theory results.

4.3.2 $\overline{N}_x$ acting on two $[0_6]_S$ Laminates

Two composite laminates of $[0_6]_s$ were bonded together side by side. Figure 4.6 show the stresses generated in each laminate. Once again the FEM results match with the close-form solution of 1 psi.

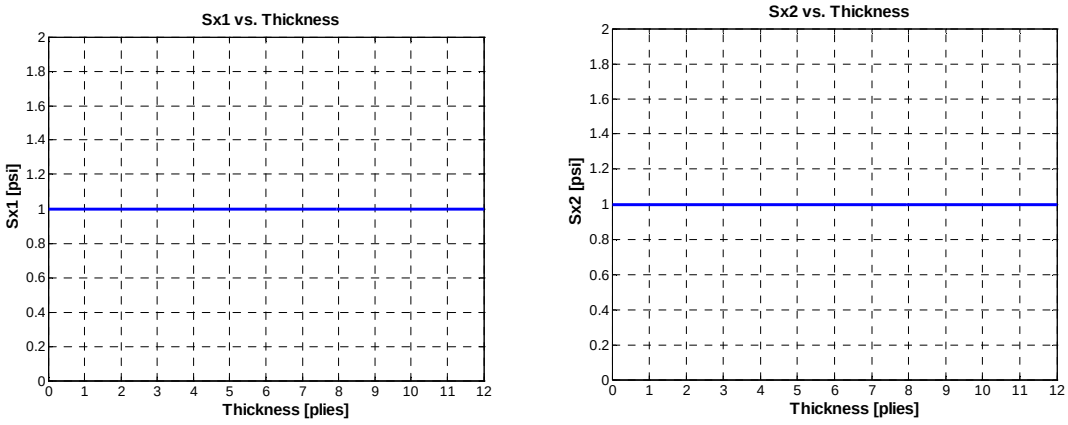

Figure 4.6 FEM axial stress through the thickness of $[0_6]_S$ laminates

a_1^{**}, a_2^{**}, $\overline{N}_{x1}$ and $\overline{N}_{x2}$ were calculated for each composite laminate. Table 4.3 shows the equivalent forces acting on each laminate and Table 4.4 lists the stresses experienced in the laminates.

Table 4.3 Calculation of the equivalent axial load for each laminate

$\overline{N}_x$=	0.045	lb			
$(a_{11})_1$=	9.1575E-07	in/lb	$(a_{11})_2$=	9.1575E-07	in/lb
$(b_{11})_1$=	2.5473E-21	1/lb	$(b_{11})_2$=	2.5473E-21	1/lb
$(d_{11})_1$=	3.0525E-03	1/lb-in	$(d_{11})_2$=	3.0525E-03	1/lb-in
a^{**}_1=	9.1575E-07	in/lb	a^{**}_2=	9.1575E-07	in/lb
w_1=	0.5	in	w_2=	0.25	in
$\overline{N}_{x1}$=	0.030	lb	$\overline{N}_{x2}$=	0.015	lb

Table 4.4 Axial stresses in each $[0_6]_s$-$[0_6]_s$ laminate

Laminate #1

			σ_x [psi]	%Diff
ply #12	0	FEM	1.00000	
		Present Method	1.00000	0.0
		Lamination Theory	1.00000	0.0
ply #11	0	FEM	1.00000	
		Present Method	1.00000	0.0
		Lamination Theory	1.00000	0.0
ply #10	0	FEM	1.00000	
		Present Method	1.00000	0.0
		Lamination Theory	1.00000	0.0
ply #9	0	FEM	1.00000	
		Present Method	1.00000	0.0
		Lamination Theory	1.00000	0.0
ply #8	0	FEM	1.00000	
		Present Method	1.00000	0.0
		Lamination Theory	1.00000	0.0
ply #7	0	FEM	1.00000	
		Present Method	1.00000	0.0
		Lamination Theory	1.00000	0.0
ply #6	0	FEM	1.00000	
		Present Method	1.00000	0.0
		Lamination Theory	1.00000	0.0
ply #5	0	FEM	1.00000	
		Present Method	1.00000	0.0
		Lamination Theory	1.00000	0.0
ply #4	0	FEM	1.00000	
		Present Method	1.00000	0.0
		Lamination Theory	1.00000	0.0
ply #3	0	FEM	1.00000	
		Present Method	1.00000	0.0
		Lamination Theory	1.00000	0.0
ply #2	0	FEM	1.00000	
		Present Method	1.00000	0.0
		Lamination Theory	1.00000	0.0
ply #1	0	FEM	1.00000	
		Present Method	1.00000	0.0
		Lamination Theory	1.00000	0.0

Laminate #2

			σ_x [psi]	%Diff
ply #12	0	FEM	1.00000	
		Present Method	1.00000	0.0
		Lamination Theory	1.00000	0.0
ply #11	0	FEM	1.00000	
		Present Method	1.00000	0.0
		Lamination Theory	1.00000	0.0
ply #10	0	FEM	1.00000	
		Present Method	1.00000	0.0
		Lamination Theory	1.00000	0.0
ply #9	0	FEM	1.00000	
		Present Method	1.00000	0.0
		Lamination Theory	1.00000	0.0
ply #8	0	FEM	1.00000	
		Present Method	1.00000	0.0
		Lamination Theory	1.00000	0.0
ply #7	0	FEM	1.00000	
		Present Method	1.00000	0.0
		Lamination Theory	1.00000	0.0
ply #6	0	FEM	1.00000	
		Present Method	1.00000	0.0
		Lamination Theory	1.00000	0.0
ply #5	0	FEM	1.00000	
		Present Method	1.00000	0.0
		Lamination Theory	1.00000	0.0
ply #4	0	FEM	1.00000	
		Present Method	1.00000	0.0
		Lamination Theory	1.00000	0.0
ply #3	0	FEM	1.00000	
		Present Method	1.00000	0.0
		Lamination Theory	1.00000	0.0
ply #2	0	FEM	1.00000	
		Present Method	1.00000	0.0
		Lamination Theory	1.00000	0.0
ply #1	0	FEM	1.00000	
		Present Method	1.00000	0.0
		Lamination Theory	1.00000	0.0

Once again the results match very well for all the plies in both composite laminates.

4.3.3 $\overline{N}_x$ acting on two $[\pm 45_2/0_2]_S$ Laminates

Now it is consider two symmetric laminates bonded together with angle plies of 45° to consider the effect of shear deformations. The results are shown in Figure 4.7.

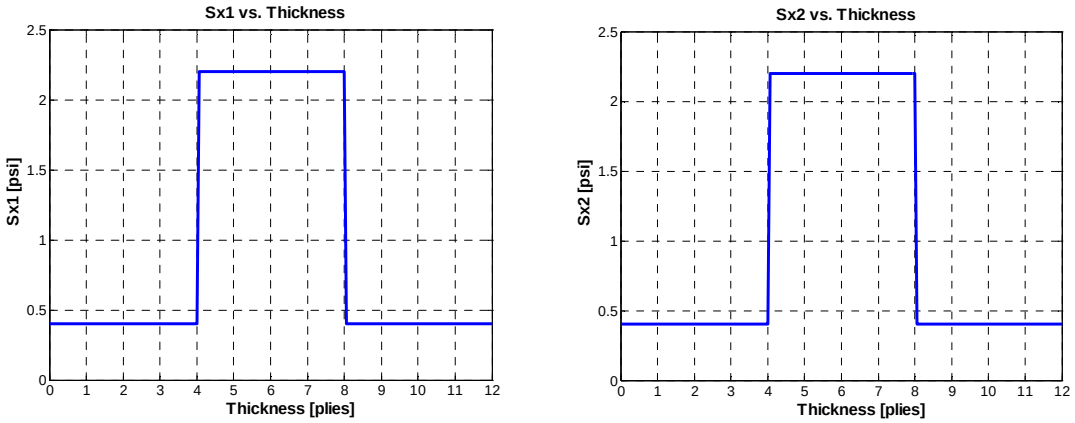

Figure 4.7 FEM axial stress through the thickness of $[\pm 45_2/0_2]_S$ laminates

In Figure 4.7, the 0° plies have higher axial stres s than the ±45° ones, since the first ones are stiffer than the second ones. Table 4.5 calculates a_1^{**}, a_2^{**}, and the equivalent axial loads for each laminate.

Table 4.5 Calculation of the equivalent axial load for each laminate

$\overline{N}_x$=	0.045	lb			
$(a_{11})_1$=	2.0268E-06	in/lb	$(a_{11})_2$=	2.0268E-06	in/lb
$(b_{11})_1$=	-4.3475E-22	1/lb	$(b_{11})_2$=	-4.3475E-22	1/lb
$(d_{11})_1$=	1.5143E-02	1/lb-in	$(d_{11})_2$=	1.5143E-02	1/lb-in
a^{**}_1=	2.0268E-06	in/lb	a^{**}_2=	2.0268E-06	in/lb
w_1=	0.5	in	w_2=	0.25	in
$\overline{N}_{x1}$=	0.030	lb	$\overline{N}_{x2}$=	0.015	lb

Table 4.6 lists the stresses present in the laminates.

Table 4.6 Axial stresses in each $[\pm 45_2/0_2]_S$ $[\pm 45_2/0_2]_S$ laminate

Laminate #1

			σ_x [psi]	%Diff
ply #12	45	FEM	0.40245	
		Present Method	0.40221	-0.1
		Lamination Theory	0.40221	-0.1
ply #11	-45	FEM	0.40243	
		Present Method	0.40221	-0.1
		Lamination Theory	0.40221	-0.1
ply #10	45	FEM	0.40247	
		Present Method	0.40221	-0.1
		Lamination Theory	0.40221	-0.1
ply #9	-45	FEM	0.40252	
		Present Method	0.40221	-0.1
		Lamination Theory	0.40221	-0.1
ply #8	0	FEM	2.19700	
		Present Method	2.19558	-0.1
		Lamination Theory	2.19558	-0.1
ply #7	0	FEM	2.19700	
		Present Method	2.19558	-0.1
		Lamination Theory	2.19558	-0.1
ply #6	0	FEM	2.19700	
		Present Method	2.19558	-0.1
		Lamination Theory	2.19558	-0.1
ply #5	0	FEM	2.19700	
		Present Method	2.19558	-0.1
		Lamination Theory	2.19558	-0.1
ply #4	-45	FEM	0.40252	
		Present Method	0.40221	-0.1
		Lamination Theory	0.40221	-0.1
ply #3	45	FEM	0.40247	
		Present Method	0.40221	-0.1
		Lamination Theory	0.40221	-0.1
ply #2	-45	FEM	0.40244	
		Present Method	0.40221	-0.1
		Lamination Theory	0.40221	-0.1
ply #1	45	FEM	0.40245	
		Present Method	0.40221	-0.1
		Lamination Theory	0.40221	-0.1

Laminate #2

			σ_x [psi]	%Diff
ply #12	45	FEM	0.40291	
		Present Method	0.40221	-0.2
		Lamination Theory	0.40221	-0.2
ply #11	-45	FEM	0.40281	
		Present Method	0.40221	-0.1
		Lamination Theory	0.40221	-0.1
ply #10	45	FEM	0.40278	
		Present Method	0.40221	-0.1
		Lamination Theory	0.40221	-0.1
ply #9	-45	FEM	0.40291	
		Present Method	0.40221	-0.2
		Lamination Theory	0.40221	-0.2
ply #8	0	FEM	2.19720	
		Present Method	2.19558	-0.1
		Lamination Theory	2.19558	-0.1
ply #7	0	FEM	2.19700	
		Present Method	2.19558	-0.1
		Lamination Theory	2.19558	-0.1
ply #6	0	FEM	2.19700	
		Present Method	2.19558	-0.1
		Lamination Theory	2.19558	-0.1
ply #5	0	FEM	2.19720	
		Present Method	2.19558	-0.1
		Lamination Theory	2.19558	-0.1
ply #4	-45	FEM	0.40290	
		Present Method	0.40221	-0.2
		Lamination Theory	0.40221	-0.2
ply #3	45	FEM	0.40279	
		Present Method	0.40221	-0.1
		Lamination Theory	0.40221	-0.1
ply #2	-45	FEM	0.40279	
		Present Method	0.40221	-0.1
		Lamination Theory	0.40221	-0.1
ply #1	45	FEM	0.40293	
		Present Method	0.40221	-0.2
		Lamination Theory	0.40221	-0.2

The present method results agree very well with the finite element and lamination theory results for all the plies including the 45°angle p lies.

4.3.4 $\overline{N}_x$ acting on [±45₂/0₄/±45₂]$_T$ and [±45₂/0₂]$_S$ Laminates

Now it is studied the effect of an anti-symmetric laminate bonded with a symmetric laminate. Once again, the 0° plies have much more axial stress than the ±45° ones as explained before. The results are presented in Figure 4.8.

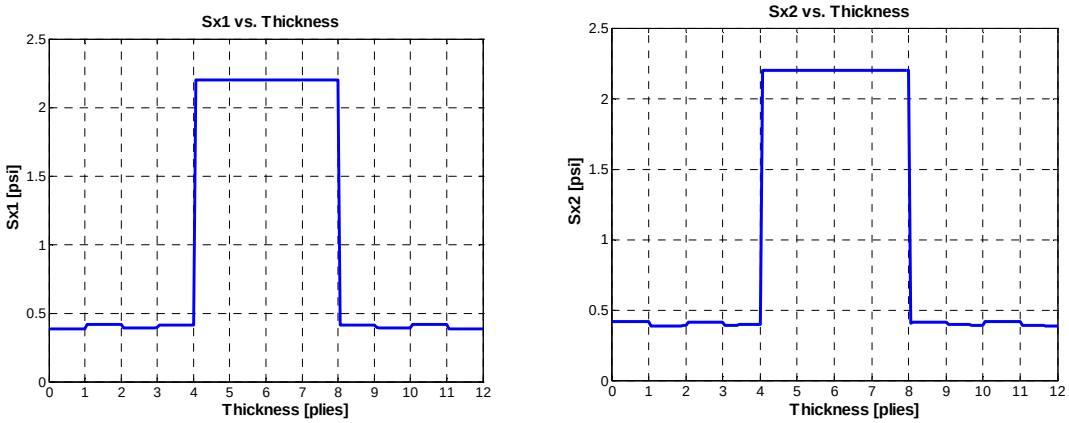

Figure 4.8 FEM axial stress through the thickness of [±45₂/0₄/±45₂]$_T$ and [±45₂/0₂]$_S$

a_1^{**}, a_2^{**}, $\overline{N}_{x1}$ and $\overline{N}_{x2}$ were calculated for each composite laminate. Table 4.7 shows the equivalent forces acting on each laminate and Table 4.8 lists the stresses experienced in the laminates.

Table 4.7 Calculation of the equivalent axial load for each laminate

$\overline{N}_x$=	0.045	lb			
$(a_{11})_1$=	2.0279E-06	in/lb	$(a_{11})_2$=	2.0268E-06	in/lb
$(b_{11})_1$=	-5.5748E-22	1/lb	$(b_{11})_2$=	-4.3475E-22	1/lb
$(d_{11})_1$=	1.5084E-02	1/lb-in	$(d_{11})_2$=	1.5143E-02	1/lb-in
a**$_1$=	2.0279E-06	in/lb	a**$_2$=	2.0268E-06	in/lb
w_1=	0.5	in	w_2=	0.25	in
$\overline{N}_{x1}$=	0.02999	lb	$\overline{N}_{x2}$=	0.01501	lb

a_1^{**} and a_2^{**} are not longer equal since they are two different types of laminates. Therefore, lamination theory can not be used in this case.

Table 4.8 Axial stresses in each $[\pm 45_2/0_4/\pm 45_2]_T$-$[\pm 45_2/0_2]_S$ laminate

Laminate #1

			σ_x [psi]	%Diff
ply #12	45	FEM	0.38570	
		Present Method	0.37837	-1.9
ply #11	-45	FEM	0.41833	
		Present Method	0.42447	1.5
ply #10	45	FEM	0.39225	
		Present Method	0.38759	-1.2
ply #9	-45	FEM	0.41187	
		Present Method	0.41525	0.8
ply #8	0	FEM	2.19800	
		Present Method	2.19615	-0.1
ply #7	0	FEM	2.19800	
		Present Method	2.19615	-0.1
ply #6	0	FEM	2.19790	
		Present Method	2.19615	-0.1
ply #5	0	FEM	2.19790	
		Present Method	2.19615	-0.1
ply #4	45	FEM	0.41183	
		Present Method	0.41525	0.8
ply #3	-45	FEM	0.39222	
		Present Method	0.38759	-1.2
ply #2	45	FEM	0.41828	
		Present Method	0.42447	1.5
ply #1	-45	FEM	0.38563	
		Present Method	0.37837	-1.9

Laminate #2

			σ_x [psi]	%Diff
ply #12	45	FEM	0.38903	
		Present Method	0.40248	3.5
ply #11	-45	FEM	0.41888	
		Present Method	0.40248	-3.9
ply #10	45	FEM	0.39413	
		Present Method	0.40248	2.1
ply #9	-45	FEM	0.41175	
		Present Method	0.40248	-2.3
ply #8	0	FEM	2.19820	
		Present Method	2.19704	-0.1
ply #7	0	FEM	2.19790	
		Present Method	2.19704	0.0
ply #6	0	FEM	2.19780	
		Present Method	2.19704	0.0
ply #5	0	FEM	2.19800	
		Present Method	2.19704	0.0
ply #4	-45	FEM	0.39415	
		Present Method	0.40248	2.1
ply #3	45	FEM	0.41174	
		Present Method	0.40248	-2.2
ply #2	-45	FEM	0.38669	
		Present Method	0.40248	4.1
ply #1	45	FEM	0.41722	
		Present Method	0.40248	-3.5

The results match well. As expected the 45° angle p lies have a larger error than the 0° angle plies. This is because there is not shear deformation in the last ones.

4.3.5 $\overline{N}_x$ acting on [45₄/0₂]$_S$ and [±45₂/0₂]$_S$ Laminates

Finally it is being considered an un-balanced laminate bonded together with a symmetric and balanced laminate (Fig. 4.9).

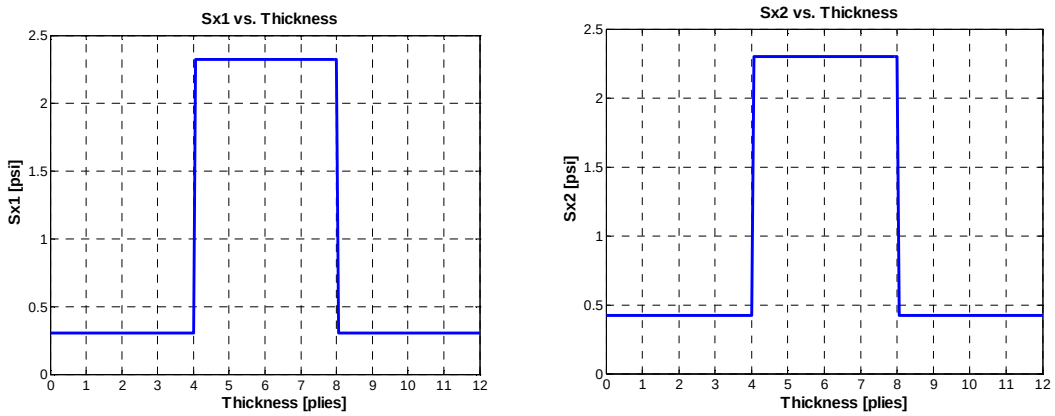

Figure 4.9 FEM axial stress through the thickness of [45₄/0₂]$_S$ and [±45₂/0₂]$_S$

Table 4.9 calculates a_1^{**}, a_2^{**}, and the equivalent axial loads for each laminate. Once again, a_1^{**} and a_2^{**} are different for each laminate.

Table 4.9 *Calculation of the equivalent axial load for each laminate*

$\overline{N}_x$=	0.045	lb			
$(a_{11})_1$=	2.1767E-06	in/lb	$(a_{11})_2$=	2.0268E-06	in/lb
$(b_{11})_1$=	1.4677E-20	1/lb	$(b_{11})_2$=	-4.3475E-22	1/lb
$(d_{11})_1$=	1.9797E-02	1/lb-in	$(d_{11})_2$=	1.5143E-02	1/lb-in
a^{**}_1=	2.1767E-06	in/lb	a^{**}_2=	2.0268E-06	in/lb
w_1=	0.5	in	w_2=	0.25	in
$\overline{N}_{x1}$=	0.02928	lb	$\overline{N}_{x2}$=	0.01572	lb

Table 4.10 lists the stresses present in the laminates.

Table 4.10 Axial stresses in each $[45_4/0_2]_S$-$[\pm 45_2/0_2]_S$ laminate

Laminate #1

			σ_x [psi]	%Diff
ply #12	45	FEM	0.30475	
		Present Method	0.30455	-0.1
ply #11	45	FEM	0.30474	
		Present Method	0.30455	-0.1
ply #10	45	FEM	0.30474	
		Present Method	0.30455	-0.1
ply #9	45	FEM	0.30468	
		Present Method	0.30455	0.0
ply #8	0	FEM	2.32030	
		Present Method	2.31890	-0.1
ply #7	0	FEM	2.32040	
		Present Method	2.31890	-0.1
ply #6	0	FEM	2.32040	
		Present Method	2.31890	-0.1
ply #5	0	FEM	2.32030	
		Present Method	2.31890	-0.1
ply #4	45	FEM	0.30468	
		Present Method	0.30455	0.0
ply #3	45	FEM	0.30474	
		Present Method	0.30455	-0.1
ply #2	45	FEM	0.30474	
		Present Method	0.30455	-0.1
ply #1	45	FEM	0.30475	
		Present Method	0.30455	-0.1

Laminate #2

			σ_x [psi]	%Diff
ply #12	45	FEM	0.42205	
		Present Method	0.42152	-0.1
ply #11	-45	FEM	0.42192	
		Present Method	0.42152	-0.1
ply #10	45	FEM	0.42191	
		Present Method	0.42152	-0.1
ply #9	-45	FEM	0.42194	
		Present Method	0.42152	-0.1
ply #8	0	FEM	2.30230	
		Present Method	2.30096	-0.1
ply #7	0	FEM	2.30220	
		Present Method	2.30096	-0.1
ply #6	0	FEM	2.30230	
		Present Method	2.30096	-0.1
ply #5	0	FEM	2.30220	
		Present Method	2.30096	-0.1
ply #4	-45	FEM	0.42193	
		Present Method	0.42152	-0.1
ply #3	45	FEM	0.42192	
		Present Method	0.42152	-0.1
ply #2	-45	FEM	0.42190	
		Present Method	0.42152	-0.1
ply #1	45	FEM	0.42207	
		Present Method	0.42152	-0.1

The present method results agree very well with the finite element results for all the plies. The next step is to consider the axial stresses due to bending for isotropic and composite laminates bonded together.

4.3.6 $\overline{M}_x$ acting on two Isotropic Laminates

Two isotropic laminate were bonded together under bending. The results are presented in Fig. 4.10.

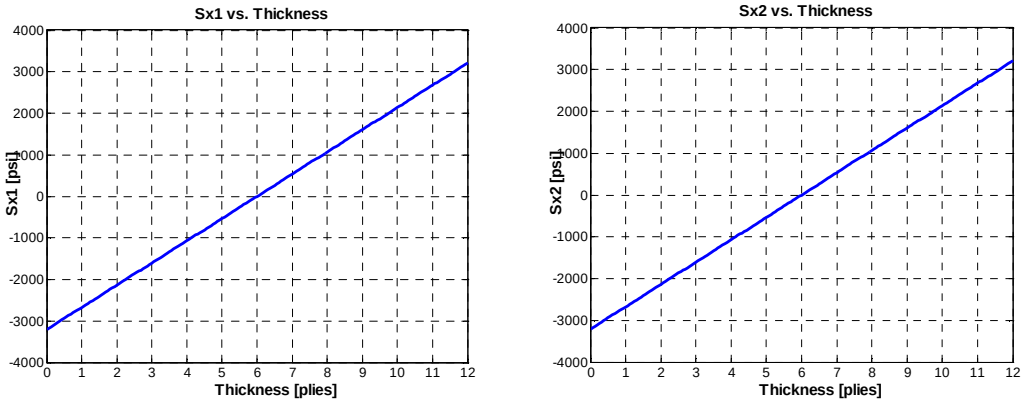

Figure 4.10 FEM axial stress through the thickness of each laminates

As expected the axial stress is a linear function. As explained earlier the applied moment is $\overline{M}_x = 1.4330\ lb-in$. The theoretical solution for the isotropic case is $\sigma_x = \frac{\overline{M}_x c}{I}$ (Table 4.12). d_1^{**} and d_2^{**} are calculated for each laminate using lamination theory and $\overline{M}_{x1}$ and $\overline{M}_{x2}$ are calculating through Equations 4.10 and 4.11. The results are shown in Table 4.11.

Table 4.11 Calculation of the equivalent moment for each laminate

$\overline{M}_x$=	1.4430	lb-in			
$(a_{11})_1$=	1.5876E-06	in/lb	$(a_{11})_2$=	1.5876E-06	in/lb
$(b_{11})_1$=	2.3327E-21	1/lb	$(b_{11})_2$=	2.3327E-21	1/lb
$(d_{11})_1$=	5.2920E-03	1/lb-in	$(d_{11})_2$=	5.2920E-03	1/lb-in
d^{**}_1=	5.2920E-03	1/lb-in	d^{**}_2=	5.2920E-03	1/lb-in
w_1=	0.5	in	w_2=	0.25	in
$\overline{M}_{x1}$=	0.9620	lb-in	$\overline{M}_{x2}$=	0.4810	lb-in

Table 4.12 Axial stresses in each ISO-ISO laminate

Laminate #1

			σ_x [psi]	%Diff
ply #12	ISO	FEM	2937.9	
		Present Method	2939.4	0.1
		Lamination Theory	2939.4	0.1
		Theoretical Sol.	2939.4	0.1
ply #11	ISO	FEM	2404.9	
		Present Method	2405.0	0.0
		Lamination Theory	2405.0	0.0
		Theoretical Sol.	2405.0	0.0
ply #10	ISO	FEM	1870.8	
		Present Method	1870.6	0.0
		Lamination Theory	1870.6	0.0
		Theoretical Sol.	1870.6	0.0
ply #9	ISO	FEM	1336.3	
		Present Method	1336.1	0.0
		Lamination Theory	1336.1	0.0
		Theoretical Sol.	1336.1	0.0
ply #8	ISO	FEM	802.0	
		Present Method	801.7	0.0
		Lamination Theory	801.7	0.0
		Theoretical Sol.	801.7	0.0
ply #7	ISO	FEM	267.8	
		Present Method	267.2	-0.2
		Lamination Theory	267.2	-0.2
		Theoretical Sol.	267.2	-0.2
ply #6	ISO	FEM	-267.8	
		Present Method	-267.2	-0.2
		Lamination Theory	-267.2	-0.2
		Theoretical Sol.	-267.2	-0.2
ply #5	ISO	FEM	-802.2	
		Present Method	-801.7	-0.1
		Lamination Theory	-801.7	-0.1
		Theoretical Sol.	-801.7	-0.1
ply #4	ISO	FEM	-1336.4	
		Present Method	-1336.1	0.0
		Lamination Theory	-1336.1	0.0
		Theoretical Sol.	-1336.1	0.0
ply #3	ISO	FEM	-1870.9	
		Present Method	-1870.6	0.0
		Lamination Theory	-1870.6	0.0
		Theoretical Sol.	-1870.6	0.0
ply #2	ISO	FEM	-2405.1	
		Present Method	-2405.0	0.0
		Lamination Theory	-2405.0	0.0
		Theoretical Sol.	-2405.0	0.0
ply #1	ISO	FEM	-2938.1	
		Present Method	-2939.4	0.0
		Lamination Theory	-2939.4	0.0
		Theoretical Sol.	-2939.4	0.0

Laminate #2

			σ_x [psi]	%Diff
ply #12	ISO	FEM	2937.9	
		Present Method	2939.4	0.1
		Lamination Theory	2939.4	0.1
		Theoretical Sol.	2939.4	0.1
ply #11	ISO	FEM	2404.9	
		Present Method	2405.0	0.0
		Lamination Theory	2405.0	0.0
		Theoretical Sol.	2405.0	0.0
ply #10	ISO	FEM	1870.8	
		Present Method	1870.6	0.0
		Lamination Theory	1870.6	0.0
		Theoretical Sol.	1870.6	0.0
ply #9	ISO	FEM	1336.3	
		Present Method	1336.1	0.0
		Lamination Theory	1336.1	0.0
		Theoretical Sol.	1336.1	0.0
ply #8	ISO	FEM	802.0	
		Present Method	801.7	0.0
		Lamination Theory	801.7	0.0
		Theoretical Sol.	801.7	0.0
ply #7	ISO	FEM	267.8	
		Present Method	267.2	-0.2
		Lamination Theory	267.2	-0.2
		Theoretical Sol.	267.2	-0.2
ply #6	ISO	FEM	-267.8	
		Present Method	-267.2	-0.2
		Lamination Theory	-267.2	-0.2
		Theoretical Sol.	-267.2	-0.2
ply #5	ISO	FEM	-802.2	
		Present Method	-801.7	-0.1
		Lamination Theory	-801.7	-0.1
		Theoretical Sol.	-801.7	-0.1
ply #4	ISO	FEM	-1336.4	
		Present Method	-1336.1	0.0
		Lamination Theory	-1336.1	0.0
		Theoretical Sol.	-1336.1	0.0
ply #3	ISO	FEM	-1870.9	
		Present Method	-1870.6	0.0
		Lamination Theory	-1870.6	0.0
		Theoretical Sol.	-1870.6	0.0
ply #2	ISO	FEM	-2405.1	
		Present Method	-2405.0	0.0
		Lamination Theory	-2405.0	0.0
		Theoretical Sol.	-2405.0	0.0
ply #1	ISO	FEM	-2938.1	
		Present Method	-2939.4	0.0
		Lamination Theory	-2939.4	0.0
		Theoretical Sol.	-2939.4	0.0

The finite element method axial stresses in each ply match perfectly with the present method, lamination theory, and theoretical solution. The next step is to consider composites.

4.3.7 $\overline{M}_x$ acting on two $[0_6]_S$ Laminates

Two composite laminates of $[0_6]_s$ bonded together side by side are studied under bending. Figure 4.11 shows the stresses generated in each laminate.

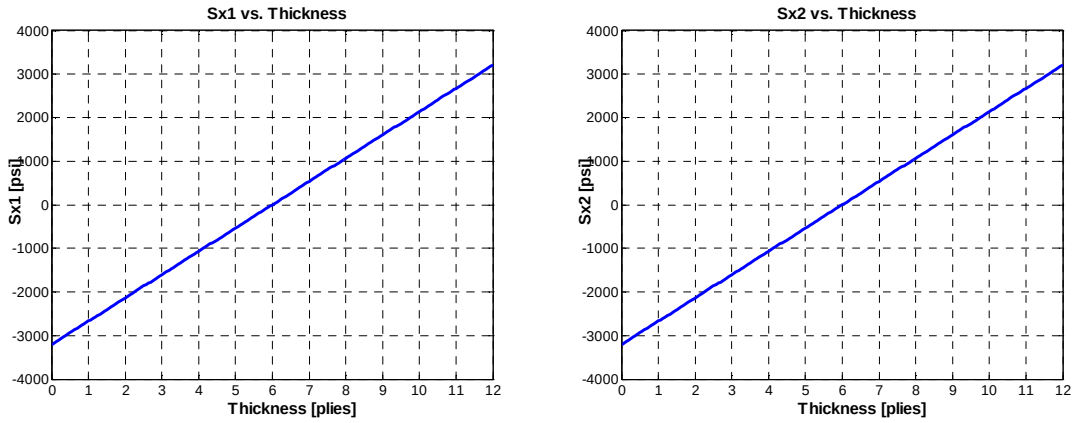

Figure 4.11 FEM axial stress through the thickness of each $[0_6]_S$ laminate

d_1^{**}, d_2^{**}, $\overline{M}_{x1}$ and $\overline{M}_{x2}$ were calculated for each composite laminate. Table 4.13 shows the equivalent moments acting on each laminate and Table 4.14 lists the stresses experienced in the laminates.

Table 4.13 Calculation of the equivalent moment for each laminate

$\overline{M}_x$=	1.4430	lb-in			
$(a_{11})_1$=	9.1575E-07	in/lb	$(a_{11})_2$=	9.1575E-07	in/lb
$(b_{11})_1$=	2.5473E-21	1/lb	$(b_{11})_2$=	2.5473E-21	1/lb
$(d_{11})_1$=	3.0525E-03	1/lb-in	$(d_{11})_2$=	3.0525E-03	1/lb-in
d^{**}_1=	3.0525E-03	1/lb-in	d^{**}_2=	3.0525E-03	1/lb-in
w_1=	0.5	in	w_2=	0.25	in
$\overline{M}_{x1}$=	0.9620	lb-in	$\overline{M}_{x2}$=	0.4810	lb-in

Table 4.14 Axial stresses in each $[0_6]_s$-$[0_6]_s$ laminate

Laminate #1

			σ_x [psi]	%Diff
ply #12	0	FEM	2939.3	
		Present Method	2939.4	0.0
		Lamination Theory	2939.4	0.0
ply #11	0	FEM	2404.9	
		Present Method	2405.0	0.0
		Lamination Theory	2405.0	0.0
ply #10	0	FEM	1870.5	
		Present Method	1870.6	0.0
		Lamination Theory	1870.6	0.0
ply #9	0	FEM	1336.1	
		Present Method	1336.1	0.0
		Lamination Theory	1336.1	0.0
ply #8	0	FEM	801.7	
		Present Method	801.7	0.0
		Lamination Theory	801.7	0.0
ply #7	0	FEM	267.2	
		Present Method	267.2	0.0
		Lamination Theory	267.2	0.0
ply #6	0	FEM	-267.2	
		Present Method	-267.2	0.0
		Lamination Theory	-267.2	0.0
ply #5	0	FEM	-801.7	
		Present Method	-801.7	0.0
		Lamination Theory	-801.7	0.0
ply #4	0	FEM	-1336.1	
		Present Method	-1336.1	0.0
		Lamination Theory	-1336.1	0.0
ply #3	0	FEM	-1870.5	
		Present Method	-1870.6	0.0
		Lamination Theory	-1870.6	0.0
ply #2	0	FEM	-2404.9	
		Present Method	-2405.0	0.0
		Lamination Theory	-2405.0	0.0
ply #1	0	FEM	-2939.3	
		Present Method	-2939.4	0.0
		Lamination Theory	-2939.4	0.0

Laminate #2

			σ_x [psi]	%Diff
ply #12	0	FEM	2939.3	
		Present Method	2939.4	0.0
		Lamination Theory	2939.4	0.0
ply #11	0	FEM	2404.9	
		Present Method	2405.0	0.0
		Lamination Theory	2405.0	0.0
ply #10	0	FEM	1870.5	
		Present Method	1870.6	0.0
		Lamination Theory	1870.6	0.0
ply #9	0	FEM	1336.1	
		Present Method	1336.1	0.0
		Lamination Theory	1336.1	0.0
ply #8	0	FEM	801.7	
		Present Method	801.7	0.0
		Lamination Theory	801.7	0.0
ply #7	0	FEM	267.2	
		Present Method	267.2	0.0
		Lamination Theory	267.2	0.0
ply #6	0	FEM	-267.2	
		Present Method	-267.2	0.0
		Lamination Theory	-267.2	0.0
ply #5	0	FEM	-801.7	
		Present Method	-801.7	0.0
		Lamination Theory	-801.7	0.0
ply #4	0	FEM	-1336.1	
		Present Method	-1336.1	0.0
		Lamination Theory	-1336.1	0.0
ply #3	0	FEM	-1870.5	
		Present Method	-1870.6	0.0
		Lamination Theory	-1870.6	0.0
ply #2	0	FEM	-2404.9	
		Present Method	-2405.0	0.0
		Lamination Theory	-2405.0	0.0
ply #1	0	FEM	-2939.3	
		Present Method	-2939.4	0.0
		Lamination Theory	-2939.4	0.0

Once again the results match very well for all the plies in both $[0_6]_s$ composite laminates.

4.3.8 $\overline{M}_x$ acting on two $[\pm 45_2/0_2]_S$ Laminates

Now it is consider two symmetric $[\pm 45_2/0_2]_S$ laminates bonded together under bending. Figure 4.12 presents the stresses experience in each laminate.

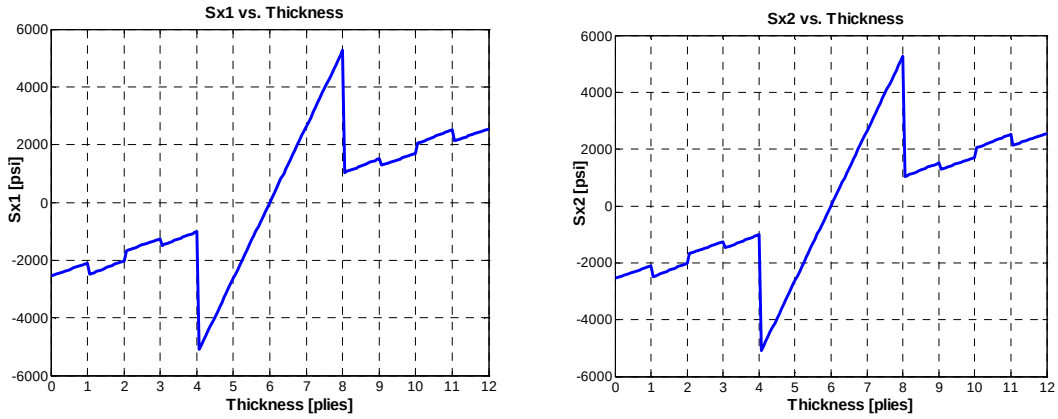

Figure 4.12 FEM axial stress through the thickness of $[\pm 45_2/0_2]_S$ laminates

Once again, the axial stress is a linear function with jumps according to the stacking sequence which makes perfectly sense. The 0° plies have much more axial stress than the ±45° ones, because the first ones are stiffer than the second ones. Table 4.15 shows the equivalent moment acting on each laminate, and Table 4.16 lists the stresses generated in the laminates.

Table 4.15 Calculation of the equivalent moment for each laminate

$\overline{M}_x$=	1.4430	lb-in			
$(a_{11})_1$=	2.0268E-06	in/lb	$(a_{11})_2$=	2.0268E-06	in/lb
$(b_{11})_1$=	-4.3475E-22	1/lb	$(b_{11})_2$=	-4.3475E-22	1/lb
$(d_{11})_1$=	1.5143E-02	1/lb-in	$(d_{11})_2$=	1.5143E-02	1/lb-in
d^{**}_1=	1.5143E-02	1/lb-in	d^{**}_2=	1.5143E-02	1/lb-in
w_1=	0.5	in	w_2=	0.25	in
$\overline{M}_{x1}$=	0.9620	lb-in	$\overline{M}_{x2}$=	0.4810	lb-in

Table 4.16 Axial stresses in each $[\pm 45_2/0_2]_S$ -$[\pm 45_2/0_2]_S$ laminate

Laminate #1			σ_x [psi]	%Diff
ply #12	45	FEM	2324.0	
		Present Method	2327.3	0.1
		Lamination Theory	2327.3	0.1
ply #11	-45	FEM	2270.3	
		Present Method	2264.1	-0.3
		Lamination Theory	2264.1	-0.3
ply #10	45	FEM	1479.6	
		Present Method	1481.0	0.1
		Lamination Theory	1481.0	0.1
ply #9	-45	FEM	1261.6	
		Present Method	1257.8	-0.3
		Lamination Theory	1257.8	-0.3
ply #8	0	FEM	3946.1	
		Present Method	3942.5	-0.1
		Lamination Theory	3942.5	-0.1
ply #7	0	FEM	1315.3	
		Present Method	1314.2	-0.1
		Lamination Theory	1314.2	-0.1
ply #6	0	FEM	-1315.4	
		Present Method	-1314.2	-0.1
		Lamination Theory	-1314.2	-0.1
ply #5	0	FEM	-3946.1	
		Present Method	-3942.5	-0.1
		Lamination Theory	-3942.5	-0.1
ply #4	-45	FEM	-1261.6	
		Present Method	-1257.8	-0.3
		Lamination Theory	-1257.8	-0.3
ply #3	45	FEM	-1479.6	
		Present Method	-1481.0	0.1
		Lamination Theory	-1481.0	0.1
ply #2	-45	FEM	-2270.3	
		Present Method	-2264.1	-0.3
		Lamination Theory	-2264.1	-0.3
ply #1	45	FEM	-2324.0	
		Present Method	-2327.3	0.1
		Lamination Theory	-2327.3	0.1

Laminate #2			σ_x [psi]	%Diff
ply #12	45	FEM	2324.0	
		Present Method	2327.3	0.1
		Lamination Theory	2327.3	0.1
ply #11	-45	FEM	2270.3	
		Present Method	2264.1	-0.3
		Lamination Theory	2264.1	-0.3
ply #10	45	FEM	1479.6	
		Present Method	1481.0	0.1
		Lamination Theory	1481.0	0.1
ply #9	-45	FEM	1261.6	
		Present Method	1257.8	-0.3
		Lamination Theory	1257.8	-0.3
ply #8	0	FEM	3946.1	
		Present Method	3942.5	-0.1
		Lamination Theory	3942.5	-0.1
ply #7	0	FEM	1315.3	
		Present Method	1314.2	-0.1
		Lamination Theory	1314.2	-0.1
ply #6	0	FEM	-1315.4	
		Present Method	-1314.2	-0.1
		Lamination Theory	-1314.2	-0.1
ply #5	0	FEM	-3946.1	
		Present Method	-3942.5	-0.1
		Lamination Theory	-3942.5	-0.1
ply #4	-45	FEM	-1261.6	
		Present Method	-1257.8	-0.3
		Lamination Theory	-1257.8	-0.3
ply #3	45	FEM	-1479.6	
		Present Method	-1481.0	0.1
		Lamination Theory	-1481.0	0.1
ply #2	-45	FEM	-2270.3	
		Present Method	-2264.1	-0.3
		Lamination Theory	-2264.1	-0.3
ply #1	45	FEM	-2324.0	
		Present Method	-2327.3	0.1
		Lamination Theory	-2327.3	0.1

The present method results agree very well with the finite element results for all the plies including the 45° angle plies.

4.3.9 $\overline{M}_x$ acting on $[\pm 45_2/0_4/\pm 45_2]_T$ and $[\pm 45_2/0_2]_S$ Laminates

Now it is studied the effect of an anti-symmetric laminate bonded with a symmetric laminate under bending. The stresses are shown in Figure 4.13.

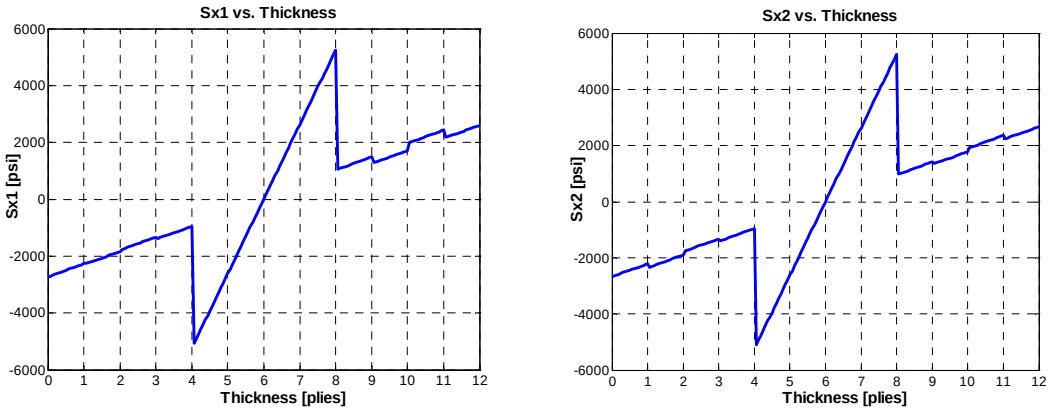

Figure 4.13 FEM axial stress through the thickness of $[\pm 45_2/0_4/\pm 45_2]_T$ laminates

d_1^{**} and d_2^{**} are calculated for each laminate using lamination theory and $\overline{M}_{x1}$ and $\overline{M}_{x2}$ are calculating through Equations 4.10 and 4.11. The results are shown in Table 4.17. Table 4.18 presents the stresses experienced in each laminate.

Table 4.17 Calculation of the equivalent moment for each laminate

$\overline{M}_x$=	1.4430	lb-in			
$(a_{11})_1$=	2.0279E-06	in/lb	$(a_{11})_2$=	2.0268E-06	in/lb
$(b_{11})_1$=	-5.5748E-22	1/lb	$(b_{11})_2$=	-4.3475E-22	1/lb
$(d_{11})_1$=	1.5084E-02	1/lb-in	$(d_{11})_2$=	1.5143E-02	1/lb-in
d^{**}_1=	1.5084E-02	1/lb-in	d^{**}_2=	1.5143E-02	1/lb-in
w_1=	0.5	in	w_2=	0.25	in
$\overline{M}_{x1}$=	0.963242	lb-in	$\overline{M}_{x2}$=	0.481172	lb-in

Table 4.18 Axial stresses in each $[\pm 45_2/0_4/\pm 45_2]_T$ - $[\pm 45_2/0_2]_S$ laminate

Laminate #1

			σ_x [psi]	%Diff
ply #12	45	FEM	2370.9	
		Present Method	2436.8	2.8
ply #11	-45	FEM	2196.6	
		Present Method	2134.5	-2.8
ply #10	45	FEM	1482.8	
		Present Method	1522.6	2.7
ply #9	-45	FEM	1256.9	
		Present Method	1220.3	-2.9
ply #8	0	FEM	3935.2	
		Present Method	3931.6	-0.1
ply #7	0	FEM	1312.9	
		Present Method	1310.5	-0.2
ply #6	0	FEM	-1309.3	
		Present Method	-1310.5	0.1
ply #5	0	FEM	-3931.6	
		Present Method	-3931.6	0.0
ply #4	45	FEM	-1184.9	
		Present Method	-1220.3	3.0
ply #3	-45	FEM	-1563.5	
		Present Method	-1522.6	-2.6
ply #2	45	FEM	-2073.6	
		Present Method	-2134.5	2.9
ply #1	-45	FEM	-2502.5	
		Present Method	-2436.8	-2.6

Laminate #2

			σ_x [psi]	%Diff
ply #12	45	FEM	2441.5	
		Present Method	2328.1	-4.6
ply #11	-45	FEM	2127.5	
		Present Method	2264.9	6.5
ply #10	45	FEM	1552.8	
		Present Method	1481.5	-4.6
ply #9	-45	FEM	1183.2	
		Present Method	1258.3	6.3
ply #8	0	FEM	3931.8	
		Present Method	3943.9	0.3
ply #7	0	FEM	1309.1	
		Present Method	1314.6	0.4
ply #6	0	FEM	-1313.1	
		Present Method	-1314.6	0.1
ply #5	0	FEM	-3936.0	
		Present Method	-3943.9	0.2
ply #4	-45	FEM	-1183.4	
		Present Method	-1258.3	6.3
ply #3	45	FEM	-1553.0	
		Present Method	-1481.5	-4.6
ply #2	-45	FEM	-2127.5	
		Present Method	-2264.9	6.5
ply #1	45	FEM	-2441.8	
		Present Method	-2328.1	-4.7

The results match well. As expected the 45° angle p lies have a larger error than the 0° angle plies. This is because there is not shear deformation in the last ones.

4.3.10 $\overline{M}_x$ acting on $[45_4/0_2]_S$ and $[\pm 45_2/0_2]_S$ Laminates

Finally it is being considered an un-balanced laminate bonded together with a symmetric and balanced laminate under bending. Figure 4.14 presents the results.

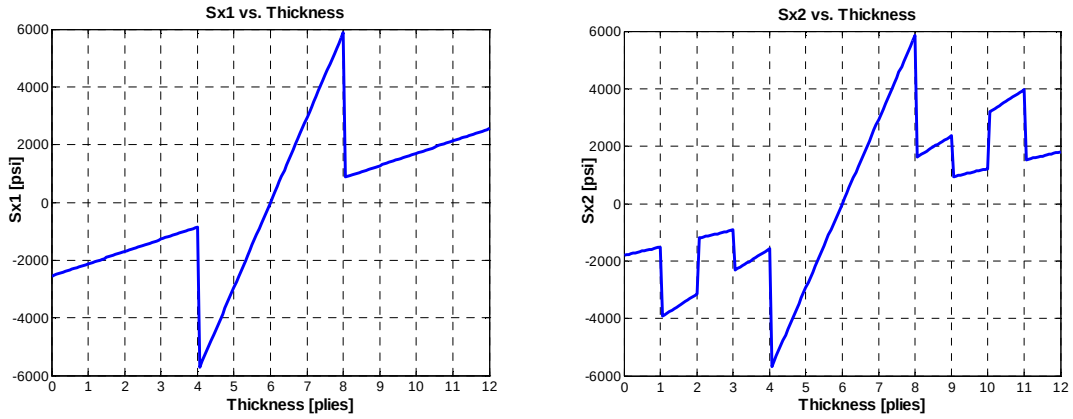

Figure 4.14 FEM axial stress through the thickness of $[45_4/0_2]_S$ laminates

Table 4.19 shows the equivalent moment acting on each laminate, and Table 4.20 lists the stresses generated in the laminates.

Table 4.19 Calculation of the equivalent moment for each laminate

$\overline{M}_x$=	1.4430	lb-in			
$(a_{11})_1$=	2.1767E-06	in/lb	$(a_{11})_2$=	2.0268E-06	in/lb
$(b_{11})_1$=	1.4677E-20	1/lb	$(b_{11})_2$=	-4.3475E-22	1/lb
$(d_{11})_1$=	1.9797E-02	1/lb-in	$(d_{11})_2$=	1.5143E-02	1/lb-in
d^{**}_1=	1.9797E-02	1/lb-in	d^{**}_2=	1.5143E-02	1/lb-in
w_1=	0.5	in	w_2=	0.25	in
$\overline{M}_{x1}$=	0.872601	lb-in	$\overline{M}_{x2}$=	0.504139	lb-in

Table 4.20 Axial stresses in each laminate $[45_4/0_2]_S$-$[\pm 45_2/0_2]_S$

Laminate #1

			σ_x [psi]	%Diff
ply #12	45	FEM	2338.5	
		Present Method	2102.8	-10.1
ply #11	45	FEM	1913.8	
		Present Method	1720.5	-10.1
ply #10	45	FEM	1488.8	
		Present Method	1338.2	-10.1
ply #9	45	FEM	1063.5	
		Present Method	955.8	-10.1
ply #8	0	FEM	4408.7	
		Present Method	4722.5	7.1
ply #7	0	FEM	1469.5	
		Present Method	1574.2	7.1
ply #6	0	FEM	-1469.6	
		Present Method	-1574.2	7.1
ply #5	0	FEM	-4408.7	
		Present Method	-4722.5	7.1
ply #4	45	FEM	-1063.5	
		Present Method	-955.8	-10.1
ply #3	45	FEM	-1488.8	
		Present Method	-1338.2	-10.1
ply #2	45	FEM	-1913.9	
		Present Method	-1720.5	-10.1
ply #1	45	FEM	-2338.5	
		Present Method	-2102.8	-10.1

Laminate #2

			σ_x [psi]	%Diff
ply #12	45	FEM	1657.2	
		Present Method	2439.3	47.2
ply #11	-45	FEM	3564.0	
		Present Method	2373.0	-33.4
ply #10	45	FEM	1068.0	
		Present Method	1552.3	45.3
ply #9	-45	FEM	1968.8	
		Present Method	1318.3	-33.0
ply #8	0	FEM	4388.9	
		Present Method	4132.1	-5.9
ply #7	0	FEM	1463.0	
		Present Method	1377.4	-5.9
ply #6	0	FEM	-1463.1	
		Present Method	-1377.4	-5.9
ply #5	0	FEM	-2926.2	
		Present Method	-4132.1	41.2
ply #4	-45	FEM	-1968.8	
		Present Method	-1318.3	-33.0
ply #3	45	FEM	-1068.1	
		Present Method	-1552.3	45.3
ply #2	-45	FEM	-3563.8	
		Present Method	-2373.0	-33.4
ply #1	45	FEM	-1657.2	
		Present Method	-2439.3	47.2

The results diverge comparing with the finite element results.

4.4 Axial Stiffness

The axial stiffness can be obtained as follow. From Equation 4.1,

$$\overline{N}_x = \overline{N}_{x1} + \overline{N}_{x2}$$

On the other hand, the axial strain can be related to the actual applied force (Eq. 4.2), $\overline{N}_x = \frac{w}{a^{**}}\varepsilon_x^o$; substituting this in the previous equation and since all the axial strains are equal $(\varepsilon_{x1}^o = \varepsilon_{x2}^o = \varepsilon_x^o)$,

$$\varepsilon_x^o = \frac{a^{**}}{w}\left[\frac{w_1}{a_1^{**}} + \frac{w_2}{a_2^{**}}\right]\varepsilon_x^o \tag{4.12}$$

From Equation 4.12 it is possible to extract that,

$$\boxed{\frac{1}{a^{**}} = \frac{v_1}{a_1^{**}} + \frac{v_2}{a_2^{**}}} \tag{4.13}$$

where $v_1 = w_1 / w$ and $v_2 = w_2 / w$. For a symmetric layup, a^{**} reduces to a_{11}.

4.5 Bending Stiffness

A similar procedure can be used to obtain the equivalent bending stiffness. From Equation 4.6,

$$\overline{M}_x = \overline{M}_{x1} + \overline{M}_{x2}$$

On the other hand, the curvature can be related to the actual applied moment (Eq. 4.7), $\overline{M}_x = \frac{w}{d^{**}}\kappa_x$; substituting this in the previous equation and since all the curvatures are equal ($\kappa_{x1} = \kappa_{x2} = \kappa_x$),

$$\kappa_x = \frac{d^{**}}{w}\left[\frac{w_1}{d_1^{**}} + \frac{w_2}{d_2^{**}}\right]\kappa_x \tag{4.14}$$

From the previous equation it is possible to extract that,

$$\boxed{\frac{1}{d^{**}} = \frac{v_1}{d_1^{**}} + \frac{v_2}{d_2^{**}}} \tag{4.15}$$

where $v_1 = w_1 / w$ and $v_2 = w_2 / w$. For a symmetric layup, d^{**} reduces to d_{11}.

4.6 Comparison of the Axial and Bending Stiffnesses

The axial stiffnesses can be extracted from Equation 4.2, $\overline{N}_x = w\frac{1}{a^{**}}\varepsilon_x^0$. The equivalent a^{**} for the two laminates can be calculated with the help of Equation 4.13.

$$\boxed{\overline{A}_x = \frac{w}{a^{**}}} \tag{4.16}$$

It is important to highlight that if the layup is symmetric, Equation 4.16 and 4.13 become

$$\overline{A}_x^{Sym} = \frac{w}{a_{11}} \quad \text{and} \quad \frac{1}{a_{11}} = \frac{v_1}{(a_{11})_1} + \frac{v_2}{(a_{11})_2}$$

A similar procedure can be used to extract the bending stiffness from Equation 4.7, $\overline{M}_x = w\frac{1}{d^{**}}\kappa_x$. The equivalent d^{**} for the two laminates is calculated through Equation 4.15.

$$\boxed{\overline{D}_x = \frac{w}{d^{**}}} \tag{4.17}$$

Once again, if the layup is symmetric, Equation 4.17 and 4.15 reduces to,

$$\overline{D}_x^{Sym} = \frac{w}{d_{11}} \quad \text{and} \quad \frac{1}{d_{11}} = \frac{v_1}{(d_{11})_1} + \frac{v_2}{(d_{11})_2}$$

The axial stiffnesses were calculated from the FEM model multiplying the applied load by the length and dividing by the axial displacement. To avoid distortions of the results by the boundary conditions or the applied load, the results were read half way through the length of the beam; that is at L/2. And in the bonding between the two laminates.

$$\overline{A}_x = \frac{FL}{2(U_{x|at\ x=L/2})}$$

The bending stiffnesses were calculated from the FEM model by first determining the curvature of the beam, and then dividing the applied moment by it.

$$\overline{M}_x = \overline{D}_x \kappa_x \quad \rightarrow \quad \overline{D}_x = \frac{\overline{M}_x}{\kappa_x}$$

All the results are listed in Table 4.21. First an isotropic material was used to be able to calculate the axial and bending stiffnesses by theoretical solution. The results matched very well. When possible, the results were compared to the smeared property approach. For the isotropic and $[0_6]_s$ cases the results converge but for the $[\pm 45_2/0_2]_s$ the smeared property results diverge for the bending stiffness. For the other cases, it is not possible to use the smeared property approach. On the other hand, the present method can be use in all the cases and the results agree with the finite element results.

Table 4.21 Axial and bending stiffnesses of two laminates bonded side by side

			units	Present Method	FEM	Diff%	Smeared Prop. Approach	Diff%	Theoretical Solution	Diff%
ISO	ISO	$\overline{A}_x$	[lb]	472,410	474,133	0.4	472,410	0.0	472,410	0.0
		$\overline{D}_x$	[lb-in²]	141.7	144.3	1.8	141.7	0.0	141.7	0.0
$[0_6]_s$	$[0_6]_s$	$\overline{A}_x$	[lb]	819,000	819,195	0.0	819,000	0.0	819,000	0.0
		$\overline{D}_x$	[lb-in²]	245.7	245.9	0.1	245.7	0.0	245.7	0.0
$[\pm 45_2/0_2]_s$	$[\pm 45_2/0_2]_s$	$\overline{A}_x$	[lb]	370,035	371,882	0.5	370,035	0.0	N/A	
		$\overline{D}_x$	[lb-in²]	49.5	53.2	6.9	111.0	124.1		
$[\pm 45_2/0_4/\pm 45_2]_T$	$[\pm 45_2/0_2]_s$	$\overline{A}_x$	[lb]	369,902	371,796	0.5	N/A		N/A	
		$\overline{D}_x$	[lb-in²]	49.7	53.1	6.6				
$[45_4/0_2]_s$	$[\pm 45_2/0_2]_s$	$\overline{A}_x$	[lb]	353,051	357,444	1.2	N/A		N/A	
		$\overline{D}_x$	[lb-in²]	41.8	47.9	12.9				

CHAPTER 5

ARBITRARY CLOSED CROSS-SECTION BEAM

The idea of this chapter is to develop a closed-form method able to calculate the axial and bending stiffnesses of an arbitrary closed cross-section beam. Some attempts have been done in this area for specific cross-section as circular, elliptical, or hat [38-41]. However, the present method will generalize the parametrization to include any cross-section. The results will be compared to smeared property, previous methods, and FEM results.

5.1 Smeared Property Approach

As presented in Chapter 2, smeared property approach is a widely used procedure to calculate the stiffnesses of a composite beam with certain cross-section. A equivalent averaged Young's Modulus of the material and lay-up is calculated and then multiplied by the area or the inertia in order to calculate the axial (Eq. 2.25) or bending stiffness (Eq. 2.26), respectively.

$$\overline{A}_x = \tilde{\tilde{E}}_x A = \frac{w}{a_{11}} \tag{5.1}$$

$$\overline{D}_x^{Smeared} = \tilde{\tilde{E}}_x I = \frac{1}{h a_{11}} I \tag{5.2}$$

5.2 Previous Method

The previous methods have attempted to calculate the axial, bending, and torsional stiffness of a composite beam with a specific cross-section. Chan and Demirhan [38] developed a method to calculate the axial and bending stiffness of a circular cross-section beam (Figure 5.1.).

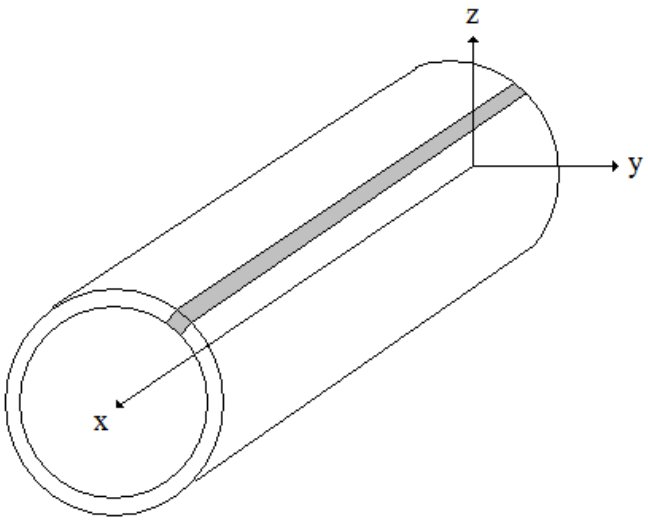

Figure 5.1 Circular cross-section beam with an infinitesimal section

The method considered the cross-section formed by infinitesimal sections inclined certain angle θ_x with respect to the horizontal coordinate y as shown in Figure 5.2.

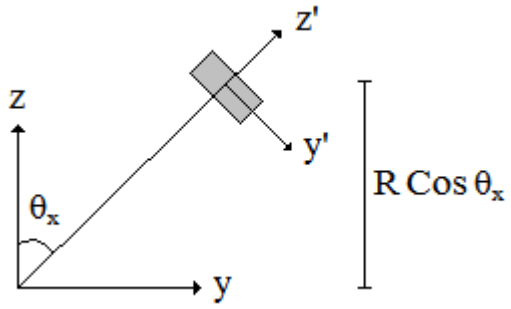

Figure 5.2 Cross-sectional view of the infinitesimal section

Therefore, the idea was to rotate the reduced stiffness matrix [Q] around x certain angle θ_x, then do the rotation around z according to each angle ply θ_z in the lay-up of the composite, and lastly translate it to the actual position in the cross-section. Finally, the overall stiffness of the composite tube is obtained by integrating over the entire θ_x domain. From there, the term $\bar{d}_{11}$ was extracted and inverted to calculate the bending stiffness of the circular cross-section beam. The procedure is better described in the following flow chart (Fig. 5.3),

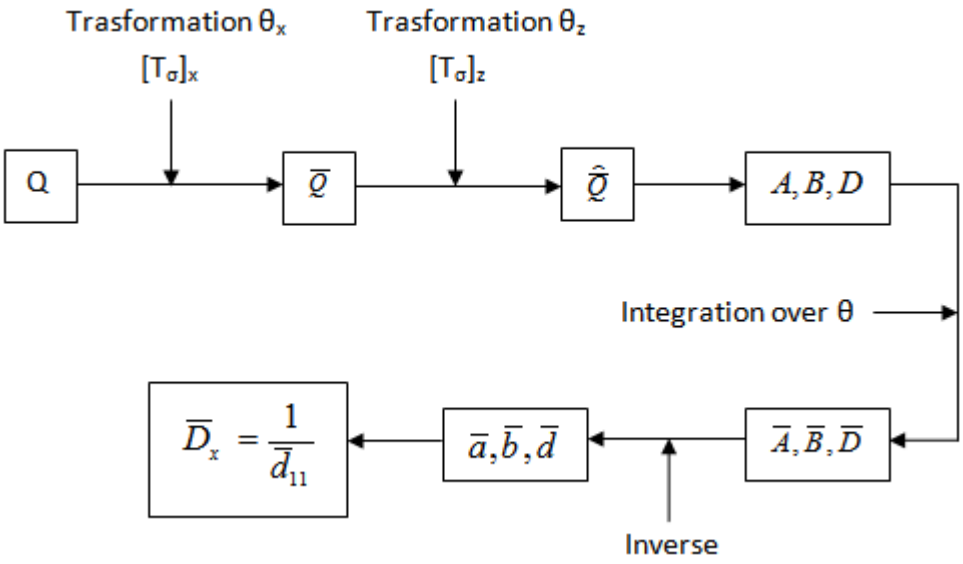

Figure 5.3 Flow chart of the previous method

In a similar way the stiffness of an elliptical cross-section was developed by Lin and Chan [39]. On the other hand, Rao and Chan [41] used a similar procedure to calculate the torsional stiffness of a tapered circular cross-section beam.

5.3 Modified Method

The previous method considers first the rotation about x-coordinate and then the rotation about z-coordinate. A modified method was developed by Syed and Chan [40] in calculating the stiffness matrix of a slant laminate. They reversed the previous procedure by rotating z-axis first, and then x-axis as shown in Figure 5.4. In addition, if the beam cross-section is un-symmetric, the bending stiffness of the beam should be calculated by Equation 2.34 as shown in section 2.5.1.

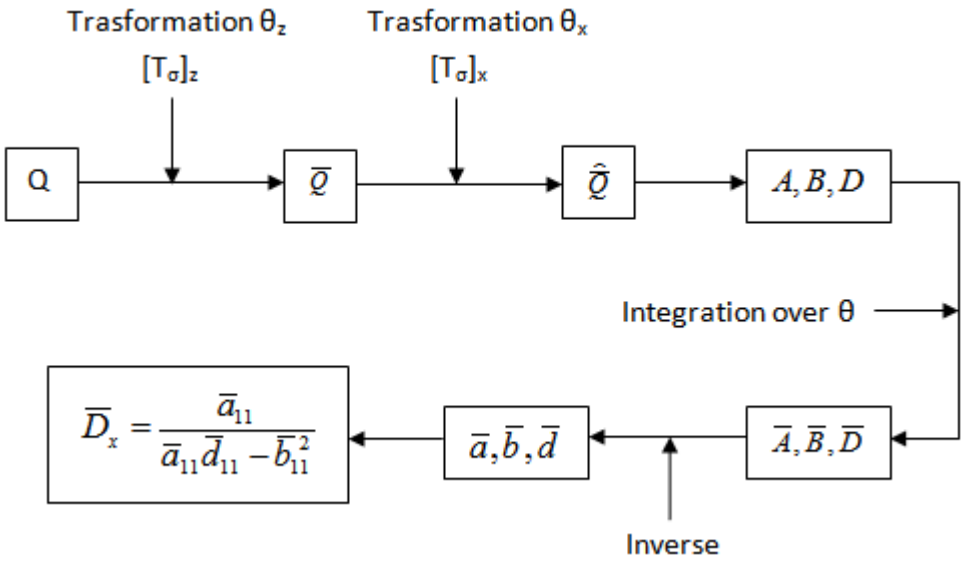

Figure 5.4 Flow chart of the modified method

5.4 Present Method

The present method doesn't consider a rotation about the x-coordinate. In this way, it is very similar to the smeared property approach with the difference that the present method is capable of working with any arbitrary cross-section. The parametrization was generalized to include all possible cross-sections: circular, elliptical, airfoil, and so on.

5.4.1 Line Integration of Structural Properties

Consider C to be the median curve of the thin-walled section. A point P(x,y,z) on the curve can be defined as $\vec{\psi}$, as shown in the Figure 5.5.

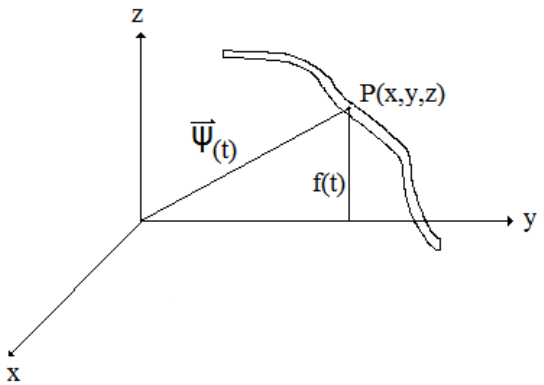

Figure 5.5 Parametrization of an arbitrary cross-section

$$\vec{\psi} = x\hat{i} + y\hat{j} + z\hat{k}$$

Let t be a position parameter over a closed interval [a,b]. Then $\vec{\psi}$ can be rewritten as

$$\vec{\psi} = x(t)\hat{i} + y(t)\,\hat{j} + z(t)\hat{k}$$

Let f be a function of any structural property over a given domain. Then the overall structural property can be evaluated in the following integral,

$$F = \int_C f(x,y,z)ds = \int_a^b f(x(t),y(t),z(t))\sqrt{\vec{\psi}'(t)\cdot\vec{\psi}'(t)}dt \tag{5.3}$$

5.4.1.1. Circular Cross-section

For a point on a circular cross-section, we have

$$\vec{\psi} = RCos(t)\,\hat{j} + RSin(t)\hat{k}$$

where R is the radius of the circular cross-section.

Then, we have

$$\int_C f(y,z)ds = \int_a^b f(y(t),z(t))\sqrt{\vec{\psi}'(t)\cdot\vec{\psi}'(t)}dt = R\int_a^b f(y(t),z(t))dt$$

5.4.1.2. Generalized Circular Cross-section

Let the circular cross-section be in y-z plane. Then, we have

$$z = \pm\sqrt{R_m^2 - y^2}$$

where R_m is the mean radius of the cross-section.

Using the parametrization, we have

$$y = t$$

$$z = \pm\sqrt{R^2 - t^2} = f(t)$$

$$\vec{\psi}(t) = t\hat{j} + f(t)\hat{k}$$

$$\vec{\psi}'(t) \cdot \vec{\psi}'(t) = 1 + [f'(t)]^2 = \frac{R^2}{R^2 - t^2}$$

5.4.2 Stiffness Matrices of Thin-walled Section

Considerinbg an infinitesimal element of the walled laminate. Its stiffness matrices are [A], [B], and [D] defined in section 2.1. These stiffness matrices translated to the centroid of the cross-section are given in Equation 2.28 and shown below:

$$\begin{aligned} [A'] &= [A] \\ [B'] &= [B] - \rho[A] \\ [D'] &= [D] - 2\rho B] + \rho^2[A] \end{aligned} \tag{5.4}$$

where $\rho = f(t)$, which is the function of the cross-section.

Integrating over the domain t to obtain the equivalent stiffness matrices for the arbitrary cross section.

$$[\overline{A}] = \int_a^b [A']\sqrt{\vec{\psi}'(t) \cdot \vec{\psi}'(t)}dt \tag{5.5}$$

$$[\overline{B}] = \int_a^b [B']\sqrt{\vec{\psi}'(t) \cdot \vec{\psi}'(t)}dt \tag{5.6}$$

$$[\bar{D}] = \int_a^b [D'] \sqrt{\vec{\psi}'(t) \cdot \vec{\psi}'(t)}\, dt \tag{5.7}$$

Then, building the large equivalent stiffness matrix and inverting it to obtain the equivalent compliance matrices.

$$\begin{bmatrix} \bar{A} & \bar{B} \\ \bar{B} & \bar{D} \end{bmatrix}^{-1} = \begin{bmatrix} \bar{a} & \bar{b} \\ \bar{b}^T & \bar{d} \end{bmatrix} \tag{5.8}$$

From there, it is easy to extract the terms needed to calculate the axial and bending stiffnesses for a composite beam with arbitrary cross section. The process is shown in Figure 5.6.

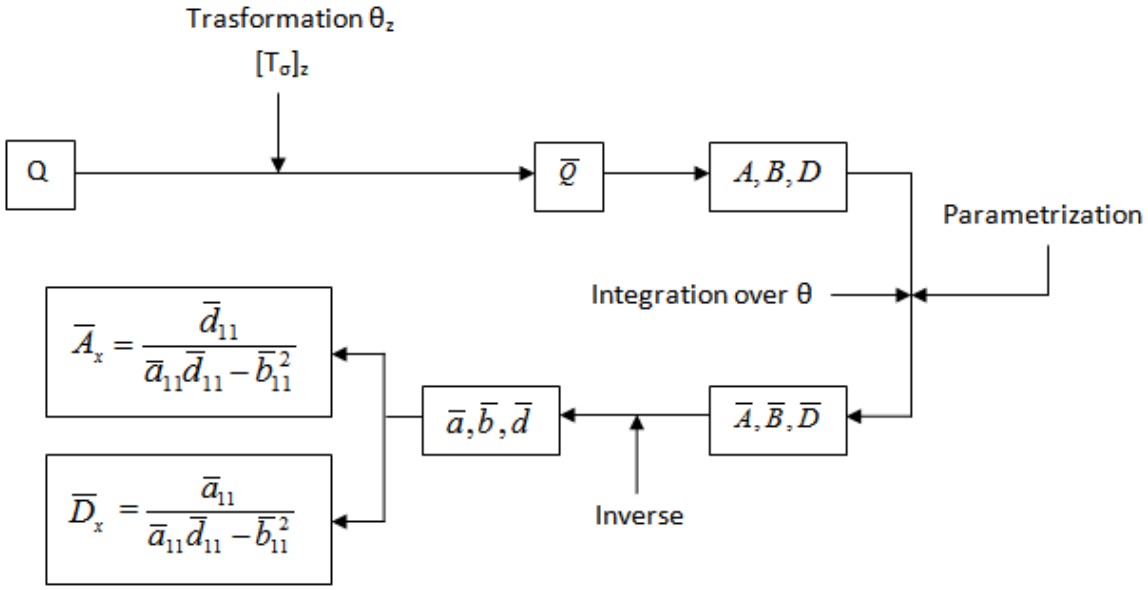

Figure 5.6 Flow chart of the present method

5.5 Finite Element Model of Beam with Circular Cross-section

Several models were created in ANSYS to simulate the composite tubes. The outer radius was varied from 0.2 to 2.6 inches. The length was established in 15 times the outer radius for each case. The mesh was 44 elements per length and 160 elements around the circumference. The composites had 16 plies with a thickness of 0.0052 inches, resulting the total thickness of 0.0832 inches. One element per ply through the thickness was used. As a result, the

total number of nodes used in the mesh was 122,400 nodes. Once again, the element used was solid46, a 3D block element with 8 nodes and 3 degrees of freedom per node.

Two cases were considered an axial load and a moment were applied. For the axial case, a unit axial load was applied to the model; in addition a rigid region was introduced to constrain the deformation (Figure 5.7). On the other hand, for the bending case the loads were applied to all the nodes in the free side, in that way, it simulates a distribute load (Figure 5.8).

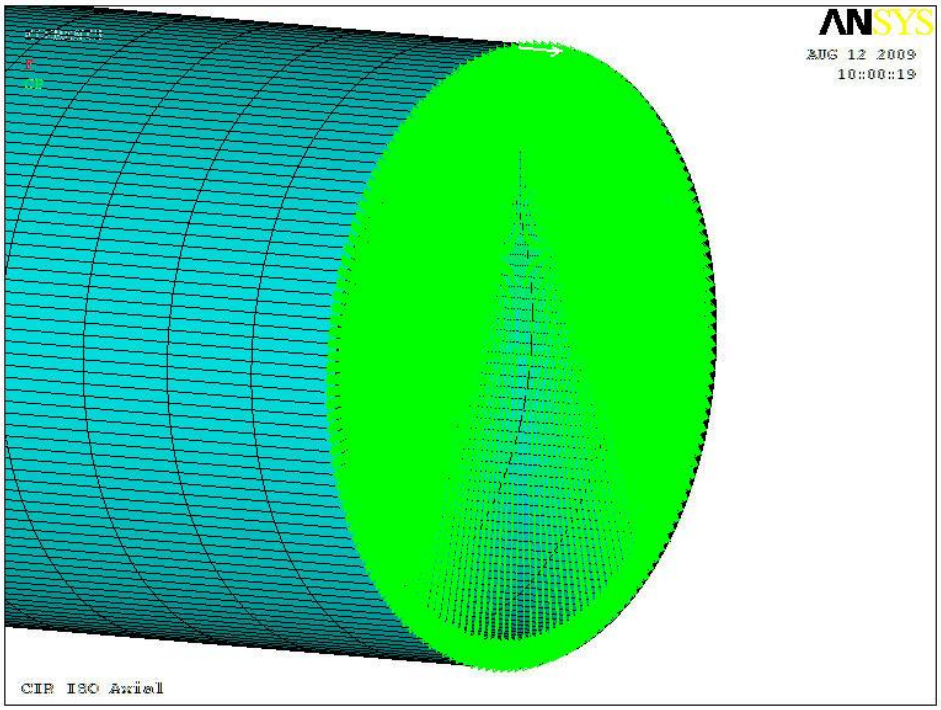

Figure 5.7 Axial load applied to the circular cross-section beam with a rigid region defined

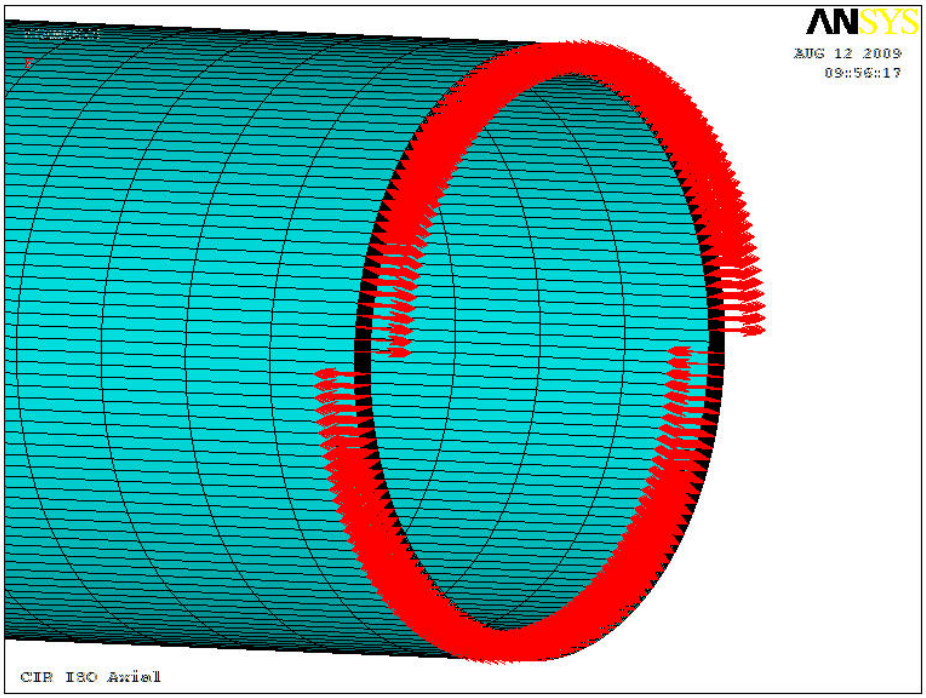

Figure 5.8 Distribute force generating the bending moment

The boundary conditions were applied has follows: the whole plane on the other side of the beam were constricted in the x-direction (axial direction). The mid-plane of the beam in the y-direction was constricted in that direction (U_y=0). And the mid-plane of the beam in the z-direction was constricted in that direction (U_z=0) as well as shown in Figure 5.9.

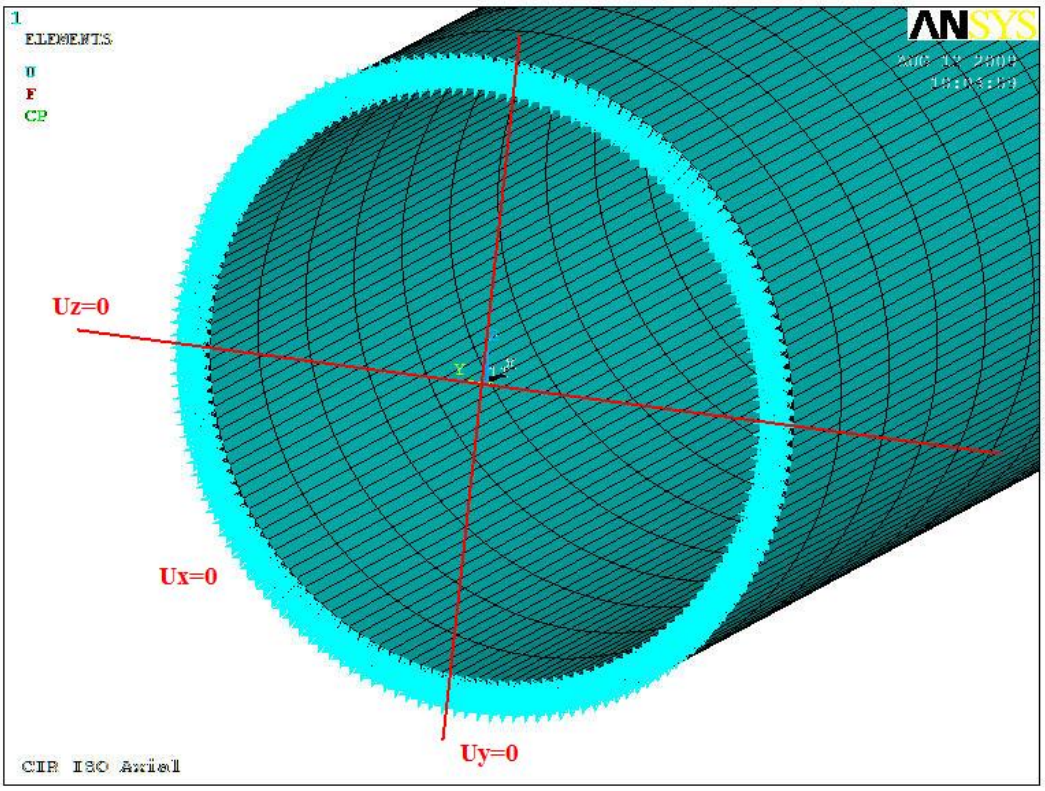

Figure 5.9 Applied Boundary Conditions

5.6 Result Comparison of Beam with Circular Cross-section

5.6.1 Smeared Property, Previous, Modified, and Present Method in Isotropic Tube

The materials were the same used in the work of Chan and Demirhan [38] to compare the results. First, an isotropic material was used to compare results from the models with the theoretical solutions. Steel was chosen with a Young Modulus of 30 Msi and a Poisson ratio of 0.3. Using this isotropic material, the previous method, the modified method and the present method were compared against the FEM and smeared property approach results. Two nodes in the mid-plane of the side of the beam were selected to read the vertical displacement. Those displacements were used to calculate its curvature. The, the total applied moment were divided by this curvature to calculate the bending stiffness. The outer radius was varied from 0.2 to 2.6 inches. The length was established in 15 times the outer radius. And the moments were applied as a distribute load across the cross-section and it was calculate for each specific case.

The parametrization was done as follow

$$\vec{\psi}(t) = t\hat{j} \pm \sqrt{R_m^2 - t^2}\,\hat{k} \qquad t \in [-R_m, R_m] \tag{5.9}$$

where R_m is the mean radius; the integration was done from $-R_m$ to R_m.

Figure 5.10 shows the results obtained by three different methods. It indicates that the present method agrees well with FEM and smeared property approaches.

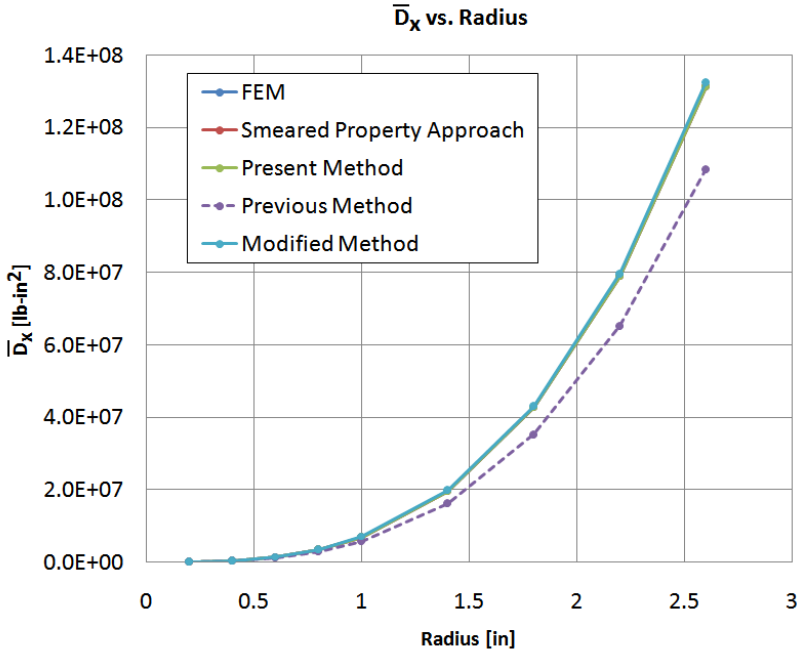

Figure 5.10 Comparison of the different methods for isotropic material

5.6.2 Smeared Property, Previous, Modified, and Present Method in Composite Tube

Similar to the previous section, the composite material used is the same used in the work of Chan and Demirhan [38] to compare the results. It had the following properties: E_1=24.8e6 psi, E_2=E_3=1.41e6, v_{12}= v_{23}= v_{13}=0.329, and G_{12}=G_{23}=G_{13}=0.90e6 psi. The lay-up used was $[\pm 45_2/0_2/\pm 45]_s$ and the model and the radius was varied in the same manner used in the isotropic case in the previous section.

The results are plotted in Figure 5.11. The FEM results match well with the smeared property approach and the present method. The previous method and the modified method results are distant.

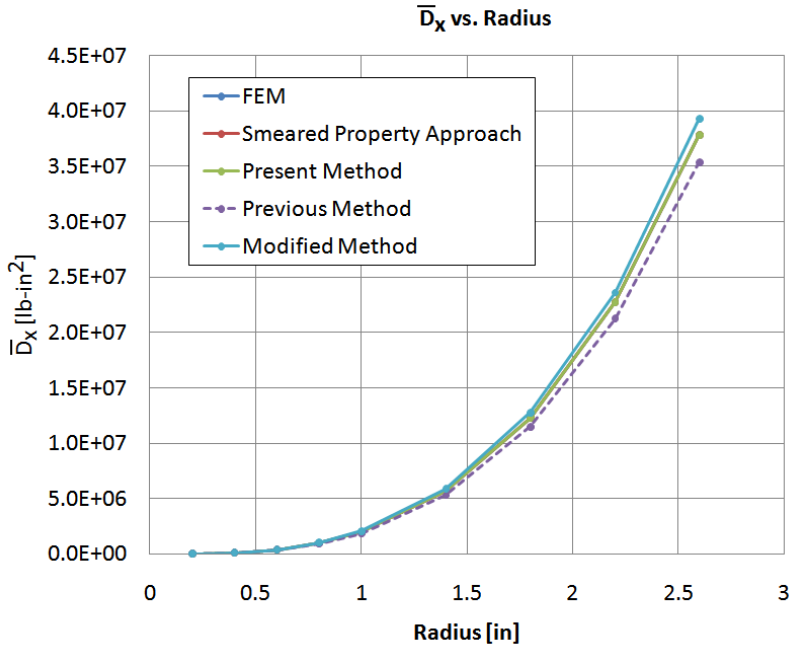

Figure 5.11 Comparison of the different methods for composite material

5.7 Present Method Results

For this section, the present method was compared against FEM results and when possible against theoretical solution, lamination theory, and smeared property approach. Another composite material was selected for this section with the following properties E_1=18.2e6 psi, E_2=E_3=1.41e6, v_{12}= v_{23}= v_{13}=0.27, and G_{12}=G_{23}=G_{13}=0.92e6 psi. Three different lay-ups were used $[0_8]_s$, $[45_2/-45_2/0_2/90_2]_s$, and $[90/0/-45/45]_{4T}$. The outer radius was kept at 1 in for all the cases.

5.7.1 Axial Stiffness and Stress for Isotropic Beam under Axial Load

A steel beam is simulated under a 1 lb axial load. The mesh and loads were as defined before. The deformation is uniform as expected because the rigid region as shown in Figure 5.12. The axial stresses are shown in Figure 5.13.

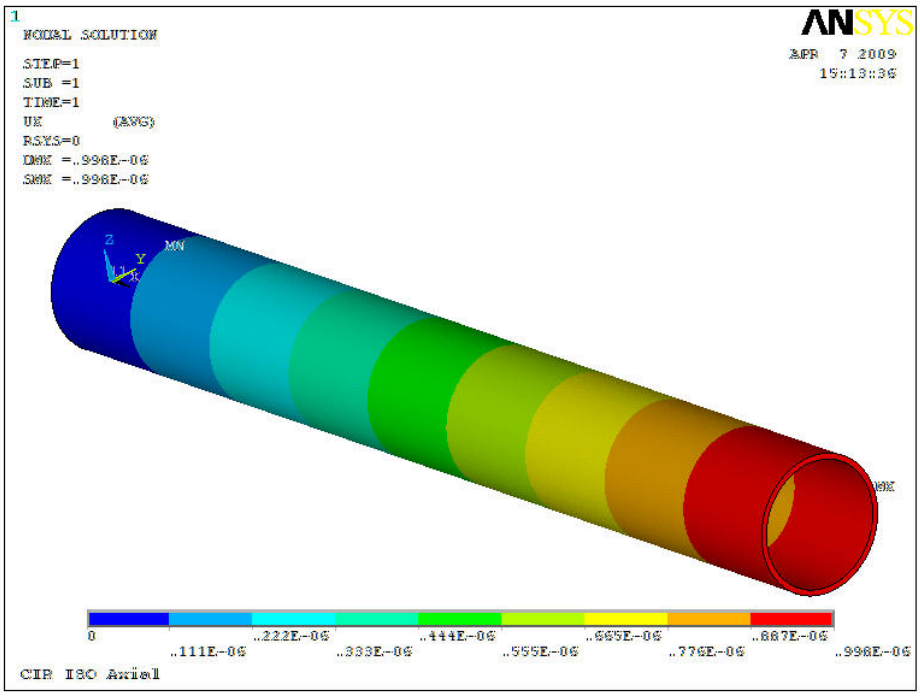

Figure 5.12 FEM axial displacements

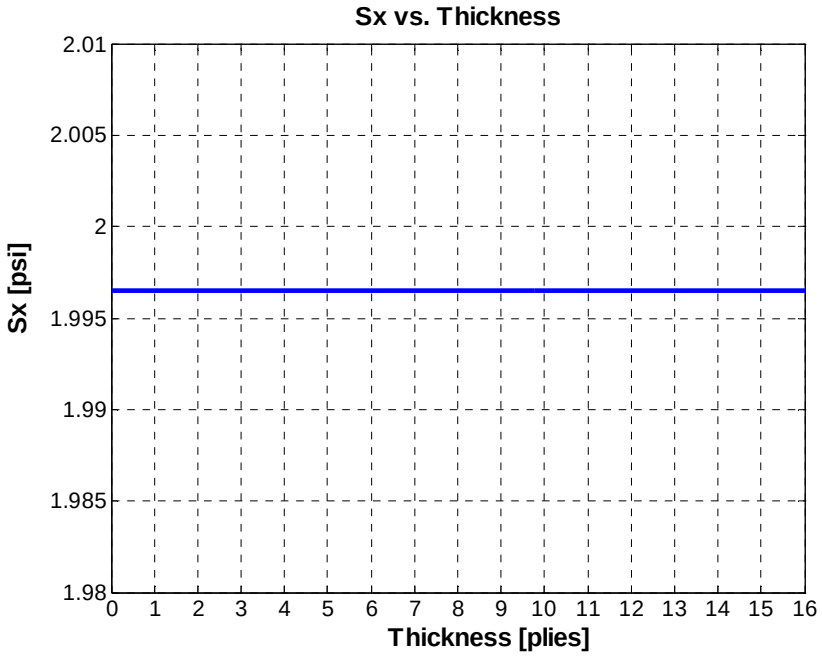

Figure 5.13 FEM axial stresses present in isotropic tube

Table 5.1 lists the axial stiffness of an isotropic tube calculated through different methods. All the results agree extremely well.

Table 5.1 Axial stiffness for isotropic tube

		$\overline{A_x}$ [lb]	%Diff
Theoretical Value	EA	1.5030E+07	
Smeared Property	$1/h[d_{11}/(a_{11}*d_{11}-b_{11}^2)]A$	1.5030E+07	0.0
Present Method	$\overline{d_{11}}/(\overline{a_{11}}*\overline{d_{11}}-\overline{b_{11}}^2)$	1.5030E+07	0.0
FEM		1.5027E+07	0.0

Table 5.2 shows the axial stresses developed in the isotropic tube due to the axial loading. The FEM, theoretical solution, and present method results agree very well.

Table 5.2 Axial stresses in isotropic tube

			σ_x [psi]	%Diff				σ_x [psi]	%Diff
ply #16	ISO	FEM	1.9965		ply #8	ISO	FEM	1.9965	
		Theoretical Solution	1.9960	0.0			Theoretical Solution	1.9960	0.0
		Present Method	1.9960	0.0			Present Method	1.9960	0.0
ply #15	ISO	FEM	1.9965		ply #7	ISO	FEM	1.9965	
		Theoretical Solution	1.9960	0.0			Theoretical Solution	1.9960	0.0
		Present Method	1.9960	0.0			Present Method	1.9960	0.0
ply #14	ISO	FEM	1.9965		ply #6	ISO	FEM	1.9965	
		Theoretical Solution	1.9960	0.0			Theoretical Solution	1.9960	0.0
		Present Method	1.9960	0.0			Present Method	1.9960	0.0
ply #13	ISO	FEM	1.9965		ply #5	ISO	FEM	1.9965	
		Theoretical Solution	1.9960	0.0			Theoretical Solution	1.9960	0.0
		Present Method	1.9960	0.0			Present Method	1.9960	0.0
ply #12	ISO	FEM	1.9965		ply #4	ISO	FEM	1.9965	
		Theoretical Solution	1.9960	0.0			Theoretical Solution	1.9960	0.0
		Present Method	1.9960	0.0			Present Method	1.9960	0.0
ply #11	ISO	FEM	1.9965		ply #3	ISO	FEM	1.9965	
		Theoretical Solution	1.9960	0.0			Theoretical Solution	1.9960	0.0
		Present Method	1.9960	0.0			Present Method	1.9960	0.0
ply #10	ISO	FEM	1.9965		ply #2	ISO	FEM	1.9965	
		Theoretical Solution	1.9960	0.0			Theoretical Solution	1.9960	0.0
		Present Method	1.9960	0.0			Present Method	1.9960	0.0
ply #9	ISO	FEM	1.9965		ply #1	ISO	FEM	1.9965	
		Theoretical Solution	1.9960	0.0			Theoretical Solution	1.9960	0.0
		Present Method	1.9960	0.0			Present Method	1.9960	0.0

5.7.2 Axial Stiffness and Stress for Composite Beam $[0_8]_s$ under Axial Load

Figure 5.14 presents the axial stress in the composite tube with all angle plies equal to 0°.

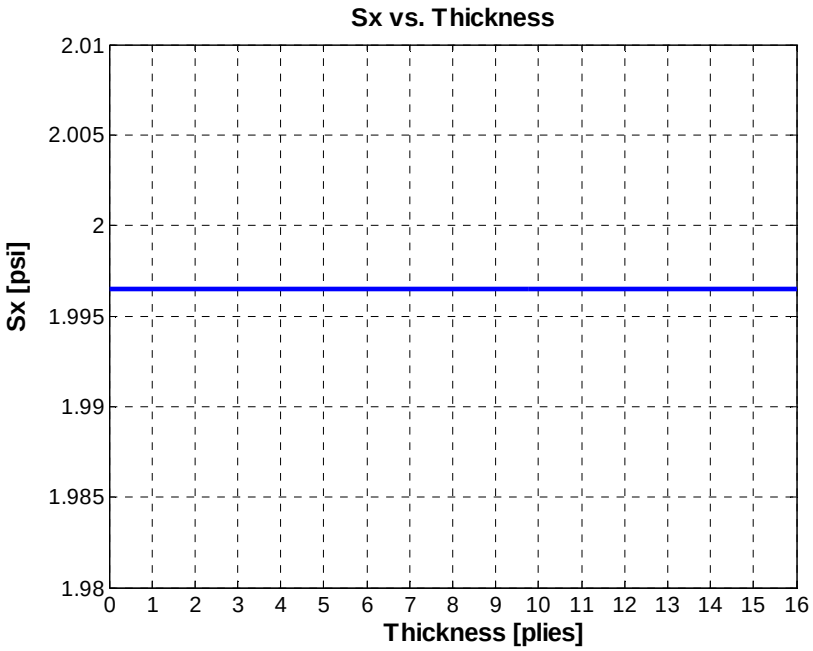

Figure 5.14 FEM axial stresses present in $[0_8]_s$ composite tube

Table 5.3 shows the axial stiffness for $[0_8]_s$ composite tube. FEM, smeared property, and present method results match perfectly.

Table 5.3 Axial stiffness for $[0_8]_s$ composite tube

		$\overline{A}_x$ [lb]	%Diff
FEM		9.1163E+06	
Smeared Property	$1/h[d_{11}/(a_{11}*d_{11}-b_{11}^2)]A$	9.1185E+06	0.0
Present Method	$\overline{d}_{11}/(\overline{a}_{11}*\overline{d}_{11}-\overline{b}_{11}^2)$	9.1185E+06	0.0

Table 5.4 lists the axial stresses present in the composite tube. Once again, the FEM and present method results agree very well.

Table 5.4 Axial stresses in $[0_8]_s$ composite tube

			σ_x	
			[psi]	%Diff
ply #16	0	FEM	1.9965	
		Present Method	1.9960	0.0
ply #15	0	FEM	1.9965	
		Present Method	1.9960	0.0
ply #14	0	FEM	1.9965	
		Present Method	1.9960	0.0
ply #13	0	FEM	1.9965	
		Present Method	1.9960	0.0
ply #12	0	FEM	1.9965	
		Present Method	1.9960	0.0
ply #11	0	FEM	1.9965	
		Present Method	1.9960	0.0
ply #10	0	FEM	1.9965	
		Present Method	1.9960	0.0
ply #9	0	FEM	1.9965	
		Present Method	1.9960	0.0
ply #8	0	FEM	1.9965	
		Present Method	1.9960	0.0
ply #7	0	FEM	1.9965	
		Present Method	1.9960	0.0
ply #6	0	FEM	1.9965	
		Present Method	1.9960	0.0
ply #5	0	FEM	1.9965	
		Present Method	1.9960	0.0
ply #4	0	FEM	1.9965	
		Present Method	1.9960	0.0
ply #3	0	FEM	1.9965	
		Present Method	1.9960	0.0
ply #2	0	FEM	1.9965	
		Present Method	1.9960	0.0
ply #1	0	FEM	1.9965	
		Present Method	1.9960	0.0

5.7.3 Axial Stiffness and Stress for Composite Beam $[45_2/-45_2/0_2/90_2]_s$ under Axial Load

The axial stresses are shown in Figure 5.15. The 0° plies have higher axial stress than the ±45° as shown. In addition, the 90° plies have the l east axial stress since it is the one with the least axial stiffness.

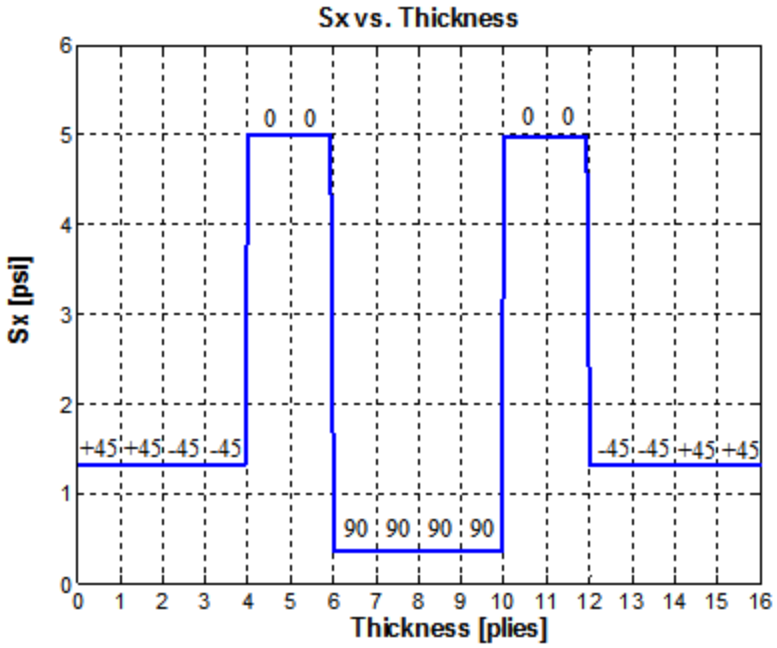

Figure 5.15 FEM axial stresses present in $[45_2/-45_2/0_2/90_2]_s$ composite tube

Table 5.5 and 5.6 lists the axial stiffness and stress; the results agree very well.

Table 5.5 Axial stiffness for $[45_2/-45_2/0_2/90_2]_s$ composite tube

		$\overline{A}_x$ [lb]	%Diff
FEM		3.6511E+06	
Smeared Property	$1/h[d_{11}/(a_{11}*d_{11}-b_{11}^2)]A$	3.6526E+06	0.0
Present Method	$\overline{d}_{11}/(\overline{a}_{11}*\overline{d}_{11}-\overline{b}_{11}^2)$	3.6526E+06	0.0

Table 5.6 Axial stresses in $[45_2/-45_2/0_2/90_2]_s$ composite tube

			σ_x [psi]	%Diff
ply #16	45	FEM	1.3194	
		Present Method	1.3225	**0.2**
ply #15	45	FEM	1.3211	
		Present Method	1.3225	**0.1**
ply #14	-45	FEM	1.3232	
		Present Method	1.3225	**-0.1**
ply #13	-45	FEM	1.3249	
		Present Method	1.3225	**-0.2**
ply #12	0	FEM	4.9877	
		Present Method	4.9809	**-0.1**
ply #11	0	FEM	4.9877	
		Present Method	4.9809	**-0.1**
ply #10	90	FEM	0.3611	
		Present Method	0.3580	**-0.9**
ply #9	90	FEM	0.3592	
		Present Method	0.3580	**-0.3**
ply #8	90	FEM	0.3572	
		Present Method	0.3580	**0.2**
ply #7	90	FEM	0.3553	
		Present Method	0.3580	**0.8**
ply #6	0	FEM	4.9780	
		Present Method	4.9809	**0.1**
ply #5	0	FEM	4.9780	
		Present Method	4.9809	**0.1**
ply #4	-45	FEM	1.3208	
		Present Method	1.3225	**0.1**
ply #3	-45	FEM	1.3221	
		Present Method	1.3225	**0.0**
ply #2	45	FEM	1.3232	
		Present Method	1.3225	**-0.1**
ply #1	45	FEM	1.3247	
		Present Method	1.3225	**-0.2**

5.7.4 Axial Stiffness and Stress for Composite Beam $[90/0/-45/45]_{4T}$ under Axial Load

Figure 5.16 presents the axial stress in the $[90/0/-45/45]_{4T}$ composite tube.

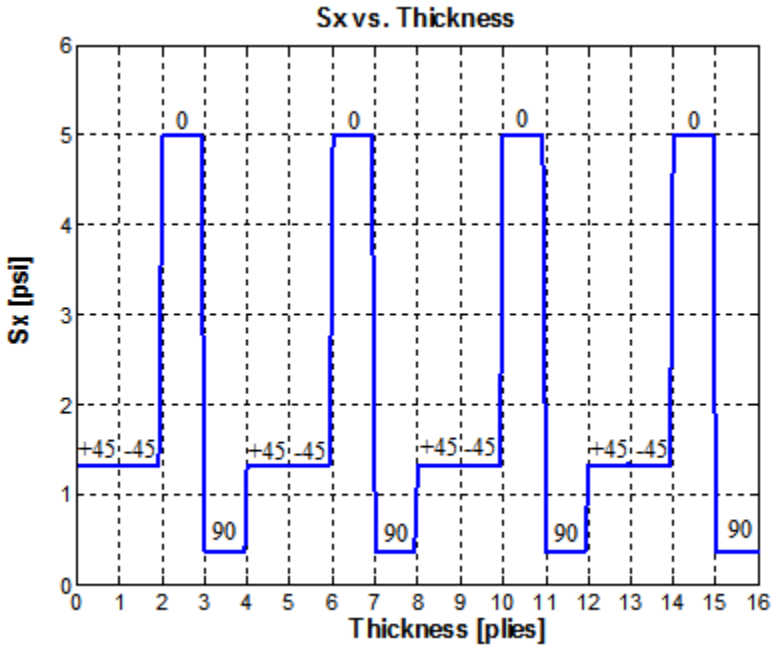

Figure 5.16 FEM axial stresses present in $[90/0/-45/45]_{4T}$ composite tube

Table 5.7 shows the axial stiffness for $[90/0/-45/45]_{4T}$ composite tube. FEM, smeared property, and present method results match perfectly.

Table 5.7 Axial stiffness for $[90/0/-45/45]_{4T}$ composite tube

		$\overline{A_x}$ [lb]	%Diff
FEM		3.6539E+06	
Smeared Property	$1/h[d_{11}/(a_{11}*d_{11}-b_{11}^2)]A$	3.6207E+06	-0.9
Present Method	$\overline{d}_{11}/(\overline{a}_{11}*\overline{d}_{11}-\overline{b}_{11}^2)$	3.6526E+06	0.0

Table 5.8 lists the axial stresses present in the composite tube. Once again, the FEM and present method results agree very well.

Table 5.8 Axial stresses in $[90/0/-45/45]_{4T}$ composite tube

			σ_x [psi]	%Diff
ply #16	45	FEM	1.3213	
		Present Method	1.3225	**0.1**
ply #15	-45	FEM	1.3161	
		Present Method	1.3225	**0.5**
ply #14	0	FEM	4.9813	
		Present Method	4.9809	**0.0**
ply #13	90	FEM	0.3586	
		Present Method	0.3580	**-0.2**
ply #12	45	FEM	1.3234	
		Present Method	1.3225	**-0.1**
ply #11	-45	FEM	1.3181	
		Present Method	1.3225	**0.3**
ply #10	0	FEM	4.9814	
		Present Method	4.9809	**0.0**
ply #9	90	FEM	0.3587	
		Present Method	0.3580	**-0.2**
ply #8	45	FEM	1.3255	
		Present Method	1.3225	**-0.2**
ply #7	-45	FEM	1.3199	
		Present Method	1.3225	**0.2**
ply #6	0	FEM	4.9815	
		Present Method	4.9809	**0.0**
ply #5	90	FEM	0.3589	
		Present Method	0.3580	**-0.2**
ply #4	45	FEM	1.3275	
		Present Method	1.3225	**-0.4**
ply #3	-45	FEM	1.3217	
		Present Method	1.3225	**0.1**
ply #2	0	FEM	4.9816	
		Present Method	4.9809	**0.0**
ply #1	90	FEM	0.3591	
		Present Method	0.3580	**-0.3**

5.7.5 Bending Stiffness and Stress for Isotropic Beam under Bending

A steel beam is simulated under a moment of 1.659358 lb-in. The axial stresses are shown in Figure 5.17.

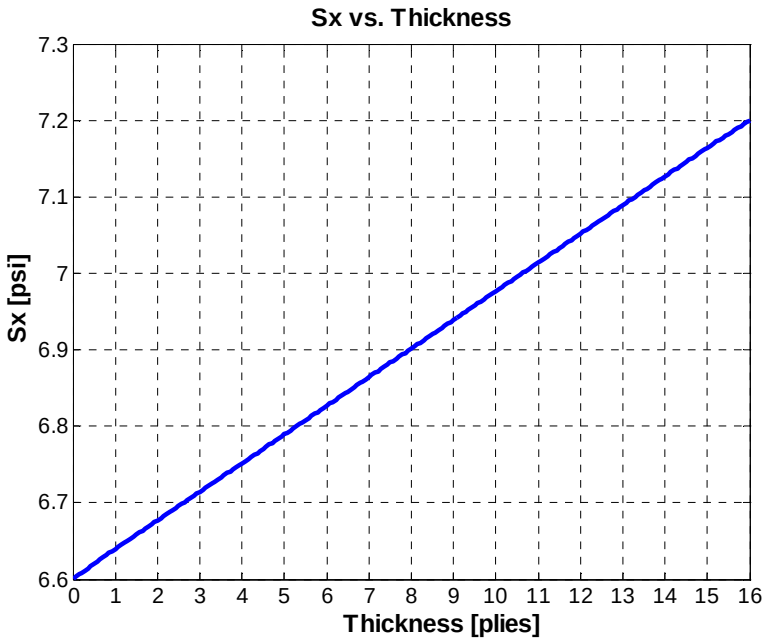

Figure 5.17 FEM axial stresses present in isotropic tube

Table 5.9 lists the bending stiffness of an isotropic tube calculated through different methods. All the results agree extremely well.

Table 5.9 Bending stiffness for isotropic tube

		$\overline{D}_x$ [lb-in^2]	%Diff
Theoretical Value	EI/L	6.9160E+06	
Smeared Property	$1/h[d_{11}/(a_{11}*d_{11}-b_{11}^2)]I$	6.9160E+06	0.0
Present Method	$\overline{a}_{11}/(\overline{a}_{11}*\overline{d}_{11}-\overline{b}_{11}^2)$	6.9116E+06	-0.1
FEM		6.9154E+06	0.0

Table 5.10 shows the axial stresses developed in the isotropic tube due to bending. The FEM, theoretical solution, and present method results agree very well.

Table 5.10 Axial stresses in isotropic tube

			σ_x [psi]	%Diff
ply #16	ISO	FEM	7.1822	
		Theoretical Solution	7.1792	0.0
		Present Method	7.1837	0.0
ply #15	ISO	FEM	7.1456	
		Theoretical Solution	7.1418	-0.1
		Present Method	7.1463	0.0
ply #14	ISO	FEM	7.1080	
		Theoretical Solution	7.1044	-0.1
		Present Method	7.1088	0.0
ply #13	ISO	FEM	7.0704	
		Theoretical Solution	7.0669	0.0
		Present Method	7.0714	0.0
ply #12	ISO	FEM	7.0329	
		Theoretical Solution	7.0295	0.0
		Present Method	7.0339	0.0
ply #11	ISO	FEM	6.9954	
		Theoretical Solution	6.9921	0.0
		Present Method	6.9965	0.0
ply #10	ISO	FEM	6.9579	
		Theoretical Solution	6.9547	0.0
		Present Method	6.9590	0.0
ply #9	ISO	FEM	6.9204	
		Theoretical Solution	6.9172	0.0
		Present Method	6.9216	0.0
ply #8	ISO	FEM	6.8830	
		Theoretical Solution	6.8798	0.0
		Present Method	6.8841	0.0
ply #7	ISO	FEM	6.8455	
		Theoretical Solution	6.8424	0.0
		Present Method	6.8467	0.0
ply #6	ISO	FEM	6.8080	
		Theoretical Solution	6.8049	0.0
		Present Method	6.8092	0.0
ply #5	ISO	FEM	6.7706	
		Theoretical Solution	6.7675	0.0
		Present Method	6.7718	0.0
ply #4	ISO	FEM	6.7332	
		Theoretical Solution	6.7301	0.0
		Present Method	6.7343	0.0
ply #3	ISO	FEM	6.6959	
		Theoretical Solution	6.6927	0.0
		Present Method	6.6969	0.0
ply #2	ISO	FEM	6.6585	
		Theoretical Solution	6.6552	0.0
		Present Method	6.6594	0.0
ply #1	ISO	FEM	6.6201	
		Theoretical Solution	6.6178	0.0
		Present Method	6.6219	0.0

5.7.6 Bending Stiffness and Stress for Composite Beam $[0_8]_s$ under Bending

Figure 5.18 presents the axial stress in the composite tube with all angle plies equal to 0°.

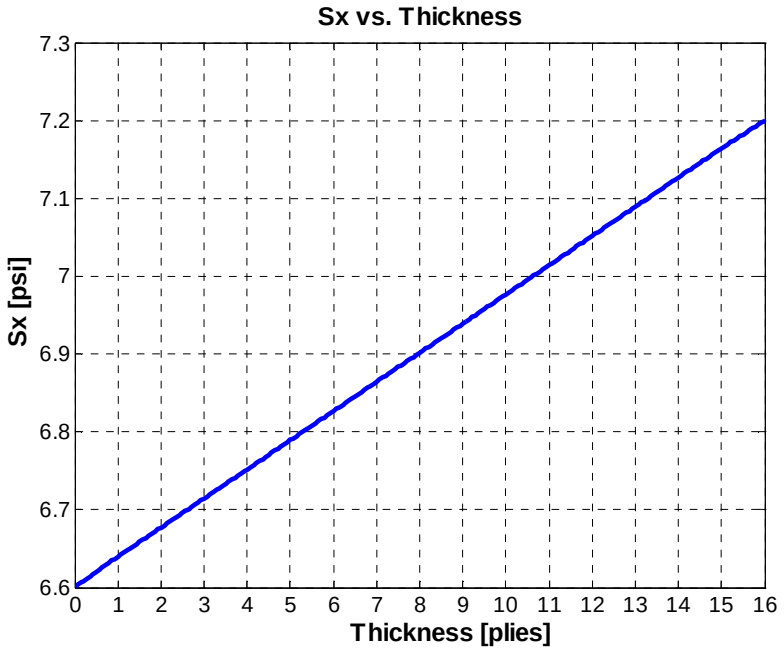

Figure 5.18 FEM axial stresses present in $[0_8]_s$ composite tube

Table 5.11 shows the axial stiffness for $[0_8]_s$ composite tube. FEM, smeared property, and present method results very well.

Table 5.11 Bending stiffness for $[0_8]_s$ composite tube

		$\overline{D}_x$ [lb-in^2]	%Diff
FEM		4.1924E+06	
Smeared Property	$1/h[d_{11}/(a_{11}*d_{11}-b_{11}^2)]$	4.1957E+06	0.1
Present Method	$\overline{a}_{11}/(\overline{a}_{11}*\overline{d}_{11}-\overline{b}_{11}^2)$	4.1931E+06	0.0

Table 5.12 lists the axial stresses present in the composite tube. The FEM and present method results agree very well.

Table 5.12 Axial stresses in $[0_8]_s$ composite tube

			σ_x	
			[psi]	%Diff
ply #16	0	FEM	7.1908	
		Present Method	7.1837	-0.1
ply #15	0	FEM	7.1532	
		Present Method	7.1463	-0.1
ply #14	0	FEM	7.1143	
		Present Method	7.1088	-0.1
ply #13	0	FEM	7.0760	
		Present Method	7.0714	-0.1
ply #12	0	FEM	7.0377	
		Present Method	7.0339	-0.1
ply #11	0	FEM	6.9993	
		Present Method	6.9965	0.0
ply #10	0	FEM	6.9610	
		Present Method	6.9590	0.0
ply #9	0	FEM	6.9227	
		Present Method	6.9216	0.0
ply #8	0	FEM	6.8844	
		Present Method	6.8841	0.0
ply #7	0	FEM	6.8460	
		Present Method	6.8467	0.0
ply #6	0	FEM	6.8077	
		Present Method	6.8092	0.0
ply #5	0	FEM	6.7694	
		Present Method	6.7718	0.0
ply #4	0	FEM	6.7310	
		Present Method	6.7343	0.0
ply #3	0	FEM	6.6926	
		Present Method	6.6969	0.1
ply #2	0	FEM	6.6549	
		Present Method	6.6594	0.1
ply #1	0	FEM	6.6158	
		Present Method	6.6219	0.1

5.7.7 Bending Stiffness and Stress for Composite Beam $[45_2/-45_2/0_2/90_2]_s$ under Bending

The axial stresses are shown in Figure 5.19. As explained before, the 0° plies have much more axial stress than the ±45° ones, and 90° plies because they are the most s tiffer.

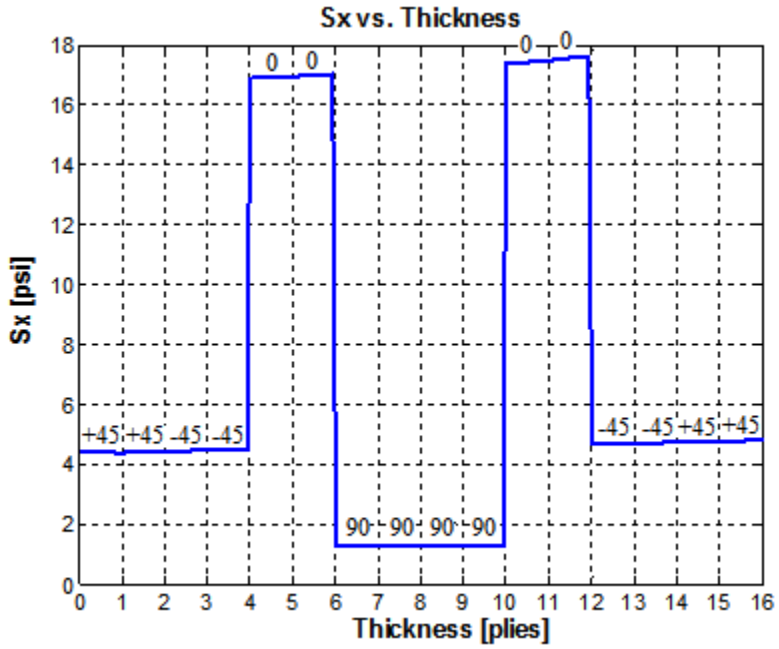

Figure 5.19 FEM axial stresses present in $[45_2/-45_2/0_2/90_2]_s$ composite tube

Table 5.13 and 5.14 lists the axial stiffness and stress; the results agree very well.

Table 5.13 Bending stiffness for $[45_2/-45_2/0_2/90_2]_s$ composite tube

		$\overline{D}_x$ [lb-in²]	%Diff
FEM		1.6577E+06	
Smeared Property	$1/h[d_{11}/(a_{11}*d_{11}-b_{11}^2)]$	1.6807E+06	1.4
Present Method	$\overline{a}_{11}/(\overline{a}_{11}*\overline{d}_{11}-\overline{b}_{11}^2)$	1.6791E+06	1.3

Table 5.14 Axial stresses in $[45_2/-45_2/0_2/90_2]_s$ composite tube

			σ_x [psi]	%Diff
ply #16	45	FEM	4.7748	
		Present Method	4.7582	-0.3
ply #15	45	FEM	4.7240	
		Present Method	4.7334	0.2
ply #14	-45	FEM	4.7067	
		Present Method	4.7117	0.1
ply #13	-45	FEM	4.6797	
		Present Method	4.6869	0.2
ply #12	0	FEM	17.5460	
		Present Method	17.5579	0.1
ply #11	0	FEM	17.4180	
		Present Method	17.4644	0.3
ply #10	90	FEM	1.2490	
		Present Method	1.2484	0.0
ply #9	90	FEM	1.2609	
		Present Method	1.2417	-1.5
ply #8	90	FEM	1.2611	
		Present Method	1.2350	-2.1
ply #7	90	FEM	1.2494	
		Present Method	1.2283	-1.7
ply #6	0	FEM	16.9840	
		Present Method	16.9970	0.1
ply #5	0	FEM	16.9220	
		Present Method	16.9035	-0.1
ply #4	-45	FEM	4.4712	
		Present Method	4.4634	-0.2
ply #3	-45	FEM	4.4382	
		Present Method	4.4386	0.0
ply #2	45	FEM	4.3916	
		Present Method	4.4109	0.4
ply #1	45	FEM	4.3829	
		Present Method	4.3861	0.1

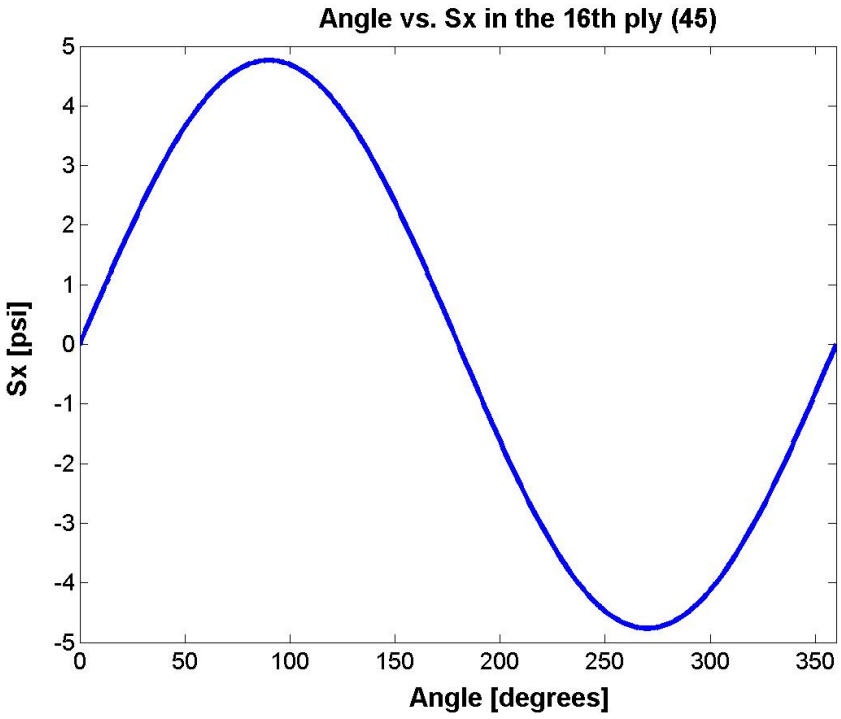

Figure 5.20 Axial stresses in $[45_2/-45_2/0_2/90_2]_s$ composite tube in the 16th ply

5.7.8 Bending Stiffness and Stress for Composite Beam $[90/0/-45/45]_{4T}$ under Bending

Figure 5.21 presents the axial stress in the $[90/0/-45/45]_{4T}$ composite tube.

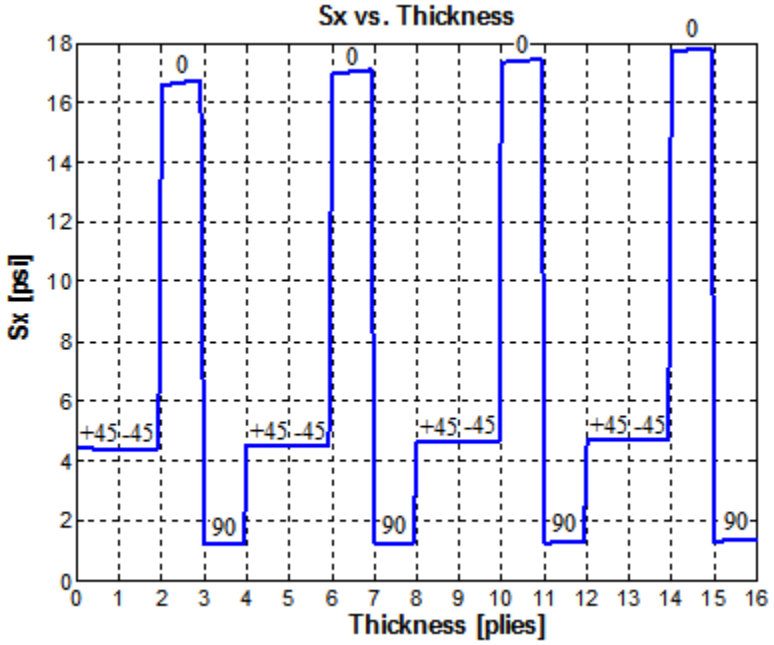

Figure 5.21 FEM axial stresses present in $[90/0/-45/45]_{4T}$ composite tube

Table 5.15 shows the axial stiffness for $[90/0/-45/45]_{4T}$ composite tube. FEM, smeared property, and present method results match well.

Table 5.15 Bending stiffness for $[90/0/-45/45]_{4T}$ composite tube

		$\bar{D}_x$ [lb-in^2]	%Diff
FEM		1.6843E+06	
Smeared Property	$1/h[d_{11}/(a_{11}*d_{11}-b_{11}^2)]$	1.6660E+06	-1.1
Present Method	$\bar{a}_{11}/(\bar{a}_{11}*\bar{d}_{11}-\bar{b}_{11}^2)$	1.6834E+06	-0.1

Table 5.16 lists the axial stresses present in the composite tube. The FEM and present method results agree very well.

Table 5.16 Axial stresses in $[90/0/-45/45]_{4T}$ composite tube

			σ_x [psi]	%Diff
ply #16	90	FEM	1.3337	
		Present Method	1.3265	-0.5
ply #15	0	FEM	17.7410	
		Present Method	17.8192	0.4
ply #14	-45	FEM	4.7223	
		Present Method	4.7088	-0.3
ply #13	45	FEM	4.7217	
		Present Method	4.6953	-0.6
ply #12	90	FEM	1.2701	
		Present Method	1.2613	-0.7
ply #11	0	FEM	17.3990	
		Present Method	17.4453	0.3
ply #10	-45	FEM	4.6148	
		Present Method	4.6095	-0.1
ply #9	45	FEM	4.6147	
		Present Method	4.5961	-0.4
ply #8	90	FEM	1.2425	
		Present Method	1.2344	-0.6
ply #7	0	FEM	17.0230	
		Present Method	17.0714	0.3
ply #6	-45	FEM	4.5084	
		Present Method	4.5102	0.0
ply #5	45	FEM	4.5093	
		Present Method	4.4968	-0.3
ply #4	90	FEM	1.2153	
		Present Method	1.2076	-0.6
ply #3	0	FEM	16.6510	
		Present Method	16.6976	0.3
ply #2	-45	FEM	4.3938	
		Present Method	4.4110	0.4
ply #1	45	FEM	4.3971	
		Present Method	4.3975	0.0

5.8 Kollar's Method

Another method to calculate the bending stiffness of a circular cross-section beam was developed by Kollar and Springer [12].

$$\overline{D}_x = \pi\left(\frac{R_m^3}{a_{11}} + \frac{R_m}{d_{11}}\right) \tag{5.10}$$

5.9 Varying the Radius

A composite beam was studied under bending with different radiuses. Using the material properties for the composite from the previous section E_1=18.2e6 psi, E_2=E_3=1.41e6, v_{12}= v_{23}= v_{13}=0.27, and G_{12}=G_{23}=G_{13}=0.92e6 psi, and with a lay-up of $[\pm 45_2/90]_s$; the model was built. The number of plies was 10 and it thickness was 0.005 inches. This time the median radii of the cross-section varied from 2 to 0.0625 inches (Fig. 5.22). The length was fixed for all the cases in 30 inches. The idea was to understand what happen when the radius become very small.

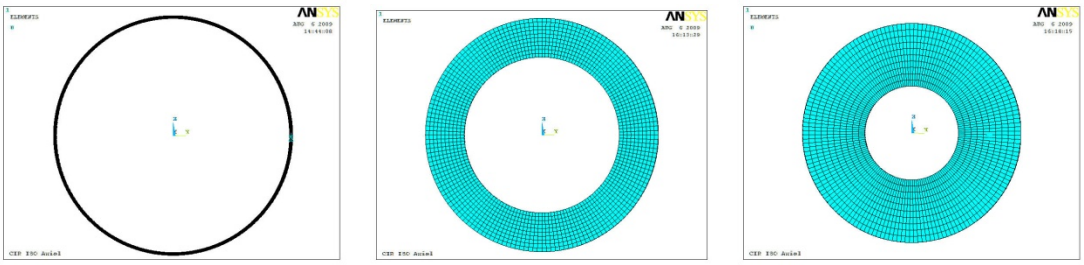

Figure 5.22 Radius of 2 in, 0.125 in, and 0.0625 in

Table 5.17 list the results for the bending stiffness calculated through FEM, smeared property, present, and Kollar methods. The averaged radius was varied from 2 in to 0.0625 in.

Table 5.17 Bending stiffness for different radiuses

Rm	t/Rm	FEM $\overline{D}_x=\overline{M}_x/k_x$	Smeared Prop. E*I	Diff %	Present Method $\overline{D}_x$	Diff %	Kollar's Eq. $\overline{D}_x$	Diff %
[in]		[lb-in^2]	[lb-in^2]		[lb-in^2]		[lb-in^2]	
2.00	0.025	4.68E+06	4.68E+06	0.1	4.68E+06	0.1	4.68E+06	0.1
1.00	0.05	5.85E+05	5.86E+05	0.1	5.85E+05	0.0	5.85E+05	0.0
0.50	0.1	7.33E+04	7.33E+04	0.1	7.33E+04	0.0	7.32E+04	-0.1
0.125	0.4	1.18E+03	1.19E+03	0.7	1.17E+03	-0.7	1.16E+03	-2.1
0.0625	0.8	1.63E+02	1.66E+02	2.0	1.58E+02	-3.0	1.49E+02	-8.1

All the results agree very well. In addition, as the radius becomes small, the results start to diverge as expected.

5.10 Varying the Lay-up

Since the smeared property approach does not take into consideration the lay-up, it was varied to see how well this method behaves. Table 5.18 shows the results for the same model where only the lay-up was changed.

Table 5.18 Bending stiffness for different lay-ups

	Rm	FEM $\overline{D}_x=\overline{M}_x/k_x$	Smeared Prop. E*I	Diff %	Present Method $\overline{D}_x$	Diff %	Kollar's Eq. $\overline{D}_x$	Diff %
	[in]	[lb-in^2]	[lb-in^2]		[lb-in^2]		[lb-in^2]	
$[0/30/\pm45/90]_s$	0.0625	359	331	-8.0	333	-7.4	308	-14.2
$[90/\pm45/30/0]_s$	0.0625	305	331	8.3	301	-1.5	292	-4.2

As expected the smeared property method results doesn't change. Therefore, their answer is not so accurate. Kollar method even though it changes according to the lay-up, the results still far. Finally, the present method which takes into account the lay-ups predicts very well the bending stiffness and their results are the closest one.

5.11 Airfoil Beam

The advantage of the present method is that not only works for circular cross-section beam but for any arbitrary cross-section as an airfoil (Fig. 5.23 and 5.24). The curve of airfoil laminate is defined in two parts. First a semi-circle with outer radius in 1 inches. In the second part, the angle of the airfoil was selected to be 10°. Therefore, their parametrization are the following

$$\rho\psi_1(t) = t\hat{j} \pm \sqrt{R_m^2 - t^2}\,\hat{k} \qquad t \in [-R_m, 0] \tag{5.11}$$

where R_m=0.9584 in. and it is the mean radius; the integration was done from $-R_m$ to 0.

For the airfoil, the parametrization was done as follow

$$\vec{\psi}_2(t) = t\hat{j} \pm \left(-\frac{R_m}{L_o} t + R_m \right) \hat{k} \qquad t \in [0, L_o] \tag{5.12}$$

where L_o=5.4353565 in. and it is the width of the airfoil as shown in Figure 5.24; the integration was done from 0 to L_o.

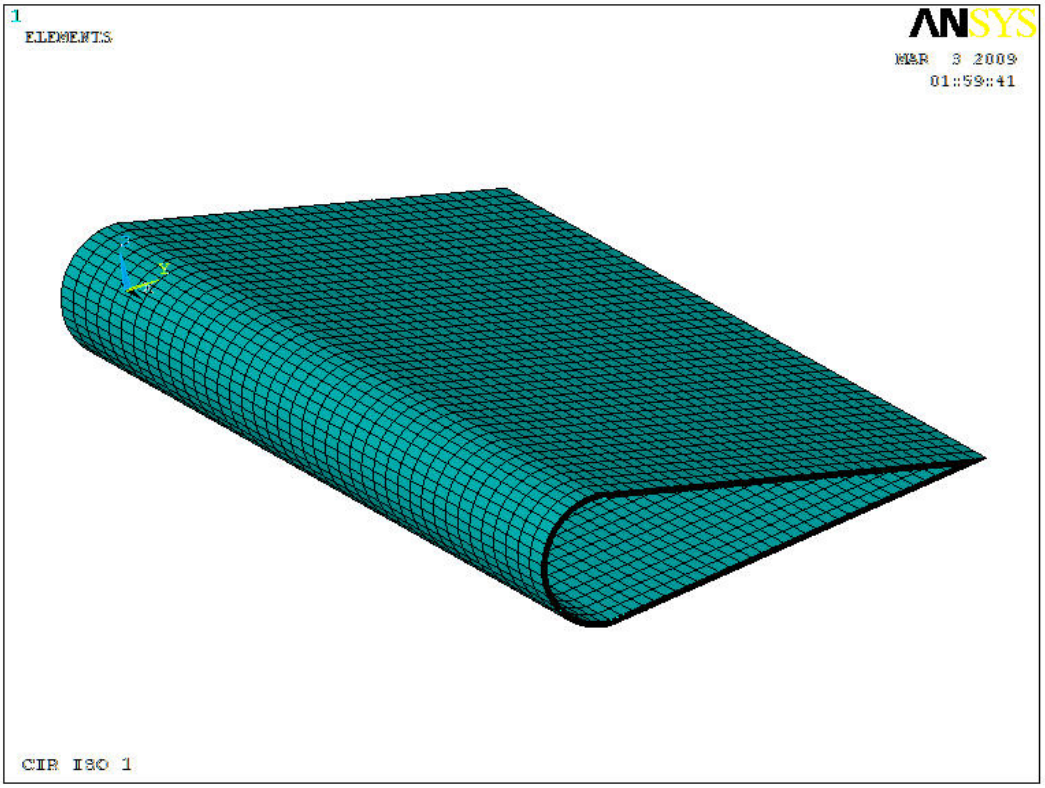

Figure 5.23 Airfoil model

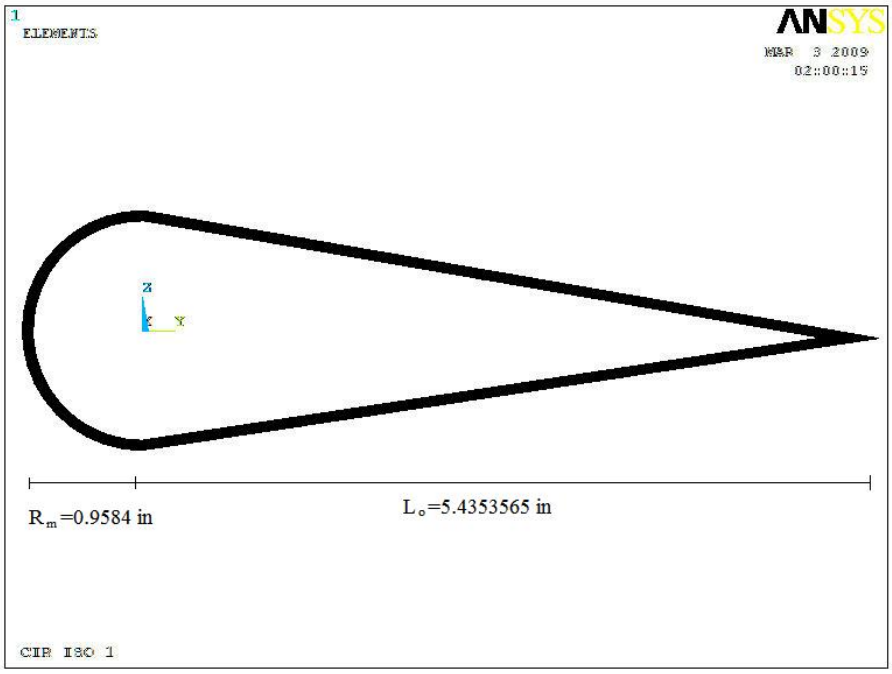

Figure 5.24 Airfoil cross-section

5.11.1 Finite Element Model

Two models were built in order make the simulations: an isotropic steel model, and a composite model with different lay-ups. The length of the beam was fixed in 15 inches. The model had 16 plies of 0.0052 inches with a total of 169,692 nodes.

Two cases were defined: axial and bending load (Fig. 5.25 and 5.26). In the axial case, a 10.434 lb load was applied and a rigid region was defined to constrain the deformation. For the bending case, a distribute load was applied to create a total moment of 0.72839 lb-in. In both case, the other end was constrained in all the 3 directions (cantilever beam).

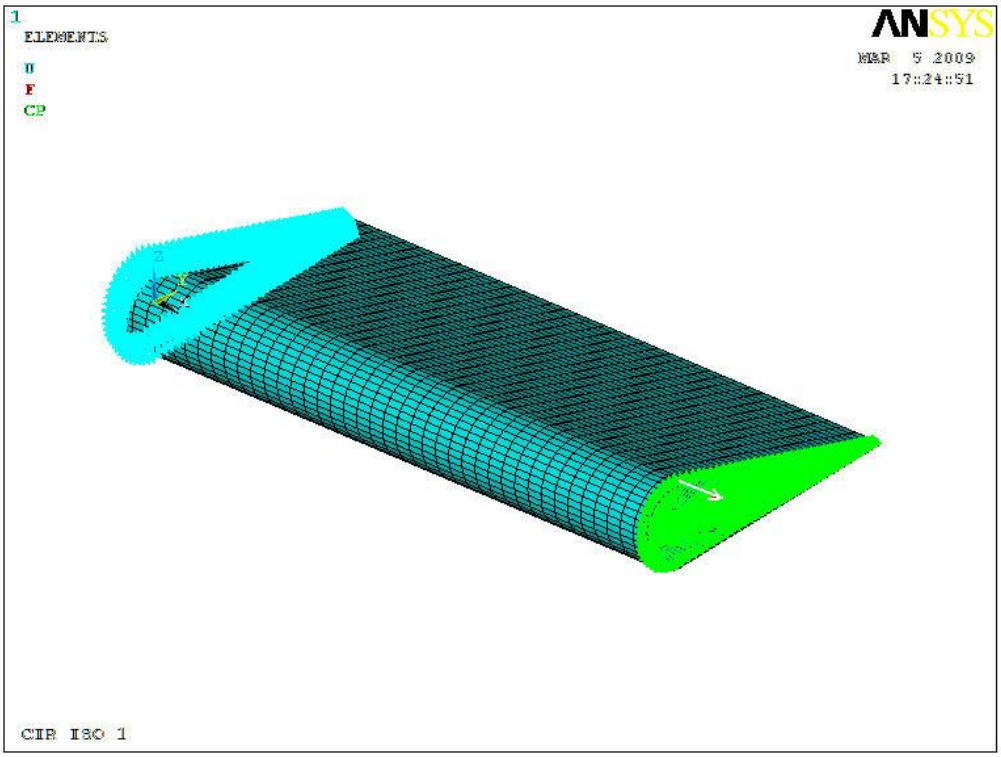

Figure 5.25 Axial loading

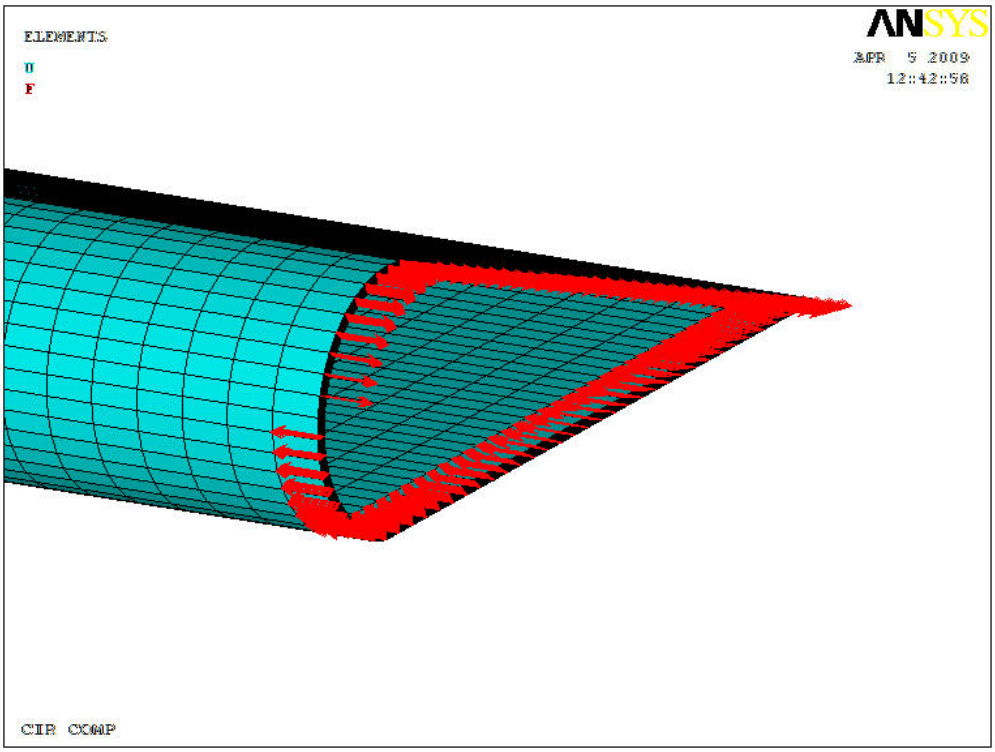

Figure 5.26 Bending loading

5.11.2 Isotropic Airfoil under Axial Load

First, an isotropic airfoil was simulated in order to compare the results with the theoretical solution. Figure 5.27 shows that the deformation of the airfoil is indeed unformed as desired.

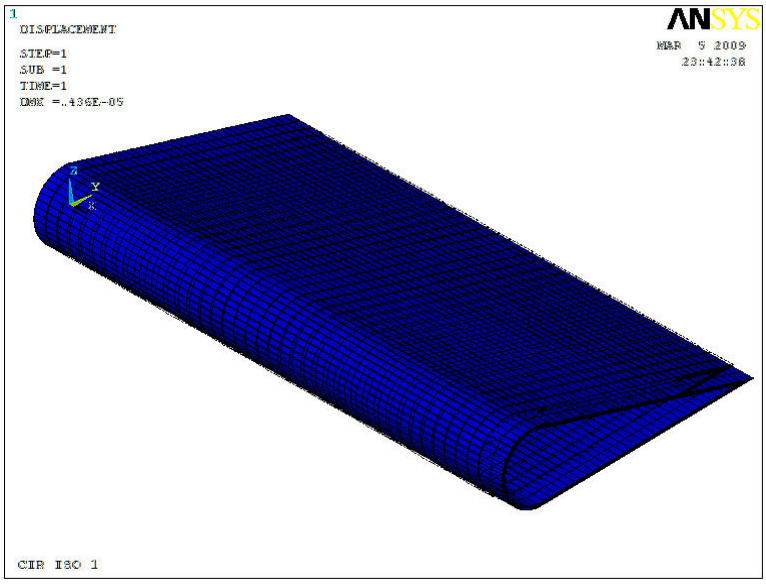

Figure 5.27 Deformation of isotropic airfoil

Figure 5.28 shows the axial stress generated in the airfoil due to the axial load

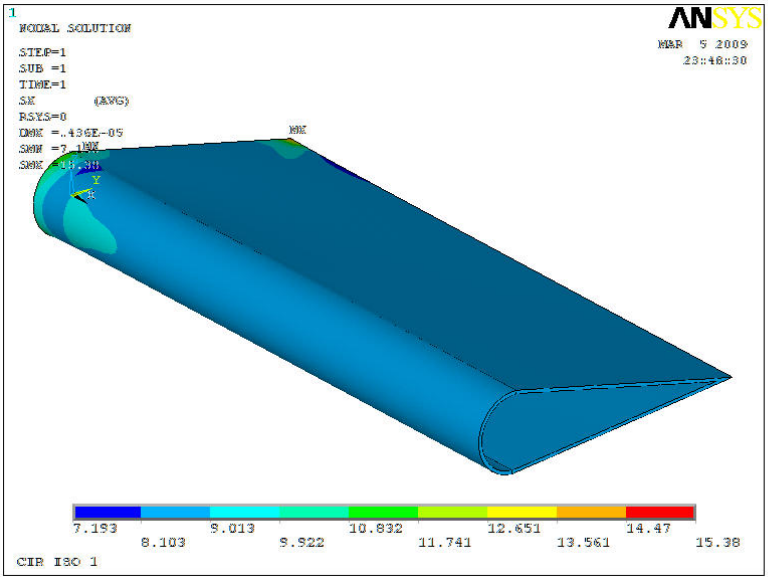

Figure 5.28 Axial stress in isotropic airfoil

Table 5.19 compares the axial stress in the airfoil between the FEM model and the theoretical solution. The results agree very well.

Table 5.19 Axial stress in isotropic airfoil

	σ_x	
	[psi]	%Diff
Theoretical Value	8.7372	
FEM	8.7428	-0.1

Table 5.20 lists the axial stiffnesses calculated through the present method and compared against the FEM and theoretical results. The results are close to each other.

Table 5.20 Axial stiffness of isotropic airfoil

		$\overline{A}_x$	
		[lb]	%Diff
Theoretical Value ISO	EA	3.5826E+07	
Present Method	$\overline{d}_{11}/(\overline{a}_{11}*\overline{d}_{11}-\overline{b}_{11}^2)$	3.7008E+07	3.3
FEM		3.6016E+07	0.5

5.11.3 Composite Airfoil $[0_8]_s$ under Axial Load

A composite airfoil was simulated with all the plies equal to 0° angle ply. Table 5.21 shows the comparison between the axial stress of the FEM model and the theoretical solution.

Table 5.21 Axial stress in $[0_8]_s$ composite airfoil

	σ_x	
	[psi]	%Diff
Theoretical Value	0.86584	
FEM	0.86817	-0.3

The axial stiffness are listed in Table 5.22. The results agree.

Table 5.22 Axial stiffness of $[0_8]_s$ composite airfoil

		$\overline{A}_x$	
		[lb]	%Diff
FEM		2.1012E+07	
Present Method	$\bar{d}_{11}/(\bar{a}_{11}*\bar{d}_{11}-\bar{b}_{11}^2)$	2.0330E+07	-3.2

5.11.4 Composite Airfoil $[45_2/-45_2/0_2/90_2]_s$ under axial load

A $[45_2/-45_2/0_2/90_2]_s$ composite airfoil was simulated. The axial displacements are presented in Figure 5.29 and the axial stress is plotted in Figure 5.30. The ply by ply stresses are shown in Figure 5.31. Once again, the stiffest plies take the largest stresses.

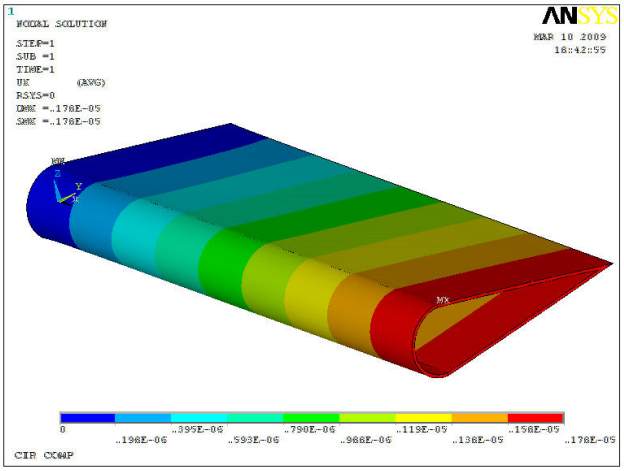

Figure 5.29 Axial displacement in $[45_2/-45_2/0_2/90_2]_s$ composite airfoil

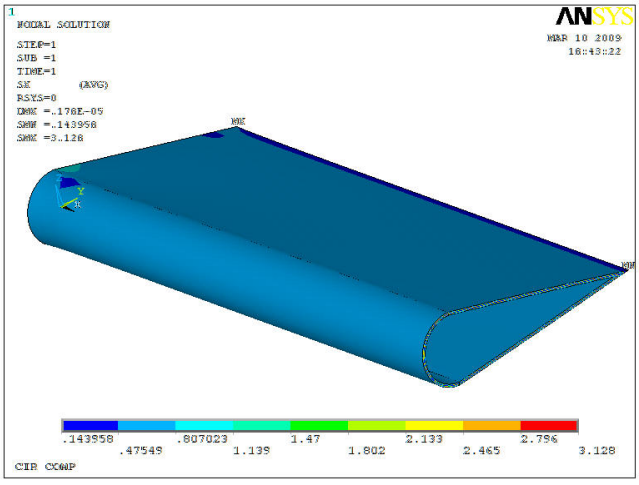

Figure 5.30 Axial stress in $[45_2/-45_2/0_2/90_2]_s$ composite airfoil

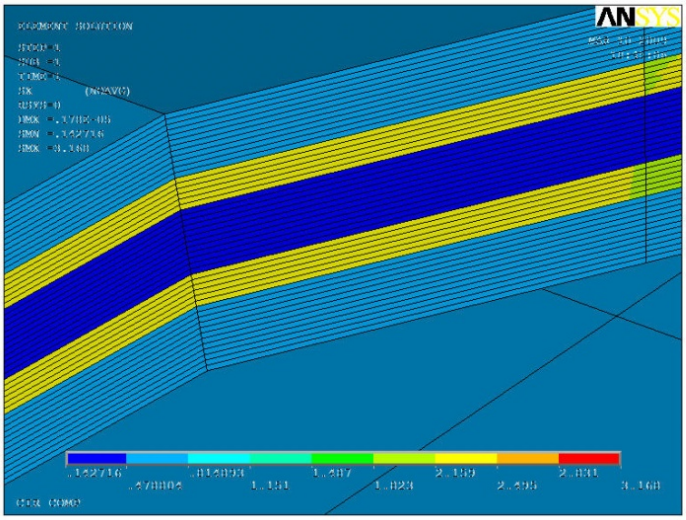

Figure 5.31 Axial stress in the plies of $[45_2/-45_2/0_2/90_2]_s$ composite airfoil

Table 5.23 lists the axial stiffness of the composite airfoil calculated by the FEM model and the present method. The results agree.

Table 5.23 Axial stiffness of $[45_2/-45_2/0_2/90_2]_s$ composite airfoil

		$\overline{A_x}$	
		[lb]	%Diff
FEM		8.4379E+06	
Present Method	$\overline{d}_{11}/(\overline{a}_{11}*\overline{d}_{11}-\overline{b}_{11}^2)$	8.1435E+06	-3.5

5.11.5 Isotropic Airfoil under Bending

The same airfoil was simulated under bending. The deformation is presented in Figure 5.32.

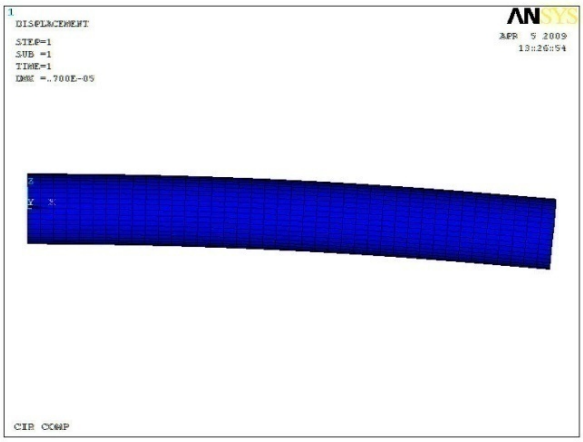

Figure 5.32 Deformation of isotropic airfoil under bending

Table 5.24 list the bending stiffness calculated through the present method and compared against the theoretical and FEM results. They agree very well.

Table 5.24 Bending stiffness of isotropic airfoil

		$\overline{D}_x$ [lb-in^2]	%Diff
Theoretical Value ISO	EI	1.1909E+07	
Present Method	$\bar{a}_{11}/(\bar{a}_{11}*\bar{d}_{11}-\bar{b}_{11}^2)$	1.1903E+07	-0.1
FEM		1.1848E+07	-0.5

5.11.6 Composite Airfoil $[0_8]_s$ under bending

For a composite airfoil with all the angle ply equal to 0°, the axial stiffness are listed in Table 5.25. The results agree well.

Table 5.25 Bending stiffness of $[0_8]_s$ composite airfoil

		$\overline{D_x}$ [lb-in²]	%Diff
FEM		7.4378E+06	
Present Method	$\bar{a}_{11}/(\bar{a}_{11}*\bar{d}_{11}-\bar{b}_{11}^2)$	7.2209E+06	-2.9

5.11.7 Composite Airfoil $[45_2/-45_2/0_2/90_2]_s$ under bending

A $[45_2/-45_2/0_2/90_2]_s$ composite airfoil was simulated under bending. Table 5.26 lists the bending stiffness of the composite airfoil calculated by the FEM model and the present method. The results agree very well.

Table 5.26 Bending stiffness of $[45_2/-45_2/0_2/90_2]_s$ composite airfoil

		$\overline{D_x}$ [lb-in²]	%Diff
FEM		2.8604E+06	
Present Method	$\bar{a}_{11}/(\bar{a}_{11}*\bar{d}_{11}-\bar{b}_{11}^2)$	2.8914E+06	1.1

5.11.8 Composite Airfoil $[90_8]_s$ under bending

Finally a composite airfoil with all the angle ply equal to 90°, the axial stiffness are listed in Table 5.27. Once again, the results agree well.

Table 5.27 Bending stiffness of $[90_8]_s$ composite airfoil

		$\overline{D_x}$ [lb-in²]	%Diff
FEM		5.5390E+05	
Present Method	$\bar{a}_{11}/(\bar{a}_{11}*\bar{d}_{11}-\bar{b}_{11}^2)$	5.5942E+05	1.0

CHAPTER 6

CONCLUSIVE REMARKS AND FUTURE WORK

An analytical method was developed to calculate the centroid, axial and bending stiffnesses, and ply stresses due to axial loading and bending of two laminated composite beams aligned bonded together one on the top of the other one. The results were compared with lamination theory, smeared property approach, and finite element method. The method was extended to calculate the centroid, axial and the bending stiffnesses of two laminate non-aligned top-and-bottom bonded together. This method reduces the two-dimensional properties of composite materials into one-dimensional structures or beams. The uniqueness of this method is that it includes the coupling effect due to the us-symmetry of the laminate as well as the structural configuration while smeared property approach does not.

In addition, another method was developed to calculate the equivalent axial and bending stiffnesses as well as the axial stresses in two laminates bonded side by side. The results were compared with, smeared property approach, theoretical solution and finite element method.

A new method is developed to calculate the axial and bending stiffnesses, and ply stresses for thin walled composite beam with arbitrary cross-section. The results were compared with finite element method, smeared property, previous, and modified method.

From this research, the following conclusions can be made.

- For the two laminate aligned bonded together one on the top of the other one method, the centroid shows excellent agreement with lamination theory for all the cases.
- For the two laminate aligned bonded together one on the top of the other one method, the axial and bending stiffnesses shows excellent agreement with finite element method

for all the cases. Smeared property approach results are deviated; especially for the bending stiffness case.

- For the two laminate aligned bonded together one on the top of the other one method, the stresses agree when all the plies are zero degree. For the symmetric case, the axial stresses are close from lamination theory and finite element method, especially for the zero degree plies. For the un-symmetric case, the stresses diverge.
- For the two laminate non-aligned bonded together one on the top of the other one method, the centroid, axial and bending stiffnesses are in excellent match with the finite element method and theoretical solution. The only case where there results are far is for the product of inertia of the un-symmetric laminate case.
- This method was extended to include the case of a Z-stiffener. The centroid, axial and bending stiffnesses match very well with the finite element and theoretical results.
- For the two laminates bonded side by side method, the stresses, axial and bending stiffnesses results match well with the finite element method one for all the cases less for the axial stresses for un-balanced laminate under bending and its bending stiffness.
- For the arbitrary cross-section method, the stress, axial and bending stiffnesses for a circular cross-section beam agree very well for all the cases with the finite element method and smeared property approach results. On the other hand, the previous method results diverge.
- For the arbitrary cross-section method, axial and bending stiffnesses for an airfoil cross-section beam agree very well for all the cases with the finite element method.

In future studies, the analysis could be extended to include hygrothermal effects, interlamina shear, torsion stiffness, failure analysis, and shear flow for thin walled structures.

In addition, there is room for improvement for the present method; especially, when treating un-symmetric laminates. Moreover, other kind of reinforcements can be studied; for example, I-beams type.

On the other hand, the present method for arbitrary cross-section can be used to study any other arbitrary cross-section other than circular and airfoil. In addition, it can be included the case of open cross-sections which was not included.

APPENDIX A

DERIVATION OF PARALLEL THEOREM FOR COMPLAINCE MATRICES OF LAMINATE

The following shows the detail procedure to obtain the shifted compliance matrices. The primed and unprimed notations refer to the new and original coordinate systems (Fig. A.1), respectively. ρ is the distance measure from the original coordinate system to the new coordinate system.

$$
\begin{aligned}
[A'] &= [A] \\
[B'] &= [B] - \rho[A] \\
[D'] &= [D] - 2\rho B] + \rho^2[A]
\end{aligned}
\tag{A.1}
$$

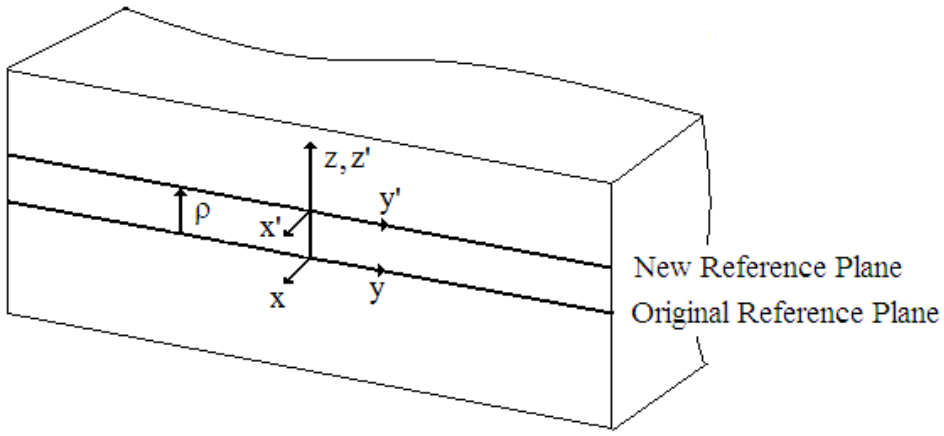

Figure A.1 References planes

On the other hand, inverting the stiffness matrices is given in [59] as

$$
\begin{pmatrix} N \\ M \end{pmatrix} = \begin{bmatrix} A & B \\ B & D \end{bmatrix} \begin{pmatrix} \varepsilon^o \\ \kappa \end{pmatrix}
$$

$$
\begin{aligned} N &= A\varepsilon^o + B\kappa \\ M &= B\varepsilon^o + D\kappa \end{aligned} \quad \rightarrow \quad \begin{aligned} \varepsilon^o &= A^{-1}N - A^{-1}B\kappa \\ M &= BA^{-1}N + (D - BA^{-1}B)\kappa \end{aligned}
$$

$$
\begin{pmatrix} \varepsilon^o \\ M \end{pmatrix} = \begin{bmatrix} A^* & B^* \\ H^* & D^* \end{bmatrix} \begin{pmatrix} N \\ \kappa \end{pmatrix}
$$

where

$$A^* = A^{-1}$$
$$B^* = -A^{-1}B$$
$$H^* = BA^{-1}$$
$$D^* = D - BA^{-1}B$$

$$\begin{matrix} \varepsilon^o = A^*N + B^*\kappa \\ M = H^*N + D^*\kappa \end{matrix} \rightarrow \begin{matrix} \varepsilon^o = A^*N + B^*(D^{*-1}M - D^{*-1}H^*N) \\ \kappa = D^{*-1}M - D^{*-1}H^*N \end{matrix}$$

$$\varepsilon^o = (A^* - B^*D^{*-1}H^*)N + B^*D^{*-1}M$$

$$\begin{pmatrix} \varepsilon^o \\ \kappa \end{pmatrix} = \begin{bmatrix} A^* - B^*D^{*-1}H^* & B^*D^{*-1} \\ -D^{*-1}H^* & D^{*-1} \end{bmatrix} \begin{pmatrix} N \\ M \end{pmatrix}$$

Therefore, it is possible to relate the stiffness matrices and the compliance matrices by

$$\begin{bmatrix} A & B \\ B & D \end{bmatrix}^{-1} = \begin{bmatrix} A^* - B^*D^{*-1}H^* & B^*D^{*-1} \\ -D^{*-1}H^* & D^{*-1} \end{bmatrix} = \begin{bmatrix} a & b \\ b^T & d \end{bmatrix}$$

However, considering a shift of a distance ρ (Eq. A.1), the stiffness and compliance matrices become

$$\begin{bmatrix} A & B-\rho A \\ B-\rho A & D-2\rho B+\rho^2 A \end{bmatrix}^{-1} = \begin{bmatrix} A'^* - B'^*D'^{*-1}H'^* & B'^*D'^{*-1} \\ -D'^{*-1}H'^* & D'^{*-1} \end{bmatrix} = \begin{bmatrix} a' & b' \\ b'^T & d' \end{bmatrix} \quad \text{(A.2)}$$

From the above equation it is possible to equate,

$$\begin{aligned} A'^* &= A^{-1} \\ B'^* &= -A^{-1}(B-\rho A) \\ H'^* &= (B-\rho A)A^{-1} \\ D'^* &= (D-2\rho B+\rho^2 A) - (B-\rho A)A^{-1}(B-\rho A) \end{aligned} \quad \text{(A.3)}$$

Expanding these equations,

$$A'^* = A^{-1}$$

$$B'^{*} = -A^{-1}(B - \rho A) = -A^{-1}B + A^{-1}\rho A = -A^{-1}B + \rho$$

$$H'^{*} = (B - \rho A)A^{-1} = BA^{-1} - \rho AA^{-1} = BA^{-1} - \rho$$

$$D'^{*} = (D - 2\rho B + \rho^2 A) - (B - \rho A)A^{-1}(B - \rho A)$$

$$D'^{*} = D - BA^{-1}B = D^{*}$$

This proof that,

$$D'^{*} = D^{*} \quad \text{or} \quad \boxed{d' = d} \tag{A.4}$$

On the other hand,

$$b' = B'^{*}D'^{*-1} \tag{A.5}$$

Substituting back Eqs. A.2 and A.4 into A.5,

$$b' = B'^{*}d'$$

In addition $B'^{*} = -A^{-1}B + \rho$,. Therefore,

$$b' = -A^{-1}Bd' + \rho d'$$

It is also known that, $B^{*} = -A^{-1}B$. Therefore,

$$b' = B^{*}d' + \rho d'$$

Finally, changing back $d' = D'^{*-1}$,

$$b' = B^{*}D'^{*-1} + \rho d'$$

And realizing that $b = B^{*}D^{*-1}$ and $d' = d$,

$$\boxed{b' = b + \rho d} \tag{A.6}$$

Finally, from A.2 it is known that,

$$a' = A'^{*} - B'^{*} D'^{*-1} H'^{*}$$

Substituting back Eq. A.3 and A.4 in this equation,

$$a' = A^{-1} + (A^{-1}B - \rho)d(BA^{-1} - \rho)$$

$$a' = A^{-1} + A^{-1}BdBA^{-1} - \rho A^{-1}Bd - \rho dBA^{-1} + \rho^2 d$$

$$a' = a + \rho(-A^{-1}BD'^{*-1} - D'^{*-1}BA^{-1}) + \rho^2 d$$

$$\boxed{a' = a + \rho(b + b^T) + \rho^2 d} \qquad \text{(A.7)}$$

APPENDIX B

PROOF THAT THE CENTROID EQUATIONS 3.19 AND 3.22 ARE EQUIVALENT

This section proofs that equation 3.19 expands to equation 3.22 and both are equivalent.

$$\bar{z}_c = \frac{\bar{z}_{c1} w_1 A_1^* + \bar{z}_{c2} w_2 A_2^*}{w_1 A_1^* + w_2 A_2^*}$$

However,

$$\bar{z}_{c1} = \bar{z}_1 + \rho_1$$
$$\bar{z}_{c2} = \bar{z}_2 + \rho_2$$

Substituting them back,

$$\bar{z}_c = \frac{(\bar{z}_1 + \rho_1) w_1 A_1^* + (\bar{z}_2 + \rho_2) w_2 A_2^*}{w_1 A_1^* + w_2 A_2^*}$$

In addition,

$$\rho_1 = -\left(\frac{b_{11}}{d_{11}}\right)_1 \qquad \text{and} \qquad \rho_2 = -\left(\frac{b_{11}}{d_{11}}\right)_2$$

$$A_1^* = \left(\frac{d_{11}}{a_{11} d_{11} - b_{11}^2}\right)_1 \quad \text{and} \quad A_2^* = \left(\frac{d_{11}}{a_{11} d_{11} - b_{11}^2}\right)_2$$

Substituting back,

$$\bar{z}_c = \frac{\left(\bar{z}_1 - \left(\frac{b_{11}}{d_{11}}\right)_1\right) w_1 \left(\frac{d_{11}}{a_{11} d_{11} - b_{11}^2}\right)_1 + \left(\bar{z}_2 - \left(\frac{b_{11}}{d_{11}}\right)_2\right) w_2 \left(\frac{d_{11}}{a_{11} d_{11} - b_{11}^2}\right)_2}{w_1 A_1^* + w_2 A_2^*}$$

$$\bar{z}_c = \frac{\bar{z}_1 w_1 \left(\frac{d_{11}}{a_{11}d_{11} - b_{11}^2} \right)_1 - w_1 \left(\frac{b_{11}}{d_{11}} \right)_1 \left(\frac{d_{11}}{a_{11}d_{11} - b_{11}^2} \right)_1 + \bar{z}_2 w_2 \left(\frac{d_{11}}{a_{11}d_{11} - b_{11}^2} \right)_2 - w_2 \left(\frac{b_{11}}{d_{11}} \right)_2 \left(\frac{d_{11}}{a_{11}d_{11} - b_{11}^2} \right)_2}{w_1 A_1^* + w_2 A_2^*}$$

$$\bar{z}_c = \frac{\bar{z}_1 w_1 A_1^* + w_1 \left(\frac{-b_{11}}{a_{11}d_{11} - b_{11}^2} \right)_1 + \bar{z}_2 w_2 A_2^* + w_2 \left(\frac{-b_{11}}{a_{11}d_{11} - b_{11}^2} \right)_2}{w_1 A_1^* + w_2 A_2^*}$$

And since,

$$B_1^* = \left(\frac{-b_{11}}{a_{11}d_{11} - b_{11}^2} \right)_1 \quad \text{and} \quad B_2^* = \left(\frac{-b_{11}}{a_{11}d_{11} - b_{11}^2} \right)_2$$

Therefore,

$$\bar{z}_c = \frac{\bar{z}_1 w_1 A_1^* + w_1 B_1^* + \bar{z}_2 w_2 A_2^* + w_2 B_2^*}{w_1 A_1^* + w_2 A_2^*}$$

which is equation 3.22.

APPENDIX C

MATLAB Files

Typical MATLAB file for Stiffener Reinforced Laminated Beam Symmetric Case $[0_4/-45/45/-45/45]_T$ and $[\pm 45_2]_T$ under bending.

```
% Bottom Laminate

E1=18.2e6;
E2=1.41e6;
v12=0.27;
G12=0.92e6;

ply=0.005;

h0=-4*ply;
h1=-3*ply;
h2=-2*ply;
h3=-1*ply;
h4=0*ply;
h5=1*ply;
h6=2*ply;
h7=3*ply;
h8=4*ply;

S11=1/E1;
S22=1/E2;
S12=-v12/E1;
S21=S12;
S33=1/G12;
S=[S11 S12 0;S21 S22 0;0 0 S33];
Q=inv(S);

b=0*pi/180;
n=sin(b);
m=cos(b);
TStress=[m^2 n^2 2*m*n;n^2 m^2 -2*m*n;-m*n m*n m^2-n^2];
TStrain=[m^2 n^2 m*n;n^2 m^2 -m*n;-2*m*n 2*m*n m^2-n^2];
QB_0=inv(TStress)*Q*TStrain;

b=45*pi/180;
n=sin(b);
m=cos(b);
TStress=[m^2 n^2 2*m*n;n^2 m^2 -2*m*n;-m*n m*n m^2-n^2];
TStrain=[m^2 n^2 m*n;n^2 m^2 -m*n;-2*m*n 2*m*n m^2-n^2];
QB_45=inv(TStress)*Q*TStrain;

b=-45*pi/180;
n=sin(b);
m=cos(b);
TStress=[m^2 n^2 2*m*n;n^2 m^2 -2*m*n;-m*n m*n m^2-n^2];
TStrain=[m^2 n^2 m*n;n^2 m^2 -m*n;-2*m*n 2*m*n m^2-n^2];
QB_N45=inv(TStress)*Q*TStrain;

P8=QB_0;
P7=QB_0;
P6=QB_0;
P5=QB_0;
```

```
P4=QB_N45;
P3=QB_45;
P2=QB_N45;
P1=QB_45;

A=P1*(h1-h0)+P2*(h2-h1)+P3*(h3-h2)+P4*(h4-h3)+P5*(h5-h4)+P6*(h6-h5)+P7*(h7-h6)+P8*(h8-
h7);
B=1/2*(P1*(h1^2-h0^2)+P2*(h2^2-h1^2)+P3*(h3^2-h2^2)+P4*(h4^2-h3^2)+P5*(h5^2-
h4^2)+P6*(h6^2-h5^2)+P7*(h7^2-h6^2)+P8*(h8^2-h7^2));
D=1/3*(P1*(h1^3-h0^3)+P2*(h2^3-h1^3)+P3*(h3^3-h2^3)+P4*(h4^3-h3^3)+P5*(h5^3-
h4^3)+P6*(h6^3-h5^3)+P7*(h7^3-h6^3)+P8*(h8^3-h7^3));

ABD=[A(1,1) A(1,2) A(1,3) B(1,1) B(1,2) B(1,3);
    A(2,1) A(2,2) A(2,3) B(2,1) B(2,2) B(2,3);
    A(3,1) A(3,2) A(3,3) B(3,1) B(3,2) B(3,3);
    B(1,1) B(1,2) B(1,3) D(1,1) D(1,2) D(1,3);
    B(2,1) B(2,2) B(2,3) D(2,1) D(2,2) D(2,3);
    B(3,1) B(3,2) B(3,3) D(3,1) D(3,2) D(3,3)];

abd1=inv(ABD);

p1=-abd1(1,4)/abd1(4,4)

% Top Laminate

E1=18.2e6;
E2=1.41e6;
v12=0.27;
G12=0.92e6;

ply=0.005;

h0=-2*ply;
h1=-1*ply;
h2=0*ply;
h3=1*ply;
h4=2*ply;

S11=1/E1;
S22=1/E2;
S12=-v12/E1;
S21=S12;
S33=1/G12;
S=[S11 S12 0;S21 S22 0;0 0 S33];
Q=inv(S);

b=45*pi/180;
n=sin(b);
m=cos(b);
TStress=[m^2 n^2 2*m*n;n^2 m^2 -2*m*n;-m*n m*n m^2-n^2];
TStrain=[m^2 n^2 m*n;n^2 m^2 -m*n;-2*m*n 2*m*n m^2-n^2];
QB_45=inv(TStress)*Q*TStrain;

b=-45*pi/180;
n=sin(b);
m=cos(b);
```

```
TStress=[m^2 n^2 2*m*n;n^2 m^2 -2*m*n;-m*n m*n m^2-n^2];
TStrain=[m^2 n^2 m*n;n^2 m^2 -m*n;-2*m*n 2*m*n m^2-n^2];
QB_N45=inv(TStress)*Q*TStrain;

P4=QB_45;
P3=QB_N45;
P2=QB_45;
P1=QB_N45;

A=P1*(h1-h0)+P2*(h2-h1)+P3*(h3-h2)+P4*(h4-h3);
B=1/2*(P1*(h1^2-h0^2)+P2*(h2^2-h1^2)+P3*(h3^2-h2^2)+P4*(h4^2-h3^2));
D=1/3*(P1*(h1^3-h0^3)+P2*(h2^3-h1^3)+P3*(h3^3-h2^3)+P4*(h4^3-h3^3));

ABD=[A(1,1) A(1,2) A(1,3) B(1,1) B(1,2) B(1,3);
    A(2,1) A(2,2) A(2,3) B(2,1) B(2,2) B(2,3);
    A(3,1) A(3,2) A(3,3) B(3,1) B(3,2) B(3,3);
    B(1,1) B(1,2) B(1,3) D(1,1) D(1,2) D(1,3);
    B(2,1) B(2,2) B(2,3) D(2,1) D(2,2) D(2,3);
    B(3,1) B(3,2) B(3,3) D(3,1) D(3,2) D(3,3)];

abd2=inv(ABD);

p2=-abd2(1,4)/abd2(4,4)


% Centroids, Stiffnesses, and Stresses

tply=0.005;
w1=0.5;
w2=0.5;

zb1=4*tply;
zb2=10*tply;

c1=-1/((abd1(1,6)^2-abd1(1,1)*abd1(6,6))*abd1(4,4)-
2*abd1(1,4)*abd1(1,6)*abd1(4,6)+abd1(1,1)*abd1(4,6)^2+abd1(1,4)^2*abd1(6,6))
c2=-1/((abd2(1,6)^2-abd2(1,1)*abd2(6,6))*abd2(4,4)-
2*abd2(1,4)*abd2(1,6)*abd2(4,6)+abd2(1,1)*abd2(4,6)^2+abd2(1,4)^2*abd2(6,6))

A1ss=c1*(abd1(4,4)*abd1(6,6)-abd1(4,6)^2);
A2ss=c2*(abd2(4,4)*abd2(6,6)-abd2(4,6)^2);
B1ss=c1*(-abd1(1,4)*abd1(6,6)+abd1(1,6)*abd1(4,6));
B2ss=c2*(-abd2(1,4)*abd2(6,6)+abd2(1,6)*abd2(4,6));
D1ss=c1*(-abd1(1,6)^2+abd1(1,1)*abd1(6,6));
D2ss=c2*(-abd2(1,6)^2+abd2(1,1)*abd2(6,6));

zc=((zb1+p1)*w1*A1ss+(zb2+p2)*w2*A2ss)/(w1*A1ss+w2*A2ss);

z1=(zb1)-zc;
z2=(zb2)-zc;

yb1=0.5/2;
yb2=0.5/2;

yc=((yb1)*w1*A1ss+(yb2)*w2*A2ss)/(w1*A1ss+w2*A2ss);
```

```
z1=(zb1)-zc;
z2=(zb2)-zc;

EA=w1*A1ss+w2*A2ss

y1=(yb1)-yc;
y2=(yb2)-yc;

EI=w1*A1ss*z1^2+2*w1*B1ss*z1+w1*D1ss+w2*A2ss*z2^2+2*w2*B2ss*z2+w2*D2ss

exc=0/EA;
kxc=0.01/EI;

stiff1=[A1ss B1ss+z1*A1ss;
  B1ss D1ss+z1*B1ss];

stiff2=[A2ss B2ss+z2*A2ss;
  B2ss D2ss+z2*B2ss];

NM1=stiff1*[exc;kxc];
NM2=stiff2*[exc;kxc];

Mxy1=-1/abd1(6,6)*(abd1(1,6)*NM1(1)+abd1(4,6)*NM1(2));
Mxy2=-1/abd2(6,6)*(abd2(1,6)*NM2(1)+abd2(4,6)*NM2(2));

midplane1=[abd1(1,1) abd1(1,4) abd1(1,6);
        abd1(2,1) abd1(2,4) abd1(2,6);
        abd1(3,1) abd1(3,4) abd1(3,6);
        abd1(4,1) abd1(4,4) abd1(4,6);
        abd1(5,1) abd1(5,4) abd1(5,6);
        abd1(6,1) abd1(6,4) abd1(6,6)]*[NM1(1);NM1(2);Mxy1];

midplane2=[abd2(1,1) abd2(1,4) abd2(1,6);
        abd2(2,1) abd2(2,4) abd2(2,6);
        abd2(3,1) abd2(3,4) abd2(3,6);
        abd2(4,1) abd2(4,4) abd2(4,6);
        abd2(5,1) abd2(5,4) abd2(5,6);
        abd2(6,1) abd2(6,4) abd2(6,6)]*[NM2(1);NM2(2);Mxy2];

% Stresses on the Bottom Laminate
z=-3.5*tply;
strain1=[midplane1(1);midplane1(2);midplane1(3)]+z*[midplane1(4);midplane1(5);midplane1(6)];
stress1=QB_45*strain1

% Stresses on the Top Laminate
z=1.5*tply;
strain2=[midplane2(1);midplane2(2);midplane2(3)]+z*[midplane2(4);midplane2(5);midplane2(6)];
stress2=QB_45*strain2
```

Typical MATLAB file for Non-Aligned Stiffener Reinforced Laminated Beam Un-symmetric Case $[\pm 45/0/90]_{3T}$.

```
% Bottom Laminate

E1=18.2e6;
E2=1.41e6;
v12=0.27;
G12=0.92e6;

ply=0.005;

h0=-4*ply;
h1=-3*ply;
h2=-2*ply;
h3=-1*ply;
h4=0*ply;
h5=1*ply;
h6=2*ply;
h7=3*ply;
h8=4*ply;

S11=1/E1;
S22=1/E2;
S12=-v12/E1;
S21=S12;
S33=1/G12;
S=[S11 S12 0;S21 S22 0;0 0 S33];
Q=inv(S);

b=0*pi/180;
n=sin(b);
m=cos(b);
TStress=[m^2 n^2 2*m*n;n^2 m^2 -2*m*n;-m*n m*n m^2-n^2];
TStrain=[m^2 n^2 m*n;n^2 m^2 -m*n;-2*m*n 2*m*n m^2-n^2];
QB_0=inv(TStress)*Q*TStrain;

b=45*pi/180;
n=sin(b);
m=cos(b);
TStress=[m^2 n^2 2*m*n;n^2 m^2 -2*m*n;-m*n m*n m^2-n^2];
TStrain=[m^2 n^2 m*n;n^2 m^2 -m*n;-2*m*n 2*m*n m^2-n^2];
QB_45=inv(TStress)*Q*TStrain;

b=-45*pi/180;
n=sin(b);
m=cos(b);
TStress=[m^2 n^2 2*m*n;n^2 m^2 -2*m*n;-m*n m*n m^2-n^2];
TStrain=[m^2 n^2 m*n;n^2 m^2 -m*n;-2*m*n 2*m*n m^2-n^2];
QB_N45=inv(TStress)*Q*TStrain;

b=90*pi/180;
n=sin(b);
m=cos(b);
TStress=[m^2 n^2 2*m*n;n^2 m^2 -2*m*n;-m*n m*n m^2-n^2];
```

```
TStrain=[m^2 n^2 m*n;n^2 m^2 -m*n;-2*m*n 2*m*n m^2-n^2];
QB_90=inv(TStress)*Q*TStrain;

P8=QB_45;
P7=QB_N45;
P6=QB_0;
P5=QB_90;
P4=QB_45;
P3=QB_N45;
P2=QB_0;
P1=QB_90;

A=P1*(h1-h0)+P2*(h2-h1)+P3*(h3-h2)+P4*(h4-h3)+P5*(h5-h4)+P6*(h6-h5)+P7*(h7-h6)+P8*(h8-
h7);
B=1/2*(P1*(h1^2-h0^2)+P2*(h2^2-h1^2)+P3*(h3^2-h2^2)+P4*(h4^2-h3^2)+P5*(h5^2-
h4^2)+P6*(h6^2-h5^2)+P7*(h7^2-h6^2)+P8*(h8^2-h7^2));
D=1/3*(P1*(h1^3-h0^3)+P2*(h2^3-h1^3)+P3*(h3^3-h2^3)+P4*(h4^3-h3^3)+P5*(h5^3-
h4^3)+P6*(h6^3-h5^3)+P7*(h7^3-h6^3)+P8*(h8^3-h7^3));

ABD=[A(1,1) A(1,2) A(1,3) B(1,1) B(1,2) B(1,3);
    A(2,1) A(2,2) A(2,3) B(2,1) B(2,2) B(2,3);
    A(3,1) A(3,2) A(3,3) B(3,1) B(3,2) B(3,3);
    B(1,1) B(1,2) B(1,3) D(1,1) D(1,2) D(1,3);
    B(2,1) B(2,2) B(2,3) D(2,1) D(2,2) D(2,3);
    B(3,1) B(3,2) B(3,3) D(3,1) D(3,2) D(3,3)];

abd1=inv(ABD);

a111=abd1(1,1)
d111=abd1(4,4)
p1=-abd1(1,4)/abd1(4,4)

% Top Laminate

E1=18.2e6;
E2=1.41e6;
v12=0.27;
G12=0.92e6;

ply=0.005;

h0=-2*ply;
h1=-1*ply;
h2=0*ply;
h3=1*ply;
h4=2*ply;

S11=1/E1;
S22=1/E2;
S12=-v12/E1;
S21=S12;
S33=1/G12;
S=[S11 S12 0;S21 S22 0;0 0 S33];
Q=inv(S);

b=0*pi/180;
```

```
n=sin(b);
m=cos(b);
TStress=[m^2 n^2 2*m*n;n^2 m^2 -2*m*n;-m*n m*n m^2-n^2];
TStrain=[m^2 n^2 m*n;n^2 m^2 -m*n;-2*m*n 2*m*n m^2-n^2];
QB_0=inv(TStress)*Q*TStrain;

b=45*pi/180;
n=sin(b);
m=cos(b);
TStress=[m^2 n^2 2*m*n;n^2 m^2 -2*m*n;-m*n m*n m^2-n^2];
TStrain=[m^2 n^2 m*n;n^2 m^2 -m*n;-2*m*n 2*m*n m^2-n^2];
QB_45=inv(TStress)*Q*TStrain;

b=-45*pi/180;
n=sin(b);
m=cos(b);
TStress=[m^2 n^2 2*m*n;n^2 m^2 -2*m*n;-m*n m*n m^2-n^2];
TStrain=[m^2 n^2 m*n;n^2 m^2 -m*n;-2*m*n 2*m*n m^2-n^2];
QB_N45=inv(TStress)*Q*TStrain;

b=90*pi/180;
n=sin(b);
m=cos(b);
TStress=[m^2 n^2 2*m*n;n^2 m^2 -2*m*n;-m*n m*n m^2-n^2];
TStrain=[m^2 n^2 m*n;n^2 m^2 -m*n;-2*m*n 2*m*n m^2-n^2];
QB_90=inv(TStress)*Q*TStrain;

P4=QB_45;
P3=QB_N45;
P2=QB_0;
P1=QB_90;

A=P1*(h1-h0)+P2*(h2-h1)+P3*(h3-h2)+P4*(h4-h3);
B=1/2*(P1*(h1^2-h0^2)+P2*(h2^2-h1^2)+P3*(h3^2-h2^2)+P4*(h4^2-h3^2));
D=1/3*(P1*(h1^3-h0^3)+P2*(h2^3-h1^3)+P3*(h3^3-h2^3)+P4*(h4^3-h3^3));

ABD=[A(1,1) A(1,2) A(1,3) B(1,1) B(1,2) B(1,3);
    A(2,1) A(2,2) A(2,3) B(2,1) B(2,2) B(2,3);
    A(3,1) A(3,2) A(3,3) B(3,1) B(3,2) B(3,3);
    B(1,1) B(1,2) B(1,3) D(1,1) D(1,2) D(1,3);
    B(2,1) B(2,2) B(2,3) D(2,1) D(2,2) D(2,3);
    B(3,1) B(3,2) B(3,3) D(3,1) D(3,2) D(3,3)];

abd2=inv(ABD);

a112=abd2(1,1)
d112=abd2(4,4)
p2=-abd2(1,4)/abd2(4,4)

%  Centroids and Stiffnesses

tply=0.005;
w1=0.5;
w2=0.25;

zb1=4*tply;
```

```
zb2=10*tply;

A1s=abd1(4,4)/(abd1(1,1)*abd1(4,4)-abd1(1,4)^2);
A2s=abd2(4,4)/(abd2(1,1)*abd2(4,4)-abd2(1,4)^2);
B1s=abd1(1,4)/(abd1(1,4)^2-abd1(1,1)*abd1(4,4));
B2s=abd2(1,4)/(abd2(1,4)^2-abd2(1,1)*abd2(4,4));
D1s=abd1(1,1)/(abd1(1,1)*abd1(4,4)-abd1(1,4)^2);
D2s=abd2(1,1)/(abd2(1,1)*abd2(4,4)-abd2(1,4)^2);

zc=((zb1+p1)*w1*A1s+(zb2+p2)*w2*A2s)/(w1*A1s+w2*A2s);

z1=(zb1)-zc;
z2=(zb2)-zc;

yb1=0.5/2;
yb2=0.25/2+0.0625;

yc=((yb1)*w1/abd1(1,1)+(yb2+p2)*w2/abd2(1,1))/(w1/abd1(1,1)+w2/abd2(1,1));

z1=(zb1)-zc;
z2=(zb2)-zc;

EA=w1*A1s+w2*A2s

y1=(yb1)-yc;
y2=(yb2)-yc;

EIyy=w1*A1s*z1^2+2*w1*B1s*z1+w1*D1s+w2*A2s*z2^2+2*w2*B2s*z2+w2*D2s
EIzz=A1s*(w1^3/12+y1^2*w1)+A2s*(w2^3/12+y2^2*w2)
EIyz=w1*(A1s*z1+B1s)*y1+w2*(A2s*z2+B2s)*y2
```

Typical MATLAB file for the Z-stiffener.

```
% Flanges 1

E1=18.2e6;
E2=1.41e6;
v12=0.27;
G12=0.92e6;

ply=0.005;

h0=-6*ply;
h1=-5*ply;
h2=-4*ply;
h3=-3*ply;
h4=-2*ply;
h5=-1*ply;
h6=0*ply;
h7=1*ply;
h8=2*ply;
h9=3*ply;
h10=4*ply;
h11=5*ply;
h12=6*ply;

S11=1/E1;
S22=1/E2;
S12=-v12/E1;
S21=S12;
S33=1/G12;
S=[S11 S12 0;S21 S22 0;0 0 S33];
Q=inv(S);

b=45*pi/180;
n=sin(b);
m=cos(b);
TStress=[m^2 n^2 2*m*n;n^2 m^2 -2*m*n;-m*n m*n m^2-n^2];
TStrain=[m^2 n^2 m*n;n^2 m^2 -m*n;-2*m*n 2*m*n m^2-n^2];
QB_45=inv(TStress)*Q*TStrain;

b=-45*pi/180;
n=sin(b);
m=cos(b);
TStress=[m^2 n^2 2*m*n;n^2 m^2 -2*m*n;-m*n m*n m^2-n^2];
TStrain=[m^2 n^2 m*n;n^2 m^2 -m*n;-2*m*n 2*m*n m^2-n^2];
QB_N45=inv(TStress)*Q*TStrain;



b=0*pi/180;
n=sin(b);
m=cos(b);
TStress=[m^2 n^2 2*m*n;n^2 m^2 -2*m*n;-m*n m*n m^2-n^2];
TStrain=[m^2 n^2 m*n;n^2 m^2 -m*n;-2*m*n 2*m*n m^2-n^2];
QB_0=inv(TStress)*Q*TStrain;
```

```
P12=QB_45;
P11=QB_N45;
P10=QB_0;
P9=QB_0;
P8=QB_N45;
P7=QB_45;
P6=QB_45;
P5=QB_N45;
P4=QB_0;
P3=QB_0;
P2=QB_N45;
P1=QB_45;

A=P1*(h1-h0)+P2*(h2-h1)+P3*(h3-h2)+P4*(h4-h3)+P5*(h5-h4)+P6*(h6-h5)+P7*(h7-h6)+P8*(h8-
h7)+P9*(h9-h8)+P10*(h10-h9)+P11*(h11-h10)+P12*(h12-h11);
B=1/2*(P1*(h1^2-h0^2)+P2*(h2^2-h1^2)+P3*(h3^2-h2^2)+P4*(h4^2-h3^2)+P5*(h5^2-
h4^2)+P6*(h6^2-h5^2)+P7*(h7^2-h6^2)+P8*(h8^2-h7^2)+P9*(h9^2-h8^2)+P10*(h10^2-
h9^2)+P11*(h11^2-h10^2)+P12*(h12^2-h11^2));
D=1/3*(P1*(h1^3-h0^3)+P2*(h2^3-h1^3)+P3*(h3^3-h2^3)+P4*(h4^3-h3^3)+P5*(h5^3-
h4^3)+P6*(h6^3-h5^3)+P7*(h7^3-h6^3)+P8*(h8^3-h7^3)+P9*(h9^3-h8^3)+P10*(h10^3-
h9^3)+P11*(h11^3-h10^3)+P12*(h12^3-h11^3));

ABD=[A(1,1) A(1,2) A(1,3) B(1,1) B(1,2) B(1,3);
    A(2,1) A(2,2) A(2,3) B(2,1) B(2,2) B(2,3);
    A(3,1) A(3,2) A(3,3) B(3,1) B(3,2) B(3,3);
    B(1,1) B(1,2) B(1,3) D(1,1) D(1,2) D(1,3);
    B(2,1) B(2,2) B(2,3) D(2,1) D(2,2) D(2,3);
    B(3,1) B(3,2) B(3,3) D(3,1) D(3,2) D(3,3)];

abdf1=inv(ABD);

Asf1=1/(abdf1(1,1)-abdf1(1,4)^2/abdf1(4,4))
Bsf1=1/(abdf1(1,4)-abdf1(1,1)*abdf1(4,4)/abdf1(1,4))
Dsf1=1/(abdf1(4,4)-abdf1(1,4)^2/abdf1(1,1))

% Flanges 2

E1=18.2e6;
E2=1.41e6;
v12=0.27;
G12=0.92e6;

ply=0.005;

h0=-6*ply;
h1=-5*ply;
h2=-4*ply;
h3=-3*ply;
h4=-2*ply;
h5=-1*ply;
h6=0*ply;
h7=1*ply;
h8=2*ply;
h9=3*ply;
h10=4*ply;
h11=5*ply;
```

```
h12=6*ply;

S11=1/E1;
S22=1/E2;
S12=-v12/E1;
S21=S12;
S33=1/G12;
S=[S11 S12 0;S21 S22 0;0 0 S33];
Q=inv(S);

b=45*pi/180;
n=sin(b);
m=cos(b);
TStress=[m^2 n^2 2*m*n;n^2 m^2 -2*m*n;-m*n m*n m^2-n^2];
TStrain=[m^2 n^2 m*n;n^2 m^2 -m*n;-2*m*n 2*m*n m^2-n^2];
QB_45=inv(TStress)*Q*TStrain;

b=-45*pi/180;
n=sin(b);
m=cos(b);
TStress=[m^2 n^2 2*m*n;n^2 m^2 -2*m*n;-m*n m*n m^2-n^2];
TStrain=[m^2 n^2 m*n;n^2 m^2 -m*n;-2*m*n 2*m*n m^2-n^2];
QB_N45=inv(TStress)*Q*TStrain;

b=0*pi/180;
n=sin(b);
m=cos(b);
TStress=[m^2 n^2 2*m*n;n^2 m^2 -2*m*n;-m*n m*n m^2-n^2];
TStrain=[m^2 n^2 m*n;n^2 m^2 -m*n;-2*m*n 2*m*n m^2-n^2];
QB_0=inv(TStress)*Q*TStrain;

P12=QB_45;
P11=QB_N45;
P10=QB_0;
P9=QB_0;
P8=QB_N45;
P7=QB_45;
P6=QB_45;
P5=QB_N45;
P4=QB_0;
P3=QB_0;
P2=QB_N45;
P1=QB_45;

A=P1*(h1-h0)+P2*(h2-h1)+P3*(h3-h2)+P4*(h4-h3)+P5*(h5-h4)+P6*(h6-h5)+P7*(h7-h6)+P8*(h8-
h7)+P9*(h9-h8)+P10*(h10-h9)+P11*(h11-h10)+P12*(h12-h11);
B=1/2*(P1*(h1^2-h0^2)+P2*(h2^2-h1^2)+P3*(h3^2-h2^2)+P4*(h4^2-h3^2)+P5*(h5^2-
h4^2)+P6*(h6^2-h5^2)+P7*(h7^2-h6^2)+P8*(h8^2-h7^2)+P9*(h9^2-h8^2)+P10*(h10^2-
h9^2)+P11*(h11^2-h10^2)+P12*(h12^2-h11^2));
D=1/3*(P1*(h1^3-h0^3)+P2*(h2^3-h1^3)+P3*(h3^3-h2^3)+P4*(h4^3-h3^3)+P5*(h5^3-
h4^3)+P6*(h6^3-h5^3)+P7*(h7^3-h6^3)+P8*(h8^3-h7^3)+P9*(h9^3-h8^3)+P10*(h10^3-
h9^3)+P11*(h11^3-h10^3)+P12*(h12^3-h11^3));

ABD=[A(1,1) A(1,2) A(1,3) B(1,1) B(1,2) B(1,3);
    A(2,1) A(2,2) A(2,3) B(2,1) B(2,2) B(2,3);
    A(3,1) A(3,2) A(3,3) B(3,1) B(3,2) B(3,3);
```

```
    B(1,1) B(1,2) B(1,3) D(1,1) D(1,2) D(1,3);
    B(2,1) B(2,2) B(2,3) D(2,1) D(2,2) D(2,3);
    B(3,1) B(3,2) B(3,3) D(3,1) D(3,2) D(3,3)];

abdf2=inv(ABD);

Asf2=1/(abdf2(1,1)-abdf2(1,4)^2/abdf2(4,4))
Bsf2=1/(abdf2(1,4)-abdf2(1,1)*abdf2(4,4)/abdf2(1,4))
Dsf2=1/(abdf2(4,4)-abdf2(1,4)^2/abdf2(1,1))

% Web

E1=18.2e6;
E2=1.41e6;
v12=0.27;
G12=0.92e6;

ply=0.005;

h0=-2*ply;
h1=-1*ply;
h2=0*ply;
h3=1*ply;
h4=2*ply;

S11=1/E1;
S22=1/E2;
S12=-v12/E1;
S21=S12;
S33=1/G12;
S=[S11 S12 0;S21 S22 0;0 0 S33];
Q=inv(S);

b=45*pi/180;
n=sin(b);
m=cos(b);
TStress=[m^2 n^2 2*m*n;n^2 m^2 -2*m*n;-m*n m*n m^2-n^2];
TStrain=[m^2 n^2 m*n;n^2 m^2 -m*n;-2*m*n 2*m*n m^2-n^2];
QB_45=inv(TStress)*Q*TStrain;

b=-45*pi/180;
n=sin(b);
m=cos(b);
TStress=[m^2 n^2 2*m*n;n^2 m^2 -2*m*n;-m*n m*n m^2-n^2];
TStrain=[m^2 n^2 m*n;n^2 m^2 -m*n;-2*m*n 2*m*n m^2-n^2];
QB_N45=inv(TStress)*Q*TStrain;

P4=QB_45;
P3=QB_N45;
P2=QB_N45;
P1=QB_45;

A=P1*(h1-h0)+P2*(h2-h1)+P3*(h3-h2)+P4*(h4-h3);
B=1/2*(P1*(h1^2-h0^2)+P2*(h2^2-h1^2)+P3*(h3^2-h2^2)+P4*(h4^2-h3^2));
D=1/3*(P1*(h1^3-h0^3)+P2*(h2^3-h1^3)+P3*(h3^3-h2^3)+P4*(h4^3-h3^3));
```

```
ABD=[A(1,1) A(1,2) A(1,3) B(1,1) B(1,2) B(1,3);
    A(2,1) A(2,2) A(2,3) B(2,1) B(2,2) B(2,3);
    A(3,1) A(3,2) A(3,3) B(3,1) B(3,2) B(3,3);
    B(1,1) B(1,2) B(1,3) D(1,1) D(1,2) D(1,3);
    B(2,1) B(2,2) B(2,3) D(2,1) D(2,2) D(2,3);
    B(3,1) B(3,2) B(3,3) D(3,1) D(3,2) D(3,3)];

abdw=inv(ABD);

Asw=1/(abdw(1,1)-abdw(1,4)^2/abdw(4,4))
Bsw=1/(abdw(1,4)-abdw(1,1)*abdw(4,4)/abdw(1,4))
Dsw=1/(abdw(4,4)-abdw(1,4)^2/abdw(1,1))

% Stiffnesses

tply=0.005;

w1=0.25;
w2=0.25;
hw=0.5;

yb1=-w1/2+2*tply;
yb2=w1/2-2*tply;

zb1=12*tply+hw+6*tply;
zb2=6*tply;
zc=12*tply+hw/2;
yc=0;
z1=zb1-zc;
z2=zb2-zc;
y1=yb1-yc;
y2=yb2-yc;

Ax=w1*(Asf1+(z1)*Bsf1)+w2*(Asf2-(z2)*Bsf2)+hw*Asw
Dx=w1*(Asf1*z1^2+2*z1*Bsf1+Dsf1)+w2*(Asf2*z2^2+2*z2*Bsf2+Dsf2)+Asw*(1/12*hw^3)
Dxy=w1*(Asf1*z1+Bsf1)*y1+w2*(Asf2*z2+Bsf2)*y2
Dy=Asf1*(1/12*w1^3+y1^2*w1)+Asf2*(1/12*w2^3+y2^2*w2)+hw*Dsw
```

Typical MATLAB file for Laminates Bonded Side by Side Un-symmetric Case $[\pm 45_2/0_4/\pm 45_2]_T$ - $[\pm 45_2/0_2]_S$ under Axial load.

```
% Laminate 1

E1=18.2e6;
E2=1.41e6;
v12=0.27;
G12=0.92e6;

ply=0.005;
total_t=12*ply;

h0=-6*ply;
h1=-5*ply;
h2=-4*ply;
h3=-3*ply;
h4=-2*ply;
h5=-1*ply;
h6=0*ply;
h7=1*ply;
h8=2*ply;
h9=3*ply;
h10=4*ply;
h11=5*ply;
h12=6*ply;

S11=1/E1;
S22=1/E2;
S12=-v12/E1;
S21=S12;
S33=1/G12;
S=[S11 S12 0;S21 S22 0;0 0 S33];
Q=inv(S);

b=0*pi/180;
n=sin(b);
m=cos(b);
TStress=[m^2 n^2 2*m*n;n^2 m^2 -2*m*n;-m*n m*n m^2-n^2];
TStrain=[m^2 n^2 m*n;n^2 m^2 -m*n;-2*m*n 2*m*n m^2-n^2];
QB_0=inv(TStress)*Q*TStrain;

b=45*pi/180;
n=sin(b);
m=cos(b);
TStress=[m^2 n^2 2*m*n;n^2 m^2 -2*m*n;-m*n m*n m^2-n^2];
TStrain=[m^2 n^2 m*n;n^2 m^2 -m*n;-2*m*n 2*m*n m^2-n^2];
QB_45=inv(TStress)*Q*TStrain;

b=-45*pi/180;
n=sin(b);
m=cos(b);
TStress=[m^2 n^2 2*m*n;n^2 m^2 -2*m*n;-m*n m*n m^2-n^2];
TStrain=[m^2 n^2 m*n;n^2 m^2 -m*n;-2*m*n 2*m*n m^2-n^2];
```

```
QB_N45=inv(TStress)*Q*TStrain;

P12=QB_45;
P11=QB_N45;
P10=QB_45;
P9=QB_N45;
P8=QB_0;
P7=QB_0;
P6=QB_0;
P5=QB_0;
P4=QB_45;
P3=QB_N45;
P2=QB_45;
P1=QB_N45;

A=P1*(h1-h0)+P2*(h2-h1)+P3*(h3-h2)+P4*(h4-h3)+P5*(h5-h4)+P6*(h6-h5)+P7*(h7-h6)+P8*(h8-
h7)+P9*(h9-h8)+P10*(h10-h9)+P11*(h11-h10)+P12*(h12-h11);
B=1/2*(P1*(h1^2-h0^2)+P2*(h2^2-h1^2)+P3*(h3^2-h2^2)+P4*(h4^2-h3^2)+P5*(h5^2-
h4^2)+P6*(h6^2-h5^2)+P7*(h7^2-h6^2)+P8*(h8^2-h7^2)+P9*(h9^2-h8^2)+P10*(h10^2-
h9^2)+P11*(h11^2-h10^2)+P12*(h12^2-h11^2));
D=1/3*(P1*(h1^3-h0^3)+P2*(h2^3-h1^3)+P3*(h3^3-h2^3)+P4*(h4^3-h3^3)+P5*(h5^3-
h4^3)+P6*(h6^3-h5^3)+P7*(h7^3-h6^3)+P8*(h8^3-h7^3)+P9*(h9^3-h8^3)+P10*(h10^3-
h9^3)+P11*(h11^3-h10^3)+P12*(h12^3-h11^3));

ABD=[A(1,1) A(1,2) A(1,3) B(1,1) B(1,2) B(1,3);
    A(2,1) A(2,2) A(2,3) B(2,1) B(2,2) B(2,3);
    A(3,1) A(3,2) A(3,3) B(3,1) B(3,2) B(3,3);
    B(1,1) B(1,2) B(1,3) D(1,1) D(1,2) D(1,3);
    B(2,1) B(2,2) B(2,3) D(2,1) D(2,2) D(2,3);
    B(3,1) B(3,2) B(3,3) D(3,1) D(3,2) D(3,3)];

abd1=inv(ABD);

ass1=(abd1(1,1)*abd1(4,4)-abd1(1,4)^2)/abd1(4,4)
dss1=(abd1(1,1)*abd1(4,4)-abd1(1,4)^2)/abd1(1,1)

% Laminate 2

E1=18.2e6;
E2=1.41e6;
v12=0.27;
G12=0.92e6;

ply=0.005;
total_t=12*ply;

h0=-6*ply;
h1=-5*ply;
h2=-4*ply;
h3=-3*ply;
h4=-2*ply;
h5=-1*ply;
h6=0*ply;
h7=1*ply;
h8=2*ply;
h9=3*ply;
```

```
h10=4*ply;
h11=5*ply;
h12=6*ply;

S11=1/E1;
S22=1/E2;
S12=-v12/E1;
S21=S12;
S33=1/G12;
S=[S11 S12 0;S21 S22 0;0 0 S33];
Q=inv(S);

b=0*pi/180;
n=sin(b);
m=cos(b);
TStress=[m^2 n^2 2*m*n;n^2 m^2 -2*m*n;-m*n m*n m^2-n^2];
TStrain=[m^2 n^2 m*n;n^2 m^2 -m*n;-2*m*n 2*m*n m^2-n^2];
QB_0=inv(TStress)*Q*TStrain;

b=45*pi/180;
n=sin(b);
m=cos(b);
TStress=[m^2 n^2 2*m*n;n^2 m^2 -2*m*n;-m*n m*n m^2-n^2];
TStrain=[m^2 n^2 m*n;n^2 m^2 -m*n;-2*m*n 2*m*n m^2-n^2];
QB_45=inv(TStress)*Q*TStrain;

b=-45*pi/180;
n=sin(b);
m=cos(b);
TStress=[m^2 n^2 2*m*n;n^2 m^2 -2*m*n;-m*n m*n m^2-n^2];
TStrain=[m^2 n^2 m*n;n^2 m^2 -m*n;-2*m*n 2*m*n m^2-n^2];
QB_N45=inv(TStress)*Q*TStrain;

P12=QB_45;
P11=QB_N45;
P10=QB_45;
P9=QB_N45;
P8=QB_0;
P7=QB_0;
P6=QB_0;
P5=QB_0;
P4=QB_N45;
P3=QB_45;
P2=QB_N45;
P1=QB_45;

A=P1*(h1-h0)+P2*(h2-h1)+P3*(h3-h2)+P4*(h4-h3)+P5*(h5-h4)+P6*(h6-h5)+P7*(h7-h6)+P8*(h8-
h7)+P9*(h9-h8)+P10*(h10-h9)+P11*(h11-h10)+P12*(h12-h11);
B=1/2*(P1*(h1^2-h0^2)+P2*(h2^2-h1^2)+P3*(h3^2-h2^2)+P4*(h4^2-h3^2)+P5*(h5^2-
h4^2)+P6*(h6^2-h5^2)+P7*(h7^2-h6^2)+P8*(h8^2-h7^2)+P9*(h9^2-h8^2)+P10*(h10^2-
h9^2)+P11*(h11^2-h10^2)+P12*(h12^2-h11^2));
D=1/3*(P1*(h1^3-h0^3)+P2*(h2^3-h1^3)+P3*(h3^3-h2^3)+P4*(h4^3-h3^3)+P5*(h5^3-
h4^3)+P6*(h6^3-h5^3)+P7*(h7^3-h6^3)+P8*(h8^3-h7^3)+P9*(h9^3-h8^3)+P10*(h10^3-
h9^3)+P11*(h11^3-h10^3)+P12*(h12^3-h11^3));

ABD=[A(1,1) A(1,2) A(1,3) B(1,1) B(1,2) B(1,3);
```

```
    A(2,1) A(2,2) A(2,3) B(2,1) B(2,2) B(2,3);
    A(3,1) A(3,2) A(3,3) B(3,1) B(3,2) B(3,3);
    B(1,1) B(1,2) B(1,3) D(1,1) D(1,2) D(1,3);
    B(2,1) B(2,2) B(2,3) D(2,1) D(2,2) D(2,3);
    B(3,1) B(3,2) B(3,3) D(3,1) D(3,2) D(3,3)];

abd2=inv(ABD);

ass2=(abd2(1,1)*abd2(4,4)-abd2(1,4)^2)/abd2(4,4)
dss2=(abd2(1,1)*abd2(4,4)-abd2(1,4)^2)/abd2(1,1)

% Stress Laminate 1

NM=[0.02999/0.5;0;0;0;0;0];

strain=abd1*NM;

strain0=[strain(1);strain(2);strain(3)];
curvature0=[strain(4);strain(5);strain(6)];

zk=5.5*ply;

strain_xy=strain0+zk*curvature0;

stress_xy=QB_45*strain_xy;

 vpa(stress_xy(1))

% Stress Laminate 2

NM=[0.01501/0.25;0;0;0;0;0];

strain=abd2*NM;

strain0=[strain(1);strain(2);strain(3)];
curvature0=[strain(4);strain(5);strain(6)];

zk=5.5*ply;

strain_xy=strain0+zk*curvature0;

stress_xy=QB_45*strain_xy;

 vpa(stress_xy(1))
% Stiffnesses

v1=0.5/0.75;
v2=0.25/0.75;

ass=inv(v1/ass1+v2/ass2);
dss=inv(v1/dss1+v2/dss2);

Ax=0.75/ass
Dx=0.75/dss
```

Typical MATLAB file for the Circular Cross-section Beam Symmetric Case $[45_2/-45_2/0_2/90_2]_S$ under Axial load.

```
clear all
clc

E1=18.2e6;
E2=1.41e6;
v12=0.27;
G12=0.92e6;

ply=0.0052;

R=1-8*ply;
Ro=R+8*ply;
Ri=R-8*ply;

syms t
f=sqrt(R^2-t^2);

h0=-f-8*ply;
h1=-f-7*ply;
h2=-f-6*ply;
h3=-f-5*ply;
h4=-f-4*ply;
h5=-f-3*ply;
h6=-f-2*ply;
h7=-f-1*ply;
h8=-f+0*ply;
h9=-f+1*ply;
h10=-f+2*ply;
h11=-f+3*ply;
h12=-f+4*ply;
h13=-f+5*ply;
h14=-f+6*ply;
h15=-f+7*ply;
h16=-f+8*ply;

h17=f-8*ply;
h18=f-7*ply;
h19=f-6*ply;
h20=f-5*ply;
h21=f-4*ply;
h22=f-3*ply;
h23=f-2*ply;
h24=f-1*ply;
h25=f+0*ply;
h26=f+1*ply;
h27=f+2*ply;
h28=f+3*ply;
h29=f+4*ply;
h30=f+5*ply;
h31=f+6*ply;
h32=f+7*ply;
h33=f+8*ply;
```

```
S11=1/E1;
S22=1/E2;
S12=-v12/E1;
S21=S12;
S33=1/G12;
S=[S11 S12 0;S21 S22 0;0 0 S33];
Q=inv(S);

b=0*pi/180;
n=sin(b);
m=cos(b);
TStress=[m^2 n^2 2*m*n;n^2 m^2 -2*m*n;-m*n m*n m^2-n^2];
TStrain=[m^2 n^2 m*n;n^2 m^2 -m*n;-2*m*n 2*m*n m^2-n^2];
QB_0=inv(TStress)*Q*TStrain;

b=45*pi/180;
n=sin(b);
m=cos(b);
TStress=[m^2 n^2 2*m*n;n^2 m^2 -2*m*n;-m*n m*n m^2-n^2];
TStrain=[m^2 n^2 m*n;n^2 m^2 -m*n;-2*m*n 2*m*n m^2-n^2];
QB_45=inv(TStress)*Q*TStrain;

b=-45*pi/180;
n=sin(b);
m=cos(b);
TStress=[m^2 n^2 2*m*n;n^2 m^2 -2*m*n;-m*n m*n m^2-n^2];
TStrain=[m^2 n^2 m*n;n^2 m^2 -m*n;-2*m*n 2*m*n m^2-n^2];
QB_N45=inv(TStress)*Q*TStrain;

b=90*pi/180;
n=sin(b);
m=cos(b);
TStress=[m^2 n^2 2*m*n;n^2 m^2 -2*m*n;-m*n m*n m^2-n^2];
TStrain=[m^2 n^2 m*n;n^2 m^2 -m*n;-2*m*n 2*m*n m^2-n^2];
QB_90=inv(TStress)*Q*TStrain;

P32=QB_45;
P31=QB_45;
P30=QB_N45;
P29=QB_N45;
P28=QB_0;
P27=QB_0;
P26=QB_90;
P25=QB_90;
P24=QB_90;
P23=QB_90;
P22=QB_0;
P21=QB_0;
P20=QB_N45;
P19=QB_N45;
P18=QB_45;
P17=QB_45;
P16=QB_45;
P15=QB_45;
P14=QB_N45;
P13=QB_N45;
```

```
P12=QB_0;
P11=QB_0;
P10=QB_90;
P9=QB_90;
P8=QB_90;
P7=QB_90;
P6=QB_0;
P5=QB_0;
P4=QB_N45;
P3=QB_N45;
P2=QB_45;
P1=QB_45;

A=P1*(h1-h0)+P2*(h2-h1)+P3*(h3-h2)+P4*(h4-h3)+P5*(h5-h4)+P6*(h6-h5)+P7*(h7-h6)+P8*(h8-
h7)+P9*(h9-h8)+P10*(h10-h9)+P11*(h11-h10)+P12*(h12-h11)+P13*(h13-h12)+P14*(h14-
h13)+P15*(h15-h14)+P16*(h16-h15)+P17*(h18-h17)+P18*(h19-h18)+P19*(h20-h19)+P20*(h21-
h20)+P21*(h22-h21)+P22*(h23-h22)+P23*(h24-h23)+P24*(h25-h24)+P25*(h26-h25)+P26*(h27-
h26)+P27*(h28-h27)+P28*(h29-h28)+P29*(h30-h29)+P30*(h31-h30)+P31*(h32-h31)+P32*(h33-
h32);
B=1/2*(P1*(h1^2-h0^2)+P2*(h2^2-h1^2)+P3*(h3^2-h2^2)+P4*(h4^2-h3^2)+P5*(h5^2-
h4^2)+P6*(h6^2-h5^2)+P7*(h7^2-h6^2)+P8*(h8^2-h7^2)+P9*(h9^2-h8^2)+P10*(h10^2-
h9^2)+P11*(h11^2-h10^2)+P12*(h12^2-h11^2)+P13*(h13^2-h12^2)+P14*(h14^2-
h13^2)+P15*(h15^2-h14^2)+P16*(h16^2-h15^2)+P17*(h18^2-h17^2)+P18*(h19^2-
h18^2)+P19*(h20^2-h19^2)+P20*(h21^2-h20^2)+P21*(h22^2-h21^2)+P22*(h23^2-
h22^2)+P23*(h24^2-h23^2)+P24*(h25^2-h24^2)+P25*(h26^2-h25^2)+P26*(h27^2-
h26^2)+P27*(h28^2-h27^2)+P28*(h29^2-h28^2)+P29*(h30^2-h29^2)+P30*(h31^2-
h30^2)+P31*(h32^2-h31^2)+P32*(h33^2-h32^2));
D=1/3*(P1*(h1^3-h0^3)+P2*(h2^3-h1^3)+P3*(h3^3-h2^3)+P4*(h4^3-h3^3)+P5*(h5^3-
h4^3)+P6*(h6^3-h5^3)+P7*(h7^3-h6^3)+P8*(h8^3-h7^3)+P9*(h9^3-h8^3)+P10*(h10^3-
h9^3)+P11*(h11^3-h10^3)+P12*(h12^3-h11^3)+P13*(h13^3-h12^3)+P14*(h14^3-
h13^3)+P15*(h15^3-h14^3)+P16*(h16^3-h15^3)+P17*(h18^3-h17^3)+P18*(h19^3-
h18^3)+P19*(h20^3-h19^3)+P20*(h21^3-h20^3)+P21*(h22^3-h21^3)+P22*(h23^3-
h22^3)+P23*(h24^3-h23^3)+P24*(h25^3-h24^3)+P25*(h26^3-h25^3)+P26*(h27^3-
h26^3)+P27*(h28^3-h27^3)+P28*(h29^3-h28^3)+P29*(h30^3-h29^3)+P30*(h31^3-
h30^3)+P31*(h32^3-h31^3)+P32*(h33^3-h32^3));

AB=int(A*sqrt(1+(diff(f,t))^2),t,-R,R);
BB=int(B*sqrt(1+(diff(f,t))^2),t,-R,R);
DB=int(D*sqrt(1+(diff(f,t))^2),t,-R,R);

ABDB=[AB(1,1) AB(1,2) AB(1,3) BB(1,1) BB(1,2) BB(1,3);
    AB(2,1) AB(2,2) AB(2,3) BB(2,1) BB(2,2) BB(2,3);
    AB(3,1) AB(3,2) AB(3,3) BB(3,1) BB(3,2) BB(3,3);
    BB(1,1) BB(1,2) BB(1,3) DB(1,1) DB(1,2) DB(1,3);
    BB(2,1) BB(2,2) BB(2,3) DB(2,1) DB(2,2) DB(2,3);
    BB(3,1) BB(3,2) BB(3,3) DB(3,1) DB(3,2) DB(3,3)];

abdb=inv(ABDB);

% Stiffnesses

our_EAx=1/(abdb(1,1))

our_EIx=vpa(abdb(1,1)/(abdb(1,1)*abdb(4,4)-abdb(1,4)^2))

% Stresses
```

```
NM=[1;0;0;0;0;0];

strain=abdb*NM;

strain0=[strain(1);strain(2);strain(3)];
curvature0=[strain(4);strain(5);strain(6)];

zk=R+(0.5)*ply;

strain_xy=strain0+zk*curvature0;

stress_xy=QB_90*strain_xy;

vpa(stress_xy(1))
```

Typical MATLAB file for the Airfoil Beam with $[90_8]_S$ under Bending.

```
clear all
clc

E1=18.2e6;
E2=1.41e6;
v12=0.27;
G12=0.92e6;

ply=0.0052;
syms t
f=(-0.9584/5.43535649594*t+0.9584);

h0=-f-8*ply;
h1=-f-7*ply;
h2=-f-6*ply;
h3=-f-5*ply;
h4=-f-4*ply;
h5=-f-3*ply;
h6=-f-2*ply;
h7=-f-1*ply;
h8=-f+0*ply;
h9=-f+1*ply;
h10=-f+2*ply;
h11=-f+3*ply;
h12=-f+4*ply;
h13=-f+5*ply;
h14=-f+6*ply;
h15=-f+7*ply;
h16=-f+8*ply;

h17=f-8*ply;
h18=f-7*ply;
h19=f-6*ply;
h20=f-5*ply;
h21=f-4*ply;
h22=f-3*ply;
h23=f-2*ply;
h24=f-1*ply;
h25=f+0*ply;
h26=f+1*ply;
h27=f+2*ply;
h28=f+3*ply;
h29=f+4*ply;
h30=f+5*ply;
h31=f+6*ply;
h32=f+7*ply;
h33=f+8*ply;

S11=1/E1;
S22=1/E2;
S12=-v12/E1;
S21=S12;
S33=1/G12;
S=[S11 S12 0;S21 S22 0;0 0 S33];
```

```
Q=inv(S);

b=90*pi/180;
n=sin(b);
m=cos(b);
TStress=[m^2 n^2 2*m*n;n^2 m^2 -2*m*n;-m*n m*n m^2-n^2];
TStrain=[m^2 n^2 m*n;n^2 m^2 -m*n;-2*m*n 2*m*n m^2-n^2];
QB_90=inv(TStress)*Q*TStrain;

P32=QB_90;
P31=QB_90;
P30=QB_90;
P29=QB_90;
P28=QB_90;
P27=QB_90;
P26=QB_90;
P25=QB_90;
P24=QB_90;
P23=QB_90;
P22=QB_90;
P21=QB_90;
P20=QB_90;
P19=QB_90;
P18=QB_90;
P17=QB_90;
P16=QB_90;
P15=QB_90;
P14=QB_90;
P13=QB_90;
P12=QB_90;
P11=QB_90;
P10=QB_90;
P9=QB_90;
P8=QB_90;
P7=QB_90;
P6=QB_90;
P5=QB_90;
P4=QB_90;
P3=QB_90;
P2=QB_90;
P1=QB_90;

A=P1*(h1-h0)+P2*(h2-h1)+P3*(h3-h2)+P4*(h4-h3)+P5*(h5-h4)+P6*(h6-h5)+P7*(h7-h6)+P8*(h8-
h7)+P9*(h9-h8)+P10*(h10-h9)+P11*(h11-h10)+P12*(h12-h11)+P13*(h13-h12)+P14*(h14-
h13)+P15*(h15-h14)+P16*(h16-h15)+P17*(h18-h17)+P18*(h19-h18)+P19*(h20-h19)+P20*(h21-
h20)+P21*(h22-h21)+P22*(h23-h22)+P23*(h24-h23)+P24*(h25-h24)+P25*(h26-h25)+P26*(h27-
h26)+P27*(h28-h27)+P28*(h29-h28)+P29*(h30-h29)+P30*(h31-h30)+P31*(h32-h31)+P32*(h33-
h32);
B=1/2*(P1*(h1^2-h0^2)+P2*(h2^2-h1^2)+P3*(h3^2-h2^2)+P4*(h4^2-h3^2)+P5*(h5^2-
h4^2)+P6*(h6^2-h5^2)+P7*(h7^2-h6^2)+P8*(h8^2-h7^2)+P9*(h9^2-h8^2)+P10*(h10^2-
h9^2)+P11*(h11^2-h10^2)+P12*(h12^2-h11^2)+P13*(h13^2-h12^2)+P14*(h14^2-
h13^2)+P15*(h15^2-h14^2)+P16*(h16^2-h15^2)+P17*(h18^2-h17^2)+P18*(h19^2-
h18^2)+P19*(h20^2-h19^2)+P20*(h21^2-h20^2)+P21*(h22^2-h21^2)+P22*(h23^2-
h22^2)+P23*(h24^2-h23^2)+P24*(h25^2-h24^2)+P25*(h26^2-h25^2)+P26*(h27^2-
h26^2)+P27*(h28^2-h27^2)+P28*(h29^2-h28^2)+P29*(h30^2-h29^2)+P30*(h31^2-
h30^2)+P31*(h32^2-h31^2)+P32*(h33^2-h32^2));
```

```
D=1/3*(P1*(h1^3-h0^3)+P2*(h2^3-h1^3)+P3*(h3^3-h2^3)+P4*(h4^3-h3^3)+P5*(h5^3-
h4^3)+P6*(h6^3-h5^3)+P7*(h7^3-h6^3)+P8*(h8^3-h7^3)+P9*(h9^3-h8^3)+P10*(h10^3-
h9^3)+P11*(h11^3-h10^3)+P12*(h12^3-h11^3)+P13*(h13^3-h12^3)+P14*(h14^3-
h13^3)+P15*(h15^3-h14^3)+P16*(h16^3-h15^3)+P17*(h18^3-h17^3)+P18*(h19^3-
h18^3)+P19*(h20^3-h19^3)+P20*(h21^3-h20^3)+P21*(h22^3-h21^3)+P22*(h23^3-
h22^3)+P23*(h24^3-h23^3)+P24*(h25^3-h24^3)+P25*(h26^3-h25^3)+P26*(h27^3-
h26^3)+P27*(h28^3-h27^3)+P28*(h29^3-h28^3)+P29*(h30^3-h29^3)+P30*(h31^3-
h30^3)+P31*(h32^3-h31^3)+P32*(h33^3-h32^3));

AB=int(A*sqrt(1+(diff(f,t))^2),t,0,5.43535649594);
BB=int(B*sqrt(1+(diff(f,t))^2),t,0,5.43535649594);
DB=int(D*sqrt(1+(diff(f,t))^2),t,0,5.43535649594);

ABDB1=[AB(1,1) AB(1,2) AB(1,3) BB(1,1) BB(1,2) BB(1,3);
    AB(2,1) AB(2,2) AB(2,3) BB(2,1) BB(2,2) BB(2,3);
    AB(3,1) AB(3,2) AB(3,3) BB(3,1) BB(3,2) BB(3,3);
    BB(1,1) BB(1,2) BB(1,3) DB(1,1) DB(1,2) DB(1,3);
    BB(2,1) BB(2,2) BB(2,3) DB(2,1) DB(2,2) DB(2,3);
    BB(3,1) BB(3,2) BB(3,3) DB(3,1) DB(3,2) DB(3,3)];

ply=0.0052;

R=0.9584;

syms t
f=sqrt(R^2-t^2);

h0=f-8*ply;
h1=f-7*ply;
h2=f-6*ply;
h3=f-5*ply;
h4=f-4*ply;
h5=f-3*ply;
h6=f-2*ply;
h7=f-1*ply;
h8=f+0*ply;
h9=f+1*ply;
h10=f+2*ply;
h11=f+3*ply;
h12=f+4*ply;
h13=f+5*ply;
h14=f+6*ply;
h15=f+7*ply;
h16=f+8*ply;

P16=QB_90;
P15=QB_90;
P14=QB_90;
P13=QB_90;
P12=QB_90;
P11=QB_90;
P10=QB_90;
P9=QB_90;
P8=QB_90;
P7=QB_90;
P6=QB_90;
```

```
P5=QB_90;
P4=QB_90;
P3=QB_90;
P2=QB_90;
P1=QB_90;

A=P1*(h1-h0)+P2*(h2-h1)+P3*(h3-h2)+P4*(h4-h3)+P5*(h5-h4)+P6*(h6-h5)+P7*(h7-h6)+P8*(h8-
h7)+P9*(h9-h8)+P10*(h10-h9)+P11*(h11-h10)+P12*(h12-h11)+P13*(h13-h12)+P14*(h14-
h13)+P15*(h15-h14)+P16*(h16-h15);
B=1/2*(P1*(h1^2-h0^2)+P2*(h2^2-h1^2)+P3*(h3^2-h2^2)+P4*(h4^2-h3^2)+P5*(h5^2-
h4^2)+P6*(h6^2-h5^2)+P7*(h7^2-h6^2)+P8*(h8^2-h7^2)+P9*(h9^2-h8^2)+P10*(h10^2-
h9^2)+P11*(h11^2-h10^2)+P12*(h12^2-h11^2)+P13*(h13^2-h12^2)+P14*(h14^2-
h13^2)+P15*(h15^2-h14^2)+P16*(h16^2-h15^2));
D=1/3*(P1*(h1^3-h0^3)+P2*(h2^3-h1^3)+P3*(h3^3-h2^3)+P4*(h4^3-h3^3)+P5*(h5^3-
h4^3)+P6*(h6^3-h5^3)+P7*(h7^3-h6^3)+P8*(h8^3-h7^3)+P9*(h9^3-h8^3)+P10*(h10^3-
h9^3)+P11*(h11^3-h10^3)+P12*(h12^3-h11^3)+P13*(h13^3-h12^3)+P14*(h14^3-
h13^3)+P15*(h15^3-h14^3)+P16*(h16^3-h15^3));

AB=int(A*sqrt(1+(diff(f,t))^2),t,-R+0.001,-0.001);
BB=int(B*sqrt(1+(diff(f,t))^2),t,-R+0.001,-0.001);
DB=int(D*sqrt(1+(diff(f,t))^2),t,-R+0.001,-0.001);

ABDB2=[AB(1,1) AB(1,2) AB(1,3) BB(1,1) BB(1,2) BB(1,3);
    AB(2,1) AB(2,2) AB(2,3) BB(2,1) BB(2,2) BB(2,3);
    AB(3,1) AB(3,2) AB(3,3) BB(3,1) BB(3,2) BB(3,3);
    BB(1,1) BB(1,2) BB(1,3) DB(1,1) DB(1,2) DB(1,3);
    BB(2,1) BB(2,2) BB(2,3) DB(2,1) DB(2,2) DB(2,3);
    BB(3,1) BB(3,2) BB(3,3) DB(3,1) DB(3,2) DB(3,3)];

m11=vpa(real(ABDB2(1,1)));
m12=vpa(real(ABDB2(1,2)));
m13=vpa(real(ABDB2(1,3)));
m14=vpa(real(ABDB2(1,4)));
m15=vpa(real(ABDB2(1,5)));
m16=vpa(real(ABDB2(1,6)));
m21=vpa(real(ABDB2(2,1)));
m22=vpa(real(ABDB2(2,2)));
m23=vpa(real(ABDB2(2,3)));
m24=vpa(real(ABDB2(2,4)));
m25=vpa(real(ABDB2(2,5)));
m26=vpa(real(ABDB2(2,6)));
m31=vpa(real(ABDB2(3,1)));
m32=vpa(real(ABDB2(3,2)));
m33=vpa(real(ABDB2(3,3)));
m34=vpa(real(ABDB2(3,4)));
m35=vpa(real(ABDB2(3,5)));
m36=vpa(real(ABDB2(3,6)));
m41=vpa(real(ABDB2(4,1)));
m42=vpa(real(ABDB2(4,2)));
m43=vpa(real(ABDB2(4,3)));
m44=vpa(real(ABDB2(4,4)));
m45=vpa(real(ABDB2(4,5)));
m46=vpa(real(ABDB2(4,6)));
m51=vpa(real(ABDB2(5,1)));
m52=vpa(real(ABDB2(5,2)));
m53=vpa(real(ABDB2(5,3)));
```

```
m54=vpa(real(ABDB2(5,4)));
m55=vpa(real(ABDB2(5,5)));
m56=vpa(real(ABDB2(5,6)));
m61=vpa(real(ABDB2(6,1)));
m62=vpa(real(ABDB2(6,2)));
m63=vpa(real(ABDB2(6,3)));
m64=vpa(real(ABDB2(6,4)));
m65=vpa(real(ABDB2(6,5)));
m66=vpa(real(ABDB2(6,6)));

ABDB2p=[real(m11) real(m12) real(m13) real(m14) real(m15) real(m16);
       real(m21) real(m22) real(m23) real(m24) real(m25) real(m26);
       real(m31) real(m32) real(m33) real(m34) real(m35) real(m36);
       real(m41) real(m42) real(m43) real(m44) real(m45) real(m46);
       real(m51) real(m52) real(m53) real(m54) real(m55) real(m56);
       real(m61) real(m62) real(m63) real(m64) real(m65) real(m66)];


ABDBT=ABDB1+2*ABDB2p;

abdb=inv(ABDBT);

our_EIx=vpa(abdb(1,1)/(abdb(1,1)*abdb(4,4)-abdb(1,4)^2))
```

APPENDIX D

ANSYS FILES

Typical ANSYS file for Stiffener Reinforced Laminated Beam Symmetric Case $[0_4/-45/45/-45/45]_T$ and $[\pm 45_2]_T$ under Axial Load.

```
/FILNAM, Laminate
/title, Laminate
/prep7

MP,EX,1,18.2E6
MP,EY,1,1.41E6
MP,EZ,1,1.41E6
MP,PRXY,1,0.27
MP,PRYZ,1,0.27
MP,PRXZ,1,0.27
MP,GXY,1,0.92E6
MP,GYZ,1,0.92E6
MP,GXZ,1,0.92E6

L=10
b1=0.5
tply=0.005
force=1

n=1

*DO,i,1,12,1
k,n,0,-b1/2,(i-7)*tply
k,n+1,L,-b1/2,(i-7)*tply
k,n+2,L,b1/2,(i-7)*tply
k,n+3,0,b1/2,(i-7)*tply
k,n+4,0,-b1/2,(i-6)*tply
k,n+5,L,-b1/2,(i-6)*tply
k,n+6,L,b1/2,(i-6)*tply
k,n+7,0,b1/2,(i-6)*tply
V,n,n+1,n+2,n+3,n+4,n+5,n+6,n+7
n=n+8
*ENDDO

allsel
nummrg,kp

ET,1,SOLID46

R,1
RMODIF,1,1,1,0,0,0,0
RMODIF,1,7,0
RMODIF,1,13,1,45,tply

R,2
RMODIF,2,1,1,0,0,0,0
RMODIF,2,7,0
RMODIF,2,13,1,-45,tply

R,3
RMODIF,3,1,1,0,0,0,0
RMODIF,3,7,0
```

```
RMODIF,3,13,1,45,tply

R,4
RMODIF,4,1,1,0,0,0,0
RMODIF,4,7,0
RMODIF,4,13,1,-45,tply

R,5
RMODIF,5,1,1,0,0,0,0
RMODIF,5,7,0
RMODIF,5,13,1,0,tply

R,6
RMODIF,6,1,1,0,0,0,0
RMODIF,6,7,0
RMODIF,6,13,1,0,tply

R,7
RMODIF,7,1,1,0,0,0,0
RMODIF,7,7,0
RMODIF,7,13,1,0,tply

R,8
RMODIF,8,1,1,0,0,0,0
RMODIF,8,7,0
RMODIF,8,13,1,0,tply

R,9
RMODIF,9,1,1,0,0,0,0
RMODIF,9,7,0
RMODIF,9,13,1,-45,tply

R,10
RMODIF,10,1,1,0,0,0,0
RMODIF,10,7,0
RMODIF,10,13,1,45,tply

R,11
RMODIF,11,1,1,0,0,0,0
RMODIF,11,7,0
RMODIF,11,13,1,-45,tply

R,12
RMODIF,12,1,1,0,0,0,0
RMODIF,12,7,0
RMODIF,12,13,1,45,tply

*DO,i,1,12,1
VSEL,S,VOLU,,i
VATT,1,i,1,0
*ENDDO

dx=320
xx=1
LSEL,s,Lenght,,L
LESIZE,all,,,dx,xx
```

```
dy=16
yy=1
LSEL,S,Lenght,,b1
LESIZE,all,,,dy,yy

dz=2
zz=1
LSEL,S,Lenght,,tply
LESIZE,ALL,,,dz,zz

allsel
VMESH,ALL

tol=1e-5

NSEL,S,LOC,x,0
D,ALL,Ux,0

NSEL,S,LOC,x,0
NSEL,R,LOC,y,0
D,ALL,Uy,0

NSEL,S,LOC,x,0
NSEL,R,LOC,z,0
D,ALL,Uz,0

NSEL,S,LOC,X,L-tol,L+tol
NSEL,R,LOC,y,0-tol,0+tol
NSEL,R,LOC,Z,0-tol,0+tol
F,ALL,FX,force

allsel

FINISH
/SOL

SOLVE
FINISH
```

Typical ANSYS file for Non-Aligned Stiffener Reinforced Laminated Beam Un-symmetric Case $[\pm 45/0/90]_{3T}$ under M_x.

```
/FILNAM, Laminate
/title, Laminate
/prep7

MP,EX,1,18.2E6
MP,EY,1,1.41E6
MP,EZ,1,1.41E6
MP,PRXY,1,0.27
MP,PRYZ,1,0.27
MP,PRXZ,1,0.27
MP,GXY,1,0.92E6
MP,GYZ,1,0.92E6
MP,GXZ,1,0.92E6

L=10
b1=0.5
b2=0.25
s=0.0625
tply=0.005
force=1
zc=4.93926269104891*tply
yc=0.23866025259459
e=0.5/16
vx=0.0625

n=1

*DO,i,1,3,1
k,n,0,0,(i-1)*tply
k,n+1,L,0,(i-1)*tply
k,n+2,L,6*e,(i-1)*tply
k,n+3,0,6*e,(i-1)*tply
k,n+4,0,0,(i)*tply
k,n+5,L,0,(i)*tply
k,n+6,L,6*e,(i)*tply
k,n+7,0,6*e,(i)*tply
V,n,n+1,n+2,n+3,n+4,n+5,n+6,n+7
n=n+8
*ENDDO

*DO,i,1,3,1
k,n,0,6*e,(i-1)*tply
k,n+1,L,6*e,(i-1)*tply
k,n+2,L,yc-7*e+6*e,(i-1)*tply
k,n+3,0,yc-7*e+6*e,(i-1)*tply
k,n+4,0,6*e,(i)*tply
k,n+5,L,6*e,(i)*tply
k,n+6,L,yc-7*e+6*e,(i)*tply
k,n+7,0,yc-7*e+6*e,(i)*tply
V,n,n+1,n+2,n+3,n+4,n+5,n+6,n+7
n=n+8
*ENDDO
```

```
*DO,i,1,3,1
k,n,0,yc-7*e+6*e,(i-1)*tply
k,n+1,L,yc-7*e+6*e,(i-1)*tply
k,n+2,L,7*e,(i-1)*tply
k,n+3,0,7*e,(i-1)*tply
k,n+4,0,yc-7*e+6*e,(i)*tply
k,n+5,L,yc-7*e+6*e,(i)*tply
k,n+6,L,7*e,(i)*tply
k,n+7,0,7*e,(i)*tply
V,n,n+1,n+2,n+3,n+4,n+5,n+6,n+7
n=n+8
*ENDDO

*DO,i,1,3,1
k,n,0,7*e,(i-1)*tply
k,n+1,L,7*e,(i-1)*tply
k,n+2,L,yc,(i-1)*tply
k,n+3,0,yc,(i-1)*tply
k,n+4,0,7*e,(i)*tply
k,n+5,L,7*e,(i)*tply
k,n+6,L,yc,(i)*tply
k,n+7,0,yc,(i)*tply
V,n,n+1,n+2,n+3,n+4,n+5,n+6,n+7
n=n+8
*ENDDO

*DO,i,1,3,1
k,n,0,yc,(i-1)*tply
k,n+1,L,yc,(i-1)*tply
k,n+2,L,8*e,(i-1)*tply
k,n+3,0,8*e,(i-1)*tply
k,n+4,0,yc,(i)*tply
k,n+5,L,yc,(i)*tply
k,n+6,L,8*e,(i)*tply
k,n+7,0,8*e,(i)*tply
V,n,n+1,n+2,n+3,n+4,n+5,n+6,n+7
n=n+8
*ENDDO

*DO,i,1,3,1
k,n,0,8*e,(i-1)*tply
k,n+1,L,8*e,(i-1)*tply
k,n+2,L,yc-7*e+8*e,(i-1)*tply
k,n+3,0,yc-7*e+8*e,(i-1)*tply
k,n+4,0,8*e,(i)*tply
k,n+5,L,8*e,(i)*tply
k,n+6,L,yc-7*e+8*e,(i)*tply
k,n+7,0,yc-7*e+8*e,(i)*tply
V,n,n+1,n+2,n+3,n+4,n+5,n+6,n+7
n=n+8
*ENDDO

*DO,i,1,3,1
k,n,0,yc-7*e+8*e,(i-1)*tply
k,n+1,L,yc-7*e+8*e,(i-1)*tply
k,n+2,L,9*e,(i-1)*tply
```

```
k,n+3,0,9*e,(i-1)*tply
k,n+4,0,yc-7*e+8*e,(i)*tply
k,n+5,L,yc-7*e+8*e,(i)*tply
k,n+6,L,9*e,(i)*tply
k,n+7,0,9*e,(i)*tply
V,n,n+1,n+2,n+3,n+4,n+5,n+6,n+7
n=n+8
*ENDDO

*DO,i,1,3,1
k,n,0,9*e,(i-1)*tply
k,n+1,L,9*e,(i-1)*tply
k,n+2,L,b1,(i-1)*tply
k,n+3,0,b1,(i-1)*tply
k,n+4,0,9*e,(i)*tply
k,n+5,L,9*e,(i)*tply
k,n+6,L,b1,(i)*tply
k,n+7,0,b1,(i)*tply
V,n,n+1,n+2,n+3,n+4,n+5,n+6,n+7
n=n+8
*ENDDO

k,n,0,0,3*tply
k,n+1,L,0,3*tply
k,n+2,L,6*e,3*tply
k,n+3,0,6*e,3*tply
k,n+4,0,0,zc-4*tply+3*tply
k,n+5,L,0,zc-4*tply+3*tply
k,n+6,L,6*e,zc-4*tply+3*tply
k,n+7,0,6*e,zc-4*tply+3*tply
V,n,n+1,n+2,n+3,n+4,n+5,n+6,n+7
n=n+8

k,n,0,6*e,3*tply
k,n+1,L,6*e,3*tply
k,n+2,L,yc-7*e+6*e,3*tply
k,n+3,0,yc-7*e+6*e,3*tply
k,n+4,0,6*e,zc-4*tply+3*tply
k,n+5,L,6*e,zc-4*tply+3*tply
k,n+6,L,yc-7*e+6*e,zc-4*tply+3*tply
k,n+7,0,yc-7*e+6*e,zc-4*tply+3*tply
V,n,n+1,n+2,n+3,n+4,n+5,n+6,n+7
n=n+8

k,n,0,yc-7*e+6*e,3*tply
k,n+1,L,yc-7*e+6*e,3*tply
k,n+2,L,7*e,3*tply
k,n+3,0,7*e,3*tply
k,n+4,0,yc-7*e+6*e,zc-4*tply+3*tply
k,n+5,L,yc-7*e+6*e,zc-4*tply+3*tply
k,n+6,L,7*e,zc-4*tply+3*tply
k,n+7,0,7*e,zc-4*tply+3*tply
V,n,n+1,n+2,n+3,n+4,n+5,n+6,n+7
n=n+8

k,n,0,7*e,3*tply
```

```
k,n+1,L,7*e,3*tply
k,n+2,L,yc,3*tply
k,n+3,0,yc,3*tply
k,n+4,0,7*e,zc-4*tply+3*tply
k,n+5,L,7*e,zc-4*tply+3*tply
k,n+6,L,yc,zc-4*tply+3*tply
k,n+7,0,yc,zc-4*tply+3*tply
V,n,n+1,n+2,n+3,n+4,n+5,n+6,n+7
n=n+8

k,n,0,yc,3*tply
k,n+1,L,yc,3*tply
k,n+2,L,8*e,3*tply
k,n+3,0,8*e,3*tply
k,n+4,0,yc,zc-4*tply+3*tply
k,n+5,L,yc,zc-4*tply+3*tply
k,n+6,L,8*e,zc-4*tply+3*tply
k,n+7,0,8*e,zc-4*tply+3*tply
V,n,n+1,n+2,n+3,n+4,n+5,n+6,n+7
n=n+8

k,n,0,8*e,3*tply
k,n+1,L,8*e,3*tply
k,n+2,L,yc-7*e+8*e,3*tply
k,n+3,0,yc-7*e+8*e,3*tply
k,n+4,0,8*e,zc-4*tply+3*tply
k,n+5,L,8*e,zc-4*tply+3*tply
k,n+6,L,yc-7*e+8*e,zc-4*tply+3*tply
k,n+7,0,yc-7*e+8*e,zc-4*tply+3*tply
V,n,n+1,n+2,n+3,n+4,n+5,n+6,n+7
n=n+8

k,n,0,yc-7*e+8*e,3*tply
k,n+1,L,yc-7*e+8*e,3*tply
k,n+2,L,9*e,3*tply
k,n+3,0,9*e,3*tply
k,n+4,0,yc-7*e+8*e,zc-4*tply+3*tply
k,n+5,L,yc-7*e+8*e,zc-4*tply+3*tply
k,n+6,L,9*e,zc-4*tply+3*tply
k,n+7,0,9*e,zc-4*tply+3*tply
V,n,n+1,n+2,n+3,n+4,n+5,n+6,n+7
n=n+8

k,n,0,9*e,3*tply
k,n+1,L,9*e,3*tply
k,n+2,L,b1,3*tply
k,n+3,0,b1,3*tply
k,n+4,0,9*e,zc-4*tply+3*tply
k,n+5,L,9*e,zc-4*tply+3*tply
k,n+6,L,b1,zc-4*tply+3*tply
k,n+7,0,b1,zc-4*tply+3*tply
V,n,n+1,n+2,n+3,n+4,n+5,n+6,n+7
n=n+8

k,n,0,0,zc-4*tply+3*tply
k,n+1,L,0,zc-4*tply+3*tply
```

```
k,n+2,L,6*e,zc-4*tply+3*tply
k,n+3,0,6*e,zc-4*tply+3*tply
k,n+4,0,0,4*tply
k,n+5,L,0,4*tply
k,n+6,L,6*e,4*tply
k,n+7,0,6*e,4*tply
V,n,n+1,n+2,n+3,n+4,n+5,n+6,n+7
n=n+8

k,n,0,6*e,zc-4*tply+3*tply
k,n+1,L,6*e,zc-4*tply+3*tply
k,n+2,L,yc-7*e+6*e,zc-4*tply+3*tply
k,n+3,0,yc-7*e+6*e,zc-4*tply+3*tply
k,n+4,0,6*e,4*tply
k,n+5,L,6*e,4*tply
k,n+6,L,yc-7*e+6*e,4*tply
k,n+7,0,yc-7*e+6*e,4*tply
V,n,n+1,n+2,n+3,n+4,n+5,n+6,n+7
n=n+8

k,n,0,yc-7*e+6*e,zc-4*tply+3*tply
k,n+1,L,yc-7*e+6*e,zc-4*tply+3*tply
k,n+2,L,7*e,zc-4*tply+3*tply
k,n+3,0,7*e,zc-4*tply+3*tply
k,n+4,0,yc-7*e+6*e,4*tply
k,n+5,L,yc-7*e+6*e,4*tply
k,n+6,L,7*e,4*tply
k,n+7,0,7*e,4*tply
V,n,n+1,n+2,n+3,n+4,n+5,n+6,n+7
n=n+8

k,n,0,7*e,zc-4*tply+3*tply
k,n+1,L,7*e,zc-4*tply+3*tply
k,n+2,L,yc,zc-4*tply+3*tply
k,n+3,0,yc,zc-4*tply+3*tply
k,n+4,0,7*e,4*tply
k,n+5,L,7*e,4*tply
k,n+6,L,yc,4*tply
k,n+7,0,yc,4*tply
V,n,n+1,n+2,n+3,n+4,n+5,n+6,n+7
n=n+8

k,n,0,yc,zc-4*tply+3*tply
k,n+1,L,yc,zc-4*tply+3*tply
k,n+2,L,8*e,zc-4*tply+3*tply
k,n+3,0,8*e,zc-4*tply+3*tply
k,n+4,0,yc,4*tply
k,n+5,L,yc,4*tply
k,n+6,L,8*e,4*tply
k,n+7,0,8*e,4*tply
V,n,n+1,n+2,n+3,n+4,n+5,n+6,n+7
n=n+8

k,n,0,8*e,zc-4*tply+3*tply
k,n+1,L,8*e,zc-4*tply+3*tply
k,n+2,L,yc-7*e+8*e,zc-4*tply+3*tply
```

```
k,n+3,0,yc-7*e+8*e,zc-4*tply+3*tply
k,n+4,0,8*e,4*tply
k,n+5,L,8*e,4*tply
k,n+6,L,yc-7*e+8*e,4*tply
k,n+7,0,yc-7*e+8*e,4*tply
V,n,n+1,n+2,n+3,n+4,n+5,n+6,n+7
n=n+8

k,n,0,yc-7*e+8*e,zc-4*tply+3*tply
k,n+1,L,yc-7*e+8*e,zc-4*tply+3*tply
k,n+2,L,9*e,zc-4*tply+3*tply
k,n+3,0,9*e,zc-4*tply+3*tply
k,n+4,0,yc-7*e+8*e,4*tply
k,n+5,L,yc-7*e+8*e,4*tply
k,n+6,L,9*e,4*tply
k,n+7,0,9*e,4*tply
V,n,n+1,n+2,n+3,n+4,n+5,n+6,n+7
n=n+8

k,n,0,9*e,zc-4*tply+3*tply
k,n+1,L,9*e,zc-4*tply+3*tply
k,n+2,L,b1,zc-4*tply+3*tply
k,n+3,0,b1,zc-4*tply+3*tply
k,n+4,0,9*e,4*tply
k,n+5,L,9*e,4*tply
k,n+6,L,b1,4*tply
k,n+7,0,b1,4*tply
V,n,n+1,n+2,n+3,n+4,n+5,n+6,n+7
n=n+8

k,n,0,0,4*tply
k,n+1,L,0,4*tply
k,n+2,L,6*e,4*tply
k,n+3,0,6*e,4*tply
k,n+4,0,0,zc
k,n+5,L,0,zc
k,n+6,L,6*e,zc
k,n+7,0,6*e,zc
V,n,n+1,n+2,n+3,n+4,n+5,n+6,n+7
n=n+8

k,n,0,6*e,4*tply
k,n+1,L,6*e,4*tply
k,n+2,L,yc-7*e+6*e,4*tply
k,n+3,0,yc-7*e+6*e,4*tply
k,n+4,0,6*e,zc
k,n+5,L,6*e,zc
k,n+6,L,yc-7*e+6*e,zc
k,n+7,0,yc-7*e+6*e,zc
V,n,n+1,n+2,n+3,n+4,n+5,n+6,n+7
n=n+8

k,n,0,yc-7*e+6*e,4*tply
k,n+1,L,yc-7*e+6*e,4*tply
k,n+2,L,7*e,4*tply
k,n+3,0,7*e,4*tply
```

```
k,n+4,0,yc-7*e+6*e,zc
k,n+5,L,yc-7*e+6*e,zc
k,n+6,L,7*e,zc
k,n+7,0,7*e,zc
V,n,n+1,n+2,n+3,n+4,n+5,n+6,n+7
n=n+8

k,n,0,7*e,4*tply
k,n+1,L,7*e,4*tply
k,n+2,L,yc,4*tply
k,n+3,0,yc,4*tply
k,n+4,0,7*e,zc
k,n+5,L,7*e,zc
k,n+6,L,yc,zc
k,n+7,0,yc,zc
V,n,n+1,n+2,n+3,n+4,n+5,n+6,n+7
n=n+8

k,n,0,yc,4*tply
k,n+1,L,yc,4*tply
k,n+2,L,8*e,4*tply
k,n+3,0,8*e,4*tply
k,n+4,0,yc,zc
k,n+5,L,yc,zc
k,n+6,L,8*e,zc
k,n+7,0,8*e,zc
V,n,n+1,n+2,n+3,n+4,n+5,n+6,n+7
n=n+8

k,n,0,8*e,4*tply
k,n+1,L,8*e,4*tply
k,n+2,L,yc-7*e+8*e,4*tply
k,n+3,0,yc-7*e+8*e,4*tply
k,n+4,0,8*e,zc
k,n+5,L,8*e,zc
k,n+6,L,yc-7*e+8*e,zc
k,n+7,0,yc-7*e+8*e,zc
V,n,n+1,n+2,n+3,n+4,n+5,n+6,n+7
n=n+8

k,n,0,yc-7*e+8*e,4*tply
k,n+1,L,yc-7*e+8*e,4*tply
k,n+2,L,9*e,4*tply
k,n+3,0,9*e,4*tply
k,n+4,0,yc-7*e+8*e,zc
k,n+5,L,yc-7*e+8*e,zc
k,n+6,L,9*e,zc
k,n+7,0,9*e,zc
V,n,n+1,n+2,n+3,n+4,n+5,n+6,n+7
n=n+8

k,n,0,9*e,4*tply
k,n+1,L,9*e,4*tply
k,n+2,L,b1,4*tply
k,n+3,0,b1,4*tply
k,n+4,0,9*e,zc
```

```
k,n+5,L,9*e,zc
k,n+6,L,b1,zc
k,n+7,0,b1,zc
V,n,n+1,n+2,n+3,n+4,n+5,n+6,n+7
n=n+8

k,n,0,0,zc
k,n+1,L,0,zc
k,n+2,L,6*e,zc
k,n+3,0,6*e,zc
k,n+4,0,0,5*tply
k,n+5,L,0,5*tply
k,n+6,L,6*e,5*tply
k,n+7,0,6*e,5*tply
V,n,n+1,n+2,n+3,n+4,n+5,n+6,n+7
n=n+8

k,n,0,6*e,zc
k,n+1,L,6*e,zc
k,n+2,L,yc-7*e+6*e,zc
k,n+3,0,yc-7*e+6*e,zc
k,n+4,0,6*e,5*tply
k,n+5,L,6*e,5*tply
k,n+6,L,yc-7*e+6*e,5*tply
k,n+7,0,yc-7*e+6*e,5*tply
V,n,n+1,n+2,n+3,n+4,n+5,n+6,n+7
n=n+8

k,n,0,yc-7*e+6*e,zc
k,n+1,L,yc-7*e+6*e,zc
k,n+2,L,7*e,zc
k,n+3,0,7*e,zc
k,n+4,0,yc-7*e+6*e,5*tply
k,n+5,L,yc-7*e+6*e,5*tply
k,n+6,L,7*e,5*tply
k,n+7,0,7*e,5*tply
V,n,n+1,n+2,n+3,n+4,n+5,n+6,n+7
n=n+8

k,n,0,7*e,zc
k,n+1,L,7*e,zc
k,n+2,L,yc,zc
k,n+3,0,yc,zc
k,n+4,0,7*e,5*tply
k,n+5,L,7*e,5*tply
k,n+6,L,yc,5*tply
k,n+7,0,yc,5*tply
V,n,n+1,n+2,n+3,n+4,n+5,n+6,n+7
n=n+8

k,n,0,yc,zc
k,n+1,L,yc,zc
k,n+2,L,8*e,zc
k,n+3,0,8*e,zc
k,n+4,0,yc,5*tply
k,n+5,L,yc,5*tply
```

```
k,n+6,L,8*e,5*tply
k,n+7,0,8*e,5*tply
V,n,n+1,n+2,n+3,n+4,n+5,n+6,n+7
n=n+8

k,n,0,8*e,zc
k,n+1,L,8*e,zc
k,n+2,L,yc-7*e+8*e,zc
k,n+3,0,yc-7*e+8*e,zc
k,n+4,0,8*e,5*tply
k,n+5,L,8*e,5*tply
k,n+6,L,yc-7*e+8*e,5*tply
k,n+7,0,yc-7*e+8*e,5*tply
V,n,n+1,n+2,n+3,n+4,n+5,n+6,n+7
n=n+8

k,n,0,yc-7*e+8*e,zc
k,n+1,L,yc-7*e+8*e,zc
k,n+2,L,9*e,zc
k,n+3,0,9*e,zc
k,n+4,0,yc-7*e+8*e,5*tply
k,n+5,L,yc-7*e+8*e,5*tply
k,n+6,L,9*e,5*tply
k,n+7,0,9*e,5*tply
V,n,n+1,n+2,n+3,n+4,n+5,n+6,n+7
n=n+8

k,n,0,9*e,zc
k,n+1,L,9*e,zc
k,n+2,L,b1,zc
k,n+3,0,b1,zc
k,n+4,0,9*e,5*tply
k,n+5,L,9*e,5*tply
k,n+6,L,b1,5*tply
k,n+7,0,b1,5*tply
V,n,n+1,n+2,n+3,n+4,n+5,n+6,n+7
n=n+8

k,n,0,0,5*tply
k,n+1,L,0,5*tply
k,n+2,L,6*e,5*tply
k,n+3,0,6*e,5*tply
k,n+4,0,0,zc-4*tply+5*tply
k,n+5,L,0,zc-4*tply+5*tply
k,n+6,L,6*e,zc-4*tply+5*tply
k,n+7,0,6*e,zc-4*tply+5*tply
V,n,n+1,n+2,n+3,n+4,n+5,n+6,n+7
n=n+8

k,n,0,6*e,5*tply
k,n+1,L,6*e,5*tply
k,n+2,L,yc-7*e+6*e,5*tply
k,n+3,0,yc-7*e+6*e,5*tply
k,n+4,0,6*e,zc-4*tply+5*tply
k,n+5,L,6*e,zc-4*tply+5*tply
k,n+6,L,yc-7*e+6*e,zc-4*tply+5*tply
```

```
k,n+7,0,yc-7*e+6*e,zc-4*tply+5*tply
V,n,n+1,n+2,n+3,n+4,n+5,n+6,n+7
n=n+8

k,n,0,yc-7*e+6*e,5*tply
k,n+1,L,yc-7*e+6*e,5*tply
k,n+2,L,7*e,5*tply
k,n+3,0,7*e,5*tply
k,n+4,0,yc-7*e+6*e,zc-4*tply+5*tply
k,n+5,L,yc-7*e+6*e,zc-4*tply+5*tply
k,n+6,L,7*e,zc-4*tply+5*tply
k,n+7,0,7*e,zc-4*tply+5*tply
V,n,n+1,n+2,n+3,n+4,n+5,n+6,n+7
n=n+8

k,n,0,7*e,5*tply
k,n+1,L,7*e,5*tply
k,n+2,L,yc,5*tply
k,n+3,0,yc,5*tply
k,n+4,0,7*e,zc-4*tply+5*tply
k,n+5,L,7*e,zc-4*tply+5*tply
k,n+6,L,yc,zc-4*tply+5*tply
k,n+7,0,yc,zc-4*tply+5*tply
V,n,n+1,n+2,n+3,n+4,n+5,n+6,n+7
n=n+8

k,n,0,yc,5*tply
k,n+1,L,yc,5*tply
k,n+2,L,8*e,5*tply
k,n+3,0,8*e,5*tply
k,n+4,0,yc,zc-4*tply+5*tply
k,n+5,L,yc,zc-4*tply+5*tply
k,n+6,L,8*e,zc-4*tply+5*tply
k,n+7,0,8*e,zc-4*tply+5*tply
V,n,n+1,n+2,n+3,n+4,n+5,n+6,n+7
n=n+8

k,n,0,8*e,5*tply
k,n+1,L,8*e,5*tply
k,n+2,L,yc-7*e+8*e,5*tply
k,n+3,0,yc-7*e+8*e,5*tply
k,n+4,0,8*e,zc-4*tply+5*tply
k,n+5,L,8*e,zc-4*tply+5*tply
k,n+6,L,yc-7*e+8*e,zc-4*tply+5*tply
k,n+7,0,yc-7*e+8*e,zc-4*tply+5*tply
V,n,n+1,n+2,n+3,n+4,n+5,n+6,n+7
n=n+8

k,n,0,yc-7*e+8*e,5*tply
k,n+1,L,yc-7*e+8*e,5*tply
k,n+2,L,9*e,5*tply
k,n+3,0,9*e,5*tply
k,n+4,0,yc-7*e+8*e,zc-4*tply+5*tply
k,n+5,L,yc-7*e+8*e,zc-4*tply+5*tply
k,n+6,L,9*e,zc-4*tply+5*tply
k,n+7,0,9*e,zc-4*tply+5*tply
```

```
V,n,n+1,n+2,n+3,n+4,n+5,n+6,n+7
n=n+8

k,n,0,9*e,5*tply
k,n+1,L,9*e,5*tply
k,n+2,L,b1,5*tply
k,n+3,0,b1,5*tply
k,n+4,0,9*e,zc-4*tply+5*tply
k,n+5,L,9*e,zc-4*tply+5*tply
k,n+6,L,b1,zc-4*tply+5*tply
k,n+7,0,b1,zc-4*tply+5*tply
V,n,n+1,n+2,n+3,n+4,n+5,n+6,n+7
n=n+8

k,n,0,0,zc-4*tply+5*tply
k,n+1,L,0,zc-4*tply+5*tply
k,n+2,L,6*e,zc-4*tply+5*tply
k,n+3,0,6*e,zc-4*tply+5*tply
k,n+4,0,0,6*tply
k,n+5,L,0,6*tply
k,n+6,L,6*e,6*tply
k,n+7,0,6*e,6*tply
V,n,n+1,n+2,n+3,n+4,n+5,n+6,n+7
n=n+8

k,n,0,6*e,zc-4*tply+5*tply
k,n+1,L,6*e,zc-4*tply+5*tply
k,n+2,L,yc-7*e+6*e,zc-4*tply+5*tply
k,n+3,0,yc-7*e+6*e,zc-4*tply+5*tply
k,n+4,0,6*e,6*tply
k,n+5,L,6*e,6*tply
k,n+6,L,yc-7*e+6*e,6*tply
k,n+7,0,yc-7*e+6*e,6*tply
V,n,n+1,n+2,n+3,n+4,n+5,n+6,n+7
n=n+8

k,n,0,yc-7*e+6*e,zc-4*tply+5*tply
k,n+1,L,yc-7*e+6*e,zc-4*tply+5*tply
k,n+2,L,7*e,zc-4*tply+5*tply
k,n+3,0,7*e,zc-4*tply+5*tply
k,n+4,0,yc-7*e+6*e,6*tply
k,n+5,L,yc-7*e+6*e,6*tply
k,n+6,L,7*e,6*tply
k,n+7,0,7*e,6*tply
V,n,n+1,n+2,n+3,n+4,n+5,n+6,n+7
n=n+8

k,n,0,7*e,zc-4*tply+5*tply
k,n+1,L,7*e,zc-4*tply+5*tply
k,n+2,L,yc,zc-4*tply+5*tply
k,n+3,0,yc,zc-4*tply+5*tply
k,n+4,0,7*e,6*tply
k,n+5,L,7*e,6*tply
k,n+6,L,yc,6*tply
k,n+7,0,yc,6*tply
V,n,n+1,n+2,n+3,n+4,n+5,n+6,n+7
```

```
n=n+8

k,n,0,yc,zc-4*tply+5*tply
k,n+1,L,yc,zc-4*tply+5*tply
k,n+2,L,8*e,zc-4*tply+5*tply
k,n+3,0,8*e,zc-4*tply+5*tply
k,n+4,0,yc,6*tply
k,n+5,L,yc,6*tply
k,n+6,L,8*e,6*tply
k,n+7,0,8*e,6*tply
V,n,n+1,n+2,n+3,n+4,n+5,n+6,n+7
n=n+8

k,n,0,8*e,zc-4*tply+5*tply
k,n+1,L,8*e,zc-4*tply+5*tply
k,n+2,L,yc-7*e+8*e,zc-4*tply+5*tply
k,n+3,0,yc-7*e+8*e,zc-4*tply+5*tply
k,n+4,0,8*e,6*tply
k,n+5,L,8*e,6*tply
k,n+6,L,yc-7*e+8*e,6*tply
k,n+7,0,yc-7*e+8*e,6*tply
V,n,n+1,n+2,n+3,n+4,n+5,n+6,n+7
n=n+8

k,n,0,yc-7*e+8*e,zc-4*tply+5*tply
k,n+1,L,yc-7*e+8*e,zc-4*tply+5*tply
k,n+2,L,9*e,zc-4*tply+5*tply
k,n+3,0,9*e,zc-4*tply+5*tply
k,n+4,0,yc-7*e+8*e,6*tply
k,n+5,L,yc-7*e+8*e,6*tply
k,n+6,L,9*e,6*tply
k,n+7,0,9*e,6*tply
V,n,n+1,n+2,n+3,n+4,n+5,n+6,n+7
n=n+8

k,n,0,9*e,zc-4*tply+5*tply
k,n+1,L,9*e,zc-4*tply+5*tply
k,n+2,L,b1,zc-4*tply+5*tply
k,n+3,0,b1,zc-4*tply+5*tply
k,n+4,0,9*e,6*tply
k,n+5,L,9*e,6*tply
k,n+6,L,b1,6*tply
k,n+7,0,b1,6*tply
V,n,n+1,n+2,n+3,n+4,n+5,n+6,n+7
n=n+8

*DO,i,7,8,1
k,n,0,0,(i-1)*tply
k,n+1,L,0,(i-1)*tply
k,n+2,L,6*e,(i-1)*tply
k,n+3,0,6*e,(i-1)*tply
k,n+4,0,0,(i)*tply
k,n+5,L,0,(i)*tply
k,n+6,L,6*e,(i)*tply
k,n+7,0,6*e,(i)*tply
V,n,n+1,n+2,n+3,n+4,n+5,n+6,n+7
```

```
n=n+8
*ENDDO

*DO,i,7,8,1
k,n,0,6*e,(i-1)*tply
k,n+1,L,6*e,(i-1)*tply
k,n+2,L,yc-7*e+6*e,(i-1)*tply
k,n+3,0,yc-7*e+6*e,(i-1)*tply
k,n+4,0,6*e,(i)*tply
k,n+5,L,6*e,(i)*tply
k,n+6,L,yc-7*e+6*e,(i)*tply
k,n+7,0,yc-7*e+6*e,(i)*tply
V,n,n+1,n+2,n+3,n+4,n+5,n+6,n+7
n=n+8
*ENDDO

*DO,i,7,8,1
k,n,0,yc-7*e+6*e,(i-1)*tply
k,n+1,L,yc-7*e+6*e,(i-1)*tply
k,n+2,L,7*e,(i-1)*tply
k,n+3,0,7*e,(i-1)*tply
k,n+4,0,yc-7*e+6*e,(i)*tply
k,n+5,L,yc-7*e+6*e,(i)*tply
k,n+6,L,7*e,(i)*tply
k,n+7,0,7*e,(i)*tply
V,n,n+1,n+2,n+3,n+4,n+5,n+6,n+7
n=n+8
*ENDDO

*DO,i,7,8,1
k,n,0,7*e,(i-1)*tply
k,n+1,L,7*e,(i-1)*tply
k,n+2,L,yc,(i-1)*tply
k,n+3,0,yc,(i-1)*tply
k,n+4,0,7*e,(i)*tply
k,n+5,L,7*e,(i)*tply
k,n+6,L,yc,(i)*tply
k,n+7,0,yc,(i)*tply
V,n,n+1,n+2,n+3,n+4,n+5,n+6,n+7
n=n+8
*ENDDO

*DO,i,7,8,1
k,n,0,yc,(i-1)*tply
k,n+1,L,yc,(i-1)*tply
k,n+2,L,8*e,(i-1)*tply
k,n+3,0,8*e,(i-1)*tply
k,n+4,0,yc,(i)*tply
k,n+5,L,yc,(i)*tply
k,n+6,L,8*e,(i)*tply
k,n+7,0,8*e,(i)*tply
V,n,n+1,n+2,n+3,n+4,n+5,n+6,n+7
n=n+8
*ENDDO

*DO,i,7,8,1
```

```
k,n,0,8*e,(i-1)*tply
k,n+1,L,8*e,(i-1)*tply
k,n+2,L,yc-7*e+8*e,(i-1)*tply
k,n+3,0,yc-7*e+8*e,(i-1)*tply
k,n+4,0,8*e,(i)*tply
k,n+5,L,8*e,(i)*tply
k,n+6,L,yc-7*e+8*e,(i)*tply
k,n+7,0,yc-7*e+8*e,(i)*tply
V,n,n+1,n+2,n+3,n+4,n+5,n+6,n+7
n=n+8
*ENDDO

*DO,i,7,8,1
k,n,0,yc-7*e+8*e,(i-1)*tply
k,n+1,L,yc-7*e+8*e,(i-1)*tply
k,n+2,L,9*e,(i-1)*tply
k,n+3,0,9*e,(i-1)*tply
k,n+4,0,yc-7*e+8*e,(i)*tply
k,n+5,L,yc-7*e+8*e,(i)*tply
k,n+6,L,9*e,(i)*tply
k,n+7,0,9*e,(i)*tply
V,n,n+1,n+2,n+3,n+4,n+5,n+6,n+7
n=n+8
*ENDDO

*DO,i,7,8,1
k,n,0,9*e,(i-1)*tply
k,n+1,L,9*e,(i-1)*tply
k,n+2,L,b1,(i-1)*tply
k,n+3,0,b1,(i-1)*tply
k,n+4,0,9*e,(i)*tply
k,n+5,L,9*e,(i)*tply
k,n+6,L,b1,(i)*tply
k,n+7,0,b1,(i)*tply
V,n,n+1,n+2,n+3,n+4,n+5,n+6,n+7
n=n+8
*ENDDO

*DO,i,9,12,1
k,n,0,vx,(i-1)*tply
k,n+1,L,vx,(i-1)*tply
k,n+2,L,6*e,(i-1)*tply
k,n+3,0,6*e,(i-1)*tply
k,n+4,0,vx,(i)*tply
k,n+5,L,vx,(i)*tply
k,n+6,L,6*e,(i)*tply
k,n+7,0,6*e,(i)*tply
V,n,n+1,n+2,n+3,n+4,n+5,n+6,n+7
n=n+8
*ENDDO

*DO,i,9,12,1
k,n,0,6*e,(i-1)*tply
k,n+1,L,6*e,(i-1)*tply
k,n+2,L,yc-7*e+6*e,(i-1)*tply
k,n+3,0,yc-7*e+6*e,(i-1)*tply
```

```
k,n+4,0,6*e,(i)*tply
k,n+5,L,6*e,(i)*tply
k,n+6,L,yc-7*e+6*e,(i)*tply
k,n+7,0,yc-7*e+6*e,(i)*tply
V,n,n+1,n+2,n+3,n+4,n+5,n+6,n+7
n=n+8
*ENDDO

*DO,i,9,12,1
k,n,0,yc-7*e+6*e,(i-1)*tply
k,n+1,L,yc-7*e+6*e,(i-1)*tply
k,n+2,L,7*e,(i-1)*tply
k,n+3,0,7*e,(i-1)*tply
k,n+4,0,yc-7*e+6*e,(i)*tply
k,n+5,L,yc-7*e+6*e,(i)*tply
k,n+6,L,7*e,(i)*tply
k,n+7,0,7*e,(i)*tply
V,n,n+1,n+2,n+3,n+4,n+5,n+6,n+7
n=n+8
*ENDDO

*DO,i,9,12,1
k,n,0,7*e,(i-1)*tply
k,n+1,L,7*e,(i-1)*tply
k,n+2,L,yc,(i-1)*tply
k,n+3,0,yc,(i-1)*tply
k,n+4,0,7*e,(i)*tply
k,n+5,L,7*e,(i)*tply
k,n+6,L,yc,(i)*tply
k,n+7,0,yc,(i)*tply
V,n,n+1,n+2,n+3,n+4,n+5,n+6,n+7
n=n+8
*ENDDO

*DO,i,9,12,1
k,n,0,yc,(i-1)*tply
k,n+1,L,yc,(i-1)*tply
k,n+2,L,8*e,(i-1)*tply
k,n+3,0,8*e,(i-1)*tply
k,n+4,0,yc,(i)*tply
k,n+5,L,yc,(i)*tply
k,n+6,L,8*e,(i)*tply
k,n+7,0,8*e,(i)*tply
V,n,n+1,n+2,n+3,n+4,n+5,n+6,n+7
n=n+8
*ENDDO

*DO,i,9,12,1
k,n,0,8*e,(i-1)*tply
k,n+1,L,8*e,(i-1)*tply
k,n+2,L,yc-7*e+8*e,(i-1)*tply
k,n+3,0,yc-7*e+8*e,(i-1)*tply
k,n+4,0,8*e,(i)*tply
k,n+5,L,8*e,(i)*tply
k,n+6,L,yc-7*e+8*e,(i)*tply
k,n+7,0,yc-7*e+8*e,(i)*tply
```

```
V,n,n+1,n+2,n+3,n+4,n+5,n+6,n+7
n=n+8
*ENDDO

*DO,i,9,12,1
k,n,0,yc-7*e+8*e,(i-1)*tply
k,n+1,L,yc-7*e+8*e,(i-1)*tply
k,n+2,L,9*e,(i-1)*tply
k,n+3,0,9*e,(i-1)*tply
k,n+4,0,yc-7*e+8*e,(i)*tply
k,n+5,L,yc-7*e+8*e,(i)*tply
k,n+6,L,9*e,(i)*tply
k,n+7,0,9*e,(i)*tply
V,n,n+1,n+2,n+3,n+4,n+5,n+6,n+7
n=n+8
*ENDDO

*DO,i,9,12,1
k,n,0,9*e,(i-1)*tply
k,n+1,L,9*e,(i-1)*tply
k,n+2,L,vx+0.25,(i-1)*tply
k,n+3,0,vx+0.25,(i-1)*tply
k,n+4,0,9*e,(i)*tply
k,n+5,L,9*e,(i)*tply
k,n+6,L,vx+0.25,(i)*tply
k,n+7,0,vx+0.25,(i)*tply
V,n,n+1,n+2,n+3,n+4,n+5,n+6,n+7
n=n+8
*ENDDO


allsel


nummrg,kp

ET,1,SOLID46

f=1
R,f
RMODIF,f,1,1,0,0,0,0
RMODIF,f,7,0
RMODIF,f,13,1,90,tply

f=2
R,f
RMODIF,f,1,1,0,0,0,0
RMODIF,f,7,0
RMODIF,f,13,1,0,tply

f=3
R,f
RMODIF,f,1,1,0,0,0,0
RMODIF,f,7,0
RMODIF,f,13,1,-45,tply
```

```
f=4
R,f
RMODIF,f,1,1,0,0,0,0
RMODIF,f,7,0
RMODIF,f,13,1,45,zc-4*tply

f=5
R,f
RMODIF,f,1,1,0,0,0,0
RMODIF,f,7,0
RMODIF,f,13,1,45,5*tply-zc

f=6
R,f
RMODIF,f,1,1,0,0,0,0
RMODIF,f,7,0
RMODIF,f,13,1,90,zc-4*tply

f=7
R,f
RMODIF,f,1,1,0,0,0,0
RMODIF,f,7,0
RMODIF,f,13,1,90,5*tply-zc

f=8
R,f
RMODIF,f,1,1,0,0,0,0
RMODIF,f,7,0
RMODIF,f,13,1,0,zc-4*tply

f=9
R,f
RMODIF,f,1,1,0,0,0,0
RMODIF,f,7,0
RMODIF,f,13,1,0,5*tply-zc

f=10
R,f
RMODIF,f,1,1,0,0,0,0
RMODIF,f,7,0
RMODIF,f,13,1,-45,tply

f=11
R,f
RMODIF,f,1,1,0,0,0,0
RMODIF,f,7,0
RMODIF,f,13,1,45,tply

f=12
R,f
RMODIF,f,1,1,0,0,0,0
RMODIF,f,7,0
RMODIF,f,13,1,90,tply

f=13
R,f
```

```
RMODIF,f,1,1,0,0,0,0
RMODIF,f,7,0
RMODIF,f,13,1,0,tply

f=14
R,f
RMODIF,f,1,1,0,0,0,0
RMODIF,f,7,0
RMODIF,f,13,1,-45,tply

f=15
R,f
RMODIF,f,1,1,0,0,0,0
RMODIF,f,7,0
RMODIF,f,13,1,45,tply

*DO,i,1,3,1
VSEL,S,VOLU,,i
VATT,1,i,1,0
*ENDDO

*DO,i,4,6,1
VSEL,S,VOLU,,i
VATT,1,i-3,1,0
*ENDDO

*DO,i,7,9,1
VSEL,S,VOLU,,i
VATT,1,i-6,1,0
*ENDDO

*DO,i,10,12,1
VSEL,S,VOLU,,i
VATT,1,i-9,1,0
*ENDDO

*DO,i,13,15,1
VSEL,S,VOLU,,i
VATT,1,i-12,1,0
*ENDDO

*DO,i,16,18,1
VSEL,S,VOLU,,i
VATT,1,i-15,1,0
*ENDDO

*DO,i,19,21,1
VSEL,S,VOLU,,i
VATT,1,i-18,1,0
*ENDDO

*DO,i,22,24,1
VSEL,S,VOLU,,i
VATT,1,i-21,1,0
*ENDDO
```

```
*DO,i,25,32,1
VSEL,S,VOLU,,i
VATT,1,4,1,0
*ENDDO

*DO,i,33,40,1
VSEL,S,VOLU,,i
VATT,1,5,1,0
*ENDDO

*DO,i,41,48,1
VSEL,S,VOLU,,i
VATT,1,6,1,0
*ENDDO

*DO,i,49,56,1
VSEL,S,VOLU,,i
VATT,1,7,1,0
*ENDDO

*DO,i,57,64,1
VSEL,S,VOLU,,i
VATT,1,8,1,0
*ENDDO

*DO,i,65,72,1
VSEL,S,VOLU,,i
VATT,1,9,1,0
*ENDDO

*DO,i,73,88,2
VSEL,S,VOLU,,i
VATT,1,10,1,0
*ENDDO

*DO,i,74,88,2
VSEL,S,VOLU,,i
VATT,1,11,1,0
*ENDDO

*DO,i,89,92,1
VSEL,S,VOLU,,i
VATT,1,i-77,1,0
*ENDDO

*DO,i,93,96,1
VSEL,S,VOLU,,i
VATT,1,i-81,1,0
*ENDDO

*DO,i,97,100,1
VSEL,S,VOLU,,i
VATT,1,i-85,1,0
*ENDDO

*DO,i,101,104,1
```

```
VSEL,S,VOLU,,i
VATT,1,i-89,1,0
*ENDDO

*DO,i,105,108,1
VSEL,S,VOLU,,i
VATT,1,i-93,1,0
*ENDDO

*DO,i,109,112,1
VSEL,S,VOLU,,i
VATT,1,i-97,1,0
*ENDDO

*DO,i,113,116,1
VSEL,S,VOLU,,i
VATT,1,i-101,1,0
*ENDDO

*DO,i,117,120,1
VSEL,S,VOLU,,i
VATT,1,i-105,1,0
*ENDDO

dx=320
xx=1
LSEL,s,Lenght,,L
LESIZE,all,,,dx,xx

dy=6
yy=1
LSEL,S,Lenght,,6*e
LESIZE,all,,,dy,yy

dy=7
yy=1
LSEL,S,Lenght,,7*e
LESIZE,all,,,dy,yy

dy=4
yy=1
LSEL,S,Lenght,,4*e
LESIZE,all,,,dy,yy

dy=1
yy=1
LSEL,S,Lenght,,1*e
LESIZE,all,,,dy,yy

dy=1
yy=1
LSEL,S,Lenght,,8*e-yc
LESIZE,all,,,dy,yy

dy=1
yy=1
```

```
LSEL,S,Lenght,,yc-7*e
LESIZE,all,,,dy,yy

dz=2
zz=1
LSEL,S,Lenght,,tply
LESIZE,ALL,,,dz,zz

dz=2
zz=1
LSEL,S,Lenght,,zc-4*tply
LESIZE,ALL,,,dz,zz

dz=1
zz=1
LSEL,S,Lenght,,5*tply-zc
LESIZE,ALL,,,dz,zz

allsel
VMESH,ALL

nummrg,node,1e-4

tol=1e-5
NSEL,S,LOC,x,0
D,ALL,Ux,0

NSEL,S,LOC,x,0
NSEL,R,LOC,y,yc
D,ALL,Uy,0

NSEL,S,LOC,x,0
NSEL,R,LOC,z,zc
D,ALL,Uz,0

NSEL,S,LOC,X,L-tol,L+tol
NSEL,R,LOC,y,yc,
NSEL,R,LOC,Z,zc+tply,
F,ALL,FX,force

NSEL,S,LOC,X,L-tol,L+tol
NSEL,R,LOC,y,yc,
NSEL,R,LOC,Z,zc-tply,
F,ALL,FX,-force

allsel

FINISH
/SOL
SOLVE
FINISH

!!!!!!!!!!!!!!!!!!!!!!!!!!!!!!!!!!!!!!!!!!!!!!!!!!!!!!!!!!!!!!!!!!!!!!!!!!!!!!!!!!!!!!!!!!!!!!!!
NSEL,S,loc,x,10/2
NSEL,r,loc,y,yc
NSEL,r,loc,z,zc
```

Typical ANSYS file for the Z-stiffener.

```
/FILNAM, CIR ISO Axial
/TITLE, CIR ISO Axial

/UNITS,BIN
/PREP7

force=1
lenght_elements=40

tply=0.005
b1=0.25
b2=0.25
w=0.5
L=10

MP,EX,1,18.2e6
MP,EY,1,1.41e6
MP,EZ,1,1.41e6
MP,PRXY,1,0.27
MP,PRYZ,1,0.27
MP,PRXZ,1,0.27
MP,GXY,1,0.92e6
MP,GYZ,1,0.92e6
MP,GXZ,1,0.92e6

ET,1,SOLID46

R,1
RMODIF,1,1,1,0,0,0,0
RMODIF,1,7,0
RMODIF,1,13,1,45,tply

R,2
RMODIF,2,1,1,0,0,0,0
RMODIF,2,7,0
RMODIF,2,13,1,-45,tply

R,3
RMODIF,3,1,1,0,0,0,0
RMODIF,3,7,0
RMODIF,3,13,1,0,tply

R,4
RMODIF,4,1,1,0,0,0,0
RMODIF,4,7,0
RMODIF,4,13,1,0,tply

R,5
RMODIF,5,1,1,0,0,0,0
RMODIF,5,7,0
RMODIF,5,13,1,-45,tply
```

```
R,6
RMODIF,6,1,1,0,0,0,0
RMODIF,6,7,0
RMODIF,6,13,1,45,tply

R,7
RMODIF,7,1,1,0,0,0,0
RMODIF,7,7,0
RMODIF,7,13,1,45,tply

R,8
RMODIF,8,1,1,0,0,0,0
RMODIF,8,7,0
RMODIF,8,13,1,-45,tply

R,9
RMODIF,9,1,1,0,0,0,0
RMODIF,9,7,0
RMODIF,9,13,1,0,tply

R,10
RMODIF,10,1,1,0,0,0,0
RMODIF,10,7,0
RMODIF,10,13,1,0,tply

R,11
RMODIF,11,1,1,0,0,0,0
RMODIF,11,7,0
RMODIF,11,13,1,-45,tply

R,12
RMODIF,12,1,1,0,0,0,0
RMODIF,12,7,0
RMODIF,12,13,1,45,tply

R,13
RMODIF,13,1,1,0,0,0,0
RMODIF,13,7,0
RMODIF,13,13,1,45,tply

R,14
RMODIF,14,1,1,0,0,0,0
RMODIF,14,7,0
RMODIF,14,13,1,-45,tply

R,15
RMODIF,15,1,1,0,0,0,0
RMODIF,15,7,0
RMODIF,15,13,1,-45,tply

R,16
RMODIF,16,1,1,0,0,0,0
RMODIF,16,7,0
RMODIF,16,13,1,45,tply
```

```
n=0
*DO,i,0,11,1
k,n+1,0,-b1+2*tply,w/2+i*tply
k,n+2,L,-b1+2*tply,w/2+i*tply
k,n+3,L,-2*tply,w/2+i*tply
k,n+4,0,-2*tply,w/2+i*tply
k,n+5,0,-b1+2*tply,w/2+(i+1)*tply
k,n+6,L,-b1+2*tply,w/2+(i+1)*tply
k,n+7,L,-2*tply,w/2+(i+1)*tply
k,n+8,0,-2*tply,w/2+(i+1)*tply
v,n+1,n+2,n+3,n+4,n+5,n+6,n+7,n+8
n=n+8
*ENDDO

*DO,i,0,11,1
k,n+1,0,-2*tply,w/2+i*tply
k,n+2,L,-2*tply,w/2+i*tply
k,n+3,L,2*tply,w/2+i*tply
k,n+4,0,2*tply,w/2+i*tply
k,n+5,0,-2*tply,w/2+(i+1)*tply
k,n+6,L,-2*tply,w/2+(i+1)*tply
k,n+7,L,2*tply,w/2+(i+1)*tply
k,n+8,0,2*tply,w/2+(i+1)*tply
v,n+1,n+2,n+3,n+4,n+5,n+6,n+7,n+8
n=n+8
*ENDDO

Local,11,0,0,0,0,0,-90,0

*DO,i,-2,1,1
k,n+1,0,-w/2,i*tply
k,n+2,L,-w/2,i*tply
k,n+3,L,w/2,i*tply
k,n+4,0,w/2,i*tply
k,n+5,0,-w/2,(i+1)*tply
k,n+6,L,-w/2,(i+1)*tply
k,n+7,L,w/2,(i+1)*tply
k,n+8,0,w/2,(i+1)*tply
v,n+1,n+2,n+3,n+4,n+5,n+6,n+7,n+8
n=n+8
*ENDDO

CSYS,0

*DO,i,0,11,1
k,n+1,0,-2*tply,-w/2-12*tply+i*tply
k,n+2,L,-2*tply,-w/2-12*tply+i*tply
k,n+3,L,2*tply,-w/2-12*tply+i*tply
k,n+4,0,2*tply,-w/2-12*tply+i*tply
k,n+5,0,-2*tply,-w/2-12*tply+(i+1)*tply
k,n+6,L,-2*tply,-w/2-12*tply+(i+1)*tply
k,n+7,L,2*tply,-w/2-12*tply+(i+1)*tply
k,n+8,0,2*tply,-w/2-12*tply+(i+1)*tply
v,n+1,n+2,n+3,n+4,n+5,n+6,n+7,n+8
n=n+8
*ENDDO
```

```
*DO,i,0,11,1
k,n+1,0,2*tply,-w/2-12*tply+i*tply
k,n+2,L,2*tply,-w/2-12*tply+i*tply
k,n+3,L,b2-2*tply,-w/2-12*tply+i*tply
k,n+4,0,b2-2*tply,-w/2-12*tply+i*tply
k,n+5,0,2*tply,-w/2-12*tply+(i+1)*tply
k,n+6,L,2*tply,-w/2-12*tply+(i+1)*tply
k,n+7,L,b2-2*tply,-w/2-12*tply+(i+1)*tply
k,n+8,0,b2-2*tply,-w/2-12*tply+(i+1)*tply
v,n+1,n+2,n+3,n+4,n+5,n+6,n+7,n+8
n=n+8
*ENDDO


NUMMRG,KP,1.0e-4

LSEL,S,LENGTH,,L
LESIZE,ALL,,,lenght_elements

LSEL,S,LENGTH,,12*tply
LESIZE,ALL,,,12

LSEL,S,LENGTH,,4*tply
LESIZE,ALL,,,4

LSEL,S,LENGTH,,w
LESIZE,ALL,,,100

LSEL,S,LENGTH,,b1-12*tply
LESIZE,ALL,,,90

LSEL,S,LENGTH,,tply
LESIZE,ALL,,,1

*DO,y,1,12,1
VSEL,S,volu,,y
VATT,1,y,1,0
*ENDDO

*DO,y,13,24,1
VSEL,S,volu,,y
VATT,1,y-12,1,0
*ENDDO

*DO,y,25,28,1
VSEL,S,volu,,y
VATT,1,y-12,1,11
*ENDDO

*DO,y,29,40,1
VSEL,S,volu,,y
VATT,1,y-28,1,0
*ENDDO

*DO,y,41,52,1
```

```
VSEL,S,volu,,y
VATT,1,y-40,1,0
*ENDDO

ALLSEL
VMESH,ALL


EPLOT

CSYS,0

TOL=0.00001

NSEL,S,LOC,X,L
NSEL,r,LOC,y,0
NSEL,r,LOC,Z,0
F,all,FX,force

NSEL,S,LOC,X,L
CP,1,ux,all

NSEL,S,LOC,X,0
D,ALL,ALL,0

ALLSEL
/SOLU
SOLVE

!!!!!!!!!!!!!!!!!!!!!!!!!!!!!!!!!!!

NSEL,S,LOC,X,0.500000*L
NSEL,r,LOC,y,0
NSEL,r,LOC,z,0
```

Typical MATLAB file for Laminates Bonded Side by Side Un-symmetric Case $[\pm 45_2/0_4/\pm 45_2]_T$ - $[\pm 45_2/0_2]_S$ under Axial load.

```
/FILNAM, Laminate
/title, Laminate
/prep7

MP,EX,1,18.2E6
MP,EY,1,1.41E6
MP,EZ,1,1.41E6
MP,PRXY,1,0.27
MP,PRYZ,1,0.27
MP,PRXZ,1,0.27
MP,GXY,1,0.92E6
MP,GYZ,1,0.92E6
MP,GXZ,1,0.92E6

L=10
b1=0.5
b2=0.25
tply=0.005
force=0.1


n=1

*DO,i,1,12,1
k,n,0,-b1,(i-7)*tply
k,n+1,L,-b1,(i-7)*tply
k,n+2,L,0,(i-7)*tply
k,n+3,0,0,(i-7)*tply
k,n+4,0,-b1,(i-6)*tply
k,n+5,L,-b1,(i-6)*tply
k,n+6,L,0,(i-6)*tply
k,n+7,0,0,(i-6)*tply
V,n,n+1,n+2,n+3,n+4,n+5,n+6,n+7
n=n+8
*ENDDO

*DO,i,1,12,1
k,n,0,0,(i-7)*tply
k,n+1,L,0,(i-7)*tply
k,n+2,L,b2,(i-7)*tply
k,n+3,0,b2,(i-7)*tply
k,n+4,0,0,(i-6)*tply
k,n+5,L,0,(i-6)*tply
k,n+6,L,b2,(i-6)*tply
k,n+7,0,b2,(i-6)*tply
V,n,n+1,n+2,n+3,n+4,n+5,n+6,n+7
n=n+8
*ENDDO

allsel
nummrg,kp
```

```
ET,1,SOLID46

R,1
RMODIF,1,1,1,0,0,0,0
RMODIF,1,7,0
RMODIF,1,13,1,-45,tply

R,2
RMODIF,2,1,1,0,0,0,0
RMODIF,2,7,0
RMODIF,2,13,1,45,tply

R,3
RMODIF,3,1,1,0,0,0,0
RMODIF,3,7,0
RMODIF,3,13,1,-45,tply

R,4
RMODIF,4,1,1,0,0,0,0
RMODIF,4,7,0
RMODIF,4,13,1,45,tply

R,5
RMODIF,5,1,1,0,0,0,0
RMODIF,5,7,0
RMODIF,5,13,1,0,tply

R,6
RMODIF,6,1,1,0,0,0,0
RMODIF,6,7,0
RMODIF,6,13,1,0,tply

R,7
RMODIF,7,1,1,0,0,0,0
RMODIF,7,7,0
RMODIF,7,13,1,0,tply

R,8
RMODIF,8,1,1,0,0,0,0
RMODIF,8,7,0
RMODIF,8,13,1,0,tply

R,9
RMODIF,9,1,1,0,0,0,0
RMODIF,9,7,0
RMODIF,9,13,1,-45,tply

R,10
RMODIF,10,1,1,0,0,0,0
RMODIF,10,7,0
RMODIF,10,13,1,45,tply

R,11
RMODIF,11,1,1,0,0,0,0
RMODIF,11,7,0
RMODIF,11,13,1,-45,tply
```

```
R,12
RMODIF,12,1,1,0,0,0,0
RMODIF,12,7,0
RMODIF,12,13,1,45,tply

R,13
RMODIF,13,1,1,0,0,0,0
RMODIF,13,7,0
RMODIF,13,13,1,45,tply

R,14
RMODIF,14,1,1,0,0,0,0
RMODIF,14,7,0
RMODIF,14,13,1,-45,tply

R,15
RMODIF,15,1,1,0,0,0,0
RMODIF,15,7,0
RMODIF,15,13,1,45,tply

R,16
RMODIF,16,1,1,0,0,0,0
RMODIF,16,7,0
RMODIF,16,13,1,-45,tply

R,17
RMODIF,17,1,1,0,0,0,0
RMODIF,17,7,0
RMODIF,17,13,1,0,tply

R,18
RMODIF,18,1,1,0,0,0,0
RMODIF,18,7,0
RMODIF,18,13,1,0,tply

R,19
RMODIF,19,1,1,0,0,0,0
RMODIF,19,7,0
RMODIF,19,13,1,0,tply

R,20
RMODIF,20,1,1,0,0,0,0
RMODIF,20,7,0
RMODIF,20,13,1,0,tply

R,21
RMODIF,21,1,1,0,0,0,0
RMODIF,21,7,0
RMODIF,21,13,1,-45,tply

R,22
RMODIF,22,1,1,0,0,0,0
RMODIF,22,7,0
RMODIF,22,13,1,45,tply
```

```
R,23
RMODIF,23,1,1,0,0,0,0
RMODIF,23,7,0
RMODIF,23,13,1,-45,tply

R,24
RMODIF,24,1,1,0,0,0,0
RMODIF,24,7,0
RMODIF,24,13,1,45,tply

*DO,i,1,12,1
VSEL,S,VOLU,,i
VATT,1,i,1,0
*ENDDO

*DO,i,13,24,1
VSEL,S,VOLU,,i
VATT,1,i,1,0
*ENDDO

dx=100
xx=1
LSEL,s,Lenght,,L
LESIZE,all,,,dx,xx

dy=24
yy=1
LSEL,S,Lenght,,b1
LESIZE,all,,,dy,yy

dy=12
yy=1
LSEL,S,Lenght,,b2
LESIZE,all,,,dy,yy

dz=2
zz=1
LSEL,S,Lenght,,tply
LESIZE,ALL,,,dz,zz

allsel
VMESH,ALL
NSEL,S,LOC,x,0
D,ALL,ALL,0

ASEL,S,AREA,,3
ASEL,A,AREA,,9
ASEL,A,AREA,,15
ASEL,A,AREA,,21
ASEL,A,AREA,,27
ASEL,A,AREA,,33
ASEL,A,AREA,,39
ASEL,A,AREA,,45
ASEL,A,AREA,,51
ASEL,A,AREA,,57
ASEL,A,AREA,,63
```

```
ASEL,A,AREA,,69
SFA,ALL,1,PRES,-1

ASEL,A,AREA,,75
ASEL,A,AREA,,81
ASEL,A,AREA,,87
ASEL,A,AREA,,93
ASEL,A,AREA,,99
ASEL,A,AREA,,105
ASEL,A,AREA,,111
ASEL,A,AREA,,117
ASEL,A,AREA,,123
ASEL,A,AREA,,129
ASEL,A,AREA,,135
ASEL,A,AREA,,141
SFA,ALL,1,PRES,-1

allsel

FINISH
/SOL

SOLVE
FINISH

!!!!!!!!!!!!!!!!!!!!!!!!!!!!!!!!!!!!!!!!!!!!!!!!!!!!!!!!!!!!!!!!!!!!!!!!!!!!!!!!!!!!!!!!!!!!!!!!!!!!!!!!!!!!!!!!!!!!!!!!!!!!!!!!!!!!
NSEL,S,loc,x,5
NSEL,r,loc,y,0
NSEL,r,loc,z,0
```

Typical MATLAB file for the Circular Cross-section Beam Symmetric Case $[45_2/-45_2/0_2/90_2]_S$ under Axial load.

```
/FILNAM, CIR COMP Axial
/TITLE, CIR COMP Axial

/UNITS,BIN
/PREP7

LOCAL,11,CYLIN,0,0,0,0,90,90

Rm=0.9584
force=1
lenght_elements=44
angular_elements=40

tply=0.0052
r=Rm+tply*8
length=15

MP,EX,1,18.2E6
MP,EY,1,1.41E6
MP,EZ,1,1.41E6
MP,PRXY,1,0.27
MP,PRYZ,1,0.27
MP,PRXZ,1,0.27
MP,GXY,1,0.92E6
MP,GYZ,1,0.92E6
MP,GXZ,1,0.92E6

ET,1,SOLID46

R,1
RMODIF,1,1,1,0,0,0,0
RMODIF,1,7,0
RMODIF,1,13,1,45,tply

R,2
RMODIF,2,1,1,0,0,0,0
RMODIF,2,7,0
RMODIF,2,13,1,45,tply

R,3
RMODIF,3,1,1,0,0,0,0
RMODIF,3,7,0
RMODIF,3,13,1,-45,tply

R,4
RMODIF,4,1,1,0,0,0,0
RMODIF,4,7,0
RMODIF,4,13,1,-45,tply

R,5
RMODIF,5,1,1,0,0,0,0
RMODIF,5,7,0
RMODIF,5,13,1,0,tply
```

```
R,6
RMODIF,6,1,1,0,0,0,0
RMODIF,6,7,0
RMODIF,6,13,1,0,tply

R,7
RMODIF,7,1,1,0,0,0,0
RMODIF,7,7,0
RMODIF,7,13,1,90,tply

R,8
RMODIF,8,1,1,0,0,0,0
RMODIF,8,7,0
RMODIF,8,13,1,90,tply

R,9
RMODIF,9,1,1,0,0,0,0
RMODIF,9,7,0
RMODIF,9,13,1,90,tply

R,10
RMODIF,10,1,1,0,0,0,0
RMODIF,10,7,0
RMODIF,10,13,1,90,tply

R,11
RMODIF,11,1,1,0,0,0,0
RMODIF,11,7,0
RMODIF,11,13,1,0,tply

R,12
RMODIF,12,1,1,0,0,0,0
RMODIF,12,7,0
RMODIF,12,13,1,0,tply

R,13
RMODIF,13,1,1,0,0,0,0
RMODIF,13,7,0
RMODIF,13,13,1,-45,tply

R,14
RMODIF,14,1,1,0,0,0,0
RMODIF,14,7,0
RMODIF,14,13,1,-45,tply

R,15
RMODIF,15,1,1,0,0,0,0
RMODIF,15,7,0
RMODIF,15,13,1,45,tply

R,16
RMODIF,16,1,1,0,0,0,0
RMODIF,16,7,0
RMODIF,16,13,1,45,tply
```

```
CSYS,11

*DO,I,1,16,1
K,1+4*(I-1),r-tply*(I-1),0,0
K,2+4*(I-1),r-tply*(I-1),90,0
K,3+4*(I-1),r-tply*(I-1),180,0
K,4+4*(I-1),r-tply*(I-1),270,0
K,69+4*(I-1),r-tply*(I-1),0,length
K,70+4*(I-1),r-tply*(I-1),90,length
K,71+4*(I-1),r-tply*(I-1),180,length
K,72+4*(I-1),r-tply*(I-1),270,length
L,1+4*(I-1),2+4*(I-1)
L,2+4*(I-1),3+4*(I-1)
L,3+4*(I-1),4+4*(I-1)
L,4+4*(I-1),1+4*(I-1)
L,69+4*(I-1),70+4*(I-1)
L,70+4*(I-1),71+4*(I-1)
L,71+4*(I-1),72+4*(I-1)
L,72+4*(I-1),69+4*(I-1)
L,1+4*(I-1),69+4*(I-1)
L,2+4*(I-1),70+4*(I-1)
L,3+4*(I-1),71+4*(I-1)
L,4+4*(I-1),72+4*(I-1)
*ENDDO

*DO,J,1,16,1
AL,1+12*(J-1),9+12*(J-1),5+12*(J-1),10+12*(J-1)
AL,2+12*(J-1),10+12*(J-1),6+12*(J-1),11+12*(J-1)
AL,3+12*(J-1),11+12*(J-1),7+12*(J-1),12+12*(J-1)
AL,4+12*(J-1),12+12*(J-1),8+12*(J-1),9+12*(J-1)
*ENDDO

*DO,K,1,64,1
VOFFST,K,-tply
*ENDDO

NUMMRG,KP,1.0e-4

LSEL,S,,,1,8,1
*DO,L,1,15,1
LSEL,A,,,1+12*L,8+12*L,1
*ENDDO
lplot
LESIZE,ALL,,,angular_elements


LSEL,S,,,9,12,1
*DO,M,1,15,1
LSEL,A,,,9+12*M,12+12*M,1
*ENDDO
lplot
LESIZE,ALL,,,lenght_elements

CSYS,0

LSEL,S,LOC,Z,0
```

```
LSEL,R,LOC,X,0
LESIZE,ALL,,,1

LSEL,S,LOC,Y,0
LSEL,R,LOC,X,0
LESIZE,ALL,,,1

LSEL,S,LOC,Z,0
LSEL,R,LOC,X,length
LESIZE,ALL,,,1

LSEL,S,LOC,Y,0
LSEL,R,LOC,X,length
LESIZE,ALL,,,1


ALLSEL
*DO,N,1,16,1
TYPE,1,
MAT,1,
REAL,17-N
VMESH,1+4*(N-1),4+4*(N-1),1
*ENDDO
EPLOT

ALLSEL
NUMMRG,NODE,1.0e-4
NUMMRG,ELEM,1.0e-4
NUMMRG,KP,1.0e-4
EPLOT

CSYS,0

TOL=0.00001

NSEL,S,LOC,X,length
NSEL,r,LOC,Z,r-TOL,r+TOL
F,all,FX,force

NSEL,S,LOC,x,length
CP,42,ux,all

NSEL,S,LOC,X,0
D,ALL,UX,0

NSEL,S,LOC,X,0
NSEL,r,LOC,Z,-rm-TOL,-rm+TOL
NSEL,r,LOC,Y,0-TOL,0+TOL
D,ALL,UY,0

NSEL,S,LOC,X,0
NSEL,r,LOC,Z,rm-TOL,rm+TOL
NSEL,r,LOC,Y,0-TOL,0+TOL
D,ALL,UY,0

NSEL,S,LOC,X,0
```

```
NSEL,r,LOC,Y,-rm-TOL,-rm+TOL
NSEL,r,LOC,Z,0-TOL,0+TOL
D,ALL,UZ,0

NSEL,S,LOC,X,0
NSEL,r,LOC,Y,rm-TOL,rm+TOL
NSEL,r,LOC,Z,0-TOL,0+TOL
D,ALL,UZ,0

ALLSEL
/SOLU
SOLVE

!!!!!!!!!!!!!!!!!!!!!!!!!!!!!!!!!!!
NSEL,S,LOC,X,0.500000*length
NSEL,r,LOC,y,-rm-TOL,-rm+TOL
NSEL,r,LOC,z,0-TOL,0+TOL
```

Typical MATLAB file for the Airfoil Beam with $[90_8]_S$ under Bending.

```
/FILNAM, CIR COMP
/TITLE, CIR COMP

/UNITS,BIN
/PREP7

LOCAL,11,CYLIN,0,0,0,0,90,90

Rm=0.9584
force=0.001
lenght_elements=40
angular_elements=10
width_elements=32
height_elements=1

tply=0.0052
r=Rm+tply*8
length=(Rm+0.0416)*15
pi=3.14159265359

MP,EX,1,18.2E6
MP,EY,1,1.41E6
MP,EZ,1,1.41E6
MP,PRXY,1,0.27
MP,PRYZ,1,0.27
MP,PRXZ,1,0.27
MP,GXY,1,0.92E6
MP,GYZ,1,0.92E6
MP,GXZ,1,0.92E6

ET,1,SOLID46

R,1
RMODIF,1,1,1,0,0,0,0
RMODIF,1,7,0
RMODIF,1,13,1,90,tply

R,2
RMODIF,2,1,1,0,0,0,0
RMODIF,2,7,0
RMODIF,2,13,1,90,tply

R,3
RMODIF,3,1,1,0,0,0,0
RMODIF,3,7,0
RMODIF,3,13,1,90,tply

R,4
RMODIF,4,1,1,0,0,0,0
RMODIF,4,7,0
RMODIF,4,13,1,90,tply
R,5
RMODIF,5,1,1,0,0,0,0
RMODIF,5,7,0
```

```
RMODIF,5,13,1,90,tply

R,6
RMODIF,6,1,1,0,0,0,0
RMODIF,6,7,0
RMODIF,6,13,1,90,tply

R,7
RMODIF,7,1,1,0,0,0,0
RMODIF,7,7,0
RMODIF,7,13,1,90,tply

R,8
RMODIF,8,1,1,0,0,0,0
RMODIF,8,7,0
RMODIF,8,13,1,90,tply

R,9
RMODIF,9,1,1,0,0,0,0
RMODIF,9,7,0
RMODIF,9,13,1,90,tply

R,10
RMODIF,10,1,1,0,0,0,0
RMODIF,10,7,0
RMODIF,10,13,1,90,tply

R,11
RMODIF,11,1,1,0,0,0,0
RMODIF,11,7,0
RMODIF,11,13,1,90,tply

R,12
RMODIF,12,1,1,0,0,0,0
RMODIF,12,7,0
RMODIF,12,13,1,90,tply

R,13
RMODIF,13,1,1,0,0,0,0
RMODIF,13,7,0
RMODIF,13,13,1,90,tply

R,14
RMODIF,14,1,1,0,0,0,0
RMODIF,14,7,0
RMODIF,14,13,1,90,tply

R,15
RMODIF,15,1,1,0,0,0,0
RMODIF,15,7,0
RMODIF,15,13,1,90,tply

R,16
RMODIF,16,1,1,0,0,0,0
RMODIF,16,7,0
RMODIF,16,13,1,90,tply
```

```
CSYS,11

*DO,I,1,16,1
K,1+4*(I-1),r-tply*(I-1),0,0
K,2+4*(I-1),r-tply*(I-1),90,0
K,3+4*(I-1),r-tply*(I-1),180,0
K,4+4*(I-1),r-tply*(I-1),270,0
K,69+4*(I-1),r-tply*(I-1),0,length
K,70+4*(I-1),r-tply*(I-1),90,length
K,71+4*(I-1),r-tply*(I-1),180,length
K,72+4*(I-1),r-tply*(I-1),270,length
L,1+4*(I-1),2+4*(I-1)
L,2+4*(I-1),3+4*(I-1)
L,3+4*(I-1),4+4*(I-1)
L,4+4*(I-1),1+4*(I-1)
L,69+4*(I-1),70+4*(I-1)
L,70+4*(I-1),71+4*(I-1)
L,71+4*(I-1),72+4*(I-1)
L,72+4*(I-1),69+4*(I-1)
L,1+4*(I-1),69+4*(I-1)
L,2+4*(I-1),70+4*(I-1)
L,3+4*(I-1),71+4*(I-1)
L,4+4*(I-1),72+4*(I-1)
*ENDDO

*DO,J,1,16,1
AL,1+12*(J-1),9+12*(J-1),5+12*(J-1),10+12*(J-1)
AL,2+12*(J-1),10+12*(J-1),6+12*(J-1),11+12*(J-1)
AL,3+12*(J-1),11+12*(J-1),7+12*(J-1),12+12*(J-1)
AL,4+12*(J-1),12+12*(J-1),8+12*(J-1),9+12*(J-1)
*ENDDO

*DO,K,1,64,1
VOFFST,K,-tply
*ENDDO

*DO,K,1,61,4
VDELE,K,,,1
*ENDDO
*DO,K,4,64,4
VDELE,K,,,1
*ENDDO

LOCAL,12,CART,0,0,Rm,0,-10,0
*DO,i,-8,8,1
K,i+9+380,0,-i*tply*tan(0.1745329252),i*tply*cos(0.1745329252)
*ENDDO
*DO,i,-8,8,1
K,i+9+398,length,-i*tply*tan(0.1745329252),i*tply*cos(0.1745329252)
*ENDDO

CSYS,0
*DO,i,0,16,1
K,i+1+415,0,5.19943117224+i*tply/tan(0.1745329252),0
*ENDDO
*DO,i,0,16,1
```

```
K,i+1+432,length,5.19943117224+i*tply/tan(0.1745329252),0
*ENDDO

CSYS,12
*DO,i,0,15,1
v,381+i,399+i,433+i,416+i,381+1+i,399+1+i,433+1+i,416+1+i
*ENDDO

LOCAL,13,CART,0,0,-Rm,0,10,0
*DO,i,-8,8,1
K,i+9+450,0,i*tply*tan(0.1745329252),i*tply*cos(0.1745329252)
*ENDDO
*DO,i,-8,8,1
K,i+9+467,length,i*tply*tan(0.1745329252),i*tply*cos(0.1745329252)
*ENDDO

*DO,i,0,15,1
v,451+i,468+i,449-i,432-i,451+1+i,468+1+i,449-1-i,432-1-i
*ENDDO

NUMMRG,KP,1.0e-3

LSEL,S,RADIUS,,Rm-8*tply,Rm+8*tply
LESIZE,ALL,,,angular_elements

LSEL,S,LENGTH,,length
LESIZE,ALL,,,lenght_elements

LSEL,S,LENGTH,,5.51920563107-0.3,5.51920563107+0.3
LESIZE,ALL,,,width_elements

LSEL,S,LENGTH,,tply,tply/tan(0.1745329252)
LESIZE,ALL,,,height_elements

LSEL,S,LENGTH,,length2-length
LESIZE,ALL,,,1

ALLSEL

TYPE,1,
MAT,1,

REAL,1
VMESH,62
REAL,2
VMESH,58
REAL,3
VMESH,54
REAL,4
VMESH,50
REAL,5
VMESH,46
REAL,6
VMESH,42
REAL,7
VMESH,38
```

```
REAL,8
VMESH,34
REAL,9
VMESH,30
REAL,10
VMESH,26
REAL,11
VMESH,22
REAL,12
VMESH,18
REAL,13
VMESH,14
REAL,13
VMESH,14
REAL,14
VMESH,10
REAL,15
VMESH,6
REAL,16
VMESH,2
REAL,16
VMESH,2

REAL,1
VMESH,3
REAL,2
VMESH,7
REAL,3
VMESH,11
REAL,4
VMESH,15
REAL,5
VMESH,19
REAL,6
VMESH,23
REAL,7
VMESH,27
REAL,8
VMESH,31
REAL,9
VMESH,35
REAL,10
VMESH,39
REAL,11
VMESH,43
REAL,12
VMESH,47
REAL,13
VMESH,51
REAL,14
VMESH,55
REAL,15
VMESH,59
REAL,16
VMESH,63
```

```
CSYS,12
REAL,1
VMESH,1
REAL,2
VMESH,4
REAL,3
VMESH,5
REAL,4
VMESH,8
REAL,5
VMESH,9
REAL,6
VMESH,12
REAL,7
VMESH,13
REAL,8
VMESH,16
REAL,9
VMESH,17
REAL,10
VMESH,20
REAL,11
VMESH,21
REAL,12
VMESH,24
REAL,13
VMESH,25
REAL,14
VMESH,28
REAL,15
VMESH,29
REAL,16
VMESH,32

CSYS,13
REAL,1
VMESH,64
REAL,2
VMESH,61
REAL,3
VMESH,60
REAL,4
VMESH,57
REAL,5
VMESH,56
REAL,6
VMESH,53
REAL,7
VMESH,52
REAL,8
VMESH,49
REAL,9
VMESH,48
REAL,10
VMESH,45
REAL,11
```

```
VMESH,44
REAL,12
VMESH,41
REAL,13
VMESH,40
REAL,14
VMESH,37
REAL,15
VMESH,36
REAL,16
VMESH,33

EPLOT

ALLSEL

CSYS,0

TOL=0.00001

NSEL,S,LOC,X,length-TOL,length+TOL,
NSEL,r,LOC,Z,0+tply/2-TOL,r+TOL
F,ALL,FX,force

NSEL,S,LOC,X,length-TOL,length+TOL,
NSEL,r,LOC,Z,0-tply/2,-r-TOL
F,ALL,FX,-force

NSEL,S,LOC,X,0
D,ALL,ALL,0

allsel
```

REFERENCES

1. Callister, W. D. Jr., 2005, *Fundamentals of Materials Science and Engineering: An integrated Approach* 2nd Edition, John Wiley & Sons, Inc., Hoboken, NJ.
2. http://en.wikipedia.org/wiki/Composite_bow
3. http://www.et.byu.edu/groups/strong/pages/articles/articles/history.pdf
4. Halpin, J. C., 1992, *Primer on composite materials analysis*, Lancaster, Pa.
5. Vlot, A., and Gunnink, Jan W., 2001, *Fibre Metal Laminates: An Introduction*, Netherlands.
6. Makeev, A., and Armanios, E., "A Finit Displacement Model for Laminated Composite Strips with Extension-twist Coupling in the Presence of Delamination", ASME Journal of Applied Mechaniocs, 65685-693, 1998.
7. Rehfield, L., and Atilgan, A. R., "Toward understanding the tailoring mechanics for thin-walled composite tubular beams", Proceeding of First USSR-USA Symposium on Mechanics of Composite Materials, ASME, 1989, pp. 187-196.
8. Smith, E. C., and Chopra, I., "Formulation and evaluation of an analytical model for composite box-beams". Journal Am Helicopter Soc, 1991, vol. 36, pp. 33-35.
9. Song, O., Libresacu, L., and Jeong, N. H., "Static response of thin-walled composite I-beams loaded at their free-end cross-section: analytical solution", ELSEVIER, Composite Structures, vol. 52, 2001, pp. 55-65.
10. Razaqpur, A. G., "Method of Analysis for Advanced composite Structures", Advanced Composites Materials in Civil Engineering Structures, Proceedings of the Specialty Conference, 1991, pp. 336-347.
11. Parnas, L., and Katirci, N., "Design of fiber-reinforced composite pressure vessels under various loading conditions", ELSEVIER, Composite Structures, vol. 58, 2002, pp. 83-95.

12. Kollar, L. P., and Springer, G. S., 2003, *Mechanics of Composite Structures*, Cambridge University Press, UK.
13. Vasiliev, V. V., 1993, *Mechanics of Composite Structures*, Taylor & Francis, Washington, DC.
14. Hodges, D. H., 2006, *Nonlinear Composite Beam Theory*, AIAA, Reston, VA.
15. Barbero, E. J., 1999, *Introduction to Composite Materials Design*, Taylor & Francis, Boca Raton, FL.
16. Altenbach, H., Altenbach, J., and Kissing, W., 2004, *Mechanics of Composite Structural Elements*, Springer-Verlag, Berlin, Germany.
17. Turtle, M. E., 2004, *Structural Analysis of Polymeric Composite Materials*, Marcel Dekker, Inc., New York, NY.
18. Barbero, E., "Pultruded Structural Shapes: Stress Analysis and Failure Prediction", Advanced Composites Materials in Civil Engineering Structures, Proceedings of the Specialty Conference, 1991, pp. 194-204.
19. Barbero, E. J., Fu, S. H., and Raftoyiannis, I., "Ultimate bending strength of composite beams", ASCE J. Mater, Civil Engng 3, 1991, pp. 293-306.
20. Suresh, R., and Malhotra, S. K., "Some studies on static analysis of composite thin-walled box beam", Pergamon, Computer & Structures, vol. 62, 1997, pp. 625-634.
21. Whitney, J. M., "Shear correction factors for orthotropic laminates under static load". ASME, J. appl. Mech., 1973, vol. 40, pp. 302-304.
22. Mamalis, A. G., Manolakos, D. E., Demosthenous, G. A., and Ioannidis, M. B., "Analysis of Failure Mechanics Observed in Axial Collapse of Thin-Walled Circular Fibreglass Composite Tubes", ELSEVIER, Thin-walled Structures, vol. 24, 1996, pp. 335-352.
23. Volovoi, V. V., and Hodges, D. H., "Single- and Multicelled Composite Thin-Walled Beams", AIAA Journal, vol. 40, No. 5, 2002, pp. 960-965.
24. Wu, Y., Zhu, Y., Lai, Y., Zhang, X., and Liu, S., "Analysis of shear lag and shear deformation effects in laminated composite box beams under bending loads", ELSEVIER, Composite Structures, vol. 55, 2002, pp. 147-156.

25. Dechao, Z., Zhongmin D., and Xingwei, W., “The Analysis of thin walled Composite Laminated helicopter rotor with hierarchical warping functions and Finite Element Method”, Chinese Journal of Mechanics Press, vol. 17, No. 3, 2001, pp. 258-268.
26. Mitra, M., Gopalakrishnan, S., and Seetharama, M., “ A new super convergent thin walled composite beam element for analysis of box beam structures”, ELSEVIER, International Journal of Solids and Structures, vol. 41, 2004, pp. 1491-1518.
27. Armanios, E., Markeev, A., and Hooke, D., “Finite-Displacement Analysis of Laminated Composite Strips with Extension-Twist Coupling”, Journal of Aerospace Engineering, vol. 9, No. 3, July 1996, pp. 80-91.
28. Bank, L. C., Xi, Z., and Mosallam, A. S., “Experimental Study of FRP Grating Reinforced Concrete Slabs”, Advanced Composites Materials in Civil Engineering Structures, Proceedings of the Specialty Conference, 1991, pp. 111-122.
29. Drummond, J. A., and Chan, W. S., “Fabrication, Analysis, and Experimentation of a Practically Constructed Laminated Composite I-Beam Under Pure Bending”, Journal of Thermoplastic Composite Materials, volume 12, May 1999, pp. 177-187.
30. Chandra, R., and Chopra, I., “Structural Behavior of Two-Cell Composite Rotor Blades with Elastic Couplings”, AIAA Journal, 1992, vol. 30, pp. 2914-2921.
31. Chandra, R., and Chopra, I., “Experimental and theoretical analysis of composite I-beams with elastic coupling”, AIAA Journal, vol. 29, 1992, pp.2197-2206.
32. Chandra, R., Stemple, A. D., and Chopra I., “Thin-walled composite beams under bending, torsional and extensional loads”, Journal Aircraft, 1990, vol. 27, 619-626.
33. Libove, C., “Stresses and Rate of Twist in Single-Cell Thin-Walled Beams with Anisotropic Walls”, AIAA Journal, 1988, vol. 26, pp. 1107-1118.
34. Stemple, A. D., and Lee, S. W., “A Finite Element Model for Composite Beams with Arbitrary Cross-Sectional Warping”, AIAA Journal, 1988, vol. 26.
35. Salim, H. A., and Davalos, J. F., “Torsion of Open and Closed thin-walled laminated composite sections”, Journal of Composite Materials, vol. 39, No. 6, 2005, pp. 497-523.
36. Gjelsvik, A., 1981, *The Theory of Thin-Walled Bars*, Wiley, New York, NY.

37. Lee, J., and Lee, S., “Flexural-torsional behavior of thin-walled composite beams”, ELSEVIER, Thin-walled Structures, vol. 42, 2004, pp. 1293-1305.
38. Chan, W. S., and Demirhan K. C., “A Simple Closed-Form Solution of Bending Stiffness for Laminated Composite Tubes”, Journal of Reinforced Plastic & Composites, vol. 19, 2000, pp. 278-291.
39. Lin, C. Y., and Chan, W. S., “A Simple Analytical Method for Analyzing Laminated Composites Elliptical Tubes”, Proceedings of the 17th Technical Conference of American Society of Composites.
40. Syed, K. A., and Chan, W. S., “Analysis of Hat-Sectioned Reinforced Composite Beams”, Proceedings of American Society for Composites Conference.
41. Rao, C., and Chan, W. S., “Analysis of Laminated Composites Tapered Tubes”, Department of Mechanical and Aerospace Engineering, University of Texas at Arlington.
42. Ascione, L., Feo, L., and Mancusi, G., “On the statical behaviour of fiber-reinforced polymer thin-walled beams”, ELSEVIER, Composites, Part B, vol. 31, 2000, pp. 643-654.
43. Bauld, N. R. Jr., and Tzeng, L., “A Vlasov theory for fiber-reinforced beams with thin-walled open cross sections”, Int Journal Solid Structures, 1984, vol. 20, pp. 277-297.
44. Wu, X., and Sun, C. T., “Simplified theory for composite thin-walled beams”, AIAA Journal, 1992, vol. 30, pp. 2945-2951.
45. Bank, L. C., and Cofie, E., “A modified beam theory for bending and twisting of open-section composite beams – numerical verification”, Composite Structures, 1992, pp. 29-30.
46. Chandra, R., Stemple, A. D., and Chopra I., “Thin-walled composite beams under bending, torsional and extensional loads”, Journal Aircraft, 1990, vol. 27, 619-626.
47. Chandra, R., and Chopra, I., “Experimental and theoretical analysis of composite I-beams with elastic coupling”, AIAA Journal, vol. 29, 1992, pp.2197-2206.
48. Ferrero, J. F. , Barrau, J. J. , Segura, J. M. , Castanie, B. , and Sudre, M., “Torsion of thin-walled composite beams with midplane symmetry”, ELSEVIER, Composite Structures, vol. 54, 2001, pp. 111-120.

49. Wu, Y., Zhu, Y., Lai, Y., Zhang, X., and Liu, S., “Analysis of thin-walled composite box beam under Torsional load without external restraint”, ELSEVIER, Thin-walled Structures, vol. 40, 2002, pp. 385-397.
50. Chuanxian, C., “Researches on bending and torsional stiffness of thin-walled carbon-epoxy box beam”, Mechanics and Practice, Beijing University Press, 1985.
51. Chandra, R., Stemple, A. D., and Chopra I., “Thin-walled composite beams under bending, torsional and extensional loads”, Journal Aircraft, 1990, vol. 27, 619-626.
52. Fei, Y., “A theory for bending and torsion of the composite single cell thin-walled beam”, Mechanics and Practice, 1994, vol. 16, pp. 37-40.
53. Min, J. S., Hyo, C. M., and In, L., “Static and dynamic analysis of composite box beams using large deflection theory. Computer & Structures, 1995, vol. 57, pp. 635-642.
54. Chattopadhyay, A., Gu, H., and Liu, Q., “Modeling of smart composite box beams with nonlinear induced strain”, ELSEVIER, Composites, Part B, vol. 30, 1999, pp. 603-612.
55. Swanson S.R., 1997, *Introduction to Design and Analysis with Advanced Composite Materials*, Prentice Hall, Upper Saddle River, New Jersey.
56. Sun, C. T., 1998, *Mechanics of Aircraft Structures*, John Wiley & Sons, Inc., New York, NY.
57. Chan, W.S., and Chou, C.J., “Effects of delamination and ply waviness on effective axial and bending stiffnesses in composite laminates”, Composite Structures, vol. 30, 1995, pp. 299-306.
58. Greenberg, M. D., 1998, *Advanced Engineering Mathematics* 2nd Edition, Prentice Hall, Upper Saddle River, New Jersey.
59. Jones, R. M., 1999, *Mechanics of Composite Materials* 2nd Edition, Taylor & Francis, Philadelphia, PA.

BIOGRAPHICAL INFORMATION

Gianfranco Rios received his B.S. degree in mechanical engineer from Simon Bolivar University, Venezuela 2004. He joined the University of Texas at Arlington in August 2004 for his Master's program in mechanical engineering and graduated in May 2006. Immediately, he started his PhD in mechanical engineering at the University of Texas at Arlington.

He received different recognitions and fellowship during his years as a graduate student, among others he received the Graduate Dean Doctoral Fellowship, the STEM Doctoral Fellowship, he was accepted as a member of the Mechanical Engineering Honor Society and the Engineering Honor Society.

He did an internship to acquire industrial experience in Fall 2005. He also worked as Graduate Research Assistant and Graduate Teacher Assistant at the University of Texas at Arlington.

His research interests include composite materials analysis, structural analysis, finite element method, finite element analysis, strength of materials, solid mechanics, materials engineering, structural dynamics, and computer aided design.

Gianfranco Rios received his PhD degree in mechanical engineering from the University of Texas at Arlington in December 2009. He completed both, his Master's and PhD programs, with a perfect GPA of 4.0.